Seismic Performance Assessment of Buildings

Volume 1 – Methodology
Second Edition

FEMA P-58-1 / December 2018

FEMA

nehrp

Seismic Performance Assessment of Buildings
Volume 1 – Methodology

Second Edition

Prepared by

APPLIED TECHNOLOGY COUNCIL
201 Redwood Shores Parkway, Suite 240
Redwood City, California 94065
www.ATCouncil.org

Prepared for

FEDERAL EMERGENCY MANAGEMENT AGENCY
Michael Mahoney, Project Officer
Robert D. Hanson, Technical Monitor
Washington, D.C.

SECOND EDITION PROJECT TEAM

APPLIED TECHNOLOGY COUNCIL
Christopher Rojahn
Jon A. Heintz (Project Executive)
Ayse Hortacsu (Project Manager)

PROJECT MANAGEMENT COMMITTEE
Ronald O. Hamburger (Project Technical Director)
John Gillengerten
William T. Holmes
John D. Hooper
Stephen A. Mahin
Jack P. Moehle
Khalid Mosalam
Laura Samant
Steven R. Winkel

PROJECT STEERING COMMITTEE
William T. Holmes (Chair)
Lucy Arendt
Deborah Beck
Christopher Deneff
H. John Price
Jonathan C. Siu
Jeffrey R. Soulages
Eric Von Berg
Williston Warren (ATC Board Contact)

STAKEHOLDER PRODUCTS TEAM
Laura Samant (Team Leader)
David Mar
Lori Peek
Maryann T. Phipps
Sharyl Rabinovici
L. Thomas Tobin

PERFORMANCE PRODUCTS TEAM
John Gillengerten (Team Leader)
David R. Bonneville
Dominic Campi
Vesna Terzic

PRODUCTS UPDATE TEAM
John D. Hooper (Team Leader)
Russell Larsen
Peter Morris

FEMA

nehrp

STAKEHOLDER PRODUCTS
  CONSULTANTS
Sandra L. Grabowski
Taline Mitten
Stacia Sydoriak
Jennifer Tobin-Gurley

PERFORMANCE PRODUCTS
  CONSULTANTS
Shreyash Chokshi
Travis Chrupalo
Erica Hays
Nirmal Kumawat
Abe Lynn
Daniel Saldana
Vinit M. Shah
Udit S. Tambe
Duy Vu To
Peny Villanueva

PRODUCTS UPDATE
  CONSULTANTS
Robert Bachman
Jack Baker
Dustin Cook
Scott Hagie
Angie Harris
Curt Haselton
Wyatt Henderson
Monica Huang
Gilberto Mosqueda
Farzad Naeim
Barbara Rodriguez
Kathrina Simonen
Siavash Sorooshian
Katherine Wade
Farzin Zareian

FIRST EDITION PROJECT TEAM

APPLIED TECHNOLOGY COUNCIL
Christopher Rojahn (Project Executive)
Jon A. Heintz (Project Manager)
Ayse Hortacsu

PROJECT MANAGEMENT COMMITTEE
Ronald O. Hamburger (Proj. Tech. Director)
John Gillengerten
William T. Holmes (ex-officio)
Peter J. May
Jack P. Moehle
Maryann T. Phipps (ATC Board Contact)

STEERING COMMITTEE
William T. Holmes (Chair)
Roger D. Borcherdt
Anne Bostrom
Bruce Burr
Kelly Cobeen
Anthony B. Court
Terry Dooley
Dan Gramer
Michael Griffin
R. Jay Love
David Mar
Steven McCabe
Brian J. Meacham
William J. Petak

RISK MANAGEMENT PRODUCTS
  TEAM
John D. Hooper (Co-Team Leader)
Craig D. Comartin (Co-Team Leader)
Mary Comerio
C. Allin Cornell
Mahmoud Hachem
Gee Heckscher
Judith Mitrani-Reiser
Peter Morris
Farzad Naeim
Keith Porter
Hope Seligson

STRUCTURAL PERFORMANCE
  PRODUCTS TEAM
Andrew S. Whittaker (Team Leader)
Gregory Deierlein
John D. Hooper
Yin-Nan Huang
Laura Lowes
Nicolas Luco
Andrew T. Merovich

NONSTRUCTURAL PERFORMANCE
  PRODUCTS TEAM
Robert E. Bachman (Team Leader)
Philip J. Caldwell
Andre Filiatrault
Robert P. Kennedy
Helmut Krawinkler
Manos Maragakis
Eduardo Miranda
Gilberto Mosqueda
Keith Porter

RISK MANAGEMENT PRODUCTS
  CONSULTANTS
Travis Chrupalo
D. Jared DeBock
Armen Der Kiureghian
Scott Hagie
Curt Haselton
Russell Larsen
Juan Murcia-Delso
Scott Shell
P. Benson Shing
Mohamed Talaat
Farzin Zareian

STRUCTURAL PERFORMANCE
  PRODUCTS AND FRAGILITY
  DEVELOPMENT CONSULTANTS
Jack Baker
Dhiman Basu
Dan Dolan
Charles Ekiert
Andre Filiatrault
Aysegul Gogus
Kerem Gulec
Dawn Lehman
Jingjuan Li
Eric Lumpkin
Juan Murcia-Delso
Hussein Okail
Charles Roeder
P. Benson Shing
Christopher Smith
Victor Victorsson
John Wallace

NONSTRUCTURAL PERFORMANCE
  PRODUCTS AND FRAGILITY
  DEVELOPMENT CONSULTANTS
Richard Behr
Greg Hardy
Christopher Higgins
Gayle Johnson
Paul Kremer
Dave McCormick
Ali M. Memari
William O'Brien
John Osteraas
Elizabeth Pahl
John Stevenson
Xin Xu

FRAGILITY REVIEW PANEL
Bruce Ellingwood
Robert P. Kennedy
Stephen Mahin

VALIDATION/VERIFICATION TEAM
Charles Scawthorn (Chair)
Jack Baker
David Bonneville
Hope Seligson

SPECIAL REVIEWERS
Thalia Anagnos
Fouad M. Bendimerad

Notice

Foreword

The Federal Emergency Management Agency (FEMA) is committed to reducing the ever-increasing cost that disasters inflict on our country. Preventing losses before they happen, by building to withstand anticipated forces, is one of the key components of mitigation, and is the only truly effective way of reducing the impact of disasters on our country. One of the most promising tools that can be used to reduce damage from an earthquake, or other similar disasters, is performance-based design.

Performance-Based Seismic Design (PBSD) is a concept that permits the design and construction of buildings with a realistic and reliable understanding of the risk of life, occupancy, and economic loss that may occur as a result of future earthquakes. PBSD is based on an assessment of a building's design to determine the probability of experiencing different types of losses, considering the range of potential earthquakes that may affect the structure. This allows a building owner or regulator to select their desired performance goal for their building.

Current building codes are prescriptive in nature and are principally intended to provide a life-safety level of protection when a design-level event, such as an earthquake, occurs. While codes are intended to produce buildings that meet a life-safety performance level for a specified level of ground shaking, they do not provide designers with a means to determine if other performance levels would be achieved. During a design level earthquake, a code-designed building could achieve the goal of preventing loss of life or life-threatening injury to building occupants, but could still sustain extensive structural and nonstructural damage and be out of service for an extended period of time. In some cases, the damage may be too costly to repair, leaving demolition as the only option.

FEMA's early work in this area included the development of FEMA 349, *Action Plan for Performance Based Seismic Design* (FEMA, 2000). PBSD development work began in earnest in 2006, when FEMA contracted with the Applied Technology Council (ATC) to initiate Phase 1 development of a seismic performance assessment methodology. This work included development of an updated project plan, published as FEMA 445, *Next-Generation, Performance-Based Seismic Design Guidelines, Program Plan for New and Existing Buildings*. Phase 1 work built upon research performed

by others, including the three Earthquake Engineering Research Centers and other universities, private industry, various construction materials trade associations, and individual product manufacturers and suppliers who have performed research to facilitate the use of their products and materials in a performance-based design environment.

Phase 1 work was completed in 2012 with the publication of FEMA P-58, *Seismic Performance Assessment of Buildings*, *Volume 1 – Methodology*, *Volume 2 – Implementation Guide*, and a series of supporting electronic materials and background technical information. For practical implementation of the methodology, work included the development of an electronic tool, referred to as the *Performance Assessment Calculation Tool*, or PACT, to help capture building inventory data, input a given earthquake shaking probability or intensity, apply specific fragilities and consequences to each building component, and present the results of a large number of runs, or realizations, in a logical format.

Unlike earlier versions of PBSD, the FEMA P-58 methodology utilizes performance measures that can be understood by decision makers. Performance objectives relate to the amount of damage the building may experience and the consequences of that damage including: potential casualties; loss of use or occupancy; and repair and reconstruction costs. They can also be used to assess potential environmental impacts.

FEMA recently completed the Phase 2 development of design guidance, which used the FEMA P-58 methodology to develop performance-based seismic design guidelines and stakeholder guidelines. This five-year effort also included an update of Volume 1 and 2 products to capture improvements to the FEMA P-58 methodology.

FEMA wishes to express its sincere gratitude to all who were involved in this project and in the development of the FEMA P-58 methodology. The entire development team numbered more than 200 individuals across all phases, and it is not possible to acknowledge them all here. However, special thanks are extended to: Ronald Hamburger, Project Technical Director; Robert Bachman, Nonstructural Team Leader; John Hooper, Risk Management Team Leader; Andrew Whittaker, Structural Products Team Leader; William Holmes, Steering Committee Chair; and Jon Heinz, ATC Project Manager. The hard work and dedication of these individuals, and all who were involved in this project, have immeasurably helped our nation move towards making performance-based seismic design a reality, and towards reducing losses suffered by the citizens of our country in future earthquakes.

Federal Emergency Management Agency

Preface

In 2001, the Applied Technology Council (ATC) was awarded the first in a series of contracts with the Federal Emergency Management Agency (FEMA) to develop Next-Generation Performance-Based Seismic Design Guidelines for New and Existing Buildings. These projects would become known as the ATC-58 series of projects. The overall program was separated into two major phases of work: Phase 1 – Developing a Methodology for Assessing the Seismic Performance of Buildings; and Phase 2 – Developing Performance-Based Seismic Design Procedures and Guidelines.

This report is one of three principal products of the Phase 1 work, which were first published in 2012, and have since been updated under the Phase 2 work:

- FEMA P-58-1, *Seismic Performance Assessment of Buildings, Volume 1 – Methodology, Second Edition*

- FEMA P-58-2, *Seismic Performance Assessment of Buildings, Volume 2 – Implementation Guide, Second Edition*

- FEMA P-58-3, *Seismic Performance Assessment of Buildings, Volume 3 – Supporting Electronic Materials and Background Documentation, Third Edition*

The three volumes together describe the seismic performance assessment methodology for individual buildings, as well as the development of basic building information, response quantities, fragilities, and consequence data used as inputs to the methodology. The procedures are probabilistic, uncertainties are explicitly considered, and performance is expressed as the probable consequences, in terms of human losses (deaths and serious injuries), direct economic losses (building repair or replacement costs), and indirect losses (repair time, unsafe placarding, and environmental impacts) resulting from building damage due to earthquake shaking. The methodology is general enough to be applied to any building type, regardless of age, construction or occupancy; however, basic data on structural and nonstructural damageability and consequence are necessary for its implementation.

To allow for practical implementation of the methodology, work included the collection of fragility and consequence data for most common structural systems and building occupancies, and the development of an electronic *Performance Assessment Calculation Tool* (PACT) for performing the probabilistic computations and accumulation of losses, which were also updated as part of the Phase 2 work.

Updates include technical improvements to the methodology, and revisions to the underlying fragility and consequence data, to take advantage of the latest research, and to bring results into better alignment with expectations based on the performance of buildings in past earthquakes. Phase 2 also included the development of additional volumes intended to expand and complete FEMA P-58 series of products to communicate seismic performance to stakeholders, quantify the seismic performance capability of typical code-conforming buildings, and provide performance-based design guidance to assist decision-makers in choosing between seismic design criteria and making seismic design decisions.

The FEMA P-58 series of products is the result of the collaborative effort of more than 200 individuals, across all phases, involved in the development of the methodology and subsequent products and reports. Phase 1 consultants were involved in the development of the basic assessment methodology, collection of available fragility data, estimation of consequences, development of supporting electronic tools, implementation of quality assurance procedures, and beta testing efforts. ATC is indebted to the Phase 1 leadership of Ron Hamburger, who served as Project Technical Director, Bob Bachman, who served as Nonstructural Performance Products Team Leader, John Hooper and Craig Comartin, who served as Risk Management Products Team Leaders, Andrew Whittaker, who served as Structural Performance Products Team Leader, and the members of the Phase 1 Project Management Committee, including John Gillengerten, Bill Holmes, Peter May, Jack Moehle, and Maryann Phipps.

Phase 2 consultants were responsible for the update of all Phase 1 products, and the development of new performance-based design guidance and stakeholder guidance. ATC is indebted to the Phase 2 leadership of Ron Hamburger, who continued to serve as the Project Technical Director, John Gillengerten, who served as Performance Products Team Leader, John Hooper, who served as Products Update Team Leader, Laura Samant, who served as Stakeholder Products Team Leader, and the members of the Phase 2 Project Management Committee, including Bill Holmes, Steve Mahin, Jack Moehle, Khalid Mosalam, and Steve Winkel.
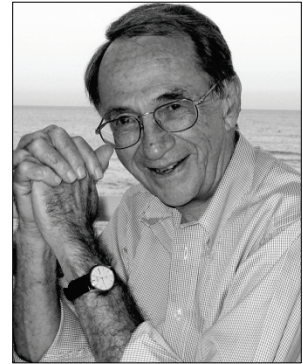
Dedication

The series of reports, collectively referred to as FEMA P-58, *Seismic Performance Assessment of Buildings, Methodology and Implementation*, is dedicated to the memory of C. Allin Cornell and Helmut Krawinkler, longtime faculty colleagues at Stanford University.

Allin brought rigorous mathematical approaches for uncertainty assessment into structural engineering, seismology, and geophysics. His continuous major contributions to risk and reliability analysis over the years have formed the basis for modern seismic risk assessment methodologies. Helmut specialized in structural design and behavior with ground-breaking research on seismic design and nonlinear structural response. His work established principles underlying modern building code provisions and formed the basis of current performance-based design methodologies.

Following the 1994 Northridge earthquake, Allin and Helmut began a close collaboration on the FEMA-funded SAC Steel Project, developing seismic design criteria for steel moment frame construction. In this regard, they were a perfect complement to one another – a combination of rigorous probabilistic thinking with an understanding of nonlinear structural behavior and design. This close collaboration continued to grow in work with the Pacific Earthquake Engineering Research Center (PEER), ultimately leading to the formalization of the PEER framework for performance-based earthquake engineering, the theoretical basis on which this report is based.

In 2000, Allin and Helmut reflected on the ultimate goal of performance-based engineering, "*The final challenge is not in predicting performance or estimating losses; it is in contributing effectively to the reduction of losses and the improvement of safety. We must never forget this.*" Allin and Helmut were true visionaries whose contributions to performance-based design and earthquake engineering are immeasurable. Their professional contributions won them both many accolades, including two of engineering's highest honors—election to the National Academy of Engineering, and receipt of the George W. Housner Medal from the Earthquake Engineering Research Institute. Beyond their professional achievements, they were both delightful, fun-loving, and thoughtful individuals whose spirits live on through their pioneering ideas and the many lives they touched in positive ways.

C. Allin Cornell
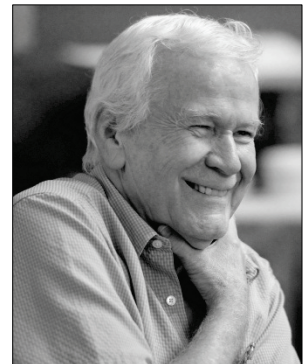
Helmut Krawinkler

Table of Contents

List of Figures

List of Tables

Chapter 1

Introduction

This report describes a general methodology and recommended procedures to assess the probable seismic performance of individual buildings based on their unique site, structural, nonstructural, and occupancy characteristics. Performance is measured in terms of the probability of incurring casualties, repair and replacement costs, repair time, selected environmental impacts, and unsafe placarding. The methodology and procedures are applicable to new or existing buildings, and can be used to: (1) assess the probable performance of a building; (2) design new buildings to be capable of providing desired performance; or (3) design seismic upgrades for existing buildings to improve their performance.

The general methodology and recommended procedures can be applied to seismic performance assessments of any building type, regardless of age, construction, or occupancy. Implementation of the methodology requires basic data on the vulnerability of structural and nonstructural components to damage (fragility), as well as estimates of potential casualties, repair costs, repair times, and environmental impacts (consequences) associated with this damage.

> In this methodology, performance is measured in terms of the probability of incurring casualties, repair and replacement costs, repair time, environmental impacts, and unsafe placarding.
>
> Performance can be assessed for a particular earthquake scenario or intensity, or considering all earthquakes that could occur, and the likelihood of each, over a specified period of time.

1.1   Background

Performance-based seismic design is a formal process for design of new buildings, or seismic upgrade of existing buildings, which includes a specific intent to achieve defined performance objectives in future earthquakes. Performance objectives relate to expectations regarding the amount of damage a building may experience in response to earthquake shaking, and the consequences of that damage.

The typical building design process is not performance-based. In the typical process, design professionals select, proportion, and detail building components to satisfy prescriptive criteria contained within the building code. Many of these criteria were developed with the intent to provide some level of seismic performance; however, the intended performance is often not obvious, and the actual ability of the resulting designs to provide the intended performance is seldom evaluated or understood.

Performance-based seismic design in its current form originated in the 1990s. Present-generation performance-based procedures are based on the Federal Emergency Management Agency (FEMA) report, FEMA 273, *NEHRP Guidelines for the Seismic Rehabilitation of Buildings* (FEMA, 1997), which addressed seismic strengthening of existing buildings, and outlined initial concepts of performance levels related to damageability and varying levels of seismic hazard. Its successor documents, FEMA 356, *Prestandard and Commentary for the Seismic Rehabilitation of Buildings* (FEMA, 2000b), and the American Society of Civil Engineers (ASCE) Standard ASCE/SEI 41-06, *Seismic Rehabilitation of Existing Buildings* (ASCE, 2007) define current practice for performance-based seismic design in the United States.
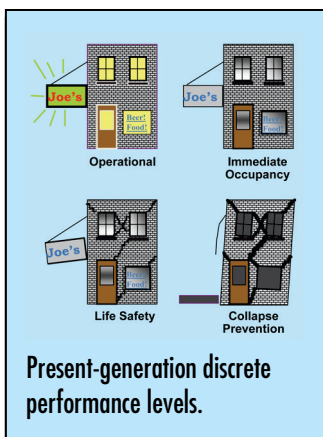
In present-generation procedures, performance is expressed in terms of a series of discrete performance levels identified as Operational, Immediate Occupancy, Life Safety, and Collapse Prevention. These performance levels are applied to both structural and nonstructural components, and are assessed at a specified seismic hazard level. Although they established a vocabulary and provided a means by which engineers could quantify and communicate seismic performance to clients and other stakeholders, implementation of present-generation procedures in practice uncovered certain limitations and identified enhancements that were needed.

Present-generation discrete performance levels.

1.2 The Need for Next-Generation Performance-Based Seismic Design Procedures

Limitations in present-generation procedures included: (1) questions regarding the accuracy and reliability of available analytical procedures in predicting actual building response; (2) questions regarding the level of conservatism underlying the acceptance criteria; (3) the inability to reliably and economically apply performance-based procedures to the design of new buildings; and (4) the need for alternative ways of communicating performance to stakeholders that is more meaningful and useful for decision-making purposes.

In order to fulfill the promise of performance-based engineering, FEMA began planning the development of next-generation procedures to address the above limitations. The FEMA 349 *Action Plan for Performance Based Seismic Design* was prepared by the Earthquake Engineering Research Institute for FEMA in 2000. Using this plan as a basis, FEMA initiated the first in a series of projects with the Applied Technology Council in 2001, which would become known as the ATC-58/ATC-58-1 Projects.

The first step in this work was to update the FEMA 349 *Action Plan*, resulting in the publication of FEMA 445, *Next-Generation Performance-*

Based Seismic Design Guidelines, Program Plan for New and Existing Buildings (FEMA, 2006). As outlined in FEMA 445, the objectives of the ATC-58/ATC-58-1 Projects were to:

- Develop a framework for performance assessment that properly accounts for, and adequately communicates to stakeholders, limitations in our ability to accurately predict response, and uncertainty in the level of earthquake hazard.

- Revise the discrete performance levels defined in present-generation procedures to create new performance measures that better relate to the decision-making needs of stakeholders.

- Create procedures for estimating these new performance measures for both new and existing buildings.

- Expand current nonstructural procedures to explicitly assess the damageability and post-earthquake condition of nonstructural components and systems.

- Modify current structural procedures to assess performance based on global response parameters, so that the response of individual components does not unnecessarily control the prediction of overall structural performance.

1.3   The Performance-Based Design Process

In the performance-based design process, design professionals, owners, and other stakeholders jointly identify the desired building performance characteristics at the outset of a project. As design decisions are made, the effects of these decisions are evaluated to verify that the final building design is capable of achieving the desired performance. Figure 1-1 presents a flowchart for the performance-based design process.

The process initiates with selection of one or more performance objectives. Each performance objective is a statement of the acceptable risk of incurring damage or loss for identified earthquake hazards. Decision-makers including owners, developers, design professionals, and building officials will typically participate in the selection of performance objectives. This process may consider the needs and desires of a wider group of stakeholders, including prospective tenants, lenders, insurers, and the general public. The needs and opinions of others can have an indirect impact on the design of a building, but these groups generally do not have an opportunity to directly participate in the design process.
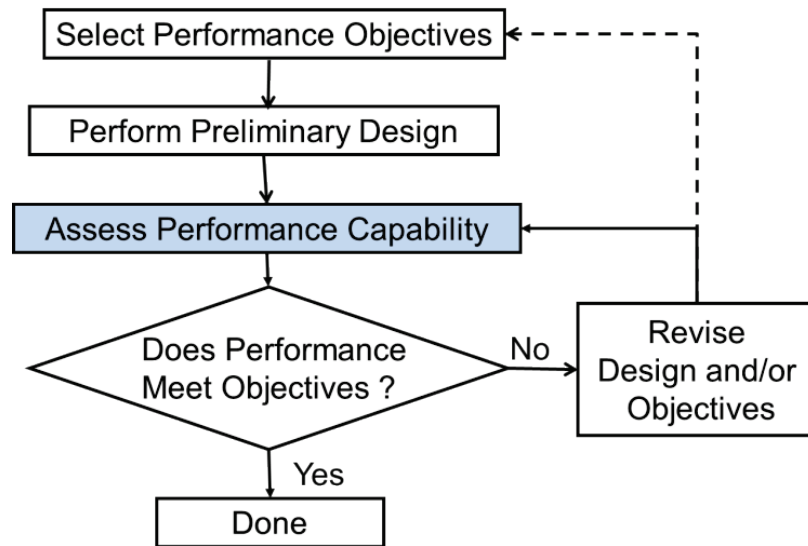
Figure 1-1   Flowchart of the performance-based design process.

Once performance objectives are selected, designs must be developed and the performance capability determined. As a minimum, basic building design information includes: (1) the location and characteristics of the site; (2) building size, configuration, and occupancy; (3) structural system type, configuration, strength, and stiffness; and (4) type, location, and character of finishes and nonstructural systems. For new buildings, preliminary design information must be developed to a sufficient level of detail to allow determination of performance capability. In the case of existing buildings, basic building design information is already defined, but preliminary retrofit measures must be developed (if necessary).

Performance assessment is the process used to determine the performance capability of a given building design. In performance assessment, engineers conduct structural analyses to predict building response to earthquake hazards, assess the likely amount of damage, and determine the probable consequences of that damage.

Following performance assessment, engineers compare the predicted performance capability with the desired performance objectives. If the assessed performance is equal to or better than the stated performance objectives, the design is adequate. If the assessed performance does not meet the performance objectives, the design must be revised or the performance objectives altered, in an iterative process, until the assessed performance and the desired objectives match.

1.4   Scope

Seismic performance assessment (shaded box in Figure 1-1), is the portion of the performance-based design process that is the primary focus of the methodology and recommended procedures contained herein. Seismic performance is expressed in terms of potential casualties, repair and replacement costs, repair time, selected environmental impacts and unsafe placarding resulting from earthquake damage. The methodology can be expanded to consider additional consequences such as other environmental impacts, and could be adapted to assess performance for other hazards and extreme loading conditions, but such enhancements are beyond the scope of the current version of the methodology.

Implementation of the methodology requires basic data on structural and nonstructural component vulnerability. Table 1-1 lists the structural systems for which fragility and consequence data have been provided.

Table 1-2 lists the building occupancies for which information on common nonstructural components, contents, normative quantities, and population models have been provided. Performance assessment for other structural systems and occupancies is possible. Data necessary for such assessments can be developed using procedures included as part of the methodology. These procedures involve the use of laboratory testing of individual components and assemblies, analytical evaluation, statistical information on the actual performance in past earthquakes, or expert judgment. It is envisioned that future research and product development activities will include the development of additional fragility and consequence data for systems and components not provided herein.

> Performance assessment is the primary focus of the general methodology and recommended procedures contained herein.

> Performance assessment for other structural systems and occupancies is possible. Data necessary for such assessments can be developed using procedures included as part of the methodology.

Table 1-1   Structural Systems and Components for which Fragility and Consequence Data have been Provided

Material	System	Comments
Concrete	Beam-column frames	Conventionally reinforced, with or without modern seismic-resistant detailing
	Shear walls	Shear- or flexurally-controlled, with or without seismic-resistant detailing
	Concrete link beams	Conventionally or diagonal reinforced with modern seismic-resistant detailing
	Slab-column systems	Post-tensioned or conventionally reinforced, with or without slab shear reinforcement
Masonry	Walls	Special or ordinary reinforced masonry walls, controlled by shear or flexure
Steel	Moment frames	Fully restrained, pre- or post-Northridge, Special, Intermediate, and Ordinary detailing
	Concentrically braced frames	"X"-braced, chevron-braced, single diagonals, special, ordinary, or nonconforming detailing

Table 1-1 Structural Systems and Components for which Fragility and Consequence Data have been Provided (continued)

Material	System	Comments
Steel (cont'd)	Buckling-restrained braced frames	"X"-braced, chevron-braced and single diagonals
	Eccentrically braced frames	Flexure or shear links at mid-span of link beam
	Light-framed walls	Structural panel sheathing, steel panel sheathing or diagonal strap bracing
	Conventional floor framing	Concrete-filled metal deck, untopped steel deck, or wood sheathing
Timber	Light-framed walls	Structural panel sheathing, gypsum board sheathing, cement plaster sheathing, let-in bracing, and with or without hold downs

Table 1-2 Building Occupancies for which Nonstructural Component Data and Population Models have been Provided

Occupancy	Comment
Commercial Office	None
Education (K-12)	Typical elementary, middle school, high school classrooms
Healthcare	General in-patient hospitals, medical equipment excluded
Hospitality	Hotels and motels
Multi-Unit Residential	Apartments; also applicable to single-family detached housing
Research Laboratories	Special purpose laboratory equipment excluded
Retail	Shopping malls and department stores
Warehouse	Inventory excluded

1.5 Basis

Performance measures serving as the basis for the assessment process were developed with input from an expanded group of stakeholders including commercial real estate investors, insurers, lenders, attorneys, and architects. This group was assembled at an invitational workshop held in Chicago, Illinois (ATC, 2002), and the collective opinions of this group were used to select the concepts of casualties, direct and indirect economic losses, and repair time, which have been used to express and measure consequences in the methodology.

The technical basis of the methodology is the framework for performance-based earthquake engineering developed by researchers at the Pacific Earthquake Engineering Research Center (PEER) during the period between 1997 and 2010. The PEER framework (Moehle and Deierlein, 2004) applies

the total probability theorem to predict earthquake consequences in terms of the probability of incurring particular values of performance measures or outcomes including casualties, repair costs, and repair time. Under the PEER framework, earthquake performance is computed as a multi-level integral of the probability of incurring earthquake effects of differing intensity, over all intensities; the probability of experiencing building response (drifts, accelerations, component demands) of different levels, given an intensity of shaking; the probability of incurring damage of different types, given building response; and the probability of incurring specific consequences given that damage occurs.

> The technical basis of the methodology is the framework for performance-based earthquake engineering developed by researchers at the Pacific Earthquake Engineering Research Center (PEER) during the period between 1997 and 2010.

Closed form solution of the multi-level integral is difficult, even for simple structural systems, and is problematic for systems as complex as real buildings. In 2004, an application of this framework was developed utilizing a modified Monte Carlo approach to implement the integration using inferred statistical distributions of building response obtained from limited suites of analyses. This application, described in Yang et al. (2009), is the basis of the performance assessment calculations and accumulation of consequences as implemented in the methodology.

1.6   Updates to the Methodology

The FEMA P-58 series of products were first published in 2012. Shortly after, a second phase of work was initiated. Major enhancements during the Phase 2 work included exercising the FEMA P-58 methodology in assessing the performance of code-conforming buildings, developing products for communicating seismic performance to stakeholders, and developing design guidance to assist decision-makers in choosing between seismic design criteria and making seismic design decisions. Technical improvements and updates to the methodology were also developed, as necessary, to take advantage of the latest research and to bring assessment results into better alignment with expectations based on performance observed in past earthquakes.

> **Second Edition Update**
>
> Significant updates in the Second Edition are identified with green margin boxes throughout the document.

As a result, Volume 1, Volume 2 – *Implementation Guide*, and Volume 3 – *Supporting Electronic Materials and Background Documentation* have all been updated, and a series of new companion products have been developed. Technical updates and improvements to the methodology include the following:

- This volume has been updated to reference currently available standards that were published after the First Edition of FEMA P-58 in 2012.

- A methodology for environmental impact assessment was developed and implemented. The environmental methodology has been incorporated throughout this volume and is demonstrated in Volume 2 – *Implementation Guide*. The algorithm is also implemented in PACT (version 3.1.2), which is provided in Volume 3. Further details about the methodology and its development are provided in FEMA P-58/BD-3.7.20 (FEMA, 2018g).

- Fragility and consequence data for selected structural and nonstructural components have been updated based on available new test data and adjusted to bring assessment results into better alignment with expectations. Updates also include revised numbering of existing fragilities as well as addition and deletion of selected fragilities. The list of provided fragility specifications in Appendix D of this volume has been updated to reflect changes to component descriptions. Detailed changes to the fragility and consequence information are documented in FEMA P-58/BD-3.7.19 (FEMA, 2018h). Note: because of these updates, a building model developed using a previous version of PACT may cause an error when used with the current version of PACT.

- Modeling considerations for nonlinear response history and simplified analyses have been updated based on recent studies, as described in Sections 5.2 and 5.3 of this volume, respectively.

- Calculation of the judgment-based collapse fragility has been updated in Section 6.4 of this volume.

- References to online tools and outside resources used in this volume and Volume 2 – *Implementation Guide* have been updated; however, the ongoing availability of resources developed external to the project is subject to change and may not be comprehensively covered herein. Other resources may become available.

1.7   Limitations

This report and its companion products provide a general methodology and recommended procedures to assess the probable seismic performance of individual buildings subjected to future earthquakes as well as design guidelines for use by structural engineers and other stakeholders including architects, owners, and tenants. The methodology assesses the likelihood that building structural and nonstructural components and systems will be damaged by earthquake shaking, and estimates the potential casualties, repair and replacement costs, repair time, selected environmental impacts, and unsafe placarding that could occur as a result of such damage. Design

guidelines assist project development teams in designing buildings that meet specific performance goals derived from these performance measures.

Performance assessment in this methodology is limited to consideration of consequences that occur within the occupied building envelope. However, earthquake shaking can also result in loss of power, water, and sewage services due to damage in offsite utilities, and earthquake casualties can occur outside the building envelope when damage generates debris that falls onto surrounding property. Earthquake shaking can also cause other significant building impacts, both inside and outside the building envelope, including initiation of fires and release of hazardous materials. Development of models to assess these additional impacts is possible, but beyond the scope of this effort.

Earthquake effects also include ground fault rupture, landslide, liquefaction, lateral spreading, seiches, and tsunamis. Although the general methodology could be used to assess impacts from these effects, such assessment is beyond the scope of the current methodology. Engineers conducting seismic performance assessments should, as a minimum, qualitatively evaluate these other effects, and, if judged significant, report appropriate limitations to decision-makers.

Assessment of building performance in future earthquakes inherently entails significant uncertainty. The methodology and procedures presented herein use state-of-the-art techniques to express the effect of these uncertainties on probable building performance. Extensive quality assurance measures were undertaken to validate the basic methodology and products as part of the developmental process. These included:

- Widespread presentation of the basic methodology and procedures at project workshops, technical conferences and symposia, and publication of interim products in refereed journals.

- Independent review of the underlying theory and methods by a validation and verification team consisting of expert researchers and practitioners with specialized knowledge in seismic performance and probabilistic theory, and implementation of a series of quality control recommendations to incrementally validate the procedures during development.

- Independent review of the component fragility development process by teams of engineers and researchers familiar with structural and nonstructural seismic performance, as well as detailed review of the quality of data and consistent application of procedures by a panel of

independent experts knowledgeable in structural reliability theory and seismic performance.

- Independent review of the consequence development process, and detailed review of the quality of the resulting cost and repair data, by a knowledgeable construction cost estimator.

- Independent review of the calculation algorithms embedded in supporting electronic materials by designated members of the project development team.

- A series of benchmark performance evaluations conducted on representative building types ranging from low-rise masonry, to mid-rise concrete and steel, to high-rise structures, by teams of researchers and graduate students that implemented the methodology under a variety of assumptions to explore the rationality of results.

Regardless of quality assurance measures undertaken, it is possible that the performance of individual buildings in actual earthquakes may be better or worse than indicated by assessments conducted in accordance with this methodology. Further, the accuracy of any performance assessment will depend on data and calculations generated by individual users. No warranty is expressed or implied regarding the accuracy, completeness, or usefulness of performance assessments made using any information, product, or procedure comprising the methodology, and users of this methodology assume all liability arising from such use.

1.8 Products

The resulting products have been organized into a series of volumes collectively referred to as FEMA P-58, *Seismic Performance Assessment of Buildings, Methodology and Implementation*. These volumes consist of a description of the basic methodology, guidance on implementation, design, and communication with stakeholders, as well as supporting electronic materials and background technical information, including:

FEMA P-58-1, *Seismic Performance Assessment of Buildings, Volume 1 – Methodology, Second Edition.* Volume 1 (this document) is the fundamental product of Phase 1 work, originally published in 2012 and updated in 2018. It presents the general methodology for conducting seismic performance assessments, and describes the necessary information and recommended procedures for developing basic building information, response quantities, fragilities, and consequence data used as inputs to the methodology. The Second Edition includes updated information regarding environmental impacts and other technical enhancements.

FEMA P-58-2, *Seismic Performance Assessment of Buildings, Volume 2 – Implementation Guide, Second Edition.* Volume 2 provides guidance on implementing a seismic performance assessment using the methodology, and includes specific instructions on how to assemble and prepare the input data necessary for the *Performance Assessment Calculation Tool* (PACT). Volume 2 was originally published in 2012 and updated in 2018. It contains a user's manual and examples illustrating the performance assessment process, including selected calculation and data generation procedures. The Second Edition (FEMA, 2018a) includes examples illustrating the calculation of environmental impacts and other technical enhancements.

FEMA P-58-3, *Seismic Performance Assessment of Buildings, Volume 3 – Supporting Electronic Materials and Background Documentation, Third Edition.* Volume 3 consists of a series of electronic products assembled to assist engineers in conducting seismic performance assessments and in understanding the technical basis of the methodology. The Second Edition (FEMA, 2016) was published in 2016 with the release of interim updates to PACT and underlying fragility and consequence data. The Third Edition (FEMA, 2018b) includes the latest version of PACT, along with additional updates to fragility and consequence data, and added tools and background documentation. The following electronic tools and documents are included:

- *Performance Assessment Calculation Tool* (PACT). PACT is an electronic calculation tool, and repository of fragility and consequence data, that performs the probabilistic calculations and accumulation of losses described in the methodology. It includes a series of utilities used to specify building properties and update or modify fragility and consequence information in the referenced databases. An executable file (.exe) is provided to facilitate installation of the tool. Appendix C of FEMA P-58 Volume 2 presents a User Manual for PACT.

- *Provided Fragility Data*. This folder contains the following products to aid management and maintenance of all provided fragility and consequence data outside of PACT and assist in the development of consequences for custom fragility specifications:

  o *Fragility Database* is an Excel workbook that is used to review and maintain all provided fragility and consequence data outside of PACT. This database has been updated for the Second Edition release and includes environmental impact consequence information.

  o *Fragility Specification* is a PDF file displaying the contents of the fragility database. Each fragility specification contains fragility and

consequence data for the component of interest, in a one-page format. Damage states are illustrated with photos of representative damage, when available.

- *PACT Input Matrix* is an Excel workbook that contains the Fragility Database in a format that is required for upload into PACT.

- *Consequence Estimation Summary* is an Excel workbook that provides the basis for provided consequence data, and can be used to assist in estimating consequences for custom fragility specifications.

- *Normative Quantity Estimation Tool* is an Excel workbook designed to assist in estimating the type and quantity of nonstructural components typically present in buildings of a given occupancy and size. Appendix D of FEMA P-58 Volume 2 presents a User Manual for this tool.

- *Performance Estimation Tool (PET)*. PET is an Excel workbook that utilizes assessment results from the application of the FEMA P-58 methodology to a group of building archetypes representative of structures conforming to the seismic design requirements of the current building code. The tool is intended for use to obtain an initial estimate of building performance in a graphical format and was developed as part of the Second Edition update.

- *Static Pushover to Incremental Dynamic Analysis* (SPO2IDA). SPO2IDA is an Excel workbook application that was originally developed by Vamvatsikos and Cornell (2006). This tool uses empirical relationships from a large database of incremental dynamic analysis results to convert static pushover curves into probability distributions for building collapse as function of ground shaking intensity.

- *Collapse Fragility Tool*. The Collapse Fragility Tool is an Excel workbook application that fits a lognormal distribution to collapse statistics obtained from a series of nonlinear dynamic analyses at different ground motion intensity levels.

- *Technical Background Documentation*. A series of reports documenting the technical background and source information for key aspects of the methodology, including simplified analysis procedures, fragility development procedures, estimation of peak floor velocity, scaling of ground motion records, residual drift computations, repair time modeling, building population modeling, validation and verification studies, results from beta testing efforts, proceedings from project workshops, and a summary of updates to fragilities in the Second Edition.

- *Structural Fragility Background Documentation.* A series of reports documenting the technical background and source data for structural fragilities provided with the methodology.

- *Nonstructural Fragility Background Documentation.* A series of reports documenting the technical background and source data for nonstructural fragilities provided with the methodology.

FEMA P-58-4, *Seismic Performance Assessment of Buildings, Volume 4 – Methodology for Assessing Environmental Impacts.* Volume 4 describes a recommended methodology for incorporating assessment of environmental impacts, along with other consequences, that are associated with the repair of damage caused by earthquake shaking (FEMA, 2018c). The findings were used to update the methodology and PACT to incorporate environmental impact consequences.

FEMA P-58-5, *Seismic Performance Assessment of Buildings, Volume 5 – Expected Seismic Performance of Code Conforming Buildings.* Volume 5 describes the application of the FEMA P-58 assessment methodology to a group of archetypical buildings representative of structures conforming to the seismic design requirements of the current building code (FEMA, 2018d).

FEMA P-58-6, *Guidelines for Performance-Based Seismic Design of Buildings.* This volume provides guidelines and recommendations for specifying seismic performance objectives in terms of FEMA P-58 performance metrics, and for selecting appropriate structural and nonstructural systems, configurations, and characteristics necessary to achieve the desired performance in varying regions of seismicity (FEMA, 2018e).

FEMA P-58-7, *Building the Performance You Need, a Guide to State-of-the-Art Tools for Seismic Design and Assessment.* This short document is intended for project managers and decision-makers, and presents a non-technical basis for using a performance-based approach for seismic design and assessment (FEMA, 2018f). This document is also supported by an online quiz.

1.9   Organization and Content

This volume presents the overall seismic performance assessment methodology and describes the recommended procedures for developing information used as inputs to the methodology. Readers are cautioned to become thoroughly acquainted with the information contained in this volume before attempting to conduct building performance assessments using PACT.

Chapter 2 presents an overview of the methodology including discussion of the specific performance measures used and the types of assessments that can be conducted.

Chapter 3 describes the development of building-specific performance models by assembling all the data necessary to assess building performance.

Chapter 4 describes methods to characterize seismic hazards for use in performance assessment.

Chapter 5 provides guidance for two alternative methods of structural analysis used to predict building response.

Chapter 6 presents alternative procedures for characterizing susceptibility to collapse as a function of ground shaking intensity.

Chapter 7 describes the calculation procedures used to determine the probable damage that a building will sustain and the consequences of damage in terms of casualties, repair costs, repair time, unsafe placarding, and other potential impacts.

Chapter 8 illustrates methods for using data obtained from performance assessment in the planning and design decision-making process.

Appendix A provides a basic tutorial on probability and statistics and the types of probability distributions used to represent uncertainty in the methodology.

Appendix B provides detailed information on seismic hazard characterization and ground motion prediction models.

Appendix C presents background information on residual drift estimation and limitations on the ability of structural analysis to reliably predict residual drift.

Appendix D lists the types of structural and nonstructural components and contents for which fragility and consequence data are provided with the methodology and accompanying databases.

Appendix E presents recommended building population models for common building occupancies.

Appendix F provides a tabulation of the typical quantities of nonstructural components and contents found in buildings of different occupancies or use.

Appendix G describes the algorithm used to generate multiple vectors of simulated demands as part of the performance assessment process.

Appendix H provides guidelines for development of fragility functions for individual building components for use in performance assessment.

Appendix I tabulates a list of building components that are generally considered rugged and, therefore, insignificant to the performance assessment process.

Appendix J describes the incremental dynamic analysis procedure, which can be used to determine the susceptibility of a building to collapse.

Appendix K describes the basis used to determine vulnerability of unanchored components to sliding or overturning.

A Glossary and list of Symbols, providing definitions of key terminology and notation used in the methodology, along with a list of References, are provided at the end of this report.

Chapter 2

Methodology Overview

2.1   Introduction

This chapter introduces key aspects of the methodology, including performance measures, uncertainty, types of performance assessment, and the basic steps of the performance assessment process.

2.2   Performance Measures

A performance measure is a means of quantifying the consequences associated with the response of a building to earthquake shaking in terms that are intended to be meaningful to decision-makers. Historically, decision-makers have used a number of different performance measures.

> Performance is expressed in terms that are intended to be meaningful to decision-makers.

Since the publication of ASCE/SEI 31-03, *Seismic Evaluation of Existing Buildings* (ASCE, 2003), and ASCE/SEI 41-06, *Seismic Rehabilitation of Existing Buildings* (ASCE, 2007), building officials and engineers have commonly used a series of standard discrete performance levels, termed Operational, Immediate Occupancy, Life Safety, and Collapse Prevention, to characterize expected building performance. These performance levels are defined by acceptable ranges of strength and deformation demands on structural and nonstructural components, with implicit qualitative relationships to probable levels of damage, casualties, post-earthquake occupancy, and repairs.

Many financial institutions including lenders, investment funds, and insurers use Probable Maximum Loss (PML), Scenario Expected Loss (SEL), and Scenario Upper Loss (SUL) as preferred performance measures. These performance measures are quantitative statements of probable building repair cost, typically expressed as a percentage of building replacement value. Some building owners, developers, and tenants have also relied on these performance measures to quantify seismic performance.

In this methodology, performance is expressed as the probable damage and resulting consequences associated with earthquake shaking using the following performance measures:

- **Casualties.** Loss of life, or serious injury requiring hospitalization, occurring within the building envelope.

- **Repair cost.** The cost, in present dollars, necessary to restore a building to its pre-earthquake condition, or in the case of total loss, to replace the building with a new structure of similar construction.

- **Repair time.** The time, in weeks, necessary to repair a damaged building to its pre-earthquake condition.

- **Environmental impacts.** The effects on the environment in terms of embodied carbon and embodied energy to restore a building to its pre-earthquake condition or, in the case of total loss, to replace the building with a new structure of similar construction.

- **Unsafe placarding.** A post-earthquake inspection rating that deems a building, or portion of a building, damaged to the point that entry, use, or occupancy poses immediate risk to safety.

For many reasons, it is not possible to precisely predict response to earthquake shaking, subsequent damage, and resulting consequences. Therefore, the methodology expresses performance in the form of probable impacts, considering inherent uncertainties. This approach has several advantages. Probable performance in terms of casualties, repair costs, repair time, and unsafe placarding is more meaningful to decision-makers and more directly useful in the decision-making process than the standard, discrete performance levels that have been used to date. Also, PML, SEL and SUL measures of performance can be directly and objectively derived using a probabilistic approach. Finally, uncertainty in performance assessment is explicitly acknowledged. If properly used, uncertainty can assist design professionals in communicating with decision-makers in a way that avoids perceived warranties and liabilities associated with performance assessments and performance-based designs.

2.3   Factors Affecting Performance

The level of damage that a building experiences in an earthquake, and the consequences of that damage in terms of casualties, repair costs, repair time, and unsafe placarding, depends on a number of factors. These include:

- the intensity of ground shaking and other earthquake effects experienced by the building;

- the response of the building to ground shaking and other earthquake effects, and the resulting force, deformation, acceleration, and velocity demands experienced by the structural and nonstructural components, contents, and occupants;

- the vulnerability of the building components, systems, and contents to damage;

- the number of people, and the type, location, and amount of contents present within the building envelope when the earthquake occurs;

- the interpretation of visible evidence of damage by inspectors performing post-earthquake safety investigations; and,

- the specific details and methods of construction used in performing repairs.

This methodology explicitly evaluates each of these factors in assessing performance. However, there are other important factors associated with the actions people take in response to future earthquakes that are not considered because they are inherently unpredictable. Factors that are not considered, but can affect the magnitude of the resulting earthquake impacts, include:

- the speed and quality of care given to injured individuals;

- the speed with which building owners engage design professionals, obtain necessary approvals, and engage contractors to implement repair actions;

- the availability of labor and materials, the efficiency of individual contractors, and their desire for profit in the post-disaster construction environment; and

- a decision to conduct repairs while a building remains occupied, or to vacate a building and allow full access for construction crews.

2.4   Uncertainty in Performance Assessment

Each factor affecting seismic performance has significant uncertainty in the ability to know or predict specific values. The fault that will produce the next earthquake, where along the fault the rupture will initiate, or the magnitude of shaking that will occur, are all not known with any certainty. Nor is there a complete understanding of the subsurface conditions that seismic waves must pass through between the fault rupture and the building site. As a result, the intensity, spectral shape, or wave form of future earthquake shaking cannot be precisely predicted.

Although the ability to develop analytical models of structures is constantly improving, models are still imprecise. Typical structural models are based on assumptions of material strength, cross-section geometry, and details of construction. Damping is estimated using rules of thumb. The effects of soil-structure interaction, elements designed to resist only gravity loads, and

> Each factor affecting seismic performance has significant uncertainty in our ability to know or predict specific values.
>
> The cumulative result of these and other uncertainties is that it is not possible to precisely assess the seismic performance of a building.

nonstructural components are commonly neglected. Therefore, response predictions are inherently uncertain, and it is not known whether structural analyses are under-predicting or over-predicting the actual response of a building.

Using response quantities from structural analyses, and the observed behavior of similar elements tested in the laboratory or in past earthquakes, it is possible to predict the levels of damage that structural and nonstructural components might sustain. However, components tested in a laboratory may not be identical to components in an actual building, and the forces and deformations imposed in the laboratory may not be identical to those predicted in the structural analysis or experienced in an actual earthquake. Therefore, predictions of the type and amount of damage are likely to be inaccurate.

Similarly, it is not possible to predict the time of day or day of the week when an earthquake will occur, the number of people that will be in the building at that time, and the type or amount of contents and furnishings that are present. Once damage is predicted, it is difficult to know the exact repair techniques that will be specified to repair damaged components, or how efficiently the repairs will be constructed.

Performance functions express the probability of incurring earthquake impacts. This methodology provides a means of determining performance functions.

The cumulative result of these and other uncertainties is that it is not possible to precisely assess the seismic performance of a building, whether that performance is measured by casualties, repair costs, repair time, or other impacts. It is, however, possible to express performance measures in the form of performance functions. Figure 2-1 presents a performance function for a hypothetical building and given intensity of shaking.

Figure 2-1   Hypothetical building performance function.

Performance functions are statistical distributions that indicate the probability that losses of a specified or smaller magnitude will be incurred as a result of future earthquakes. Appendix A provides a brief introduction to such distributions. In the figure, the horizontal axis represents the size of the impact (e.g., number of casualties, repair cost, or weeks of construction time) while the vertical axis indicates the probability that the actual impact will be equal to or less than this value. The methodology and procedures presented in this report describe a means to determine performance functions.

2.5 Types of Performance Assessment

This methodology can be used to develop three types of performance assessment: intensity-based, scenario-based, and time-based assessments.

2.5.1 Intensity-Based Assessments

Intensity-based assessments evaluate the probable performance of a building assuming that it is subjected to a specified earthquake shaking intensity. Shaking intensity is defined by 5% damped, elastic, acceleration response spectra. This type of assessment can be used to assess the performance of a building for design earthquake shaking consistent with a building code response spectrum, or to assess performance for shaking intensity represented by any other response spectrum.

> Intensity-based assessments evaluate performance for a user-selected acceleration response spectrum.

2.5.2 Scenario-Based Assessments

Scenario-based assessments evaluate the probable performance of a building assuming that it is subjected to an earthquake scenario consisting of a specific magnitude earthquake occurring at a specific location relative to the building site. Scenario assessments are useful for buildings located close to one or more known active faults. This type of assessment can be used to assess the performance of a building in the event that an historic earthquake is repeated, or a future projected earthquake occurs.

> Scenario-based assessments evaluate performance for a user-selected earthquake magnitude and distance.

Scenario-based assessments are similar to intensity-based assessments except that they consider uncertainty in the intensity of earthquake shaking, given that the scenario occurs. Results of scenario-based assessments are performance functions similar to Figure 2-1, except that the probable performance is conditioned on the occurrence of the specified earthquake scenario rather than a specified shaking intensity.

2.5.3 Time-Based Assessments

Time-based assessments evaluate the probable performance of a building over a specified period of time (e.g., 1 year, 30 years, or 50 years)

considering all earthquakes that could occur in that time period, and the probability of occurrence associated with each earthquake. Time-based assessments consider uncertainty in the magnitude and location of future earthquakes as well as the intensity of motion resulting from these earthquakes.

The time period for time-based assessment depends on the interests and needs of the decision-maker. Assessments based on a single year are useful for cost-benefit evaluations used to decide between alternative performance criteria. Assessments over longer periods of time are useful for other decision-making purposes. Chapter 8 provides additional information on the use of performance assessment results in decision-making.

Time-based assessments provide performance functions that are similar to Figure 2-1, except that the vertical axis of the function expresses the frequency that an impact of a certain size (e.g., number of casualties, repair costs, or weeks of construction time) will be exceeded in a period of time, typically one year. Once the performance function for a one-year time period has been developed, it can easily be converted to other time periods (see Appendix A).

2.6   The Methodology

Figure 2-2 is a flowchart illustrating the relationship between the steps that comprise the performance assessment methodology. It also identifies the chapters that provide more detailed discussion of each step.
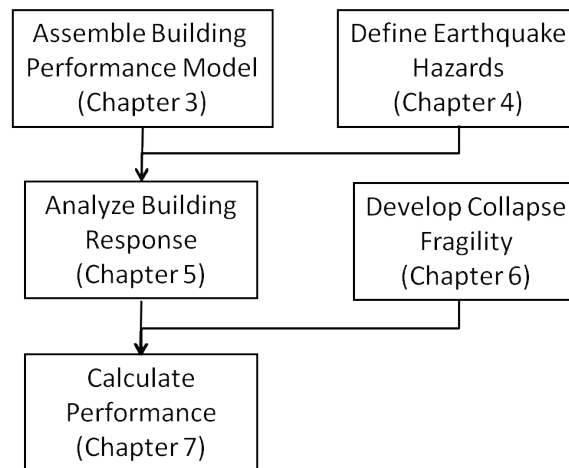
Figure 2-2   Flowchart of the performance assessment methodology.

2.6.1   Assemble Building Performance Model

The building performance model is an organized collection of data used to define the building assets at risk and their exposure to seismic hazards. This data includes definition of:

- Structural components and assemblies that can be damaged by the response of the building to earthquake shaking. Data must include information on the types of damage these components can sustain, the structural demands that cause this damage, and the consequences of this damage in terms of risk to human life, repair methods, repairs costs, repair time, and post-earthquake building occupancy due to unsafe placarding.

- Nonstructural systems, components, and contents that do not provide significant resistance to gravity or earthquake loading but can be damaged by the response of the building to earthquake shaking. Data must include the location of these components within the building, their vulnerability to different types of damage, and the consequences of this damage in terms of life-threatening debris generation, repair methods, repairs costs, repair time, selected environmental impacts, and influence on post-earthquake building occupancy.

- Occupancy, including the distribution of people within the building envelope and the variability of this distribution over time of day and day of the year.

Vulnerable building components are categorized into fragility groups and performance groups. Fragility groups are sets of similar components that have the same potential damage characteristics in terms of vulnerability and consequences. Performance groups are subsets of a fragility group that will experience the same earthquake demands in response to earthquake shaking. Chapter 3 introduces the fragility specification used to define damage and consequence data, and describes the categorization of components into fragility groups and performance groups.

2.6.2   Define Earthquake Hazards

Earthquake effects include ground shaking, ground fault rupture, liquefaction, lateral spreading, land sliding, and tsunami inundation. Each of these effects can occur with different levels of severity, or intensity, ranging from imperceptible to highly damaging. Earthquake hazard is a quantification of the intensity of these effects and the site-specific probability that effects of a given intensity will be experienced. Presently, this methodology addresses consequences associated with building damage due

to earthquake ground shaking. It can, however, be extended to include consideration of other earthquake effects.

Ground shaking hazards are specified in different ways, depending on the type of assessment and the type of structural analysis used to quantify earthquake response. These are introduced below and described in more detail in Chapter 4.

Intensity-based assessments consider building response to a single acceleration response spectrum. Depending on the type of structural analysis used, ground shaking intensity is characterized in the form of discrete spectral response accelerations extracted from a reference spectrum, or suites of ground motion records that have been selected and scaled for consistency with the reference spectrum.

Scenario-based assessments consider building response to an earthquake scenario at a defined magnitude and distance from the site. Shaking hazards are represented by a median acceleration response spectrum and period-dependent dispersions obtained from the ground motion prediction equation or attenuation relationship used to derive the spectrum. Analyses are conducted using discrete spectral response accelerations derived from the median spectrum, or ground motion records that are scaled to be consistent with the distribution of possible spectra.

For time-based assessments, ground shaking hazards are characterized by a series of mean seismic hazard curves at different sites. Each hazard curve is a plot of the mean annual frequency of exceedance of spectral response acceleration of different amplitudes at a particular structural period. These hazard curves are used to derive a series of acceleration response spectra representing a range of ground shaking intensities across a meaningful range of exceedance probabilities and structural response quantities. Analyses are conducted using discrete spectral response accelerations derived from spectra at each intensity, or ground motion records that are scaled to be consistent with these spectra at each intensity.

2.6.3   Analyze Building Response

Building response can be simulated using nonlinear response-history analysis or a simplified procedure based on equivalent lateral forces.

Structural analysis is used to predict the response of a building to earthquake shaking in the form of response quantities (i.e., demands) that can be associated with structural and nonstructural damage. Demands typically include peak values of story drift ratio in each of two orthogonal directions, floor velocity, floor acceleration, and residual drift ratio. It is possible to use other demand parameters, such as individual component strength or

deformation demands, if a building includes components for which damage is better correlated with such parameters.

Chapter 5 describes the use of two analysis procedures for response prediction: (1) nonlinear response-history analysis; and (2) simplified analysis based on equivalent lateral force methods. Nonlinear response-history analysis can be used for any structure, and can provide values for any demand parameter that is simulated in the model. Simplified analysis is valid for regular, low-rise, and mid-rise structures, with limited nonlinear response, and will provide values for peak transient floor acceleration, floor velocity and story drift ratio only. Also included in Chapter 5 is an approximate procedure to estimate residual drift ratio from peak story drift ratio and yield story drift ratio.

2.6.4 Develop Collapse Fragility

Most casualties occur as a result of partial or total building collapse. To assess potential casualties, it is necessary to define the probability of incurring structural collapse as a function of ground motion intensity along with the modes of structural collapse that are possible (e.g., single-story, multi-story, full-floor, or partial floor). These are represented in the form of collapse fragility functions. Chapter 6 describes a means of establishing collapse fragilities using a combination of structural analysis and judgment.

> Most casualties occur as a result of building collapse.

2.6.5 Calculate Performance

To account for the many uncertainties inherent in factors affecting seismic performance, the methodology uses a Monte Carlo procedure to perform loss calculations. This is a highly repetitive process in which building performance is calculated for each of a large number (hundreds to thousands) of realizations. Each realization represents one possible performance outcome for the building, considering a single combination of possible values of each uncertain factor.

> Each realization represents one possible performance outcome. The methodology uses Monte Carlo analysis to explore uncertainty in the possible range of outcomes.

Chapter 7 describes the calculation procedures used to assess probable performance with explicit consideration of uncertainty. These calculations are numerous and data-intensive for systems as complex as real buildings. As a matter of practicality, a companion *Performance Assessment Calculation Tool* (PACT) was developed along with the methodology to perform repetitive calculations and manage data.

2.6.5.1 Intensity-Based and Scenario-Based Assessments

For intensity-based and scenario-based assessments, the performance calculations are nearly identical. Figure 2-3 provides a flowchart illustrating

the performance calculation process for intensity- and scenario-based assessments. For each type of assessment, the possible consequences of building performance (casualties, repair costs, repair time, unsafe placarding) are calculated many times to explore the effect of uncertainty on the predicted outcome. Each repetition is termed a realization, and represents one possible performance outcome for the particular earthquake intensity or scenario being analyzed. Figure 2-4 provides a flowchart illustrating the process for assessing a performance outcome in each realization.

```
┌─────────────────────────┐
│     Develop "R"         │
│ Simulated Demand Sets   │
└─────────────────────────┘
            │
            ▼
┌─────────────────────────┐
│ For each of "R" Realizations │
│   Compute Consequences  │
│    (See Figure 2-4)     │
└─────────────────────────┘
            │
            ▼
┌─────────────────────────┐
│  For each Consequence   │
│  Order Realizations from│
│  Least Impact to Highest│
└─────────────────────────┘
            │
            ▼
┌─────────────────────────────────┐
│      For each Consequence       │
│ Plot Value of Realization Impact│
│            against              │
│ Percentage of Realizations Having│
│          Smaller Impact         │
└─────────────────────────────────┘
```
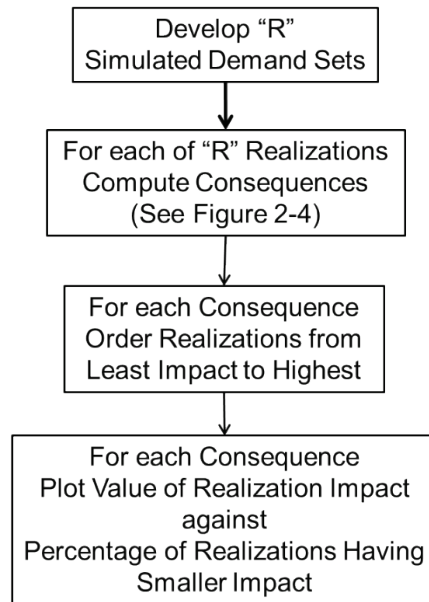
Figure 2-3   Flowchart for intensity- and scenario-based assessments.

The calculation is repeated for R realizations, where R might be on the order of 1000 or more. These outcomes are ordered from smallest to largest and a performance curve (similar to Figure 2-1) is constructed as a plot of the percentage of realizations with outcomes that exceed each value. Key steps in the process are described below.

Develop simulated demand sets. The process initiates with determining how many realizations, R, will be evaluated. Results from the structural analysis are used to generate a series of R simulated demand sets (i.e., vectors of structural response quantities). Simulated demand sets reflect the correlation between the various response quantities predicted in the analyses, uncertainties inherent in structural response prediction, and in the case of scenario-based assessment, uncertainties associated with the spectral content of the ground motion. Appendix G describes the mathematical procedure for deriving a set of simulated demands in the form of a matrix $[m \times R]$, where each column in the matrix is one set of simulated demands. For each of the R

realizations, a unique set of possible earthquake performance outcomes is determined using the steps in Figure 2-4.
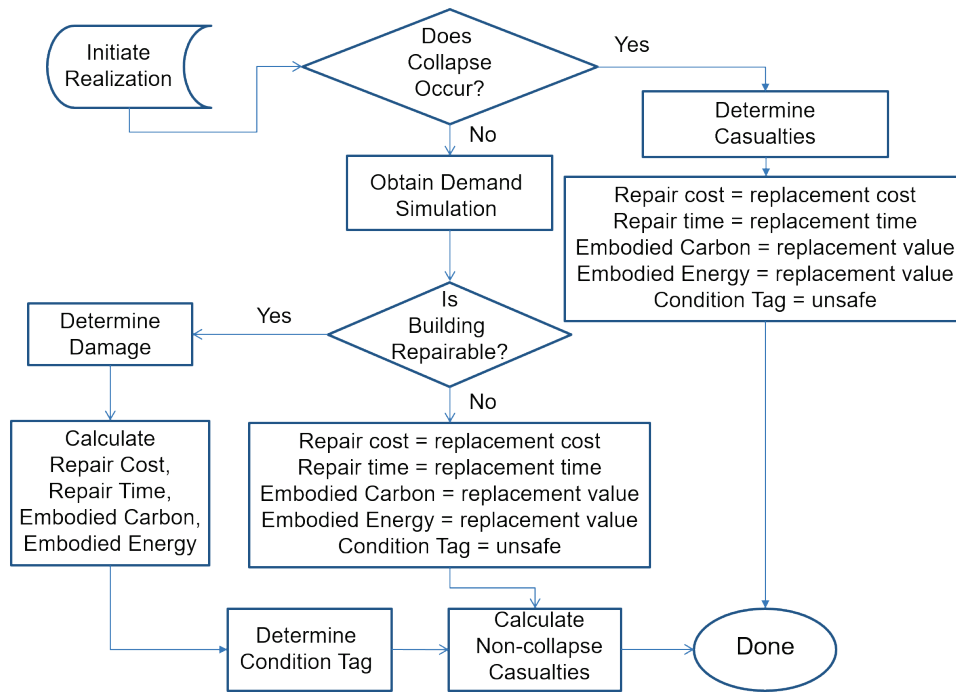
Second Edition Update

This figure has been updated to include consideration of environmental impacts, embodied carbon and embodied energy.

Figure 2-4   Flowchart for assessing a performance outcome in each realization.

Determine if collapse occurs. The first step in each realization is to determine if the building has collapsed. Collapse susceptibility is characterized by a collapse fragility function. By comparing the collapse fragility function with the intensity of ground motion for the realization, the probability of collapse is determined. Random number generation is used to determine if the collapse threshold will be exceeded. When collapse occurs, the building is assumed to be a total loss and the repair cost, repair time, and environmental impacts are taken as the values associated with building replacement, including consideration of demolition and removal of debris from the site.

Calculate collapse casualties. To calculate casualties, it is necessary to determine a time of day and day of the week at which the realization occurs. Using a time-dependent population model appropriate for the building occupancy, along with randomly generated day and time, the number of people present in the area of collapse is determined. Using casualty functions appropriate to the type of construction, percentages of the population at risk in the collapsed area are classified as serious injuries or fatalities.

The methodology does not predict casualties that could occur outside the building envelope as a result of debris falling onto adjacent properties. To make such a prediction, it would be necessary to have a population model for the area outside the building. For tall buildings, exterior population models would need to extend a considerable distance from the subject building, and would potentially include many other buildings. Although the logic could be extended to include such modeling, estimation of casualties outside the building envelope is beyond the scope of the current methodology.

Obtain simulated demands. If the building does not collapse in a given realization, it is necessary to associate one of the previously generated sets of simulated demand vectors with the realization. For intensities at which no collapses occur, all of the simulated demand sets in the $[m \times R]$ matrix of simulated demands are uniquely associated with a realization. For intensities at which some collapses occur, realizations that experience collapse are not assigned simulated demands, and some simulated demand sets are not used.

Determine if the building is repairable. Simulated demand sets for each realization include an estimate of the residual drift ratio at each level of the building. The maximum residual drift ratio is used, together with a building repair fragility, to determine if repair is practicable. A typical building repair fragility is a lognormal distribution with a median value of 1% residual drift ratio, and a dispersion of 0.3, as shown in Figure 2-5.
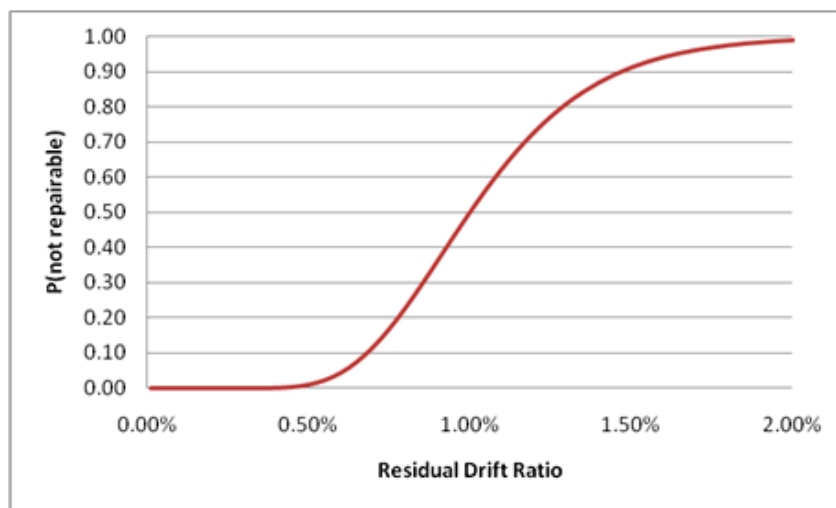
Figure 2-5   Typical building repair fragility based on residual drift ratio.

At a residual drift ratio of 0.5%, this fragility indicates that building repair is a virtual certainty. At a residual drift ratio of 2.0%, however, it is a virtual certainty that the building will not be repaired. As with collapse determination, a random number generator is used to determine if the building is deemed irreparable for that realization. If irreparable, repair cost,

repair time, and environmental impacts are taken as the building replacement values, including consideration of demolition and removal of debris from the site. The building is also assumed to be assigned an unsafe placard.

Determine damage. If the building has not collapsed and is deemed repairable in a given realization, the set of simulated demands is used to determine a damage state for each vulnerable component in the building. Damage states are assigned on a performance group basis. Each performance group has an associated series of damage states and fragility functions that describe the probability that components within the group will be damaged to a given level. Random number generation is used to determine which damage state, if any, is experienced by each component in the realization.

Calculate consequences. Using damage states and associated consequence functions, the magnitude of consequences associated with the damage in each component is determined. In calculating consequences, consideration is given to the volume of repairs that must be made, as well as uncertainties in repair technique, contractor efficiency, and pricing.

2.6.5.2 Time-Based Assessments

In time-based assessments, a more complex procedure is used. Time-based assessments compute the probable building performance outcomes considering all possible intensities of shaking that might be experienced by the building within the specified time period, and weights the outcome from each intensity by the probability that such shaking will occur.

To perform this calculation, it is necessary to obtain a hazard curve for the site that provides the annual frequency of exceedance of ground motions with different intensities. Figure 2-6 is one such curve for a hypothetical site, showing the annual frequency of exceedance of a ground motion intensity parameter, e. Chapter 4 and Appendix B provide detailed information on how to characterize seismic hazard for time-based assessments.

The hazard curve is divided into a series of intervals, illustrated as intervals Δe_i in the figure. The annual frequency of occurrence of ground motion having an intensity that falls within each interval is equal to the difference between the annual frequencies of exceedance of the ground shaking intensities at each end of the interval. For each intensity interval on the hazard curve, an intensity-based assessment is performed for the intensity at the mid-point of the interval. The resulting performance outcomes are then weighted by the annual frequency of occurrence of intensities within that

interval. The results of these assessments are summed over all of the intervals to form a time-based performance function, as shown in Figure 2-7.
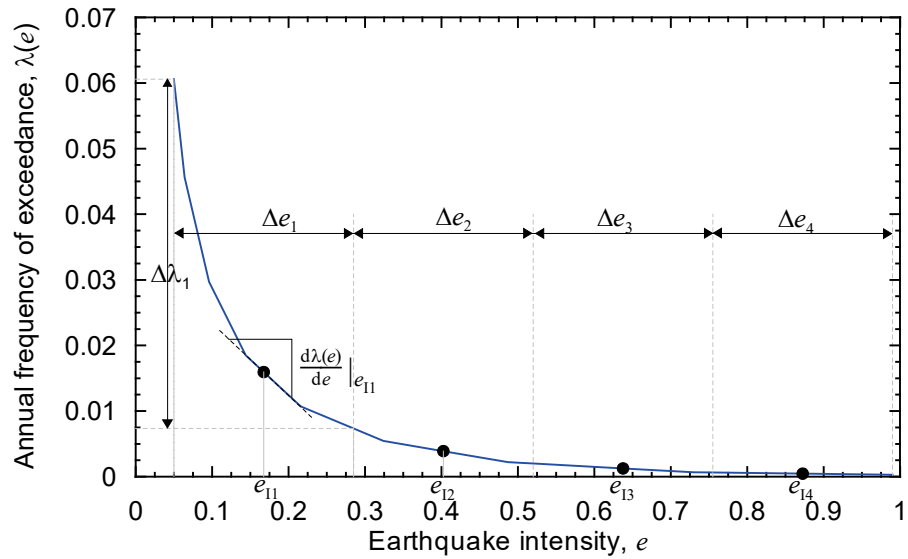
Figure 2-6   Seismic hazard curve used in time-based assessments.
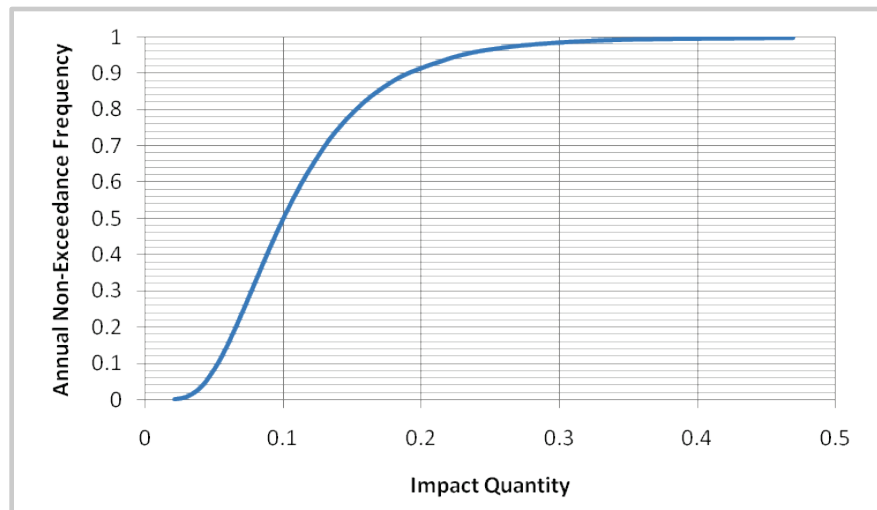
Figure 2-7   Hypothetical time-based building performance function.

Chapter 3

Assemble Building Performance Model

3.1   Introduction

This chapter describes the process for assembling the building performance model. The building performance model is an organized collection of data necessary to define building assets that are at risk and vulnerable to the effects of earthquake shaking. This includes definition of:

- Basic building data including building size, replacement cost, replacement time, and replacement quantities for embodied energy and carbon.

- Occupancy, including the distribution of people within the building envelope and the variability of this distribution over time, and the type and quantity of nonstructural components and contents present in the building.

- Vulnerable structural components and assemblies in sufficient detail to quantify their location within the building and the demands they will experience during response to earthquake shaking; their vulnerability to damage caused by earthquake-induced deformations and forces; and the consequences of this damage, in terms of collapse potential and generation of life-threatening debris, necessary repair actions, and influence on post-earthquake building occupancy due to unsafe placarding.

- Vulnerable nonstructural systems, components and contents in sufficient detail to quantify their location within the building and the demands they will experience during response to earthquake shaking; their method of installation as it effects their vulnerability to damage; and the consequences of this damage, in terms of generation of falling hazards and life-threatening debris, necessary repair actions, and influence on post-earthquake building occupancy.

The building performance model includes population models, fragility groups, and performance groups. Components and assemblies that provide measurable resistance to deformation are classified as structural whether or not they are intended to be part of the gravity or seismic-force-resisting

> The building performance model is an organized collection of all data necessary to define the building assets at risk.

systems. Elements and components that are vulnerable to damage are assigned a fragility specification within the building performance model. Fragility specifications include information on component damage states, fragility functions, and consequence functions. Elements and components that are not vulnerable to damage (i.e., rugged) are not included in the performance model, although the costs and environmental impacts associated with these elements must be considered in the total building replacement evaluation. These concepts are described in the sections that follow.

3.2 Basic Building Data

Basic building data includes:

- the number of stories, story height, floor area at each level; and

- the total replacement cost, core and shell replacement cost, replacement time, replacement quantities for embodied energy and carbon, and total loss threshold.

Figure 3-1 defines the floor level and story designation numbering system used in the building performance model. A floor level and the story immediately above it are always assigned the same number. Building roofs are designated Floor $N+1$, where N is the total number of vulnerable stories. In the figure, Floor 1 is assigned to the ground floor, which would be consistent with an assumption that the basement levels and the associated contents below grade are rugged. If significant damage and loss can occur in the basement levels, floor numbering should initiate at the lowest vulnerable level.
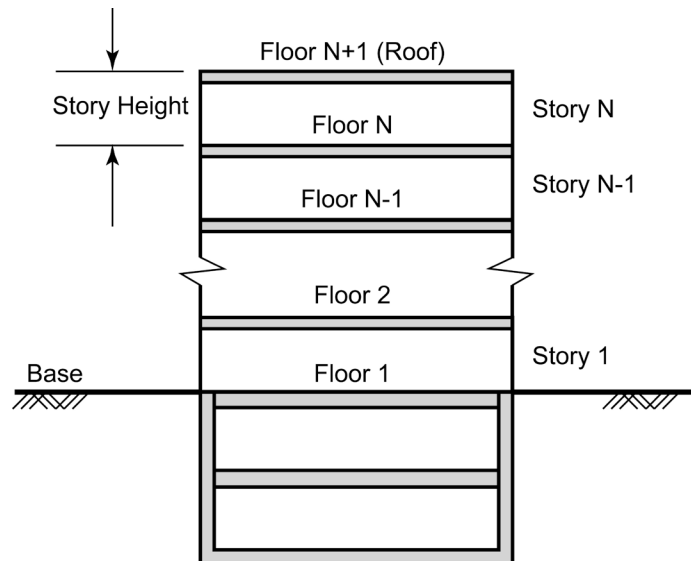
Figure 3-1   Definition of floor number, story number, and story height.

Replacement cost, replacement time, and replacement quantities for embodied energy and carbon are used to compute impacts associated with damage that renders a building irreparable. This occurs when the total cost of repairing all damaged components and systems exceeds a threshold value, when the residual story drift ratio exceeds a level that is considered practicable to repair, or when collapse occurs. Core and shell replacement cost includes replacement of the basic building structure, exterior enclosure, and mechanical, electrical, and plumbing infrastructure that is typically present in a building before tenant improvements are made. Total replacement cost includes replacement of the core, shell, and all tenant improvements and contents.

In order to replace a damaged building, it is necessary to demolish the building and remove it from the site. Therefore, replacement cost and replacement quantities for embodied energy and carbon should include the cost and energy and carbon released when demolishing the damaged building and clearing the site of debris in addition to replacing the building "in-kind." Demolition and site clearance can increase building replacement costs by as much as to 20% to 30%.

The total loss threshold is used to set a pre-determined cap on the level of repair effort. At the total loss threshold, a building is likely to be replaced rather than repaired. FEMA uses a threshold value of 50% when contemplating whether a damaged structure should be replaced or repaired. Past studies suggest that many owners elect to replace buildings when the projected repair costs exceed about 40% of the replacement cost. Many factors, including the age of a building, occupancy, status as a historic landmark, the economic health of the surrounding neighborhood, and individual profitability affect this decision.

> Past studies suggest that 40% of the replacement cost is a reasonable total loss threshold for many buildings.

The total loss threshold for carbon emissions replacement can be estimated by multiplying the total replacement cost by the appropriate construction sector impacts for global warming potential, from the Economic Input-Output Life Cycle Assessment (EIO LCA) database (Carnegie Mellon University Green Design Institute, 2008).

The total loss threshold for the embodied energy replacement can be estimated by multiplying the total replacement cost by the appropriate construction sector impacts from the EIO LCA database using the Energy category.

3.3 Occupancy

As used in this methodology, occupancy categorizes the primary use of a building or portion of a building. In the building performance model, occupancy is used to:

- establish a population model (i.e., the number of people present at different times of the day and different days of the year) for use in assessing potential casualties; and

- determine the type and quantity of nonstructural components and contents in a building, on an approximate basis, without the need for a building-specific inventory.

Population models and component inventories are provided for the following occupancies:

- Commercial Office

- Education (K-12) – typical elementary, middle school, and high school classrooms

- Healthcare – general in-patient hospitals; medical equipment excluded

- Hospitality – hotels and motels

- Multi-Unit Residential – apartments; also applicable to single-family detached housing

- Research Laboratories – special purpose laboratory equipment excluded

- Retail – shopping malls and department stores

- Warehouse – inventory excluded

It is possible to create building-specific inventories of nonstructural components for occupancies not covered by this list. Adaptive use of provided occupancy information will facilitate building performance modeling.

3.4 Population Models

Building population models define the number of people present per 1,000 square feet of building floor area. Population models include a definition of the peak population, which is the number of people likely to be present at times of peak occupancy, and the fraction of this peak population likely to be present at other times characterized by:

- time of day;

- day of the week (weekday or weekend); and

- month of the year.

Population patterns vary with time of day (e.g., hours of operation, lunch time fluctuations), and day of week (weekdays versus weekends). Variation by month is used to characterize the effects of holidays. Rather than designating specific days as holidays, population models prorate weekday populations considering the number of holidays per month and the total number of weekdays, on average, for that month.

Default values for peak population are provided in Table 3-1, along with the time of day during which peak populations are expected to occur. Figure 3-2 shows an example of the time-dependent variation in population, as a percentage of peak population, for commercial office occupancies over a 24-hour period. Population models for each occupancy are provided in Appendix E.

Population models also include an equivalent continuous occupancy (ECO), which is a time-weighted average population theoretically occupying a building on a continual basis. It represents the number of persons present, on average, throughout the year, considering all times of day and days of the week.

Table 3-1   Recommended Default Values of Peak Population by Occupancy

Occupancy	Peak Population Values (per 1000 sq. ft.)	Peak Population Time of Day
Commercial Office	4.0	Daytime (3 pm)
Education (K-12): Elementary Schools	14.0	Daytime
Education (K-12): Middle Schools	14.0	Daytime
Education (K-12): High Schools	12.0	Daytime
Healthcare	5.0	Daytime (3 pm)
Hospitality	2.5	Nighttime (3 am)
Multi-Unit Residential	3.1	Nighttime (3 am)
Research Laboratories	3.0	Daytime (3 pm)
Retail	6.0	Daytime (5 pm)
Warehouse	1.0	Daytime (3 pm)
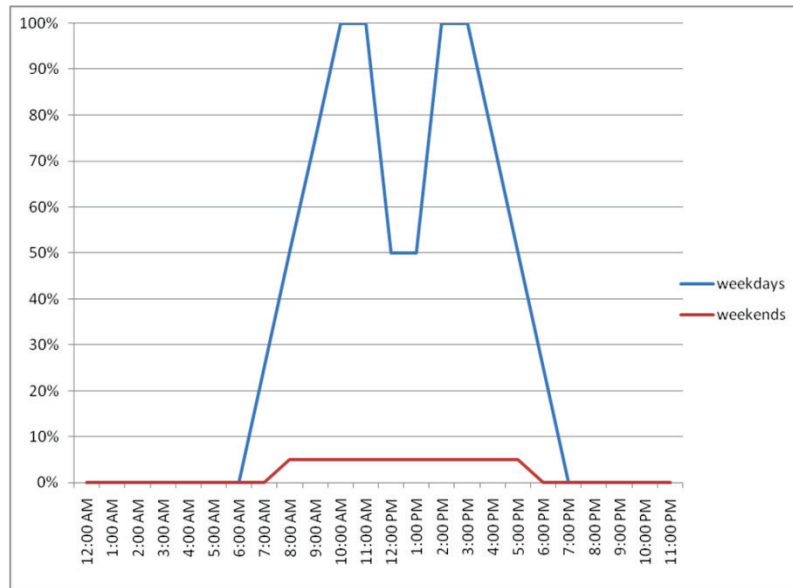
Figure 3-2   Plot of default variation in population (relative to expected peak population) by time of day for Commercial Office occupancies.

Peak population models can be used to generate "worst-case" estimates of casualties, considering earthquakes that occur at times of peak occupancy. This can be useful for evaluating the potential number of casualties in buildings with large populations that are present when the building is occupied, but full occupancy happens only occasionally (e.g., auditoriums, stadiums, and similar buildings). Equivalent continuous occupancy models enable rapid estimation of mean casualties, considering earthquake occurrence that is random in time, but use of equivalent continuous occupancy reduces the apparent dispersion in casualty estimates. Point-in-time population models can be used to develop a better understanding of the uncertainty in casualties associated with time, but it is necessary to perform a large number of realizations (on the order of several thousand) to do this in a meaningful way.

3.5   Fragility and Performance Groups

All vulnerable structural components, nonstructural components, and contents are categorized into fragility groups and performance groups. The quantity of components and contents within a building and within each performance group can be determined from a building-specific inventory. Alternatively, quantities can be assigned based on typical quantities (i.e., normative quantities) found in buildings of similar occupancy and size.

Fragility and consequence data have been collected and provided for common structural and nonstructural components found in typical buildings

and occupancies. A summary list of fragility groups available for identifying and defining the vulnerable components and contents in a building is presented in Appendix D.

Complete fragility and consequence information is contained in fragility specifications comprising the *Fragility Database*. This database is referenced by the companion *Performance Assessment Calculation Tool* (PACT), and is provided as part of *Volume 3 – Supporting Electronic Materials and Background Documentation*.

3.5.1 Fragility Groups

A fragility group is a collection of components, or assemblies, all of which have similar:

- construction characteristics, including details of construction, details of manufacture, and installation techniques;

- potential modes of damage;

- probability of incurring these damage modes, when subjected to earthquake demands; and

- potential consequences resulting from damage.

A fragility group can comprise individual components (e.g., pendant light fixtures), or assemblies of components (e.g., interior fixed partitions including metal studs, gypsum board sheathing, and wall coverings).

Components and assemblies that are of similar, but not identical, construction may need to be assigned to different fragility groups to properly characterize their susceptibility to damage and the consequences of that damage. For example, interior partitions throughout a building could be assigned to the same fragility group if they are all the same height, they are all installed in the same manner, and they all have the same finish. However, if some of the partitions are fixed and some are installed with slip tracks to permit movement, each would have different susceptibility to damage under the same earthquake shaking, and should be assigned to different fragility groups. Similarly, partitions with ceramic tile finishes would cost more to repair than walls with simple painted finishes, and should be assigned to different fragility groups.

Each fragility group is identified by a unique classification number based on recommendations contained in NISTIR 6389, *UNIFORMAT II Elemental Classification for Building Specifications, Cost Estimating and Cost Analysis* (NIST, 1999). Fragility classification numbers take the alpha-numeric form:

> A fragility group is a collection of similar components or systems with the same damageability and consequences of damage.

> Fragility groups are identified using a classification system based on UNIFORMAT II described in NISTIR 6389.

A1234.567. The first letter in the classification system indicates the overall component category, taken as one of the following:

- A – Substructure

- B – Shell

- C – Interiors

- D – Services

- E – Equipment and furnishings

- F – Special construction and demolition

The first two numbers provide the next categorization. For instance, B10 represents superstructure components while B20 represents exterior enclosures. The next two numbers identify a unique component. For example, the classification number B1044 identifies superstructure components that are reinforced concrete shear walls. The numbers after the decimal identify variations in the basic component, and are used to identify different configurations, conditions of installation, material quantities, repair actions, demand levels, and other attributes.

Table 3-2 lists a sample set of fragility groups that could be used in the building performance model for a hypothetical two-story, steel frame office building. The table includes a NISTIR fragility classification number, a description of the basic component, and the predictive demand parameter used to assess damage.

Table 3-2   Example Fragility Groups for a Two-Story Steel Frame Office Building

Fragility Classification Number	Description	Demand Parameter
B1035.001	Structural steel moment connections	Story drift ratio parallel to frame
B2022.001	Exterior curtain walls	Story drift ratio parallel to wall
C1011.001	Interior wall partitions	Story drift ratio parallel to wall
C3032.001	Suspended ceilings	Floor acceleration
D1014.011	Traction elevators	Peak ground acceleration
D3031.000	Chillers	Floor acceleration
E2022.001	Modular office workstations	Floor acceleration
E2022.112	Filing cabinets	Floor velocity

The fragility groups listed in Table 3-2 are at an elementary level. Each group typically includes a number of additional decimal subgroups assigned as necessary to identify differences between components in the group. For example, the fragility group D3031.000 associated with chillers includes D3031.011a, identifying 100-ton chillers installed without seismic anchorage and no vibration isolation, and D3031.013k, identifying 1000-ton chillers installed with seismic anchorage and vibration isolation.

Provided fragility information can be modified, and user-defined fragility groups can be developed to suit the needs of a specific building. When a new fragility group is created, or an existing fragility group is modified, a new NISTIR fragility classification number must be assigned to the new group. The following logic is recommended for establishing fragility groups when the provided information is not adequate to define the assets at risk in a particular building:

1. **Identify the components that are likely to suffer damage and contribute to potential losses.** Components that should be considered include those that can be damaged by building response to earthquake shaking, and those that will also have a measurable impact on consequences in the event that they become damaged. Components that are not subject to significant damage for credible levels of demand (i.e., rugged) need not be considered. For example, in a steel frame building, floor beams that are not part of the seismic-force-resisting system typically will not be damaged by earthquake shaking, and generally need not be included in the building performance model. Also, some nonstructural components (e.g., toilet fixtures) can often be neglected as they are generally not damaged by earthquake shaking.

   Some components may not be damaged by earthquake shaking directly, but can be affected by damage (or repairs) to other components. For example, a conduit embedded in an interior partition is inherently rugged. However, if the partition is sufficiently damaged to require complete replacement, it will become necessary to replace the conduit. In this case, the wall (not the conduit) is the component defining the fragility group, but the conduit is considered in determining the consequences of damage to the wall.

2. **Group components into logical sets considering normal design and construction practices and specification sections**. Interior partitions, for example, are constructed using a series of individual components including cold-formed steel framing, gypsum wallboard, fasteners, drywall tape, plaster, and paint. Since these items have both a design and construction relationship, and tend to be damaged as an assembly, they

can be included as a common assembly in a single fragility group. When components are grouped together as an assembly, changes to the design or construction of one component (e.g., the manner in which the studs are attached to the floors above and below) will likely affect the damageability of the entire assembly. Also, repair of damage to one component in the assembly is likely to involve work on other components in the assembly.

3. **Group components such that all components in the group are damaged by a single demand parameter.** The probability that a component (or collection of components) will become damaged must be tied to a single demand parameter (e.g., story drift ratio, floor acceleration, floor velocity, or plastic rotation). Damage to all components in a fragility group is assumed to be dependent on the same demand parameter for all possible damage states. However, not all components in a fragility group are required to experience the same level of demand. Interior partitions in one story of a building might be assigned to the same fragility group as those in other stories, but drift ratios will likely be different in each story.

4. **Group components such that fragilities, damage states, and consequence functions are logical for monitoring and repair.** All components in a fragility group should have similar damage states and similar consequences associated with that damage. For example, interior partitions and exterior curtain walls should be placed in different fragility groups because they are likely to have different types of damage, be damaged at different levels of drift, and require different repair actions necessary to restore components to their pre-earthquake condition.

3.5.2 Performance Groups

Performance groups are a sub-categorization of fragility groups. A performance group is a subset of fragility group components that are subjected to the same earthquake demands (e.g., story drift, floor acceleration, or velocity, in a particular direction, at a particular floor level). Figure 3-3 illustrates the concept of performance groups for a three-story reinforced concrete office structure.

Most performance groups are organized by story level (1st through 3rd) and direction (N-S and E-W) because a common predictive demand parameter is story drift ratio parallel to component orientation, and drift ratios would be expected to be different at each level. As depicted in the figure, N-S shear walls comprise one performance group in the first story, and N-S shear walls comprise a different performance group in the second story, even though

they are part of the same reinforced concrete shear wall fragility group, B1044.001. Similar organization is used for curtain wall and glazing performance groups.

Figure 3-3   Example performance groups for a three-story office building.

For acceleration-sensitive components such as contents, performance groups are assigned independent of direction because the predictive demand parameter is peak floor acceleration. Contents at the first, second, and third stories would each be assigned to unique performance groups because of expected differences in floor acceleration at each level. Other components that use floor acceleration as a predictive demand parameter include ceiling systems, piping systems, ductwork, and mechanical equipment.

In the building performance model, it is important to differentiate between the level at which demands are imparted to a component, and the level at which impacts will occur if the component experiences damage. In the case of suspended components (e.g., ceilings, piping, ductwork, and pendant light fixtures), acceleration demands are imparted by the floor level from which they are suspended. However, if these components fail, consequences will occur in the floor level below. In this methodology, suspended components are assigned to the floor level that is impacted by their failure (i.e., the level below). In the building performance model, special flags are used to identify that earthquake demands on such components are associated with the floor (or roof) level above the assigned level.

3.5.3 Normative Quantities

Quantities of vulnerable components and contents within a building must be specified in the building performance model. This can be determined from a building-specific inventory using design drawings (e.g., structural, architectural, mechanical, electrical, and plumbing); however, this level of detail is not typically known until late in the design process, and also is subject to change over the years.

> Normative quantities are an estimate of the quantity of nonstructural components and contents likely to be present in a building of a specific occupancy on a gross square foot (gsf) basis.

Structural quantities can be estimated based on preliminary structural designs. Quantities of nonstructural component and contents can be estimated based on typical quantities (i.e., normative quantities) found in buildings of similar occupancy and size. Normative quantities are an estimate of the quantity of components and contents likely to be present in a building of a specific occupancy on a gross square foot (gsf) basis. Databases of normative quantities are available that can be used to determine the type and total number of components that would be present in typical buildings of a certain size, which can then be used to populate the building performance model.

Normative quantity data have been developed based on a detailed analysis of approximately 3,000 buildings across typical occupancies. These data allow for estimation of quantities at the 10th, 50th, and 90th percentile levels, which enables consideration of the likely differences in quantities found in individual buildings. An example of normative quantity information provided for healthcare occupancies is shown in Table 3-3.

Table 3-3   Sample Normative Quantities for Healthcare Occupancies

Component Type	Unit of Measurement	10th Percentile Quantity	50th Percentile Quantity	90th Percentile Quantity
Gross area	SF	20,000	127,700	1,515,000
Volume	CF per 1 gsf	13.000	15.750	18.000
Cladding				
Windows or glazing area	100 SF per 1 gsf	4.0E-04	1.4E-03	3.1E-03
Interior partition length	100 LF per 1 gsf	7.5E-04	1.1E-03	1.4E-03
Ceilings				
Ceiling - lay in tile percentage	%	N/A	80%	N/A
Ceiling - gypsum board percentage	%	N/A	8%	N/A
Stairs	FL per 1 gsf	7.0E-05	8.0E-05	1.0E-04
Elevators	EA per 1 gsf	1.2E-05	2.8E-05	9.8E-05

Component Type	Unit of Measurement	10th Percentile Quantity	50th Percentile Quantity	90th Percentile Quantity
Plumbing				
Cold domestic water piping - 2½ inch diameter or smaller	1,000 LF per 1 gsf	8.0E-05	1.1E-04	1.3E-04
Gas supply piping	1,000 LF per 1 gsf	5.0E-06	1.0E-05	1.5E-05
HVAC				
Chiller capacity	TN per 1 gsf	2.9E-03	3.3E-03	3.7E-03
Boiler capacity	BTU per 1 gsf	40.000	50.000	65.000
Air handling units	CFM per 1 gsf	0.800	1.000	1.250
HVAC ducts – less than 6 sq. ft.	1,000 LF per 1 gsf	5.0E-05	7.5E-05	9.0E-05
HVAC in-line drops and diffusers	EA per 1 gsf	1.6E-02	2.0E-02	2.2E-02
Electrical				
Electrical distribution – conduits	LF per 1 gsf	3.0E-01	5.0E-01	6.0E-01
Standby generators	KVA per 1 gsf	3.5E-03	5.0E-03	1.5E-02
Fire protection				
Sprinkler piping	20 LF per 1 gsf	1.0E-02	1.1E-02	1.3E-02
Sprinkler drops	EA per 1 gsf	1.0E-02	1.2E-02	1.4E-02

Typically, 50th percentile values are appropriate for estimating quantities for most buildings. When more specific information is known about a building under consideration, 10th percentile or 90th percentile values can be selected, as appropriate.

A complete tabulation of normative quantity information provided for all occupancies covered by the methodology is provided in Appendix F. In addition, a companion *Normative Quantity Estimation Tool*, which is an Excel workbook designed to assist in estimating quantities of components and contents for building performance modeling, is provided as part of *Volume 3 – Supporting Electronic Materials and Background Documentation*.

Quantities associated with certain occupancy-specific tenant-furnished equipment and contents are not reliably estimated by normative quantities and have not been included. In the case of healthcare occupancies, for example, normative quantity information for hospital imaging equipment, surgical devices, and specialty lighting are not provided. Quantities for such

occupancy-specific items, along with the related fragility and consequence data, must be developed on a user-defined basis.

3.5.4 Fragility Units of Measure

It is necessary to identify the quantity of components in each performance group in meaningful units of measure. This methodology uses units of measure that logically relate to computation of damage and consequences for components in a performance group. Large distinct components like elevators, air handlers, and beam-column moment connections are measured in individual units (i.e., "each"). However, other components have different units of measure. For example, low aspect ratio shear walls (aspect ratios less than 1:1) are measured in units of $H \times H$ panels, where H is the height of the panel, because damage in walls can be logically segregated into panels of this size. Sprinkler piping is measured in units of thousands of lineal feet because historically, when leaks have occurred in such systems, a leak rate of 1 per 1,000 feet was commonly observed. The units of measure associated with a particular fragility group are defined in the fragility specifications comprising the *Fragility Database*.

The quantity of components in a performance group is determined by the total number of components present in a building divided by the fragility unit of measure. In the case of interior partitions, for example, the fragility unit of measure is 100 lineal feet, meaning partition quantities are expressed in units of 100 LF. Thus, for an office building that might have 2,000 lineal feet of interior partitions on a given floor oriented in a given direction, the quantity associated with the resulting performance group is $2,000/100 = 20$ units of 100-foot segments of wall partition.

3.5.5 Rugged Components

Rugged components are not vulnerable to damage, or have a very high threshold for damage given the levels of demand likely to be experienced in a building due to earthquake shaking. Because they are not considered damageable, rugged components are not expected to contribute to performance impacts. However, in the case of total building loss or collapse, replacement of rugged components must be included in the building replacement cost and replacement time estimates.

Components that are not included in the building performance model are essentially considered rugged for the purposes of that assessment. Similarly, components that are not expected to contribute to losses in a specific building can be deemed "rugged," and intentionally omitted from the building

> Units of measure are associated with components in a fragility group for the purposes of estimating consequences and damage. Components can be defined in individual units of "each," units of lineal feet (e.g., 1000 LF), units of square feet (e.g., 250 SF), or other units.

performance model. Appendix I provides a list of component types that, in most cases, can be considered rugged for most performance assessments.

3.6 Damage States

Building and component damage generally occurs as a continuum, with the scope and extent of damage increasing as demand increases. Rather than using a continuous range of possible damage states, each fragility group is assigned a series of discreet damage states to characterize the different levels of damage that can occur. Each damage state is associated with a unique set of consequences consisting of:

> Damage is characterized as a series of discrete damage states representing the different levels of possible damage.

- a unique probable repair action, with associated repair cost, repair time, and embodied energy and carbon consequences;

- a unique potential for unsafe placarding;

- a unique potential effect on the number of casualties; or

- any combination of the above.

Each damage state represents a unique set of consequences considering these performance measures. Not all damage states will contribute significantly to all types of consequences. A damage state that is important for one performance measure (e.g., repair costs) may not be equally important for other performance measures (e.g. casualties).

Considering a hypothetical exterior cladding component, meaningful damage states could include:

- Cracking of sealant joints, permitting moisture or air intrusion. Over the long term, this type of damage will present building maintenance issues and will require repair (e.g., sealant joint replacement), but it will not have consequences related to casualties, unsafe placarding, or long lead times. Consequences of this damage state will likely include limited repair costs and relatively short repair times.

- Visible cracking of the panels. This type of damage is unsightly, and will require repair in the form of removal and replacement of damaged panels, but is also not expected to impact casualties, unsafe placarding, or long lead times. This damage state will likely have more severe cost and embodied energy and carbon consequences and will result in a longer repair times.

- Panel connection failure and loss of panels from the building envelope. This damage will require replacement of missing panels and repair to significantly damaged panels. It can also have potential casualty impacts

due to falling hazards, and may have unsafe placarding impacts due to concerns over whether the building is safe to occupy. This damage state will have the most severe cost, repair time, and embodied energy and carbon consequences, and could also have casualty consequences and unsafe placarding consequences. (Note: the methodology, as developed, only tracks casualties within the building envelope, but could be expanded to consider falling hazards outside the building envelope.)

3.6.1 Damage Logic

For a particular component type, damage states must consider the relationship with other potential damage states. Possible logical relationships between damage states include:

- **Sequential.** Sequential damage states must occur in sequential order, with one state occurring before another is possible. Sequential damage states represent a progression to higher levels of damage as demand increases. Generally, as damage moves from one state to the next, more serious consequences accrue. In the case of a concrete component controlled by flexure, for example, damage states might include: (1) hairline cracking repaired with simple patching and painting; (2) large cracks requiring epoxy injection; and (3) spalling of concrete and buckling of reinforcement requiring replacement of damaged concrete and buckled reinforcing bars.

- **Mutually exclusive.** Mutually exclusive damage states exist when the occurrence of one damage state precludes the occurrence of another damage state. Each mutually exclusive damage state must have a conditional probability of occurrence, given that the component is damaged. In the case of the previous concrete example, the component might reach a level of demand at which: (1) the flexural cracks lengthen and widen (80% chance); or (2) the behavior transitions to shear-controlled, with the formation of more serious shear cracking (20% chance). The probabilities for all mutually exclusive damage states must sum to 100%.

- **Simultaneous.** Simultaneous damage states are independent and unrelated in that they can occur, but need necessarily occur, at the same time. Each simultaneous damage state is assigned a conditional probability of occurrence, given that the component is damaged. The sum of the probabilities for all simultaneous damage states will generally exceed 100%, as some damage states will occur at the same time. Elevators are an example of components with simultaneous damage states. Damage can consist of one or more conditions, each with its own

> When a fragility group has more than one damage state, damage states can be sequential, mutually exclusive, or simultaneous.

independent probability of occurrence, and each with the ability to render an elevator inoperable. For a typical traction elevator, examples include: damaged control or machinery (26% chance); damaged counterweights, rails, or guide shoes (79% chance); damaged stabilizers, cab walls, or cab doors (68% chance), and damage to the cab ceiling (17% chance).

3.6.2 Damage Correlation

Individual performance groups can be designated as having either correlated or uncorrelated damage. Correlated damage means that all components within a performance group will always have the same damage state. If a performance group is designated as uncorrelated, then each component in a performance group can have a different damage state.

> Performance groups can be identified as having correlated or uncorrelated damage. Use of correlated damage significantly reduces computational effort and time but understates the potential dispersion in performance.

Correlation of damage states can be used for conditions in which failure of one component will necessarily require simultaneous failure of all components within the performance group. One such example is a series of identical braced frames, within a single line of resistance, in a given story. If lateral deformation of the line of braces is sufficient to induce buckling in one brace, it is likely that all braces in the line will simultaneously buckle as forces redistribute to adjacent braces, triggering additional buckling to occur.

Identical braces on separate lines of resistance, however, will likely exhibit uncorrelated behavior. Because the lateral deformation along different lines of framing will likely be different, each line will have a different potential for buckling behavior. To account for this behavior, it is possible assign separate performance groups to each line of bracing, and then designate the brace components within each performance group as correlated.

Use of correlated damage states results in reduced computational effort in the performance calculation process, as it is only necessary to identify a single damage state for each performance group. In the case of uncorrelated damage states, it is necessary to determine a unique damage state for each component in the group, significantly increasing computational effort. In reality, most building components will not have perfectly correlated behavior. Use of correlated damage states when the damage is not actually correlated is not expected to significantly affect mean estimates of performance impacts, but it can significantly affect the resulting dispersion in results.

If the probability of incurring unsafe placarding is an important consequence, correlated damage states should not be used unless there is reason to believe that damage occurrence is actually correlated within a performance group. This is because the probability of incurring an unsafe placard is triggered

based on the percentage of components that are damaged. If a correlated assumption is used, then a higher number of components will be deemed damaged, and the number of realizations that reach the unsafe placard triggering threshold will be overstated, resulting in unrealistically high probabilities for unsafe placarding.

3.7   Demand Parameters

Story drift ratio, floor acceleration, and floor velocity are most typically assigned to fragility groups; however, other demand parameters can be used.

Although actual damage can occur as a result of complex relationships between damageability and component demands of various types, in this methodology, the occurrence of all damage states within a fragility group is predicted by a single demand parameter. The demand parameter assigned to a fragility group is the one that best predicts the occurrence of the potential damage states with the least amount of uncertainty. For most structural systems (e.g., shear walls, braced frames, steel and concrete moment frames), and for many nonstructural components, story drift ratio has been selected as the best indicator of potential damageability. Floor acceleration and floor velocity are also commonly used. When considered appropriate or necessary, it is possible to use other demand parameters (e.g., plastic rotations, axial forces, or other local component actions).

Since most buildings include drift-sensitive components that generally align with principal orthogonal axes of the building, drift ratios in each direction are necessary to calculate performance impacts. In most cases, failure modes related to acceleration or velocity (e.g., failure of equipment base anchorage, or sliding of unanchored contents) are insensitive to the direction of the applied demand. In some cases, such as tall book cases, failure modes may be sensitive to directionality, but it may be difficult to determine the actual orientation of such objects with respect to the building axes. For these reasons, peak values of floor acceleration or floor velocity (independent of direction) are used to calculate performance impacts.

This methodology estimates maximum peak floor acceleration and velocity by multiplying maximum values obtained from analysis by a factor of 1.2. This factor is an approximation that accounts for vector summation effects, but acknowledges that the peak value of acceleration (or velocity) is unlikely to occur simultaneously along the two building axes. It is possible to change this factor, and it is possible to designate acceleration- and velocity-sensitive performance groups as sensitive to a particular direction, if the orientation of the components is known.

3.8 Component Fragility

3.8.1 Fragility Functions

The type and extent of damage that a component will experience is uncertain. Component fragility functions are statistical distributions that indicate the conditional probability of incurring damage at a given value of demand. Fragility functions are assumed to be lognormal distributions. A unique fragility function is required for each sequential damage state, and for each group of mutually exclusive or simultaneous damage states.

Figure 3-4 shows a representative family of sequential fragility functions (i.e., fragility curves) for a reduced beam section (RBS) special steel moment frame beam-column connection. For this fragility group, three damage states are defined:

- **Damage State DS1.** Beam flange and web local buckling requiring heat straightening of the buckled region.

- **Damage State DS2.** Lateral-torsional distortion of the beam in the hinge region requiring partial replacement of the beam flange and web, and corresponding work on adjacent structural and nonstructural components.

- **Damage State DS3.** Low-cycle fatigue fracture of the beam flanges in the hinge region requiring replacement of a large section of the beam in the fractured region, and corresponding work on adjacent structural and nonstructural components.

The fragility function for each damage state is defined by a median demand value, θ, at which there is a 50% chance that the damage state will initiate, and a dispersion, β, which indicates uncertainty that the damage state will initiate at this value of demand. If a large number of components are subjected to demand, θ, and the performance of these components is uncorrelated, half of the components will experience this damage state, and half will not.

Dispersion is associated solely with uncertainty in the onset of damage as a function of demand, and is independent of uncertainty associated with the intensity of shaking or the prediction of demand. Dispersion reflects uncertainty associated with variability in construction and material quality, the level of knowledge regarding the likely behavior of a component subjected to a specified value of demand, and the extent to which the occurrence of damage can be predicted by a single demand parameter. As the value of β increases, the shape of the curve flattens, indicating a wider

> Component fragility functions are distributions that indicate the conditional probability of incurring a damage state given a value of demand. This methodology assumes that fragility functions are lognormal distributions.

range of demands over which there is significant probability that the damage state will initiate.
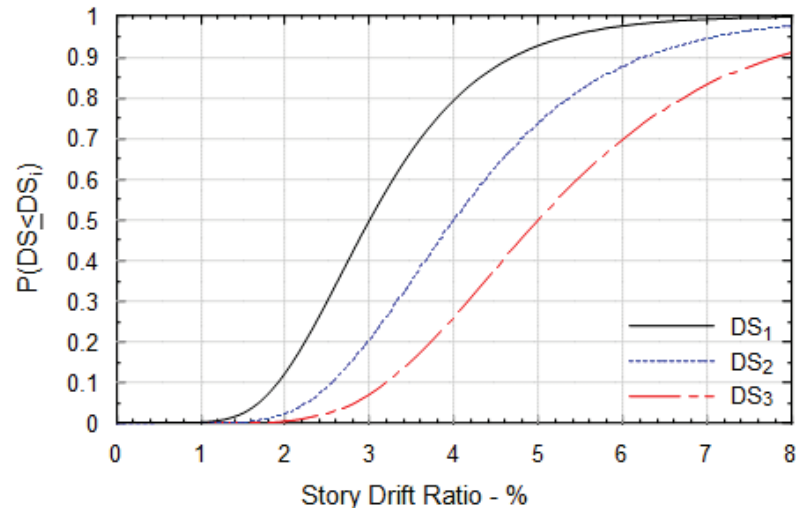
Figure 3-4   Example family of fragility curves for special steel moment frame beam-column connections.

For the damage states represented in Figure 3-4, median and dispersion values are: (1) $\theta = 3\%$ story drift ratio, $\beta = 0.35$ for DS1; (2) $\theta = 4\%$ story drift ratio, $\beta = 0.35$ for DS2; and (3) $\theta = 5\%$ story drift ratio, $\beta = 0.35$ for DS3. Therefore, at a story drift ratio of 4%:

* The probability that some damage will occur is equal to the probability that DS1 will initiate, which is 80%, since these damage states are sequential, and DS1 must occur before any of the other damage states can occur.

* The probability that no damage will occur is equal to the probability that neither DS1, DS2, nor DS3 will initiate, which is $1.00 - 0.80 = 20\%$.

* The probability that damage will be in any one damage state is equal to the difference between the probabilities associated with a given damage state and the next higher damage state. For DS1, this is $0.80 - 0.50 = 30\%$; for DS2 this is $0.5 - 0.26 = 24\%$, and for DS3, this is $0.26 - 0.0 = 26\%$.

For each realization in which collapse does not occur, fragility functions are used in conjunction with calculated demands to determine a damage state for each component. Collectively in a given realization, the set of damage states determined for all components in a building define the building damage state.

3.8.2 Fragility Development

Component fragility functions can be developed through laboratory testing, collection of earthquake experience data following damaging earthquakes, analysis, engineering judgment, or a combination of these methods. FEMA 461, *Interim Testing Protocols for Determining the Seismic Performance Characteristics of Structural and Nonstructural Components* (FEMA, 2007), provides recommended procedures for laboratory testing intended to develop fragility data. Appendix H provides quantitative procedures for developing the median, θ, and dispersion, β, for fragility functions based on various levels of available data:

> Component fragilities can be developed by laboratory testing, earthquake experience data, analysis, judgment, or a combination of these.

- **Actual Demand Data.** Data are available from a sufficient number of test specimens, and each tested specimen experienced the damage state of interest at a known value of demand.

- **Bounding Demand Data.** Test data or earthquake experience data are available from a sufficient number of specimens, but the damage state of interest only occurred in some specimens. For the other specimens, testing was terminated before the damage state of interest occurred, or the earthquake did not result in damage to the specimens. The maximum demand that each specimen was subjected to is known, but this maximum demand may not be the demand at which the damage state initiated.

- **Capable Demand Data.** Test data or earthquake experience data are available from a sufficient number of specimens, but the damage state of interest did not occur in any of the specimens. The maximum value of demand that each specimen was subjected to is known.

- **Derivation.** No data are available, but it is possible to model the behavior and analytically estimate the level of demand at which the damage state of interest will occur.

- **Expert Opinion.** No data are available and analysis of the behavior is not feasible, but one or more knowledgeable individuals can offer an opinion as to the level of demand at which damage is likely to occur, based on experience or engineering judgment.

3.8.3 Provided Fragility Functions

Each of the approaches identified in Section 3.8.2 were used in the development of fragility functions provided with the methodology. A summary list of available fragility functions is presented in Appendix D. Complete fragility information is contained in fragility specifications comprising the *Fragility Database*, provided as part of *Volume 3 –*

Supporting Electronic Materials and Background Documentation. Guidance on selecting appropriate fragilities from the list of provided fragilities, and assigning them within the building performance model, is provided in *Volume 2 – Implementation Guide.*

Fragility and consequence data have been developed for more than 700 common structural and nonstructural components and contents found in typical buildings and occupancies. Structural fragility functions cover the following common structural systems:

> **Over 700 fragilities have been developed and provided as part of this methodology.**

> **Second Edition Update**
> Fragility and consequence data have been updated. Refer to Appendix D for more details.

- Steel moment frames

- Steel concentrically braced frames

- Steel buckling-restrained braced frames

- Steel eccentrically braced frames

- Concrete moment frames

- Concrete shear walls

- Concrete link beams

- Concrete flat plates

- Masonry shear walls

- Cold-formed steel walls

- Light-framed wood walls

Fragility functions are also provided for the following common nonstructural systems and contents:

- Exterior wall construction

- Exterior glazing systems

- Roof tiles, masonry chimneys, and parapets

- Interior partitions

- Ceilings

- Stairs

- Elevators

- Mechanical equipment and distribution systems (e.g., chillers, cooling towers, air handling units, piping, and ducting)

- Electrical equipment and distribution systems (e.g., transformers, switchgear, distribution panels, battery racks, recessed lighting, and pendant lighting)

- Access floors, workstations, bookcases, filing cabinets, and storage racks

Provided structural and nonstructural fragilities capture the range of performance capability considering differences in vulnerability to damage. Variations include:

- Special versus ordinary system detailing requirements found in material design standards such as ANSI/AISC 341-16, *Seismic Provisions for Structural Steel Buildings* (AISC, 2016a), and ACI 318-14, *Building Code Requirements for Structural Concrete and Commentary* (ACI, 2014).

- Differences in behavior associated with configuration, such as steel braced frames with chevron, single diagonal, or X-brace configurations, moment frame connections with beams on one or both sides, and shear walls with slender or low aspect ratios.

- Differences in behavior associated with member properties, such as steel braced frames consisting of hollow structural section (HSS), wide flange (WF), and buckling-restrained braces (BRB).

- Designs using varying limit state assumptions, such as shear-controlled or flexure-controlled behaviors, moment frames with strong-column-weak-beam proportioning, and connections designed to develop the capacity of the members.

- Nonstructural systems and equipment installed with (or without) seismic bracing and anchorage.

The list of provided fragilities is further expanded to consider differences in consequences, especially those related to repair costs. Although damage states and repair actions for a specific fragility group might be identical, differences in cost associated with the size of a component, quantity of material, or finish quality are significant enough to warrant the development of additional fragility groups. Examples include variation in:

- Steel section weight and concrete member size

- Concrete and masonry wall thickness

- Concrete and masonry wall height

- Partition wall finishes

- Ceiling area

- Diameter of piping

- Cross-sectional area of ducting

- Capacity of equipment (e.g., tons of cooling capacity, cubic feet per minute of air flow, amps, or kilovolt-amperes)

3.8.4 Calculated Fragilities

> Some component types and damage modes require building-specific calculation of fragility parameters.

Some fragilities require building-specific calculation of fragility parameters for certain component types or damage states. Examples include fragilities related to mechanical equipment anchorage for which the possible modes of damage are known (e.g., anchorage failure), but the capacity must be determined for the specific case under consideration.

The following procedures can be used to estimate fragility parameters for components with failure modes that can be predicted using design formulations contained within industry standard design specifications, such as ACI 318-14, and ANSI/AISC 360-16, *Specification for Structural Steel Buildings* (AISC, 2016b). These procedures can also be used to develop calculation-based fragility parameters for components that lack experimental or experience data, but have failure modes that can be predicted using rational calculation procedures based on engineering mechanics. Procedures are based on the type of limit state associated with the damage, including:

- Strength-limited damage states

- Ductility-limited damage states

- Displacement-limited damage states

- Code-based limit states

- Overturning limit states (for unanchored components)

- Sliding limit states (for unanchored components)

Strength-Limited Damage States

An obvious damage state for many components is the limit of essentially elastic behavior. This procedure is applicable to the calculation of fragility parameters based on the component design strength, ϕR_n, determined in accordance with an appropriate industry design standard. For ductile behavior modes (e.g., flexure), the median strength is determined as:

$$\theta_{ductile} = C_q e^{(2.054\beta)} \phi R_n \tag{3-1}$$

For brittle failure modes, the median strength is determined as:

$$\theta_{brittle} = C_q e^{(2.81\beta)} \phi R_n \tag{3-2}$$

where the dispersion, β, and coefficient, C_q, are determined as described below.

The total dispersion, β, is a function of the uncertainty in the ability of a design equation to predict the actual failure demand, β_D, dispersion in material strength, β_M, and uncertainties associated with construction quality, β_C. The total dispersion is computed as:

$$\beta = \sqrt{\beta_D^2 + \beta_M^2 + \beta_C^2} \tag{3-3}$$

Design equations for brittle failure modes have higher inherent uncertainty than equations for ductile failure modes. For ductile failure modes that are well-predicted by classical methods of engineering mechanics (e.g., yield strength of a prismatic member loaded in flexure), a design uncertainty of $\beta_D = 0.05$ is recommended. For ductile failure modes with more complex behavioral characteristics (e.g., elastic buckling of a bar), a larger value of $\beta_D = 0.10$ is recommended.

For brittle failure modes (e.g., tensile failure of a wood post, shear failure of lightly reinforced concrete, and crushing failure of masonry or concrete), higher values of design uncertainty are recommended. Values can be obtained from the commentary underlying the applicable design standard, or from the fundamental research upon which it was based. Alternatively, a default value for brittle failure modes can be taken as $\beta_D = 0.25$.

Material strength variability is a function of the material itself. In relative terms, wood tends to have higher variability than concrete due to ambiguity associated with grading procedures and non-uniformity in individual pieces of wood. Some grades of steel (e.g., ASTM A992) have relatively low material variability, while other grades (e.g., ASTM A36) can have material variability on the order of concrete. Values for dispersion in material strength can be obtained from industry data. Alternatively, default values from Table 3-4 can be used.

Uncertainty associated with construction quality is based on consideration of the sensitivity of a particular behavior mode to the level of quality control that is provided during construction. For example, the strength of a post-installed expansion anchor will be sensitive to the quality of installation in terms of hole size and tightening torque. Other behaviors might not be as sensitive to construction quality. Table 3-5 provides recommended values for uncertainty associated with construction quality, β_C.

Table 3-4   Default Values of Dispersion, β_M, Associated with Material Strength

Material	Description	Dispersion, β_M
Steel	ASTM A36[1]	0.15
	All grades except ASTM A36	0.10
Concrete	Ready-mix conforming to ASTM C94[2]	0.12
	Other – based on cylinder test results	0.20 [3]
Wood	Machine-stress graded	0.12
	Visually graded	0.20
	Ungraded	0.30
Masonry	Engineered concrete or brick masonry conforming to TMS 402 [4]	0.15
	Other masonry	0.25

Notes: [1]   *Standard Specification for Carbon Structural Steel* (ASTM, 2012).
[2]   *Standard Specification for Ready-Mixed Concrete* (ASTM, 2013).
[3] β_M can be taken as the coefficient of variation (COV) obtained from cylinder test results. Alternatively, a default value of 0.2 can be used.
[4]   *Building Code Requirements and Specification for Masonry Structures* (TMS, 2016).

Table 3-5   Default Values of Uncertainty, β_C, Associated with Construction Quality

Sensitivity to Construction Quality	Degree of Construction Quality Control		
	Very Good	**Average**	**Low**
Low	0	0	0
Moderate	0	0.10	0.15
High	0	0.15	0.25

Coefficient, C_q, further adjusts the value of median strength based on the sensitivity of the behavior mode to construction quality. In most cases, the value of C_q can be taken as unity. However, in some cases a lesser value is warranted. Alternate values of C_q are established based on judgment, and should be used in cases where potential variations in capacity are extremely sensitive to construction quality, and the actual condition of the construction is not known. For example, in the case of post-installed expansion anchors, where it is uncertain as to whether or not the anchors have been properly set, an alternate value C_q should be considered. For tension loading, one possible value could be 0.5, representing the average between 1.0 for a proper installation (i.e., full tension capacity) and 0.0 for an improper installation (i.e., no tension capacity).

Ductility-Limited Damage States

Some damage states in ductile components will initiate when inelastic deformation reaches a particular ductility level. Without appropriate test data to characterize the ductility at which a particular damage state occurs, estimates of this threshold should be considered highly uncertain. When appropriate test data are not available, the following procedure can be used to characterize ductility-limited damage states:

1. Calculate the median value and dispersion for the elastic limit of the component (i.e., onset of yield), using the procedures for strength-limited damage states.

2. Calculate the median deformation of the component, δ_y, at the onset of yield, using elastic deformation analysis under the applied median yield load.

3. Judgmentally classify the behavior mode as one of "limited ductility" associated with $\mu = 2$, "moderate ductility" associated with $\mu = 4$, or "high ductility" associated with $\mu = 6$, where μ is the presumed ratio between the deformation at the onset of the damage state to the deformation at onset of yield.

4. Calculate the median displacement demand for the onset of the damage state as $\theta = \mu\delta_y$.

5. Calculate the dispersion, β, for the damage state as:

$$\beta = \sqrt{\beta_1^2 + 0.16} \leq 0.6 \qquad (3\text{-}4)$$

where β_1 is the dispersion associated with the onset of yield, calculated using the procedures for strength-based damage states.

Displacement-Limited Damage States

Some damage states are best characterized by an imposed displacement. Examples include beams resting on a bearing seat of limited length, or attachments for precast panels that rely on slotted connections to accommodate movement. In such cases, the median displacement demand at initiation of failure should be taken as the calculated available length of travel based on the specified travel allowance dimension (i.e., length of bearing seat, or length of slotted holes). The dispersion should be estimated based on the likelihood that the initial position of the structure is out of tolerance. Normal construction tolerances can be considered as representing one standard deviation on the displacement dimension. The dispersion can then be taken as equal to the coefficient of variation, which is approximated

by the standard deviation value (i.e., construction tolerance), divided by the median (i.e., travel allowance dimension).

Code-Based Limit States

In some cases, there may be insufficient information to calculate the capacity of a component. For example, information on the anchorage capacity of a piece of equipment may not be available because the anchorage has not yet been designed, or in the case of an existing installation, the details of the anchorage are not known. In such cases, the code-based design strength for the code in effect at the time of installation can be used to establish the capacity of the component. The following procedure can be used:

1. Identify the governing code for the installation, and compute the design strength (or displacement capacity) in terms of a convenient demand parameter, such as spectral acceleration, force, or story drift ratio. The code-based capacity is then taken as the presumed value of ϕR_n.

2. Decide whether the damage state is a ductile or brittle failure mode. If it is unknown which is likely, a separate calculation can be performed for ductile and brittle assumptions, and the results averaged.

3. Assign a default dispersion of $\beta = 0.5$.

4. If the mode is considered ductile, determine the median value of θ using use Equation 3-1. If the mode is considered nonductile, determine the median value of θ using Equation 3-2. In either case, a value of $C_q = 0.5$ should be assumed.

Overturning Limit States for Unanchored Components

In the case of unanchored components, limiting behavior modes include overturning and sliding damage states. The procedure for determining overturning fragilities for unanchored components has been adapted from ASCE/SEI 43-05, *Seismic Design Criteria for Structures, Systems, and Components in Nuclear Facilities* (ASCE, 2005). Fragility parameters include the median peak total floor velocity, V_{PT}, at which overturning initiates, and a dispersion reflecting the uncertainty in this behavior mode. The assumptions, derivation, and basis for the procedure are presented in Appendix K.

The demand parameter is peak total floor velocity, V_{PT}, defined as the peak value of the sum of the ground velocity and the relative velocity between the ground and the floor level. This can be visualized as the peak velocity of the floor relative to a fixed point in space during response to earthquake shaking.

Unanchored components are assumed to exhibit an oscillatory rocking behavior until a critical displacement is reached and the object becomes unstable. Components are assumed to have a rectangular shape with height, $2h$, and width, $2b$, uniform weight distribution, and are assumed to overturn about a single axis with the smallest base dimension, $2b$, as shown in Figure 3-5.
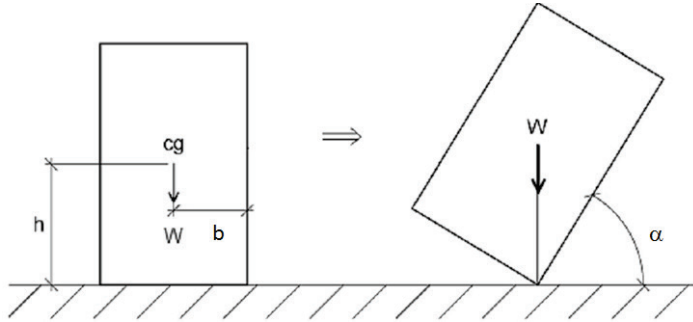
Figure 3-5   Overturning of unanchored components.

The critical tipping angle, α, at which the component will become unstable, is given by:

$$\alpha = \arctan\left(\frac{b}{h}\right) \qquad (3\text{-}5)$$

The spectral acceleration capacity for overturning of the component, S_{aO}, is determined from the critical tip angle, α, and the dimensions of the component:

$$S_{aO} = \frac{2B}{\alpha} \qquad (3\text{-}6)$$

where B is given by the equation:

$$B = \cos(\alpha) + \frac{b}{h}\sin(\alpha) - 1 \qquad (3\text{-}7)$$

To determine if behavior is controlled by overturning or sliding, the value of S_{aO} is compared with the static coefficient of friction, μ_S. A value of S_{aO} that exceeds μ_S indicates that the component will likely slide rather than overturn (i.e., enough force will be generated to overcome the static coefficient of friction before the component has been pushed to the critical tipping angle). Conversely, values of S_{aO} that are less than μ_S indicate that the object will likely overturn rather than slide.

The estimated median peak total floor velocity, V_{PT}, is obtained from the equation:

$$\hat{V}_{PT} = \frac{S_{aO}g}{2\pi f_r D_{amp}} \tag{3-8}$$

where:

$$D_{amp} = 2.31 - 0.41 \times \ln\left(100\beta_r\right) \tag{3-9}$$

and the effective rocking frequency, f_r, and damping ratio, β_r, are determined by:

$$f_r = \frac{1}{2\pi}\sqrt{\frac{2gB}{C_3\alpha^2 h}} \tag{3-10}$$

$$\beta_r = \frac{\gamma}{\sqrt{4\pi^2 + \gamma^2}} \tag{3-11}$$

where:

$$C_3 = \frac{4}{3}\left(1 + \left(\frac{b}{h}\right)^2\right) \tag{3-12}$$

$$\gamma = -2 \times \ln\left(C_R\right) \tag{3-13}$$

$$C_R = 1 - \frac{2\left(\frac{b}{h}\right)^2}{C_3} \tag{3-14}$$

A dispersion of $\beta = 0.5$ is recommended for this fragility.

Sliding Limit States for Unanchored Components

The procedure for determining sliding fragilities for unanchored components is similar to the procedure for overturning, and also has been adapted from ASCE/SEI 43-05. Fragility parameters include the median peak total floor velocity, V_{PT}, at which sliding will have exceeded a limiting displacement, and a dispersion reflecting the uncertainty in this behavior mode. The assumptions, derivation, and basis for the procedure are presented in Appendix K.

Before determining sliding fragility parameters for an unanchored component, it is necessary to determine if behavior will be controlled by sliding or overturning. As in the case of overturning, the spectral acceleration capacity for overturning, S_{aO}, is compared with the static coefficient of friction, μ_S. Values of S_{aO} that exceed μ_S indicate that the component will likely slide rather than overturn.

The sliding limit state depends on the definition of a critical sliding displacement, δ, at which the component will slide off of a supporting surface or slide into another object, resulting in damage. The median value of peak floor velocity at which the component will slide a distance, δ, is determined by:

$$\hat{V}_{PT} = \frac{\sqrt{2\mu_D g \delta}}{1.37} \qquad (3\text{-}15)$$

where μ_D is the dynamic coefficient of friction between the component and its supporting surface, g is the acceleration of gravity, and δ is the critical sliding displacement. As with overturning, a dispersion of $\beta = 0.5$ is recommended for this fragility.

3.9   Consequence Functions

Consequence functions are relationships that indicate the potential distribution of losses as a function of damage state. Consequence functions translate damage into potential repair and replacement costs, repair time, embodied energy and carbon, casualties, unsafe placarding, and other impacts.

> Consequence functions are distributions of the likely consequences of damage translated into potential repair and replacement costs, repair time, embodied energy and carbon, casualties, unsafe placarding, and other impacts.

For each damage state, fragility specifications include repair descriptions that provide information on repair actions, materials, and quantities necessary to develop repair cost, repair time and embodied energy and carbon consequences. To facilitate casualty estimation, each damage state includes a description regarding potential life safety hazards associated with the damage, and the affected area over which designated life safety hazards would exist. For unsafe placarding, each damage state also includes a description of the extent to which the occurrence of damage is likely to result in posting of an unsafe placard.

Consequence functions for each damage state were developed based on descriptions of repair actions, potential life safety hazards, and unsafe placarding, using the procedures described below. Complete consequence information is contained in fragility specifications comprising the *Fragility Database*, provided as part of *Volume 3 – Supporting Electronic Materials and Background Documentation*. Guidance on modifying available consequence functions, and developing user-defined consequences, is provided in *Volume 2 – Implementation Guide*.

3.9.1 Repair Costs

Repair costs include consideration of all necessary construction activities to return the damaged components to their pre-earthquake condition. Repair actions assume repair or replacement "in-kind," and do not include work associated with bringing a non-conforming installation or structure into compliance with newer criteria. Repair costs are based on the repair measures outlined for each damage state, and include all the steps a contractor would implement to conduct a repair including:

- Removal or protection of contents adjacent to the damaged area.

- Shoring of the surrounding structure (if necessary).

- Protection of the surrounding area (e.g., from dust and noise) with a temporary enclosure.

- Removal of architectural and mechanical, electrical, and plumbing systems, as necessary, to obtain access for the repair.

- Procurement of new materials and transport to the site.

- Conduct of the repair work.

- Replacement of architectural and mechanical, electrical, and plumbing systems, as necessary.

- Clean-up and replacement of contents.

Consequence functions for repair costs provided with the methodology were developed based on construction cost estimates computed for a reference location in the United States (Northern California) at a reference time (2011), neglecting uncertainty in contractor pricing strategies or construction cost escalation. Repair cost consequences include consideration of economies of scale and efficiencies in construction operations. When a large quantity of the same type of work is necessary, contractor mobilization, demobilization, and overhead costs can be spread over a larger volume of work, resulting in reduced unit rates. A typical consequence function for repair cost is illustrated in Figure 3-6. For each damage state, repair costs are described using the following parameters:

- **Lower quantity.** Quantity of repair actions of a give type, below which there is no discount reflecting economies of scale or efficiencies in operation.

- **Maximum cost.** The unit cost to perform a repair action, excluding any economies of scale or efficiencies in operation.

- **Upper quantity.** Quantity of repair work, above which no further economies of scale or efficiencies in operation are attainable.

- **Minimum cost.** The unit cost to perform a repair action, considering all possible economies of scale and efficiencies in operation.

- **Dispersion.** Uncertainty in values of unit cost.
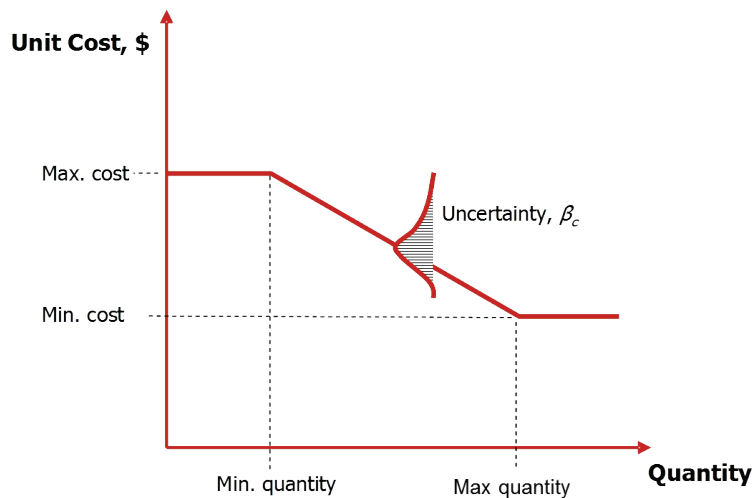
Figure 3-6   Typical consequence function for repair costs.

At each point along the consequence function, there is a distribution of potential repair costs. The distribution (and dispersion) was derived from cost data representing 10th, 50th, and 90th percentile estimates of construction cost. Both lognormal and normal distributions were developed from available repair cost data, and the curve with the best fit was used in each case.

The cost of accessing the damaged area to conduct repairs will affect repair costs. For example, it is more difficult, and, hence, more costly, to repair damage on the tenth floor of a building than on the first floor. Similarly, cost premiums associated with access restrictions and enhanced protection measures in certain occupancies (e.g., healthcare and research laboratories) can affect repair costs. Finally, the presence of hazardous materials within the damaged area will affect the repair actions and approach to construction activities. Each of these considerations will result in increased repair costs. The methodology includes provision for "macro-factors," which are provided on a story-by-story basis, to adjust repair consequences for these effects.

> Macro-factors are used to account for occupancy-specific conditions that affect repair effort, and to adjust cost data for inflation and building-specific location.

The methodology also considers factors to adjust repair costs for inflation and location relative to the reference location and time used in developing the cost data. Any convenient construction cost index can be used for this

purpose, if normalized to the reference location (Northern California) and time (2011).

3.9.2 Repair Time

The actual time that a building will be unusable for beneficial re-occupancy following an earthquake is difficult to determine. Factors that can affect the length of time for building re-occupancy (downtime) include:

- Who is responsible for performing repairs (e.g., owner or tenants).

- Financial resources available to the party responsible for performing repairs.

- Availability of design professionals to assess the condition of the building, to perform a detailed evaluation, and to design repair actions.

- The time required to secure a building permit.

- Availability of contractors, and the associated mobilization time, and availability of construction workers, equipment, and materials necessary to perform repairs.

- The time required to prepare the site.

- The time it takes to procure specialized equipment (i.e., long lead time) and materials for a specific building or occupancy.

- Whether or not the building will remain in service during repairs, which limits repair work to unoccupied areas, versus remaining vacant to provide complete access for conducting repairs on a building-wide basis.

- Whether or not the building has been posted with an unsafe placard, and the length of time necessary to convince a building official that it is safe to conduct repair operations within the building.

- The time it takes to complete the final clean-up.

Uncertainties in these factors make reliable estimation of overall occupancy interruption time intractable. As a result, the methodology uses the following measures for consequences associated with occupancy interruption:

- The length of time necessary to conduct repairs (i.e., repair time).

- The need to procure items with long lead times.

- The probability that a building will be posted with an unsafe placard.

To estimate repair time, each damage state includes a time-related consequence function that indicates the number of labor hours associated

with the specified repair actions. A key parameter for developing repair time estimates is the number of workers assumed to occupy the building at the same time. The methodology uses a "maximum worker per square foot" parameter that can be adjusted to account for whether or not the building is occupied during construction, as well as assumptions about the availability of contractor labor in the region.

Repair time consequences also include consideration of economies of scale and efficiencies in construction operations. For each damage state, repair times are described using the following parameters:

- **Lower quantity.** Quantity of repair actions of a give type, below which there is no reduction in time reflecting economies of scale or efficiencies in operation.

- **Maximum time.** The maximum number of labor hours necessary to perform a repair action, excluding any economies of scale or efficiencies in operation.

- **Upper quantity.** Quantity of repair work, above which no further economies of scale or efficiencies in operation are attainable.

- **Minimum time.** The minimum number of labor hours necessary to perform a repair action, considering all possible economies of scale and efficiencies in operation.

- **Dispersion.** Uncertainty in labor effort associated with a given repair action.

Since the detailed repair time estimate was derived from the repair cost data, the final repair time distribution and dispersion were based on the repair cost results. The median repair time estimate is taken at the 50th percentile estimate of the labor effort. The repair time dispersion, β_{RT}, is derived from the repair cost dispersion, β_{RC}, using the relationship:

$$\beta_{RT} = \sqrt{\beta_{RC}^2 + (0.25)^2} \qquad (3\text{-}16)$$

Repair cost dispersion are enriched by 0.25, as shown in Equation 3-16 to account for the additional uncertainty associated with estimating repair time for a given repair scenario.

Serial repair strategies assume work occurs sequentially between floors. Parallel repair strategies assume work occurs on all floors simultaneously. Repair time estimates include consideration of both serial and parallel repair strategies. Neither strategy is likely to represent the actual schedule used to

> Repair time is limited to the number of labor hours associated with the required repair.

> **Second Edition Update**
> The repair time consequences were revised to reflect a change from crew rate (3-person crew working 8-hour workday) to person-days, resulting in a reduction factor of 3/8 over the previous repair time estimates. The repair time consequence was updated for all fragilities.

> **Second Edition Update**
> The repair time consequence algorithm has been updated. The repair time consequence was updated for all fragilities.

repair a particular building, but the two extremes are expected to represent a reasonable bound to the probable repair time.

Repair time can be significantly affected by long lead times for procurement of critical equipment and components (e.g., HVAC equipment and elevators). Because lead times vary, and are case-specific, they are not explicitly calculated as part of the methodology. If a damage state requires replacement of a component that is associated with a long lead time, this is indicated in the fragility specification and is flagged as part of the assessment results.

3.9.3 Environmental Impacts

<div style="border:1px solid #000; background:#c9d79a; padding:4px; width:200px;">

Second Edition Update
Consideration of environmental impacts has been added.

</div>

A wide range of environmental impacts will occur due to seismic damage and repair activities. Environmental impacts associated with building construction and repair are typically quantified using environmental life cycle assessment (LCA) procedures. In this methodology, Economic Input Output LCA (EIO-LCA) data are used to estimate environmental impacts of damage and repair using two metrics: embodied carbon (in units of kg of carbon dioxide equivalents emitted, CO2e) and embodied energy use (in units of Mega Joules, MJ).

These environmental impacts are calculated directly from the repair cost estimates with the generalized EIO impact per dollar spent in each industrial sector, multiplied by the repair costs in each of these sectors. Thus, the level of precision parallels the level of precision in the repair cost estimate. The range and uncertainty of environmental impacts are estimated to match the range and uncertainty in the repair costs.

Construction repair cost estimates are divided into industrial sectors including labor, material manufacturing, equipment rental and energy use. The evaluation assumes zero environmental impact of labor (as is common in LCA) and equipment rental (assuming impact of equipment distributed over many uses).

The additional uncertainty associated with environmental impacts is not explicitly included, as complete data are not available at this time. Factors that can impact the uncertainty of environmental impacts include:

- location of material manufacturing, which impacts energy sources and manufacturing practices, and
- material make up (e.g., concrete mix design).

To account for these uncertainties in an approximate manner, the dispersion in embodied carbon and embodied energy is assumed to be directly related to that for repair cost, and is computed for each of these impacts, as shown in Equation 3-16 above.

The environmental impacts associated with manufacturing building materials and products are considered. The impacts of other life cycle stages (transportation, construction, use, and end of life) are not included at this time due to limitations in available data. The methodology could be extended to include additional environmental impacts and life cycle stages in the future. Details on the overall approach for determining environmental impacts can be found in FEMA P-58/BD-3.7.20, *Methodology for Environmental Impact Assessment* (FEMA, 2018g).

3.9.4   Unsafe Placarding

Each damage state is associated with a potential to result in an unsafe placard. In some cases, the potential is high, and in other cases the potential is low or negligible. The most severe damage states in nearly all of the structural fragility groups will trigger a potential for an unsafe placard because it is assumed that the stability of the structure has been compromised, resulting in a risk to life safety. Although nonstructural damage can be an indicator of potential structural damage, it does not, by itself, pose a life safety risk. Most nonstructural fragility groups are not associated with an unsafe placard.

The posting of an unsafe placard is a major contributor to delays in building re-occupancy following an earthquake, and can significantly affect building repair times given the presumed dangerous condition of the building. Estimation of the time associated with unsafe placarding is not explicitly calculated as part of the methodology. Instead, the likelihood of receiving an unsafe placard as a result of damage to a performance group is established. It is ant icipated that, if needed or desired, the building-specific time associated with an unsafe placard can be estimated on a case-by-case basis and added to the calculated repair time consequences.

> The time associated with unsafe placarding is not estimated. Instead, the likelihood of receiving an unsafe placard for each performance group, and the building as a whole, is established.

For damage states that are determined to have potential to result in an unsafe placard, the median quantity of damage that would trigger such a placard is provided. For example, in the case of reinforced concrete special moment frames, if 20% of the beam-column joints in a performance group reach damage state DS3 (i.e., concrete cracking, spalling of cover, crushing of the core, and fracture and buckling of reinforcement), it is expected that an unsafe placard will be likely.

3.9.5 Casualties

> Building collapse is the principle cause of earthquake casualties. This methodology also estimates casualties associated with falling debris and other component damage.

Building collapse is the principle cause of earthquake casualties. However, some damage states associated with individual components or assemblies can have potential casualty consequences. These are generally associated with falling debris (e.g., failed glazing falling out of its frame and injuring nearby occupants), but can also be associated with damage states such as the release of hot water, steam, or toxic materials.

Casualties caused by building collapse are based on possible building collapse modes and the estimated number of building occupants. Assessment of building collapse potential is discussed in Chapter 6. The estimated number of building occupants is determined using the provided population models.

For individual components, each damage state includes a description regarding potential life safety hazards associated with the damage, and the casualty-affected planar area over which designated life safety hazards would exist. The casualty-affected planar area represents the planar area proximate to a component in which damage could result in serious injury or loss of life. The affected area is typically larger than the projected area occupied by the component to account for uncertainty in the area over which debris, spray, or hazardous material release may occur.

Not all occupants within a casualty-affected area will become casualties. Because of this, it is necessary to identify the percentage of individuals that, if located within the casualty-affected area, are likely to be injured by the component. In the case of wall-mounted electronic equipment, for example, a panel might be on the order of 5 to 10 square feet. The assumed casualty-affected area could be on the order of 16 square feet, and the percentages for serious injury and loss of life might be taken as 10% and 5%, respectively. These values are judgmentally determined.

3.10 Fragility Specifications

Damage, fragility, and consequence data provided with the methodology are recorded in fragility specifications comprising the *Fragility Database*. Fragility specifications include basic identifier information, fragility units, damage state and consequence descriptions, photos illustrating damage (when available), fragility parameters, and consequence functions, as illustrated in Figure 3-7, Figure 3-8, and Figure 3-9.

FEMA P-58 Fragility Specification

NISTIR Classification	B1041.031b				Line 121

NISTIR Name ACI 318 OMF with weak joints and beam flexural response, Conc Col & Bm = 24" x 24", Beam both sides

Description ACI318 OMF, joint shear failure, beam flexural response. Meets the following requirements: (1) Sum Mcol / Sum Mbeam > 1.2, (2) Beam Vn > Veq, (3) Column Vn > Veq Costing is on a per joint basis.

Construction Quality: Not Specified
Seismic Installation Conditions: Not Specified

Quantity Rounding | Round Qty? YES
Allow sum by floor or building? NO
Demand Location (floor above?) No

Fragility Unit of Measure:	EA 1				
Demand Parameter (unit):	Story Drift Ratio	Unit less			
Number of Damage States:	3				
Damage State:	DS1	DS2	DS3		
Type of Damage State:	Sequential	Sequential	Sequential		
DS Hierarchy	Seq(DS1,DS2,DS3)				
Descriptions	Beams or joints exhibit residual crack widths > 0.06 in. No significant spalling. No fracture or buckling of reinforcing.	Beams or joints exhibit residual crack widths > 0.06 in. Spalling of cover concrete exposes beam and joint transverse reinforcement but not longitudinal reinforcement. No fracture or buckling of reinforcing.	Beams or joints exhibit residual crack widths > 0.06 in. Spalling of cover concrete exposes a significant length of beam longitudinal reinforcement. Crushing of core concrete may occur. Fracture or buckling of reinf. requiring replacement may occur.		

Figure 3-7   Basic identifier information for a typical fragility specification.
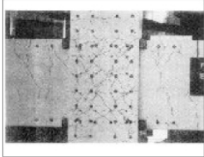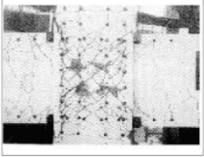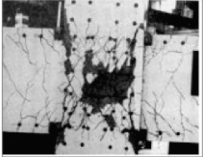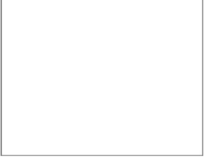
Illustrations

	B1041.031a-DS1-1.JPG	B1041.031a-DS2-1.JPG	B1041.031a-DS3-1.JPG		
Damage State Probability:	1.00	1.00	1.00		

Fragility Parameters

Median Demand, θ:	0.0175	0.0225	0.0322		
Data dispersion, β_d:	0.2	0.27	0.32		
Uncertainty, β_u:	0.3	0.13	0.15		
Total Dispersion, β:	0.4	0.4	0.4		

Correlation (Yes / No) NO

Directionality (Yes / No) YES

Quality Ratings
Data Quality Average
Data Relevance Average
Documentation Quality Superior
Rationality Superior

Consequence Functions
Repair Description

Remove furnishings, ceilings and mechanical, electrical and plumbing systems (as necessary) 8 feet either side of damaged area. Clean area adjacent to the damaged concrete. Prepare spalled concrete and adjacent cracks, as necessary, to be patched and to receive the epoxy injection. Patch concrete with grout. Replace and repair finishes. Replace furnishings, ceilings and mechanical, electrical and plumbing systems as necessary.	Remove furnishings, ceilings and mechanical, electrical and plumbing systems (as necessary) 15 feet either side of damaged area. Shore damaged member(s) a min one level below (more levels may be required). Remove damaged concrete at least 1 inch beyond the exposed reinforcing steel. Place concrete forms. Place concrete. Remove forms. Remove shores after one week. Replace and repair finishes. Replace furnishings, ceilings and mechanical, electrical and plumbing systems (as necessary).	Remove furnishings, ceilings and mechanical, electrical and plumbing systems (as necessary) 15 feet either side of damaged component. Shore damaged member(s) a minimum of one level below (more levels may be required). Remove damaged component. Place and splice (as necessary) new reinforcing steel to existing, undamaged reinforcing. Place concrete forms. Place concrete. Remove forms. Remove shores after one week. Replace and repair finishes. Replace furnishings, ceilings and mechanical, electrical and plumbing systems (as necessary).		

Figure 3-8   Fragility information for a typical fragility specification.

Long Lead Time (Yes / No)		NO			NO			NO								
Repair Costs:	P_{10}	P_{50}	P_{90}	P_{10}	P_{50}	P_{90}	P_{10}	P_{50}	P_{90}	P_{10}	P_{50}	P_{90}	P_{10}	P_{50}	P_{90}
Repair Cost by Damage State:	1.02E+04	2.14E+04	3.11E+04	1.85E+04	3.25E+04	4.44E+04	2.30E+04	4.00E+04	5.29E+04						
Best fit mean:		2.09E+04			3.18E+04			3.86E+04							
Best Fit Distribution:		Normal			Normal			Normal							
Quantity Plateau (Min Qty, Max Qty)	5.00		20.00	5.00		20.00	5.00		20.00						
Average Repair Cost (Min Qty, Max Qty)	2.57E+04		1.71E+04	3.90E+04		2.60E+04	4.80E+04		3.20E+04						
CV or beta (Min Qty, Max Qty)	0.39		0.39	0.32		0.32	0.30		0.30						
Quantity Unit:		Each			Each			Each							
Repair Time:	P_{10}	P_{50}	P_{90}	P_{10}	P_{50}	P_{90}	P_{10}	P_{50}	P_{90}	P_{10}	P_{50}	P_{90}	P_{10}	P_{50}	P_{90}
Repair Time by Damage State:	8.98E+00	1.89E+01	2.75E+01	1.63E+01	2.87E+01	3.92E+01	2.03E+01	3.53E+01	4.67E+01						
Best fit mean:		1.89E+01			2.87E+01			3.53E+01							
Best Fit Distribution:		Normal			Normal			Normal							
Quantity Plateau (Min Qty, Max Qty)	5.00		20.00	5.00		20.00	5.00		20.00						
Average Repair Time (Min Qty, Max Qty)	2.27E+01		1.51E+01	3.44E+01		2.29E+01	4.23E+01		2.82E+01						
CV or beta (Min Qty, Max Qty)	0.46		0.46	0.40		0.40	0.39		0.39						
Quantity Unit:		Each			Each			Each							
Environmental Impacts:	Median Cost	Best Fit	CV or Beta	Median Cost	Best Fit	CV or Beta	Median Cost	Best Fit	CV or Beta	Median Cost	Best Fit	CV or Beta	Median Cost	Best Fit	CV or Beta
Embodied Carbon (kg CO2eq)	3.7E+03	Normal	0.46	5.5E+03	Normal	0.40	6.7E+03	Normal	0.39						
Embodied Energy (MJ)	4.2E+04	Normal	0.46	6.3E+04	Normal	0.40	7.8E+04	Normal	0.39						
LifeSafety Hazard:															
Potential non-collapse casualties? (Yes / No)		NO			NO			NO							
Casualty-affected Planar Area (sf) per Normative Unit:		Not Applicable			Not Applicable			Not Applicable							
Serious Injury (Median, Dispersion)	0%	0.00		0%	0.00		0%	0.00							
Loss of Life (Median, Dispersion)	0%	0.00		0%	0.00		0%	0.00							
Post-event Tagging Flag:		NO			NO			YES							
Unsafe Placard Trigger (Median, Dispersion)	0%	0.00		0%	0.00		20%	0.50							

Comments:	None			Root Cost Multiplier:	1
Date Created:	Not Given				
Approved (YES / NO)?	By User				
Official (YES / NO) ?	By User				
Author:					
Revisions:	2011-08-24 Changed DS2 beta from 0.3 to 0.4 to avoid negative probability beyond 1% story drift.				

Figure 3-9   Consequence information for a typical fragility specification.

Chapter 4
Define Earthquake Hazards

4.1   Introduction

Earthquake hazards are defined in terms of earthquake shaking. Earthquake effects also include ground fault rupture, landslide, liquefaction, lateral spreading, seiches, and tsunamis, but consideration of these effects are beyond the scope of the current version of the methodology.

Earthquake shaking occurs in three dimensions and can be completely defined by two orthogonal horizontal components and one vertical component. In most cases, however, vertical shaking is not a key contributor to earthquake damage and has little impact on seismic performance. Therefore, in most performance assessments, only horizontal earthquake shaking is considered.

This chapter describes how earthquake hazards are defined, selected, and specified in the performance assessment process. Appendix B presents background information on characterization of ground shaking hazards, and procedures that can be used to characterize vertical shaking, if deemed significant for the building under consideration.

Earthquake ground shaking is characterized by target acceleration response spectra. For nonlinear response history analysis, shaking effects are assessed by simultaneously evaluating response to orthogonal pairs of horizontal ground motion components. The ground motion pairs are scaled for consistency with the target response spectrum for the desired ground shaking intensity level. For simplified analysis, shaking is characterized by spectral response accelerations at the first mode period along each axis of the building.

Characterization of earthquake hazards varies by type of performance assessment. For intensity-based assessments, ground shaking intensity can be represented by any user-defined acceleration response spectrum (e.g., a code design spectrum). For scenario-based assessments, ground shaking intensity is represented by acceleration response spectra derived for specific magnitude-distance pairs (e.g., a known event on a specified fault) using ground motion prediction equations, also called attenuation relationships. For time-based assessments, ground-shaking intensity is represented by a

> Earthquake hazards are defined in terms of earthquake shaking. Other earthquake effects are beyond the scope of the current version of the methodology.

series of seismic hazard curves, and acceleration response spectra derived from these curves, at selected annual frequencies of exceedance.

4.2   Building Location and Site Conditions

4.2.1   Seismic Environment and Hazard

Earthquake shaking hazards are determined by the location of the site relative to causative faults and sources, and regional and site-specific geologic characteristics. Local topographic conditions (e.g., hills, valleys, and canyons) can also affect the characteristics of shaking at a site, however, these are special cases that require site-specific investigation, and are not considered here.

> Earthquake hazard at a site is determined by earthquake sources in the vicinity, the propagation of seismic waves to the building, and modifications based on local site conditions.

4.2.2   Location

For intensity-based assessments, the location of the site need not be defined. For scenario-based assessments, the distance from the building site to the causative fault must be known. Time-based assessments require seismic hazard curves that predict the annual frequency of exceedance of key spectral response parameters. To develop hazard curves, the exact location of the site (in terms of latitude and longitude) must be identified. To adequately locate a site, latitude and longitude should be defined to a minimum of three decimal places.

4.2.3   Local Soil Conditions

The properties of site soils must be defined to enable:

* Selection of appropriately shaped spectra for intensity-based assessments.

* Selection of appropriate ground motion prediction equations for scenario-based assessments.

* Development of seismic hazard curves and response spectra for time-based assessments.

In the Western United States, it is generally sufficient to define the soil conditions to a depth of 30 m (100 ft) below the ground surface. As a minimum, it is necessary to have sufficient data to characterize the Site Class in accordance with ASCE/SEI 7-16, *Minimum Design Loads and Associated Criteria for Buildings and Other Structures* (ASCE, 2017) so that site coefficients can be assigned. For sites categorized as Site Class E or F, additional information will be needed for the necessary site response analysis. Such information will generally include the depth, classification, and shear wave velocity of materials in the soil column above bedrock.

4.3   Ground Motion Prediction Equations

Ground motion prediction equations are used to derive acceleration response spectra used in scenario-based assessments. They also form the basis for probabilistic seismic hazard analyses used to develop hazard curves for time-based assessments. Ground motion prediction equations provide estimated values of ground shaking intensity parameters, such as peak ground acceleration, peak ground velocity, and spectral response acceleration at particular structural periods, for user-specified combinations of earthquake magnitude and site-to-source distance.

Seismologists derive ground motion prediction equations from regression analyses on values of intensity parameters obtained from strong motion recordings in past earthquakes. Regression analyses consider site-to-source distance, earthquake magnitude, and other parameters. Strong motion recordings are typically obtained from pairs of instruments arranged to capture orthogonal components of motion. At any instant in time, each orthogonal component will have a different amplitude, and it is possible that neither component will represent the maximum amplitude at a given time. Most ground motion prediction equations provide geometric mean (geomean) spectral response accelerations represented by the quantity:

> Ground motion prediction equations provide estimates of spectral response acceleration parameters for specified earthquake magnitude and site-to-source distance based on regression analyses of past strong motion recordings.

$$S_{gm}(T) = \sqrt{S_x(T) \times S_y(T)}\qquad(4\text{-}1)$$

where $S_x(T)$ and $S_y(T)$ are orthogonal components of spectral response acceleration at period T. The X and Y directions could represent the actual recorded orientations, or they could represent a rotated axis orientation. Some equations rotate the motion to capture fault-normal and fault-parallel orientations, while others use an arbitrary rotation intended to capture a maximum orientation. The geomean approximately represents a statistical mean response. As a mean value, actual shaking in any direction has an equal probability of being higher or lower than the geomean. For example, maximum response acceleration can be as high as 130% of the geomean or more, while the minimum response acceleration can as low as 80% of the geomean, or less. Except within a few kilometers of the rupture zone, the orientation of maximum spectral response with respect to the strike of the fault is random and varies with period.

Scenario assessments can be used to assess the effects of a repeat of an historic earthquake, or to explore the effects of a selected-magnitude event on a nearby fault. The United States Geological Survey (USGS) posts information on best-estimate maximum magnitudes for active faults in the Western United States and the Inner Mountain seismic region on the USGS

website at https://earthquake.usgs.gov/hazards/qfaults/ (last accessed March 15, 2018).

Fault directivity effects can have a substantial impact on the amplitude, duration, and period content of shaking, and should be considered for scenario-based assessments if the selected earthquake is M_w 6.0 or greater, and the building site is located within 20 km to 30 km of the presumed fault rupture zone. Directivity should be specified as: (1) forward directivity (rupture progresses towards the site); (2) reverse directivity (rupture progresses away from the site); (3) null directivity; or (4) unspecified directivity (random direction of rupture progression). Appendix B and NIST GCR 11-917-15, *Selecting and Scaling Earthquake Ground Motions for Performing Response History Analyses* (NIST, 2011), provide guidance on consideration of fault-rupture directivity.

At sites located within the forward directivity region of strike-slip faulting, ground shaking often exhibits directivity effects, and shaking in the fault-normal direction contains velocity pulses and significantly larger amplitudes than shaking in the fault-parallel direction. Hazard assessments on sites within 20 km of strike-slip faults should consider these effects.

Some ground motion prediction equations are quite complex. Simpler models, often called attenuation relationships, take the basic form:

$$\ln Y = c_1 + c_2 M - c_3 \ln R - c_4 R + \gamma \qquad (4\text{-}2)$$

where Y is the median value of the strong-motion parameter of interest (e.g., geometric mean spectral acceleration at a particular period), M is the earthquake magnitude, R is the source-to-site distance, and γ is a standard error term. Additional terms can be used to account for other effects including near-source directivity, faulting mechanism (e.g., strike-slip, and reverse strike-slip), and site conditions.

Although many ground motion prediction equations have been developed, most apply to a specific geographic region based on the data set of ground motion records used to develop the relationships. It is important to ensure that the selected equation is appropriate to the particular building site and earthquake source mechanism.

Appendix B provides a list of selected ground motion prediction equations for North America. The Open Seismic Hazard Analysis (OpenSHA) website, http://www.opensha.org/ (last accessed, March 15, 2018) provides a ground motion prediction equation plotter that can be used to generate median spectra and dispersions for models including Boore and Atkinson (2008), Campbell and Bozorgnia (2008), and Chiou and Youngs (2008) used

by the USGS to produce the national seismic hazard maps referenced in ASCE/SEI 7-10. It is noted that OpenSHA requires a revision to most computers' security settings in order to provide the results. Other tools are available through the PEER Center and USGS that provide similar information.

In 2014, a new set of ground motion prediction equations (Next Generation Attenuation Relationships for Western U.S, NGA-West2) were developed and used in the development of the seismic design maps in ASCE/SEI 7-16. These new equations can be downloaded from the PEER Ground Motion Database, available at http://peer.berkeley.edu/ngawest2/ (last accessed March 15, 2018).

For a particular earthquake scenario and site, different attenuation relationships can provide significantly different estimates of the probable values of spectral response acceleration. These are caused by differences in the data set of records used to develop each relationship, as well as differences in the functional form of the relationships. Figure 4-1 plots values of 0.2 second spectral response acceleration versus site-to-source distance, derived from three ground motion prediction equations, for two earthquake magnitudes. Differences between the values predicted by each equation are evident in the figure, and these differences are sources of uncertainty in determining ground motion intensity for a scenario.
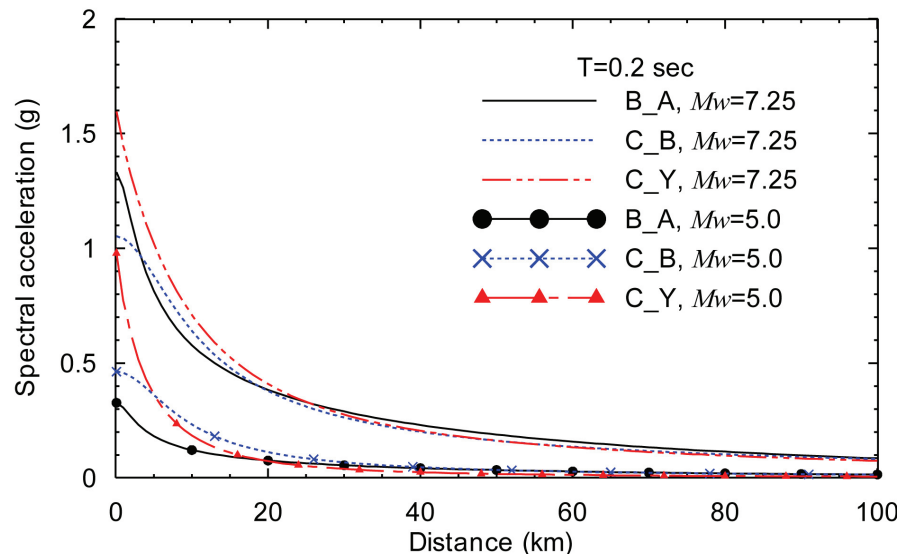
Figure 4-1   Differences between Boore and Atkinson (B_A), Campbell and Bozorgnia (C_B), and Chiou and Youngs (C_Y) ground motion prediction equations.

Ground motion prediction equations can be used to develop acceleration response spectra by repeatedly applying the equation to a range of periods.

Some prediction equations use shear-wave velocity in the upper 30 m of soil as an input variable, while others are applicable only for a particular soil type. If the selected equation has an input variable for shear wave velocity in the upper 30 m, the site-specific value should be used in seismic hazard calculations.

If the selected equation uses a generic description of the reference soil type (e.g., soft rock) and reports the reference shear wave velocity, spectra should be adjusted for the site-specific shear wave velocity in the upper 30 m of the soil column. Adjustments can be made using site-response analysis or factors for Site Class, as specified in ASCE/SEI 7-16, or other references.

Each relationship includes a measure of uncertainty associated with the lack of a perfect match between values predicted by the equation and the measured values upon which they were based. Some models permit calculation of a distribution of response acceleration values. Figure 4-2 illustrates a range of response spectra plotted for different probabilities of exceedance for a M_w 7.25 earthquake, all derived from a single ground motion prediction equation.
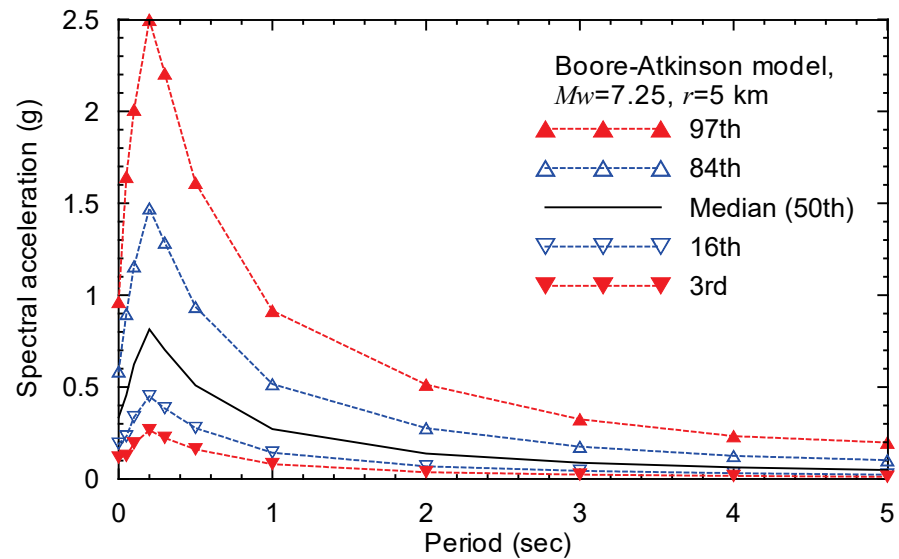
Figure 4-2   Response spectra with different probabilities of exceedance derived from a single ground-motion prediction equation for an earthquake scenario of $M_w = 7.25$ and $r = 5$ km.

4.4   Nonlinear Response History Analysis

This section describes recommended procedures for selecting and scaling acceleration histories for use with nonlinear response history analysis. These include:

- Development of an appropriate target acceleration response spectrum.

- Selection of an appropriate suite of earthquake ground motions.

- Scaling of motions for consistency with the target spectrum.

These procedures are applicable to intensity-based, scenario-based, and time-based assessments. Appendix B provides an alternate procedure for use with scenario-based assessments that explicitly considers uncertainty in ground motion.

4.4.1 Target Acceleration Response Spectra

For intensity-based assessments, any spectrum can be used as a target spectrum. The spectral shape should be consistent with the geologic characteristics of the site. For scenario-based assessments, the target spectrum should be derived directly from an appropriate ground motion prediction equation. For time-based assessments, one spectrum is required for each of the several seismic hazard intervals used in the analysis. Seismic hazard intervals are selected from the seismic hazard curve for the site.

Target spectra can be Uniform Hazard Spectra (UHS), Conditional Mean Spectra (CMS), or Conditional Spectra (CS). These are described in Appendix B. For intensities with high annual frequencies of exceedance (i.e., frequent events), Uniform Hazard and Conditional Mean Spectra should be similar in shape. For intensities with low annual frequencies of exceedance (i.e., rare events), the amplitude of Conditional Mean Spectra will be smaller at some periods than Uniform Hazard Spectra, as the Conditional Mean Spectrum considers the low likelihood of high amplitudes over the entire range of periods given the amplitude at the period of interest. In this regard, the CMS quantifies a less conservative and more realistic "scenario spectrum" for a particular intensity. Conditional Spectra differ from Conditional Mean Spectra in that they consider uncertainty as well as amplitude in determining spectral values at each period. Use of either Conditional Mean Spectra or Conditional Spectra will provide more accurate estimates of median story drift and acceleration response for a given intensity of shaking than Uniform Hazard Spectra, but additional effort is required to generate these spectra.

If Conditional Mean Spectra are used, it is necessary to select an appropriate period upon which to condition the spectrum. If a building has identifiable modes associated with translational response along two orthogonal axes, X and Y, the corresponding fundamental translational periods associated with each axis are denoted T_1^X and T_1^Y, respectively. Conditional Mean Spectra should be developed based on the hazard at period $\overline{T}$, taken as the average

of periods T_1^X and T_1^Y. For buildings without identifiable response modes in each of the X and Y axes, $\overline{T}$ should be taken as the period of the fundamental mode T_1. Development of Conditional Mean Spectra is described in in Appendix B.

4.4.2   Ground Motion Selection and Scaling

The intent of ground motion selection and scaling is to obtain a set of motions that will produce unbiased estimates of median structural response when used with nonlinear response history analysis. Ground motions are selected such that, on average, they reasonably match the target spectrum over the period range T_{min} to T_{max}. For buildings with identifiable translational response modes in each of the X and Y axes, T_{max} is taken as twice the larger value of T_1^X and T_1^Y. For buildings without identifiable response modes in each of the X and Y axes, T_{max} is taken as twice the period of the fundamental period, T_1. Period, T_{min}, is taken as the smaller of $0.2T_1^X$ and $0.2T_1^Y$. If substantial response, and corresponding damage, is expected to occur in modes with periods less than T_{min} (e.g., in tall buildings where higher modes may contribute significantly to acceleration and drift response), T_{min} should be taken as low enough to capture these important behaviors.

To the extent possible, selected pairs of earthquake ground motions should have a spectral shape that is similar to the target spectrum. In addition, selected records should have faulting mechanisms, earthquake magnitudes, site-to-source distances, and local geology that are similar to those that dominate the seismic hazard at the particular intensity level, although these considerations are not as significant as overall spectral shape. For near-fault sites in the forward directivity region, and for buildings with velocity-sensitive nonstructural components and systems, ground motion selection should also consider the amplitude and shape of the scaled velocity time series. Ground motions are available from a number of sources, including https://ngawest2.berkeley.edu/ and www.cosmos-eq.org (last accessed, March 15, 2018).

Limited study suggests that when the spectral shape of the selected motions matches the target spectrum well, relatively few records can provide a reasonable estimate of median response over the height of the building. Regardless of the fit, at least seven ground motion pairs should be used. When there is significant scatter in the spectral shape of selected records (i.e., there is a poor fit to the target spectrum), eleven or more pairs of motions may be needed to produce reasonable estimates of median response.

> Selected pairs of ground motions should have a spectral shape that is similar to the target spectrum over the period range of interest. When the fit is good, at least 7 pairs of motions should be used. When the fit is poor, 11 pairs of motions, or more, are recommended.

Intensity-Based Assessments

Intensity-based assessments require a target acceleration response spectrum and suites of n ground motions scaled for compatibility with this spectrum. The following procedure should be used to select and scale ground motions for intensity-based assessments:

1. Select the target response spectrum.

2. Select a candidate suite of ground motion pairs from available sets of recorded motions.

3. Using Equation 4-1, construct the geomean spectrum for each ground motion pair over the period range $T_{min} \leq T \leq T_{max}$. Compare the geomean shape with the shape of the target spectrum. Select ground motion pairs with geomean spectral shapes that are similar to the target spectrum over the period range $T_{min} \leq T \leq T_{max}$. Discard ground motion pairs that do not adequately fit the shape of the target spectrum.

4. Amplitude-scale both components of each ground motion pair by the ratio of $S_a(\overline{T})$ obtained from the target spectrum to the geometric mean $S_{gm}(\overline{T})$ of the recorded components, where $\overline{T}$ is the average of periods T_1^X and T_1^Y.

Scenario-Based Assessments

Scenario-based assessments require a target median response spectrum for the scenario derived from a ground motion prediction equation, a measure of the dispersion associated with this spectrum, and suites of n ground motion pairs scaled for compatibility with the spectrum. Ground motion intensity is assumed to be lognormally distributed with median value, θ, and dispersion, β. In this procedure, ground motion dispersion is indirectly considered in the modeling uncertainty assumed in response calculation (Chapter 5). Appendix B presents an alternate procedure for ground motion selection that explicitly considers ground motion dispersion. If the alternate procedure is used, assumptions for modeling uncertainty in response calculation must be adjusted accordingly.

The following procedure should be used to select and scale ground motions for scenario-based assessments:

1. Select the scenario magnitude and site-to-source distance.

2. Select an appropriate ground motion prediction equation for the region, site soil type, and source characteristics.

3. Establish the period range (T_{max}, T_{min}).

4. Construct a median spectrum over the period range $T_{min} \leq T \leq T_{max}$ using the selected ground motion prediction equation.

5. Select and scale suites of n ground motion pairs using Steps 2 through 4 for intensity-based assessments, above.

Time-Based Assessments

Time-based assessments require seismic hazard curves for spectral acceleration, $S_a(\bar{T})$, and suites of ground motion pairs selected and scaled to match spectra derived from the seismic hazard curves in the period range $T_{min} \leq T \leq T_{max}$ over a range of exceedance frequencies (i.e., intensities). Hazard curves include explicit consideration of ground motion uncertainty. The following procedure should be used to determine analysis intensities, and to select and scale ground motions for time-based assessments:

Step 1 – Select Intensity Range. An appropriate range of ground motion exceedance frequencies and corresponding spectral response accelerations, $S_a(\bar{T})$, must be selected for the building under consideration. A range of exceedance frequencies is considered appropriate if it is associated with a range of spectral acceleration intensities that would be expected to cause building damage ranging from negligible to complete loss. For new buildings designed in accordance with ASCE/SEI 7-10, an appropriate range of exceedance frequencies is:

- Minimum mean annual frequency of exceedance corresponding to $S_a(\bar{T}) = S_a^{min} = 0.05\,\mathrm{g}$ for $\bar{T} \leq 1$ second, and $S_a^{min} = 0.05 / \bar{T}\,\mathrm{g}$ otherwise.

- Maximum mean annual frequency of exceedance taken as 0.0002, with S_a^{max} taken as $S_a(\bar{T})$ at this exceedance frequency.

Older, non-ductile buildings are more likely to experience damage at low levels of shaking, and collapse at moderate levels of shaking, than modern code-conforming buildings. For weak or otherwise damageable buildings, the range of exceedance frequencies suggested above should be modified. Specifically the lower bound should be adjusted so that the corresponding spectral acceleration at that level does not result in damage to structural or nonstructural components. The upper bound should be adjusted to a level at which no more than two intensities of shaking within the range trigger collapse.

Step 2 – Select Analysis Intensities and Scale Motions. Structural analysis will be performed at a series of intensities spanning the range of intensities selected in Step 1, above. Intensities should be determined, and ground motions should be selected and scaled, as follows:

1. Develop a seismic hazard curve for $S_a(\bar{T})$.

2. Compute the range of spectral accelerations S_a^{min} and S_a^{max} per Step 1, above.

3. Split the range of spectral acceleration, S_a^{min} to S_a^{max}, into m intervals ($m = 8$ is recommended); identify the midpoint spectral acceleration and the mean annual frequency of exceedance at each end of the interval (see Figure 4-3).

4. From the hazard curve, extract the mean annual frequency of exceedance of the midpoint spectral acceleration for each interval. Calculate the mean annual probability of occurrence, which is used to determine average annual losses. The mean annual probability of occurrence of ground motions within an interval, $\Delta\lambda_i$, is the difference between the mean annual frequencies of exceedance at the end points of the interval.

5. Develop a target spectrum for each interval, using the mean annual frequency of exceedance of each midpoint spectral acceleration. This can be done using tools on the Open Seismic Hazard Analysis website, http://www.opensha.org/, or the USGS Unified Hazard Tool, available at https://earthquake.usgs.gov/hazards/interactive/ (last accessed March 15, 2018).

6. For each target spectrum, select and scale suites of n ground motion pairs using Steps 2 through 4 for intensity-based assessments, above.
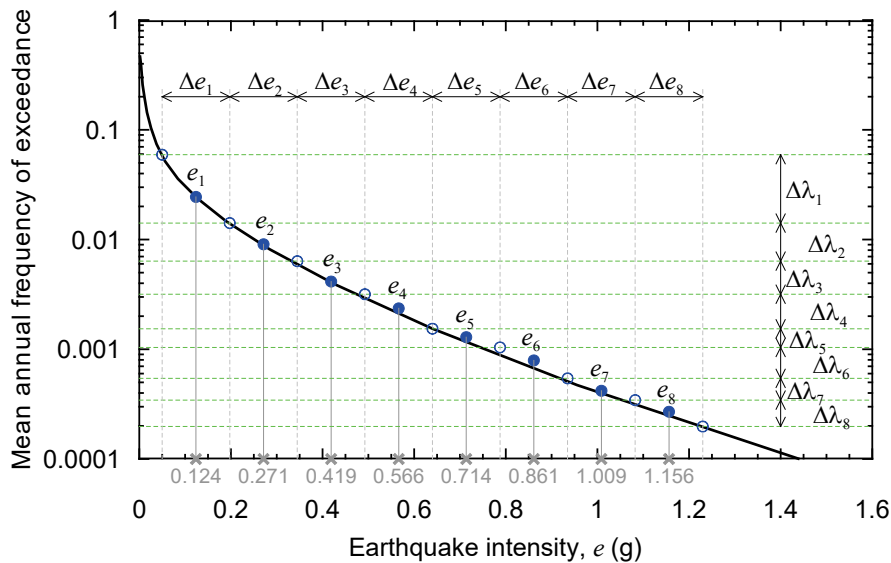
Figure 4-3   Example hazard characterization for time-based assessments showing intensity intervals, midpoint spectral accelerations, mean annual frequencies of exceedance, and mean annual probabilities of occurrence.

4.5 Simplified Analysis

This section provides procedures for earthquake hazard characterization for use in the simplified analysis procedure described in Chapter 5.

4.5.1 Intensity-Based Assessments

For intensity-based assessments, earthquake intensity is defined by any 5% damped, elastic, horizontal acceleration response spectrum. The simplified analysis procedure uses spectral response accelerations at the fundamental period of translational response in each of two orthogonal directions, T_1^X and T_1^Y, derived from that spectrum.

4.5.2 Scenario-Based Assessments

In scenario-based assessments using the simplified analysis procedure, earthquake hazard should be characterized as follows:

1. Select the magnitude and site-to-source distance for the scenario event.

2. Select an appropriate ground motion prediction equation for the region, site soil type, and source characteristics.

3. Determine the median values of the spectral response acceleration at the periods of the first translational mode along each axis of the building, T_1^X and T_1^Y.

4.5.3 Time-Based Assessments

Time-based assessments make use of site-specific seismic hazard curves. Guidance on selecting an appropriate range of intensities is provided in Section 4.4.2. In time-based assessments using the simplified analysis procedure, earthquake hazard should be characterized as follows:

1. Develop a seismic hazard curve for $S_a(\overline{T})$.

2. Compute the spectral accelerations S_a^{min} and S_a^{max}.

3. Split the range of spectral acceleration, S_a^{min} to S_a^{max}, into m intervals; ($m = 8$ is recommended); identify the midpoint spectral acceleration and the mean annual frequency of exceedance at each end of the interval (see Figure 4-3).

4. From the hazard curve, extract the mean annual frequency of exceedance of the midpoint spectral acceleration for each interval. Calculate the mean annual probability of occurrence, which is used to determine average annual losses. The mean annual probability of occurrence of ground motions within an interval, $\Delta\lambda_i$, is the difference between the mean annual frequencies of exceedance at the end points of the interval.

5. Develop a spectrum (e.g., UHS, CMS, or CS) for each mean annual frequency of exceedance of Step 3.

6. For each of the *m* spectra, determine the values of the spectral response acceleration at the periods of the first translational mode along each axis of the building, T_1^X and T_1^Y.

Chapter 5
Analyze Building Response

5.1   Introduction

Structural analysis is used to evaluate building response to earthquake shaking and produce estimated median values of structural response parameters that are predictive of structural and nonstructural damage. Key response parameters include floor accelerations, floor velocities, story drift ratios, and residual drift ratios.

This chapter presents two alternative analysis procedures that can be used to predict peak values and estimate dispersion in structural response. Section 5.2 provides guidance on using nonlinear response history analysis to predict median response and dispersion. Section 5.3 describes a simplified analysis procedure for predicting median response and dispersion using linear static analysis and the yield strength of the structure. Section 5.4 presents equations for calculating residual drift ratios based on nonlinear response history analysis or simplified analysis results.

The procedures in the chapter are not suitable for evaluation of building collapse. The procedures of Chapter 6 should be used for estimating the collapse capacity of a structure.

5.2   Nonlinear Response History Analysis

Nonlinear response history analysis can be used to assess performance of any structure at any ground shaking intensity. Nonlinear response history analysis is used to generate sets of demands, such as story drift ratios, floor accelerations, and floor velocities, which are predictive of performance. These sets are used to develop statistics including median values and dispersions for each demand parameter of interest, and to derive correlations between different demands in the set.

The following sections provide limited guidance on nonlinear modeling for performance assessment. Comprehensive guidance on nonlinear simulation of building response is beyond the scope of this report. More detailed information can be found in NIST GCR 17-917-45, *Recommended Modeling Parameters and Acceptance Criteria for Nonlinear Analysis in Support of Seismic Evaluation, Retrofit, and Design* (NIST, 2017a), NIST GCR 17-917-46v1, *Guidelines for Nonlinear Structural Analysis for Design of Buildings,*

> Structural analysis is used to provide median estimates of key response parameters that are predictive of structural and nonstructural damage.

> Analysis procedures include nonlinear response history and simplified analysis.

Part I – General (NIST, 2017b), NIST GCR 17-917-46v2, *Guidelines for Nonlinear Structural Analysis for Design of Buildings, Part IIa – Steel Moment Frames* (NIST, 2017c), NIST GCR 17-917-46v3, *Guidelines for Nonlinear Structural Analysis for Design of Buildings, Part IIb – Reinforced Concrete Moment Frames* (NIST, 2017d), NIST GCR 10-917-5, *Nonlinear Structural Analysis for Seismic Design: A Guide for Practicing Engineers* (NIST, 2010a), PEER/ATC-72-1, *Modeling and Acceptance Criteria for Seismic Design and Analysis of Tall Buildings* (ATC, 2010), and FEMA P-440A, *Effects of Strength and Stiffness Degradation on Seismic Response* (FEMA, 2009c).

5.2.1   Modeling

> Buildings should be modeled, analyzed, and assessed as three-dimensional assemblies of components, including all elements that provide measurable strength and stiffness.

> **Second Edition Update**
> Stiffening effect of gravity systems has been studied.

Buildings should be modeled, analyzed, and assessed as three-dimensional assemblies of components, including the foundation, and considering soil-structure interaction effects, as necessary. All structural framing and nonstructural components that contribute to the strength or stiffness of the building should be explicitly included in the analytical model. The stiffening effect of gravity systems and nonstructural components can result in actual building periods that are significantly shorter than that estimated using bare structural frames. Background documents FEMA P-58/BD-3.7.17 and FEMA P-58/BD-3.7.18 provided in *Volume 3 – Supporting Electronic Materials and Background Documentation* present additional discussion on these effects. The building code has long recognized stiffening effects by placing an upper limit on calculated periods used for design purposes. The reduction in estimated losses obtained using realistic models that properly account for stiffening effects can be significant, especially at low levels of ground shaking and for buildings with flexible structural systems such as moment-resisting frames or buckling-restrained braced frames.

Modeled components should typically include nonlinear representation of force-deformation behavior. Elastic component representations should only be substituted for nonlinear component models if elastic response is confirmed for the ground motion intensities under consideration. Components can be modeled using a variety of techniques, ranging from frame elements with concentrated plastic hinges, to detailed finite element and fiber element representations. Strength and stiffness degradation should be considered to the extent that these behaviors are expected to influence structural response at the intensities under consideration. Component modeling parameters should be verified against test data, or appropriate idealized backbone response curves, such as those recommended in PEER/ATC-72-1 and ASCE/SEI 41-13, *Seismic Evaluation and Retrofit of Existing Buildings* (ASCE, 2014), should be used.

The goal of an analysis used for performance assessment is to generate an estimate of the expected response of the building, and its components, to earthquake shaking. Median values of modeling parameters (e.g., initial stiffness, yield strength, plastic deformation limits) should be used, if known. However, mean values are more commonly available than median values, and can be used where insufficient information is available to accurately characterize the median and distribution of modeling parameters.

Component Force-Deformation Relationships

Element and component models are characterized by force-deformation relationships like those shown in Figure 5-1, with a single force parameter (e.g., axial load, shear, or moment), Q, plotted against a characteristic displacement (or rotation) parameter, Δ. Force-deformation behavior is typically characterized by an initial stiffness, yield strength, peak strength, plastic deformation capacity, and residual strength. The characteristic strength and deformation quantities shown in the figure are useful indices for calibration, validation, or comparison of component models.

> Nonlinear component behavior is typically characterized by an initial stiffness, yield strength, peak strength, plastic deformation capacity, and residual strength.
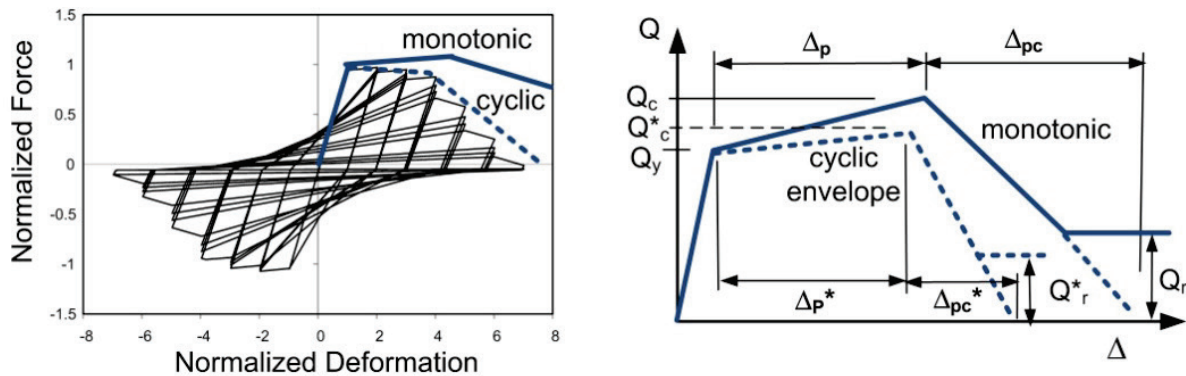
Figure 5-1   Generalized component force-deformation behaviors.

Historically, the term "backbone curve" has referred to many different things, and component backbone relationships can be envelopes of monotonic or cyclic loading response (FEMA, 2009c). The maximum strength that a component can develop at a given level of deformation is termed the force-displacement capacity boundary, and is generally equal to the response of the component to monotonic loading. A force-deformation curve that envelopes the hysteretic behavior of a component is termed the cyclic envelope. Cyclic envelopes are not unique, and they depend on the loading protocol used in component testing. Deformation capacities, peak strength, and residual strength parameters typically degrade under repeated cyclic loading.

> Historically, the term "backbone curve" has referred to many different things, and component backbone relationships can be envelopes of monotonic or cyclic loading response.

Force-deformation relationships such as those presented in ASCE/SEI 41-13 (Figure 5-2), are defined based on a cyclic envelope curve to approximately capture cyclic degradation effects that are not explicitly included in the analytical model. In Figure 5-2, the "a", "b" and "c" parameters of ASCE/SEI 41-13 nonlinear force-deformation relationships are comparable to the Δ_p*, $\Delta_{pc}*$ and Q_r* parameters of Figure 5-1.
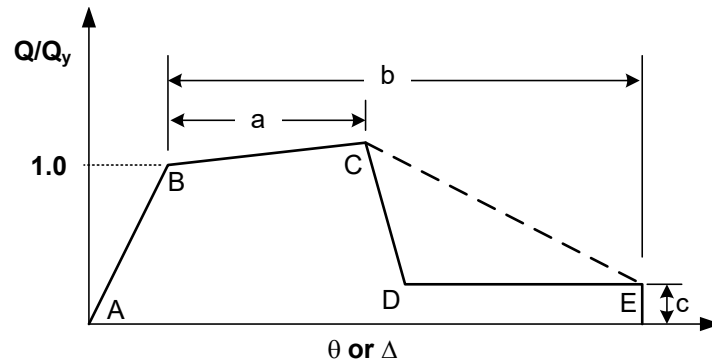
Figure 5-2   Generalized force-deformation relationship adapted from ASCE/SEI 41-13 (ASCE, 2014).

> The choice of backbone curve (monotonic or cyclic) depends on the capabilities of the analytical model.

The choice of backbone curve (monotonic or cyclic) depends on whether the analytical model is capable of explicitly simulating cyclic degradation or not. Direct modeling of cyclic degradation begins with a monotonic backbone curve, and degrades this relationship as the analysis proceeds, considering the cyclic loading history that is imposed on the component. Indirect modeling of cyclic degradation utilizes a cyclic envelope to define the component backbone curve, and additional cyclic deterioration is ignored. Although it is desirable to employ direct modeling of cyclic degradation, few commercial software packages have elements capable of doing so, and indirect modeling is most often used.

The envelope of component force-deformation behavior has a significant effect on overall building response (FEMA, 2009c). Types of degradation include cyclic degradation and in-cycle degradation, as illustrated in Figure 5-3. Cyclic degradation is characterized by loss of strength and stiffness occurring in subsequent cycles. In-cycle degradation is characterized by loss of strength and negative stiffness occurring within a single cycle. Studies have shown that components exhibiting cyclic degradation can have stable dynamic response, but components exhibiting in-cycle degradation are prone to dynamic instability (i.e., collapse). Differences are less significant for ductile components where imposed deformations do not exceed the peak strength (less than Δ_p or Δ_p* in Figure 5-1).
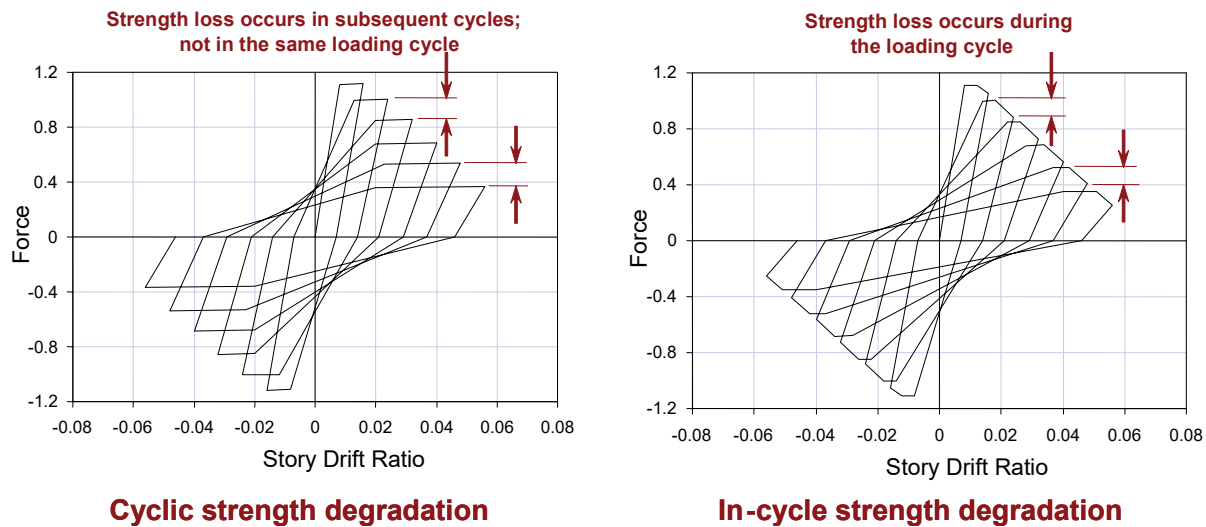
Figure 5-3   Comparison of cyclic versus in-cycle degradation of component response (FEMA, 2009c).

Ideally, the cyclic envelope should be determined based on tests conducted using several different loading protocols. One such protocol is given by ATC-24, *Guidelines for Cyclic Seismic Testing of Components of Steel Structures* (ATC, 1992), which represents the loading demands of a characteristic earthquake. Further guidance on modeling component force-deformation behavior is provided in NIST GCR 17-917 45, NIST GCR 17-917-46v1 through v3, PEER/ATC-72-1, FEMA P-440A, and Ibarra et al. (2005).

Geometric Nonlinear Effects

P-delta effects can significantly increase displacements and internal member forces in the post-yield response of a structure. *P*-delta effects should, therefore, be accounted for in nonlinear analysis, even when elastic design provisions would otherwise allow them to be neglected.

Gravity Loads

Gravity loads based on expected dead and live loading should be considered in the analysis, along with the entire seismic mass of the structure. Expected live loads typically include about 25% of the unreduced design live load.

Damping

In nonlinear response history analysis, most energy dissipation is modeled directly through the hysteretic response of structural components. Therefore, equivalent viscous damping assigned in the analytical model should be limited to energy dissipation that is not otherwise captured by element hysteresis. Generally, this includes: (1) energy dissipation associated with

> Most energy dissipation is explicitly modeled through the hysteretic response of structural components. Equivalent viscous damping assigned in the analytical model should be limited to 5% or less in typical buildings, and 3% or less in tall buildings.

components that are modeled as elastic but are expected to experience limited cracking or yielding; (2) architectural cladding, partitions and finishes, that are not modeled; and (3) interaction between the soil and foundation, when soil-structure interaction effects are not modeled. Equivalent viscous damping should typically be assigned in the range of 1% to 5% of critical damping in the predominant vibration modes of the structure. Values of 3% or less should be used for tall buildings and other structures where damping effects associated with foundations and nonstructural cladding are small relative to the structural hysteretic effects. Additional information on damping can be found in *Guidelines for Performance-Based Seismic Design of Tall Buildings* (PEER, 2017).

When energy dissipation devices (e.g., dampers) are installed in a structural system, these components should be modeled explicitly using appropriate component models, including velocity terms to capture viscous effects and nonlinear springs to capture hysteretic effects. Additional guidance on modeling of damping is provided in PEER/ATC-72-1.

Diaphragms

Diaphragms should be modeled using appropriate stiffness assumptions. A diaphragm can be classified as rigid if the maximum in-plane lateral deformation of the diaphragm is less than one half of the average drift in the stories above and below the subject diaphragm for the same intensity of shaking. Diaphragms that do not meet this criterion, and diaphragms in which significant shear transfer occurs between vertical lines of resistance (i.e., out-of-plane offset discontinuities), should be modeled explicitly using finite elements. Mass should be distributed across the floor (and roof) to capture torsional and in-plane response. If the diaphragms will not remain elastic at the ground motion intensities under consideration, a nonlinear representation should be used.

Soil-Structure Interaction

Foundations likely to uplift or slide at the ground motion intensities under consideration should be modeled to capture these effects. Where compliance at the soil-foundation interface will significantly alter the dynamic characteristics of the structure, or change the pattern of deformation response, this should also be modeled.

Soil-structure interaction effects will generally be most significant for stiff buildings founded on soft soils. NIST GCR 12-917-21, *Soil-Structure Interaction for Building Structures* (NIST, 2012), introduced the structure-to-soil stiffness ratio, $h/(V_sT)$, as a test for the significance of soil-structure

interaction effects. In this equation, h is the effective height of the structure, taken as to-thirds of the modeled building height, V_s is the average effective overburden-corrected shear wave velocity of the soil profile below the site, and T is the fixed-base period of the building in the direction under consideration. Values of $h/(V_sT)$ exceeding 0.1 indicate that soil-structure interaction effects are likely to be significant. See NIST GCR 12-917-21 for detailed guidance on the calculation and interpretation of the structure-to-soil stiffness ratio.

Appendix B provides limited guidance on modeling soil-foundation-structure systems together with a discussion on the likely impact of soil-structure interaction on foundation input motions. NIST GCR 12-917-21 provides detailed guidance on procedures that can be used to model soil-foundation springs and dashpots, together with example applications. Alternatively, approximate methods of soil-structure interaction analysis found in FEMA 440, *Improvement of Nonlinear Static Seismic Analysis Procedures* (FEMA, 2005), can also be used.

Foundation Embedment

Depending on the site characteristics and the dynamic properties of the building, foundation input motions (i.e., the ground motions imparted at the base of a structure) can be substantially different from free-field ground motions. Known as kinematic interaction effects, differences between free-field and foundation input motions are another result of soil-structure interaction effects. For structures with basements exceeding one story in depth, consideration should be given to modifying free-field motions to derive foundation input motions for analysis of the structure. Site-specific response analysis can be used for this purpose. Approximate procedures can also be used to reduce the amplitude of the target response spectrum. Appendix B and NIST GCR 12-917-21 provide more detailed guidance on this topic.

Non-Simulated Deterioration and Failure Modes

Ideally, all significant modes of component deterioration (and failure) should be incorporated directly into the analytical model. In new building designs that employ ductile detailing provisions and capacity design concepts, nonlinear analysis can often simulate the complete response of the building because nonlinear behavior is controlled in components with predictable deterioration characteristics. In certain structural systems, however, components do not have well-defined post-yield behaviors, and there can be rapid, non-ductile, strength and stiffness degradation that cannot be simulated

> Non-simulated failure modes involve the selection of criteria beyond which the response of an individual component, or the overall model, cannot be trusted to be a reliable indicator of building response.

in a nonlinear analysis. For example, premature shear failures in concrete columns or walls, torsional-flexural buckling of laterally unbraced steel members, or connection and splice failures are all behaviors that are difficult to include in an analytical model.

In such cases, steps should be taken to assure that modeling does not overestimate the available structural resistance when failure modes have not been explicitly simulated. Particular attention should be given to failure modes that might trigger building collapse. One technique involves the definition of non-simulated failure criteria, beyond which the response of an individual component, or the overall model, cannot be trusted to be a reliable indicator of building response.

Foundations are rarely included in building models, but can be damaged by earthquake shaking. Damage to vulnerable foundation components can be treated as non-simulated failure modes, but appropriate fragility and consequence functions will need to be assigned to include these impacts in loss calculations. For buildings with vulnerable foundation components, analyses that produce failure-level demands should not be considered valid for purpose of developing response statistics and generation of realizations.

5.2.2 Number of Analyses

The number of ground motion pairs necessary to obtain valid estimates of median response was discussed in Chapter 4. It depends on how well the geomean spectral shape of the scaled motions matches the shape of the target spectrum in the period range T_{min} to T_{max}. When ground motions are selected without consideration of spectral shape, analyses using 11 pairs of properly scaled motions can provide a reasonable estimate of median response, defined as 75% confidence of being within plus or minus 20% of the median (Huang et al., 2011). Limited study suggests that when a good match between the spectral shape of the selected motions and the target spectrum is obtained, use of fewer records can provide a reasonable prediction of median response. Regardless of the goodness of fit, a minimum of 7 ground motion pairs is recommended because of extremely poor prediction of record-to-record variability obtained in small suites of ground motions.

For time-based assessments, nonlinear analyses are conducted at m different intensity levels representing intervals along the seismic hazard curve. A value of $m = 8$ is recommended, although it may be possible to use fewer intervals for some structures and seismic hazard environments. At each intensity level, at least 7 ground motion pairs should be used. If the selected

motions do not have a good match to the spectral shape of the target spectrum, 11 or more motions may be necessary.

When performing nonlinear response history analysis at values of ground shaking intensity, $S_a(\overline{T})$, that approach the median collapse capacity of the structure, it is likely that one or more of the n sets of ground motion pairs will result in prediction of structural collapse, as evidenced by solution instability, predicted story drift ratios exceeding the range of validity of the analytical model, or predicted demands that suggest the onset of one or more non-simulated collapse modes. Although it is possible to obtain additional ground motions pairs and perform additional analyses to replace the motions that produce collapse, this is not always necessary, and for shaking intensities where the collapse probability is high, it is impractical to do.

The following procedures are recommended when analytically predicted collapse is encountered in q or more sets of the n ground motion pairs at a given ground motion intensity:

- Simulated demands sets used for loss calculation are conditioned on the non-collapsed state of the structure. Therefore, analysis results from any ground motion pair that results in prediction of collapse, either simulated or non-simulated, should not be included in the suites of analytical results used to generate simulated demands sets. These analyses, however, can useful in developing the collapse fragility of the structure, as described in Chapter 6.

- If the remaining number of ground motion pairs for which collapse did not occur (n-q) is greater than or equal to 7, it is acceptable to use the results from the remaining (n-q) analyses to obtain estimates of demand at this ground motion intensity. No further analyses are required at this intensity level.

- If the remaining number of ground motion pairs for which collapse did not occur (n-q) is less than or equal to 7, then additional ground motion pairs should be selected until at least 7 analyses that do not predict collapse are obtained. It is important to note that if the ground shaking intensity at which analysis is performed is associated with a collapse probability greater than 0.5, a very large number of analyses may be necessary to obtain 7 runs that do not predict collapse. At such ground motion intensities, building performance will be dominated by the probability of collapse. Therefore, it is recommended that ground motion intensities associated with collapse probabilities greater than 0.5 not be used to determine demand. Chapter 6 provides information on

> The number of analyses required for each scenario or intensity level depends on the match to the shape of the target spectrum. When the match is good, at least 7 pairs of motions should be used. When the match is poor, 11 pairs of motions, or more, are recommended.

determining the collapse probability at different ground motion intensities.

5.2.3 Floor Velocity and Floor Acceleration

Typical output from nonlinear response history analysis includes peak values of displacement, nonlinear deformation demands, and component forces. Although some component fragility functions use component force or deformation demand as the predictive demand parameter, most fragility functions are based on story drift ratio, floor acceleration or floor velocity. Most structural analysis software does not directly provide results in these forms, so some post-processing may be needed to obtain these quantities. Drift ratio is the difference in displacement at adjacent floor levels divided by the story height. Floor velocity can be calculated by numerical differentiation, which consists of dividing the difference in floor displacements at adjacent time steps by the size of the time step. If floor acceleration is not directly available, it can be obtained by taking a second numerical differential, which consists of dividing the difference in computed floor velocities at adjacent time steps by the size of the time step.

5.2.4 Effective Drift

For slender concrete shear walls, the key demand parameter is effective drift, which is the drift at the effective height of the wall. The location of the effective height varies based on the loading profile, but generally ranges between 50-75% of the building height.

5.2.5 Quality Assurance

Nonlinear analysis is a complex process. To assure meaningful results, models should be carefully checked to establish their reliability. The following steps are suggested:

- Results of linear dynamic (response spectrum) analyses should be compared to results of nonlinear response history analyses to assess the degree of nonlinearity in the structure under various ground motion intensities, and to confirm that under low intensity motions, the nonlinear model is behaving in a manner that is consistent with the linear model.

- Nonlinear static analyses under lateral and gravity loading should be used to interrogate inelastic mechanisms, plastic deformations, and inelastic force redistributions, to confirm these with expected behavior.

- Nonlinear analyses should be run both with and without *P*-delta effects to establish the sensitivity of the results to gravity loads and large deformations.

Second Edition Update
Additional guidance is provided for slender concrete shear walls.

Nonlinear analysis is a complex process. To assure meaningful results, models should be carefully checked to establish their reliability.

- Plots of the hysteretic response of selected components should be reviewed for conformance with the modeled component force-deformation behavior.

5.2.6 Uncertainty

Nonlinear response history analysis is used to provide estimates of median response. If a sufficient number of nonlinear analyses are performed on a sufficient number of models with varying modeling assumptions, it is possible to explicitly calculate uncertainties in demand associated with modeling assumptions, and the relationships (or correlations) between demand parameters. However, it is usually impractical to perform a sufficient number of analyses to obtain statistically valid information on dispersion or correlation in calculated response quantities. In this methodology, demand parameter dispersions are estimated based on judgment regarding the uncertainty inherent in response calculation. Because of probable inaccuracies in dispersion and correlation that would be observed in small suites of analyses, use of assumed values of uncertainty is considered the best available information.

> It is usually impractical to perform a sufficient number of analyses to obtain statistically reliable estimates of dispersion and correlation in calculated response quantities.

Three sources of demand parameter uncertainty are considered: (1) modeling uncertainty; (2) record-to-record variability; and (3) ground motion variability. These are discussed below. Chapter 7 and Appendix G describe how the computed variability in response is augmented to account for modeling uncertainty and, in the case of scenario-based assessments, ground motion variability, in the generation of simulated demand sets for loss computations.

Modeling Uncertainty

The demand distributions for selected ground motion intensities are characterized by median values and dispersions. These can be obtained through probabilistic analysis of a large family of building models in which component mechanical properties are random variables with user-specified distributions. However, the computational effort required to do this would be very large. Therefore, best-estimate analytical models are used for analysis, and calculated dispersions are augmented by judgmentally determined values accounting for modeling uncertainty.

> Modeling uncertainty, β_m, results from inaccuracies in component modeling, damping, and mass assumptions. These uncertainties have been associated with the level of building definition and construction quality assurance, β_c, and the quality and completeness of the nonlinear analysis model, β_q.

Modeling uncertainty, β_m, results from inaccuracies in component modeling, damping, and mass assumptions. For the purpose of estimating β_m, these uncertainties have been associated with the level of building definition and construction quality assurance, β_c, and the quality and completeness of the

nonlinear analysis model, β_q. The total modeling dispersion can be estimated as follows:

$$\beta_m = \sqrt{\beta_c^2 + \beta_q^2} \qquad (5\text{-}1)$$

Building definition and construction quality assurance, β_c. This component of modeling uncertainty accounts for the possibility that the actual properties of structural elements (e.g., material strength, section properties, and details such as rebar location) might be different than those otherwise believed to exist. Values of β_c are assigned based on the quality and confidence associated with building definition. For existing buildings, this will depend on the quality of the available drawings documenting the as-built construction, and the level of field investigation performed to verify their accuracy. For new buildings, this will be determined based on assumptions regarding how well actual construction will match the design. Table 5-1 provides recommended values for β_c under representative conditions. Judgment is necessary when selecting values from the table.

Table 5-1   Values of Dispersion for Construction Quality Assurance, β_c

Building Definition and Construction Quality Assurance	β_c
Superior Quality, New Buildings: The building is completely designed and will be constructed with rigorous construction quality assurance, including special inspection, materials testing, and structural observation. *Superior Quality, Existing Buildings*: Drawings and specifications are available and field investigation confirms they are representative of the actual construction, or if not, the actual construction is understood. Material properties are confirmed by extensive materials testing.	0.10
Average Quality, New Buildings: The building design is completed to a level typical of design development; construction quality assurance and inspection are anticipated to be of limited quality. *Average Quality, Existing Buildings:* Documents defining the building design are available and are confirmed by visual observation. Material properties are confirmed by limited materials testing.	0.25
Limited Quality, New Buildings: The building design is completed to a level typical of schematic design, or other similar level of detail. *Limited Quality, Existing Buildings*: Construction documents are not available and knowledge of the structure is based on limited field investigation. Material properties are based on default values typical for buildings of the type, location, and age of construction.	0.40

Quality and completeness of the analytical model, β_q. This component of modeling uncertainty recognizes that hysteretic models may not accurately capture the behavior of structural components, even if the details of construction are precisely known. Values of β_q are assigned based on the completeness of the mathematical model and how well the component deterioration and failure mechanisms are understood and implemented. Dispersion should be selected based on an understanding of how sensitive

response predictions are to key structural parameters (e.g., strength, stiffness, deformation capacity, in-cycle versus cyclic degradation) and the likely degree of inelastic response. Table 5-2 provides recommended values for β_q.

Table 5-2   Values of Dispersion for Quality of the Analytical Model, β_q

Quality and Completeness of the Analytical Model	β_q
Superior Quality: The numerical model is robust over the anticipated range of response. Strength and stiffness deterioration and all likely failure modes are explicitly modeled. Model accuracy is established with data from large-scale component tests through failure. *Completeness*: The mathematical model includes all structural components and nonstructural components in the building that contribute to strength or stiffness.	0.10
Average Quality: The numerical model for each component is robust over the anticipated range of displacement or deformation response. Strength and stiffness deterioration is fairly well represented, though some failure modes are simulated indirectly. Accuracy is established through a combination of judgment and large-scale component tests. *Completeness*: The mathematical model includes most structural components and nonstructural components in the building that contribute significant strength or stiffness.	0.25
Limited Quality: The numerical model for each component is based on idealized cyclic envelope curves from ASCE/SEI 41-13 or comparable guidelines, where strength and stiffness deterioration and failure modes are not directly incorporated in the model. *Completeness*: The mathematical model includes structural components in the seismic-force-resisting system.	0.40

Selection of β_q values should be guided by the expected degree of inelastic response and likelihood of component failure or building collapse. For example, component models in a building that are expected to remain elastic (i.e., no structural damage) need not address component deterioration, failure modes need not be simulated, and a value of $\beta_q = 0.1$ is likely appropriate. Conversely, if collapse simulations are being performed, robust numerical models are required for all components expected to suffer significant damage. If such models have not been validated by large-scale testing, the model confidence should be low, and a value of β_q in the range of 0.3 to 0.5 is likely appropriate.

Regardless of the relative values of β_c and β_q derived using Table 5-1 and Table 5-2, the total uncertainty computed using Equation 5-1 should not be taken greater than 0.5.

Record-to-Record Variability

In structures experiencing nonlinear response, or response in multiple modes, each record will produce somewhat different predictions of peak response quantities, resulting in record-to-record variability. Use of a small number of

ground motion pairs will either underestimate or overestimate true record-to-record variability in each response quantity as well as the correlation between response quantities.

Unless a very large number of ground motion pairs are used (on the order of 30 or more), values of dispersion obtained from limited suites of analyses will generally be inaccurate. This methodology, however, assumes that record-to-record response variability and demand correlation coefficients computed using small numbers of ground motions are sufficiently accurate for performance assessment, as augmented for other sources of uncertainty.

Ground Motion Variability

For scenario-based assessment, it is necessary to account for uncertainty in the shape and amplitude of the target spectrum. Table 5-3 lists suggested values for ground motion spectral demand dispersion, β_{gm}, based on uncertainty in attenuation relationships in widely accepted ground motion prediction equations for Western North America (WNA), the Central and Eastern United States (CEUS), and the Pacific North West (PNW). Values of β_{gm} appropriate to the specific ground motion prediction equations used to derive the target spectrum should be substituted for these, when known.

Table 5-3   Default Values of Dispersion for Ground Motion Uncertainty, β_{gm}

$\overline{T}, T_1$ (sec)	β_{gm}		
	WNA	CEUS	PNW
<0.20	0.60	0.53	0.80
0.35	0.60	0.55	0.80
0.5	0.61	0.55	0.80
0.75	0.64	0.58	0.80
1.0	0.65	0.60	0.80
1.50	0.67	0.60	0.85
≥2.0	0.70	0.60	0.90

5.3   Simplified Analysis

The simplified analysis procedure uses linear models, static analyses, and an estimate of the lateral yield strength of the structure to generate median values of demands that are predictive of damage. Structures are assumed to have independent translational response in each of two horizontal axes, denoted *X* and *Y*, and separate analyses are performed along each axis. The effects of vertical earthquake shaking, torsion, and soil-structure interaction are neglected.

The simplified analysis procedure is limited in its ability to estimate nonlinear response. Assumptions underlying the simplified analysis procedure include:

- The framing systems are independent along each horizontal axis of the building, response along each axis is uncoupled, and torsional response can be ignored.

- The building is regular in plan and elevation (i.e., there are no substantial discontinuities in strength and stiffness).

- Story drift ratios do not exceed 4 times the corresponding yield drift ratio, excessive degradation in strength and stiffness does not occur, and assumptions of bilinear elastic-plastic component behavior are reasonable.

- Story drifts ratios are limited to 4%, below which P-delta effects can be considered insignificant.

- The building is less than 15 stories tall, and higher mode contributions to response are not considered significant.

Simplified analysis of buildings that do not conform to these assumptions may not be reliable. Even for buildings that do conform to these assumptions, simplified analysis will entail greater uncertainty as to the true value of medians and dispersions associated with the calculated demands. As a result, use of the simplified analysis procedure will result in performance impacts and calculated losses that are somewhat different from those computed using nonlinear analysis methods.

5.3.1   Modeling

Mathematical models for simplified analysis should appropriately represent the distribution of mass and stiffness throughout the building. All elements that contribute significantly to lateral strength or stiffness should be included in the model, whether or not they are considered to be structural or nonstructural, or part of the seismic-force-resisting system. ASCE/SEI 41-13 provides guidance for modeling the strength and stiffness of typical building components appropriate for use in simplified analysis. The mathematical model is used to establish the fundamental period and first mode shape in each of two orthogonal directions. These periods and mode shapes are used to compute pseudo lateral forces that are applied in a static analysis of the model to determine story drift ratios. This information, together with estimates of peak ground acceleration, peak ground velocity, and the yield strength of the structure, is used to compute median estimates of peak story

drift ratio, peak floor acceleration, and peak floor velocity in each orthogonal direction.

The yield strength of the structure can be estimated using plastic analysis concepts, nonlinear static analysis in accordance with ASCE/SEI 41-13, or the response modification coefficient, R, and the overstrength factor, Ω_0, specified in ASCE/SEI 7-16, *Minimum Design Loads and Associated Criteria for Buildings and Other Structures* (ASCE, 2017). Use of R and Ω_0 is only appropriate when minimal information is available on the actual design of the structure, as may occur during schematic or preliminary design phases. In such cases, the yield strength can be taken in the range given by:

$$\frac{1.5S_a(T)W}{R/I} \le V_y \le \frac{\Omega_0 S_a(T)W}{R/I} \tag{5-2}$$

where $S_a(T)$ is the design spectral response acceleration evaluated at the fundamental period in the direction under consideration, and R, Ω_0, and I are the elastic design coefficients for structural system and occupancy of the building, as defined in ASCE/SEI 7-16.

5.3.2 Simplified Analysis Procedure

Figure 5-4 defines the floor level, story level, and floor height designation numbering system used in the simplified analysis procedure.
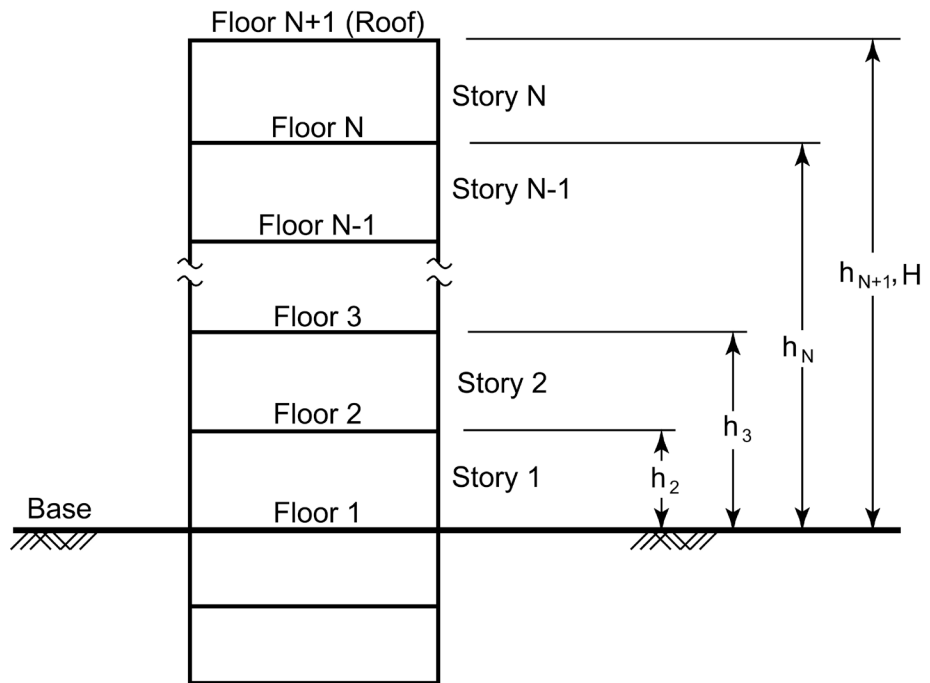
Figure 5-4   Definition of floor levels, story numbers, and floor heights used in the simplified analysis procedure.

Pseudo Lateral Force

In each direction, a pseudo lateral force, V, is used to compute story drift ratios, velocities, and accelerations. The force, V, in each direction is computed as:

$$V = C_1 C_2 S_a(T_1) W_1 \qquad (5\text{-}3)$$

where C_1 is an adjustment factor for inelastic displacements; C_2 is an adjustment factor for cyclic degradation; $S_a(T_1)$ is the 5% damped spectral acceleration at the fundamental period of the building, in the direction under consideration, for the selected level of ground shaking; and W_1 is the first modal effective weight in the direction under consideration, taken as not less than 80% of the total weight, W. If building response is elastic, coefficients C_1 and C_2 are set equal to 1.0.

The first mode effective weight, W_1, can be calculated as:

$$W_1 = \frac{\left(\sum\limits_{j=2}^{N+1} w_j \phi_{j1}\right)^2}{\sum\limits_{j=2}^{N+1} w_j \phi_{j1}^2} \qquad (5\text{-}4)$$

where w_j is the lumped weight at floor level j, ϕ_{j1} is the jth floor ordinate of the first mode deflected shape, N is the number of floors in the building above the base, and floor levels are as defined in Figure 5-4. Alternatively, W_1 can be taken as $C_m W$, where C_m is as defined in ASCE/SEI 41-13.

The adjustment factor, C_1, is computed as:

$$
\begin{aligned}
C_1 &= 1 + \frac{S-1}{0.04a} & \text{for } T_1 \le 0.2 \, \text{sec} \\
&= 1 + \frac{S-1}{aT_1^2} & \text{for } 0.2 < T_1 \le 1.0 \, \text{sec} \qquad (5\text{-}5) \\
&= 1 & \text{for } T_1 > 1.0 \, \text{sec}
\end{aligned}
$$

where T_1 is the fundamental period of the building in the direction under consideration, a is a function of the soil site class (taken as 130, 130, 90, 60, and 60 for ASCE/SEI 7-16 site classes A, B, C, D and E, respectively) and S is a strength ratio given by:

$$S = \frac{S_a(T_1) W}{V_{y1}} \qquad (5\text{-}6)$$

where V_{y1} is the estimated yield strength of the building in first mode response, and W is the total weight. The estimated yield strength, V_{y1}, should

be determined by a suitable nonlinear static analysis procedure, such as that contained in ASCE/SEI 41-13. If S has a value less than or equal to 1.0, then C_1 is taken as unity.

When the value of S is less than or equal to 1.0, C_2 is also taken as unity. When S is greater than 1.0, C_2 is computed as:

$$
\begin{aligned}
C_2 &= 1 + \frac{(S-1)^2}{32} && \text{for } T_1 \leq 0.2 \sec \\
&= 1 + \frac{1}{800}\frac{(S-1)^2}{T_1^2} && \text{for } 0.2 < T_1 \leq 0.7 \sec && \text{(5-7)} \\
&= 1 && \text{for } T_1 > 0.7 \sec
\end{aligned}
$$

If the building incorporates viscous or viscoelastic damping devices, the 5% damped spectral acceleration ordinate should be replaced by the value that corresponds to the first mode damping in the building. The procedures of ASCE/SEI 41-13 can be used to estimate the damping in a building equipped with viscous or viscoelastic energy dissipation devices, and to adjust the response spectrum for the effects of damping other than 5%.

Median Estimates of Demand

Median estimates of story drift ratio, Δ_i^*, floor acceleration, a_i^*, and floor velocity, v_i^*, from the simplified analysis procedure are computed using the following steps, as further described below:

1. Determine vertical distribution of forces by distributing the pseudo lateral force, V, over the height of the building.

2. Apply the lateral forces to the linear static model to compute floor displacements and uncorrected story drifts. Divide story drifts by story height to obtain story drift ratios.

3. Correct story drift ratios to account for inelastic behavior and higher mode effects.

4. Estimate peak floor acceleration at each floor from peak ground acceleration.

5. Estimate peak floor velocity at each floor from peak ground velocity.

Step 1 – Determine vertical distribution of forces. The pseudo lateral force, F_x, at floor level x, is given by:

$$
F_x = C_{vx}V \tag{5-8}
$$

where, C_{vx} is a vertical distribution factor given by:

$$C_{vx} = \frac{w_x h_x^k}{\displaystyle\sum_{i=2}^{N+1} w_i h_i^k} \tag{5-9}$$

and w_i is the lumped weight at floor level i; h_i (or h_x) is the height above the effective base of the building to floor level i (or x); and k is equal to 2.0 for a first mode period greater than 2.5 seconds, or equal to 1.0 for a first mode period less than or equal to 0.5 seconds (linear interpolation can be used for intermediate periods).

Step 2 – Compute floor displacements and uncorrected story drift ratios. The lateral forces, F_x, at each level are simultaneously applied to the linear static analysis model. The displacement of each floor relative to the base is computed. The uncorrected story drift ratio at each level, Δ_i, is determined as the difference between the lateral displacements of the floor levels immediately above and below the story, divided by the story height.

Step 3 – Correct story drift ratios to account for inelastic behavior and higher mode effects. Estimates of median story drift ratio, Δ_i^*, at each level i, are calculated as:

$$\Delta_i^* = H_{\Delta i}\left(S, T_1, h_i, H\right) \times \Delta_i \tag{5-10}$$

where $H_{\Delta i}\left(S, T_1, h_i, H\right)$ is the drift correction factor for story i computed from:

$$\ln\left(H_{\Delta i}\right) = a_0 + a_1 T_1 + a_2 S + a_3 \frac{h_{i+1}}{H} + a_4 \left(\frac{h_{i+1}}{H}\right)^2 + a_5 \left(\frac{h_{i+1}}{H}\right)^3 \tag{5-11}$$

$$\text{for } S \geq 1, \, i = 1 \text{ to } N$$

and the values of the coefficients a_0 through a_5 are obtained from Table 5-4 for structures less than 9 stories in height, and Table 5-5 for structures 10 to 15 stories in height; S is the strength ratio previously defined; T_1 is the first mode period; and H is the total building height above the base, as defined in Figure 5-4.

Step 4 – Estimate peak floor acceleration from peak ground acceleration. At the base of the building, peak floor acceleration is taken as equal to the peak ground acceleration. At other floor levels, i, the estimated median peak floor acceleration, a_i^*, relative to a fixed point in space, is derived from the peak ground acceleration using:

$$a_i^* = H_{ai}\left(S, T, h_i, H\right) \times PGA \quad \text{for } i = 2 \text{ to } N+1 \tag{5-12}$$

where PGA is the peak ground acceleration; $H_{ai}(S,T,h_i,H)$ is the acceleration correction factor for floor i computed from:

$$\ln(H_{ai}) = a_0 + a_1 T_1 + a_2 S + a_3 \frac{h_i}{H} + a_4 \left(\frac{h_i}{H}\right)^2 + a_5 \left(\frac{h_i}{H}\right)^3 \qquad (5\text{-}13)$$

$$\text{for } S \geq 1, i = 2 \text{ to } N+1$$

and the values of the coefficients a_0 through a_5 are obtained from Table 5-4 for structures less than 9 stories in height, and Table 5-5 for structures 10 to 15 stories in height. If the building response is elastic, S is taken as 1.0.

> **Second Edition Update**
> Tables 5-4 and 5-5 have been expanded to include correction factors for additional structural systems based on FEMA P-58/ BD-3.7.21.

Table 5-4   Correction Factors for Story Drift Ratio, Floor Velocity, and Floor Acceleration for 2-Story to 9-Story Buildings

Demand	Frame Type	a_0	a_1	a_2	a_3	a_4	a_5
Story drift ratio	Steel EBF[1]	0.90	-0.12	0.012	-2.65	2.09	0
	Steel SCBF[2]	0.75	0.18	-0.042	-2.45	1.93	0
	Steel BRBF[3]	0.33	0.14	-0.059	-0.68	0.56	0
	Moment Frame[4]	0.75	-0.044	-0.010	-2.58	2.30	0
	Wall	0.92	-0.036	-0.058	-2.56	1.39	0
Floor velocity	Steel EBF[1]	0.15	-0.10	0	-0.408	0.47	0
	Steel SCBF[2]	0.20	0.23	-0.074	-0.45	0.19	0
	Steel BRBF[3]	1.15	-0.47	-0.039	-0.043	0.47	0
	Moment Frame[4]	0.025	-0.068	0.032	-0.53	0.54	0
	Wall	-0.033	-0.085	0.055	-0.52	0.47	0
Floor acceleration	Steel EBF[1]	0.66	-0.27	-0.089	0.075	0	0
	Steel SCBF[2]	1.15	-0.47	-0.039	-0.043	0.47	0
	Steel BRBF[3]	0.92	-0.30	-0.042	-0.25	0.43	0
	Moment Frame[4]	0.66	-0.25	-0.080	-0.039	0	0
	Wall	0.66	-0.15	-0.084	-0.26	0.57	0

[1] Steel EBF = Steel eccentrically braced frames
[2] Steel SCBF = Steel special concentrically braced frames
[3] Steel BRBF = Steel buckling-restrained braced frames
[4] Moment Frame = Steel and reinforced concrete special moment-resisting frames

Step 5 – Estimate peak floor velocity from peak ground velocity. At the base of the building, peak floor velocity is taken as equal to the peak ground velocity, PGV. Peak ground velocity can be calculated by seismic hazard analysis for intensity- or time-based assessments, or by using a ground motion prediction equation for a scenario-based assessment. If detailed information on peak ground velocity is not available, PGV can be estimated along each building axis by dividing the spectral velocity at a period of one

second, $S_v(1.0 \text{ s})$, by a factor of 1.65 (Newmark and Hall, 1982; Huang and Whittaker, 2012).

Table 5-5   Correction Factors for Story Drift Ratio, Floor Velocity, and Floor Acceleration for 10-Story to 15-Story Buildings

Demand	Frame Type	a_0	a_1	a_2	a_3	a_4	a_5
Story drift ratio	Steel EBF[1]	1.91	-0.12	-0.077	-3.78	6.43	-3.42
	Steel SCBF[2]	1.26	0.053	-0.033	-6.93	10.62	-4.80
	Steel BRBF[3]	1.11	0.14	-0.057	-5.46	7.38	-2.88
	Moment Frame[4]	0.67	-0.044	-0.098	-1.37	1.71	-0.57
	Wall	0.86	-0.036	-0.076	-4.58	6.88	-3.24
Floor velocity	Steel EBF[1]	0.086	-0.10	0.041	0.45	-2.89	2.57
	Steel SCBF[2]	0.6	-0.11	-0.064	3.24	-6.69	4.45
	Steel BRBF[3]	0.81	-0.10	-0.092	2.38	-4.96	3.28
	Moment Frame[4]	-0.020	-0.068	0.034	0.32	-1.75	1.53
	Wall	-0.11	-0.085	0.11	0.87	-4.07	3.27
Floor acceleration	Steel EBF[1]	0.44	-0.27	-0.052	3.24	-9.71	6.83
	Steel SCBF[2]	0.63	-0.17	-0.046	3.52	-8.51	5.53
	Steel BRBF[3]	0.93	-0.191	-0.057	1.67	-4.60	3.06
	Moment Frame[4]	0.34	-0.25	-0.062	2.86	-7.43	5.10
	Wall	-0.13	-0.15	-0.10	7.79	-17.52	11.04

[1] Steel EBF = Steel eccentrically braced frames
[2] Steel SCBF = Steel special concentrically braced frames
[3] Steel BRBF = Steel buckling-restrained braced frames
[4] Moment Frame = Steel and reinforced concrete special moment-resisting frames

Spectral velocity at a period of 1 second can be derived from spectral acceleration at a period of one second using the formula:

$$S_v(1.0 \text{ s}) = \frac{S_a(1.0 \text{ s})}{2\pi} g \qquad (5\text{-}14)$$

where $S_a(1.0 \text{ s})$ is the spectral acceleration at 1 second period. Peak ground velocity can then be approximated as:

$$PGV = \frac{S_v(1.0 \text{ s})}{1.65} \qquad (5\text{-}15)$$

At other floor levels, i, the estimated median peak floor velocity, v_i^*, relative to a fixed point in space, is computed from the peak ground velocity using the formula:

$$v_i^* = H_{vi}(S, T, h_i, H) \times v_{si} \quad \text{for } i = 2 \text{ to } N + 1 \qquad (5\text{-}16)$$

where $H_{vi}(S, T, h_i, H)$ is computed from:

$$\ln\left(H_{vi}\right) = a_0 + a_1 T_1 + a_2 S + a_3 \frac{h_i}{H} + a_4 \left(\frac{h_i}{H}\right)^2 + a_5 \left(\frac{h_i}{h}\right)^3 \tag{5-17}$$

$$\text{for} \quad S \geq 1, \, i = 2 \text{ to } N + 1$$

and the values of the coefficients a_0 through a_5 are obtained from Table 5-4 for structures less than 9 stories in height, and Table 5-5 for structures 10 to 15 stories in height. The reference floor velocity, v_{si}, is determined from:

$$v_{si} = PGV + 0.3 \frac{T_1}{2\pi}\left(\frac{V_{y1}}{W_1/g}\Gamma_1\right)\left(\frac{\delta_i}{\delta_r}\right) \tag{5-18}$$

where T_1 is the first mode period; V_{y1} is the effective yield strength in first mode response; W_1 is the first modal effective weight in the direction under consideration, taken as not less than 80% of the total weight; Γ_1 is the first mode participation factor; δ_i is the uncorrected displacement of floor i; δ_r is the uncorrected roof displacement with respect to the base, and all other terms are as previously defined.

Dispersions in Response Calculations

To conduct performance assessments using simplified analysis, it is necessary to develop distributions of story drift, floor acceleration, and floor velocity to capture uncertainty.

Simplified analysis yields discrete values of median estimates of response quantities. To conduct performance assessments using simplified analysis, it is necessary to develop distributions of story drift, floor acceleration, and floor velocity, where the distributions capture uncertainty in ground motion intensity (β_{gm}), analysis record-to-record variability ($\beta_{a\Delta}$, β_{aa}, β_{av}), and modeling (β_m). Table 5-6 lists default values of dispersion to be used with simplified analysis results. Linear interpolation can be used to estimate values of β for intermediate values of T_1 and S.

For intensity-based and time-based assessments, separate values of total dispersion for drift, β_{SD}, floor acceleration, β_{FA}, and floor velocity, β_{FV}, are needed. These are calculated based on Table 5-6 values for analysis record-to-record dispersion for drift, $\beta_{a\Delta}$, acceleration, β_{aa}, and velocity, β_{av}, respectively, as follows:

$$\beta_{SD} = \sqrt{\beta_{a\Delta}^2 + \beta_m^2} \tag{5-19}$$

$$\beta_{FA} = \sqrt{\beta_{aa}^2 + \beta_m^2} \tag{5-20}$$

$$\beta_{FV} = \sqrt{\beta_{av}^2 + \beta_m^2} \tag{5-21}$$

Table 5-6 Default Dispersions for Record-to-Record Variability and Modeling Uncertainty for use with Simplified Analysis

T_1 (sec)	$S = \dfrac{S_a(T_1)W}{V_{y1}}$	$\beta_{a\Delta}$	β_{aa}	β_{av}	β_m
0.20	≤1.0	0.05	0.10	0.50	0.25
	2	0.35	0.10	0.51	0.25
	4	0.40	0.10	0.40	0.35
	6	0.45	0.10	0.37	0.50
	≥8	0.45	0.05	0.24	0.50
0.35	≤1.0	0.10	0.15	0.32	0.25
	2	0.35	0.15	0.38	0.25
	4	0.40	0.15	0.43	0.35
	6	0.45	0.15	0.38	0.50
	≥8	0.45	0.15	0.34	0.50
0.5	≤1.0	0.10	0.20	0.31	0.25
	2	0.35	0.20	0.35	0.25
	4	0.40	0.20	0.41	0.35
	6	0.45	0.20	0.36	0.50
	≥8	0.45	0.20	0.32	0.50
0.75	≤1.0	0.10	0.25	0.30	0.25
	2	0.35	0.25	0.33	0.25
	4	0.40	0.25	0.39	0.35
	6	0.45	0.25	0.35	0.50
	≥8	0.45	0.25	0.30	0.50
1.0	≤1.0	0.15	0.30	0.27	0.25
	2	0.35	0.30	0.29	0.25
	4	0.40	0.30	0.37	0.35
	6	0.45	0.30	0.36	0.50
	≥8	0.45	0.25	0.34	0.50
1.50	≤1.0	0.15	0.35	0.25	0.25
	2	0.35	0.35	0.26	0.25
	4	0.40	0.30	0.33	0.35
	6	0.45	0.30	0.34	0.50
	≥8	0.45	0.25	0.33	0.50
≥2.0	≤1.0	0.25	0.50	0.28	0.25
	2	0.35	0.45	0.21	0.25
	4	0.40	0.45	0.25	0.35
	6	0.45	0.40	0.26	0.50
	≥8	0.45	0.35	0.26	0.50

For scenario-based assessments, the values of total dispersion must also include uncertainty in ground motion attenuation, β_{gm}, obtained from Table 5-3. Total dispersion for drift, floor acceleration, and floor velocity including uncertainty in ground motion attenuation, β_{gm}, are given by:

$$\beta_{SD} = \sqrt{\beta_{a\Delta}^2 + \beta_m^2 + \beta_{gm}^2} \qquad (5\text{-}22)$$

$$\beta_{FA} = \sqrt{\beta_{aa}^2 + \beta_m^2 + \beta_{gm}^2} \qquad (5\text{-}23)$$

$$\beta_{FV} = \sqrt{\beta_{av}^2 + \beta_m^2 + \beta_{gm}^2} \qquad (5\text{-}24)$$

5.4   Residual Drift

> Nonlinear analysis using standard production software and typical component modeling techniques does not result in accurate assessments of residual drift.

Residual drift predicted by nonlinear analysis is highly sensitive to component modeling assumptions related to post-yield hardening/softening slope and unloading response. Accurate statistical simulation of residual drift requires the use of advanced component models, careful attention to cyclic hysteretic response, and a large number of ground motion pairs.

Since the requirements for direct simulation of residual drift are computationally complex and not practical for general implementation in design, the following equations were developed to estimate the median residual drift ratio, Δ_r, as a function of the peak transient response of the structure:

$$
\begin{aligned}
\Delta_r &= 0 & \text{for } \Delta \le \Delta_y \\
\Delta_r &= 0.3(\Delta - \Delta_y) & \text{for } \Delta_y < \Delta < 4\Delta_y \qquad (5\text{-}25) \\
\Delta_r &= (\Delta - 3\Delta_y) & \text{for } \Delta \ge 4\Delta_y
\end{aligned}
$$

where Δ is the median story drift ratio calculated by analysis, and Δ_y is the median story drift ratio calculated at yield. Appendix C provides background information on the development of these relationships.

The yield drift ratio, Δ_y, is associated with significant yielding in the structure. In steel concentrically braced frame and buckling-restrained braced systems, the yield drift ratio can be calculated as the story drift ratio associated with story shear forces equal to the expected yield strength of the braces. In low aspect ratio shear wall systems, it is the drift ratio associated with the expected shear strength of the walls. In slender shear wall systems dominated by flexural behavior, it is the drift ratio associated with the expected flexural strength of the walls under a lateral load distribution consistent with the dynamic response of the building.

In moment frame systems, the yield drift ratio can be calculated as the story drift associated with story shear forces related to: (1) beams or columns reaching their expected plastic moment capacity, including the effect of axial forces in the members; or (2) the beam-column connection panel joints reaching their expected yield strength. The distribution of forces in the story under consideration can be calculated based on equivalent lateral forces, or alternatively, by applying a shear force at the floor above the story being evaluated with a lateral support imposed at the floor below the story being evaluated.

When nonlinear response history analysis is used, the residual drift ratio, Δ_r, can be calculated at each level using Equation 5-25 and the story drift ratios calculated from the suite of analysis results. When simplified analysis is used, the residual drift, Δ_r, can be calculated at each level using a value of median transient drift, Δ_i^*, calculated using the procedures of Section 5.3.

The dispersion in the residual drift is generally larger than that of the story drift. When simplified analysis is used, the total dispersion in the residual drift due to both record-to-record variability, β_a, and modeling, β_m, should be set equal to 0.8 (Ruiz-Garcia and Miranda, 2005). When response history analysis is used, the dispersion in residual drift, β_{RD}, can be determined from the equation:

$$\beta_{RD} = \sqrt{\beta_a^2 + \beta_{ARD}^2} \qquad (5\text{-}26)$$

where β_a is the dispersion in residual drift obtained from the suite of analyses, and β_{ARD} is set equal to 0.2.

Chapter 6
Develop Collapse Fragility

6.1   Introduction

Building collapse is the principle cause of earthquake casualties. Assessment of collapse-induced earthquake casualties requires the development of a building collapse fragility, which is a relationship that defines the probability of incurring structural collapse as a function of ground motion intensity. The probability of collapse is expressed as a lognormal distribution of spectral acceleration at the first mode period, defined by a median value, $\hat{S}_a(T)$, and dispersion, β. This chapter presents several alternative procedures for establishing building-specific collapse fragility functions for input into a building performance model.

> Assessment of collapse-induced earthquake casualties requires the development of a building collapse fragility, which is a relationship that defines the probability of incurring structural collapse as a function of ground motion intensity.

The present state-of-the-art for collapse assessment is described in FEMA P-695, *Quantification of Building Seismic Performance Factors* (FEMA, 2009b). The procedures in FEMA P-695 are based on the concept of incremental dynamic analysis (IDA), which is a computationally intensive procedure that is rarely practical in non-research applications. Use of incremental dynamic analysis for the development of a collapse fragility function is described in Appendix J.

A more practical alternative, also described in FEMA P-695, is to perform limited suites of nonlinear response history analyses at key intensity levels that produce collapse predictions, and to develop collapse fragility functions from the resulting collapse statistics. Collapse fragility functions for low-rise buildings can be approximated using a simplified procedure based on nonlinear static (pushover) analysis. Collapse fragilities for buildings conforming to the requirements of recent building codes can be inferred based on the target collapse resistance inherent in the building code.

6.2   Nonlinear Response History Analysis

Nonlinear response history analysis is the most reliable method of establishing collapse fragility functions. The basic process entails performing large suites of analyses at multiple intensity levels ranging from intensities that produce near linear response to intensities that cause collapse. A smooth lognormal distribution is fit to the fraction of ground motions at each intensity level that result in collapse.

6.2.1 Definition of Collapse

Building collapse is generally associated with local or global loss of vertical-load carrying capacity, or failure of the gravity-load carrying system. Analytically, collapse is evidenced by numerical instability, large lateral drift response, or demands exceeding the failure capacity of gravity-load carrying components.

Aside from soil or foundation (e.g., pile) failures, there are few examples of building collapse due to overturning. Excessive lateral displacement, which can lead to a near-complete loss of lateral stiffness, can also trigger failure of vertical-load carrying components. In this methodology, collapse is defined as:

> Collapse is defined as sidesway failure (lateral dynamic instability), loss of vertical-load carrying capacity, or exceedance of non-simulated failure criteria.

- Sidesway failure (lateral dynamic instability), characterized by loss of lateral stiffness, and development of P-delta instability.

- Loss of vertical-load carrying capacity in gravity or seismic-force-resisting components due to earthquake-induced drifts.

- Exceedance of non-simulated failure criteria, consisting of force or deformation limits beyond which components can no longer continue to reliably resist load.

Simulation of collapse requires explicit solution techniques that are available in few commercial software packages. Typical analytical software used in engineering offices employ implicit solution techniques, which are unable to do so. As a result, collapse is assumed when numerical instability occurs, when lateral displacements exceed the range of model validity, or when non-simulated failure criteria are exceeded. Loss of vertical-load carrying capacity is predicted by excessive strength or deformation demands on gravity-load carrying components.

6.2.2 Mathematical Models

In general, three-dimensional mathematical models should be used for collapse assessment. Two-dimensional (planar) models may be sufficient in cases where buildings have regular configurations, the translational response in each orthogonal direction is independent, and torsional response is not significant. When two-dimensional models are used, the median collapse capacity, $\hat{S}_a(T)$, should be taken as the smaller of the values obtained in each direction.

Best-estimate mechanical properties should be used for each component in the mathematical model. Best-estimate models use median values for all component force-deformation parameters, such as yield strength, yield

deformation, post-yield stiffness, maximum strength, and deformation corresponding to maximum strength. If median values are unavailable, mean values can be used. Chapter 5 provides additional information, and resources for additional guidance, on modeling component force-deformation behavior.

Ideally, nonlinear models should simulate all possible modes of component deterioration and failure (e.g., axial, flexure, axial-flexure interaction, shear, and shear-flexure interaction). If a mode of deterioration or failure is not included in the model, its effect on collapse must be accounted for indirectly, through the use of non-simulated failure criteria. Some vertical-load carrying components (e.g., gravity columns) may not be included in the mathematical model, but must be checked for possible failure to ensure that they do not result in a collapse condition at the force or deformation demands predicted in the analysis.

> Ideally, nonlinear models should simulate all possible modes of deterioration or failure. Failure modes that are not directly simulated in the model must be checked for possible collapse at the force or deformation demands predicted in the analysis.

Most energy dissipation is modeled directly through the hysteretic force-deformation response of the structural components. Equivalent viscous damping assigned in the mathematical model should, therefore, be limited. For typical buildings, equivalent viscous damping should be in the range of 1% to 5% of critical damping in the predominant vibration modes of the structure. Values of 3% or less should be used for tall buildings and other structures where damping effects are small relative to structural hysteretic effects. Chapter 5 provides additional guidance on consideration of damping in structural analysis.

6.2.3 Incremental Dynamic Analysis

In incremental dynamic analysis (IDA), a large number of nonlinear response history analyses are performed using ground motions that are systematically scaled to increasing earthquake intensities until collapse occurs. Incremental dynamic analysis yields a distribution of results at varying intensities that can be used to generate a collapse fragility.

Because this method involves a large suite of suitable ground motion pairs (on the order of 20 or more), each of which is incrementally scaled to many different intensity levels, and nonlinear response history analysis is conducted for each pair at each intensity, the level of effort is computationally intensive and the method is seldom used in practice. The resulting data, however, are comprehensive, as illustrated in Figure 6-1. Use of incremental dynamic analysis for generation of a building-specific collapse fragility is described in Appendix J.

> Incremental dynamic analysis is computationally intensive and seldom used in practice, but the resulting collapse data are comprehensive.
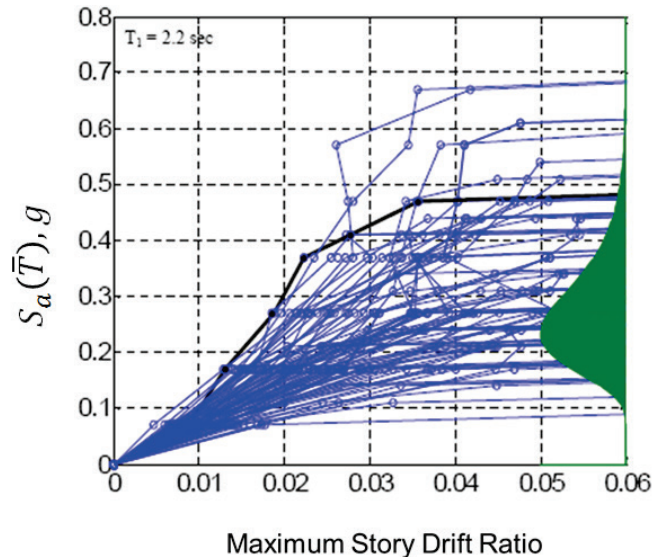
Figure 6-1   Sample incremental dynamic analysis results showing the distribution of collapse statistics for a hypothetical building.

6.2.4   Limited-Suite Nonlinear Analysis

In this approach, nonlinear response history analyses are performed at a number of intensity levels, some of which result in collapse. Such analyses will be an inherent part of time-base assessments when nonlinear response history analysis is used. At each intensity level, I, an estimated conditional probability of collapse, $P(C \mid I)$ is obtained from the equation:

$$P(C \mid I) = \frac{n}{N} \tag{6-1}$$

where n is the number of analyses at intensity, I, for which collapse is predicted, and N is the total number of analyses performed at intensity, I. A plot of the estimated conditional probability of collapse can be developed as a function of intensity, using an appropriate estimate of dispersion, and a lognormal distribution can be fitted to the data as shown in Figure 6-2.

When fitting a lognormal distribution to the data obtained from such analyses, it is best to anchor the fitted curve to data near the median collapse point, as small suites of analyses will be unreliable when only a small fraction of the analyses predict collapse. A dispersion of not less than 0.6 is recommended when this procedure is used. A companion *Collapse Fragility Tool*, which is an Excel workbook application designed to assist in fitting lognormal curves to limited sets of collapse data, is provided as part of *Volume 3 – Supporting Electronic Materials and Background Documentation*.
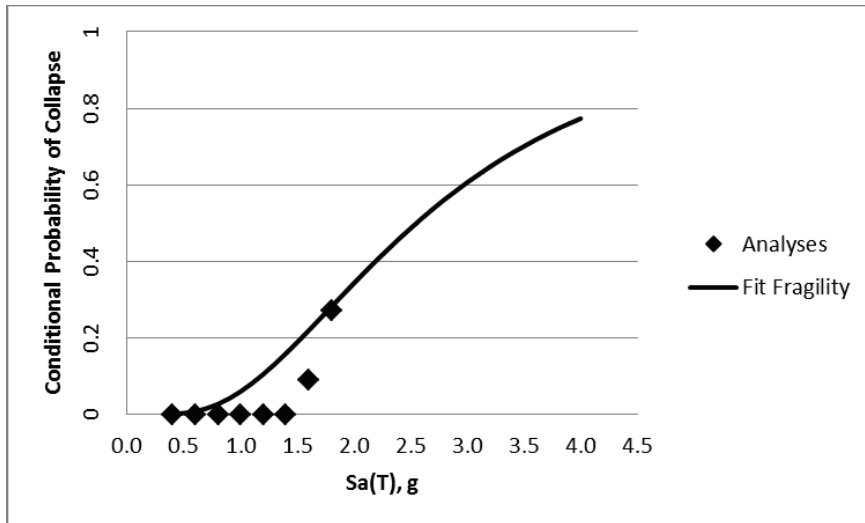
Figure 6-2   Illustration of collapse fragility estimated using nonlinear analysis at several intensity levels.

Figure 6-2 illustrates this approach for a hypothetical structure in which a time-based assessment is performed using suites of 10 nonlinear response history analyses at values of $S_a(\overline{T})$ equal to 0.4 g, 0.6 g, 0.8 g, 1.0 g, 1.2 g, 1.4 g, 1.6 g, and 1.8 g. In this example, analysis predicted three collapses at $S_a(\overline{T}) = 1.8$ g, one collapse at 1.6 g, and no collapses at lower intensities. A lognormal distribution has been fitted to these data with a judgmentally selected median of 2.6 g and a dispersion of 0.6.

To obtain reliable estimates of collapse fragility, a large number of ground motions (on the order of 20) should be used. However, it is worth noting that collapse fragility estimates obtained with as few as 7 ground motions per intensity level are likely to be of comparable quality to those obtained using the other approximate methods described in this chapter.

6.3   Simplified Nonlinear Analysis

From empirical relationships for characteristic segments of IDA curves for many systems, Vamvatsikos and Cornell (2006) suggested that static pushover curves could be used to estimate nonlinear dynamic response. The open source software tool, *Static Pushover 2 Incremental Dynamic Analysis* (SPO2IDA), was created as a product of that research. This tool, which is an Excel workbook application designed to convert static pushover curves into approximate incremental dynamic analysis results, is provided as part of *Volume 3 – Supporting Electronic Materials and Background Documentation*.

Approximate incremental dynamic analysis results derived from SPO2IDA can be used to generate collapse fragilities. Use of SPO2IDA should be

> SPO2IDA can be used to convert static pushover curves into approximate incremental dynamic analysis results for generating collapse fragilities.

limited to low-rise buildings that are regular in both plan and elevation, dominated by first mode translational behavior, with independent response along each principal axis, and negligible torsion.

To use SPO2IDA, a pushover analysis, similar to the nonlinear static procedure described in ASCE/SEI 41-13, *Seismic Evaluation and Retrofit of Existing Buildings* (ASCE, 2014), is performed, and a normalized force-displacement relationship for the global behavior is generated. The global base-shear, V, versus roof displacement, Δ, relationship is transformed into a normalized spectral acceleration versus global displacement ductility relationship, as shown in Figure 6-3.

Figure 6-3   Normalized spectral acceleration versus global ductility relationship used in SPO2IDA.

The spectral acceleration is computed as $S_a = V / (C_m W / g)$, with all terms as defined in Chapter 5. The spectral acceleration is normalized by S_y, which is equal to S_a at the first control point (i.e., $S_a / S_y = 1$). The global displacement ductility, μ, is the ratio of the roof displacement, Δ, to the roof yield displacement. The coordinate of the first control point (yield point) in SPO2IDA space is $(\mu, S_a / S_y)$, or $(1, 1)$.

Figure 6-4 presents sample output from SPO2IDA, which is based on the static pushover curve shown in Figure 6-3 as input. Results include the 16th, 50th (median) and 84th percentile estimates of normalized spectral acceleration at collapse. Since a best-estimate model is used to derive the static pushover curve and the resulting fractiles for collapse, the total dispersion used to derive the collapse fragility curve should be computed considering record-to-record variability and modeling uncertainty. A minimum default dispersion of 0.6 is recommended for deriving collapse fragility functions based on SPO2IDA results.
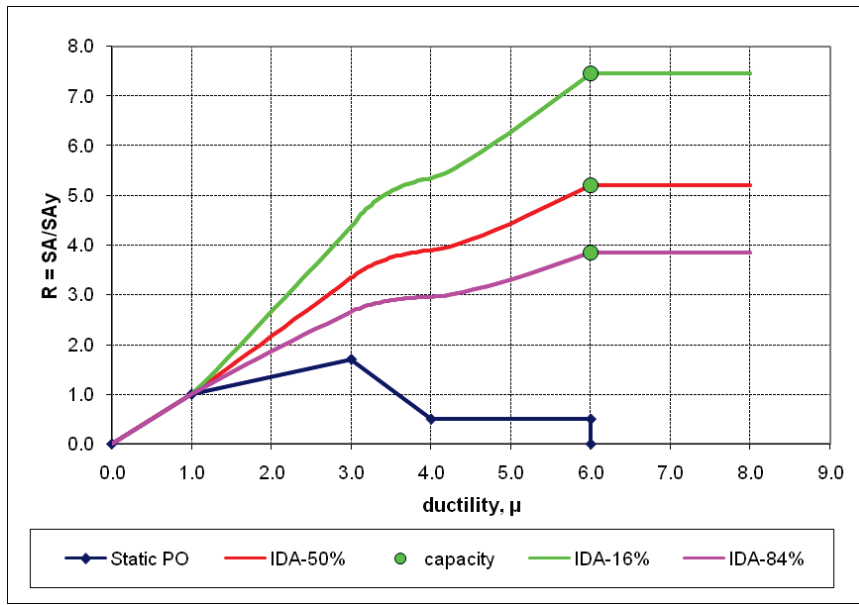
Figure 6-4   Sample SPO2IDA results and fractile estimates of normalized
                  spectral acceleration at collapse for the static pushover curve
                  shown in Figure 6-3.

6.4   Judgment-Based Collapse Fragility

Seismic design procedures contained in ASCE/SEI 7-16, *Minimum Design Loads and Associated Criteria for Buildings and Other Structures* (ASCE, 2017), are intended to provide less than a 10% chance that structures conforming to the requirements for Risk (or Occupancy) Category II will collapse when subjected to Maximum Considered Earthquake shaking, as defined in that standard. Studies have shown that conforming structures generally meet this criterion (FEMA, 2009b; NIST, 2010b). As a result, collapse fragility curves can be developed using engineering judgment based on the expected collapse capacity of code-conforming structures.

> Judgment based on the collapse resistance inherent in code-conforming buildings can be used to estimate collapse fragility, but this should not be regarded as a reliable measure of the collapse resistance of an individual building.

This approach entails significantly greater uncertainty than the other methods described in this chapter. As with any exercise of engineering judgment, the resulting performance assessments will be limited by the accuracy and uncertainty inherent in the judgment used to develop the fragility. Available collapse studies have generally considered well-configured, regular structures. Some structural systems have easily met the intended collapse criterion, while others have not. It should be expected that somewhat irregular structures with unfavorable structural configurations will not provide equivalent collapse performance as more favorable configurations permitted in ASCE/SEI 7-16.

The following procedure should be used along each principal axis of the building, and the lowest value of median collapse capacity $\hat{S}_a(\bar{T})$ should be used as the basis for the collapse fragility:

Step 1. Determine the highest value of base shear, V, calculated per ASCE/SEI 7-16, for which the structure just satisfies the applicable seismic design criteria within ASCE/SEI 7-16.

Step 2. Determine the effective value of the design spectral acceleration at the fundamental period, S_{aD}, at which the structure satisfies all applicable seismic design criteria of ASCE/SEI 7-16 from the equation:

$$S_{aD} = \frac{V}{W}R \tag{6-2}$$

where V is the base shear determined in Step 1, W is the seismic weight, and R is the response modification coefficient for the structure, as defined in ASCE/SEI 7-16.

Step 3. Compute the inferred median collapse capacity, $\hat{S}_a(T_1)$, at the fundamental period T_1:

$$\hat{S}_a(T_1) = 4S_{aD} \tag{6-3}$$

> **Second Edition Update**
>
> The computation of the inferred median collapse capacity has been updated.

Step 4. Convert the computed median collapse capacity at the fundamental period, $\hat{S}_a(T_1)$, to that of the average period, $\hat{S}_a(\bar{T}_1)$, using:

$$\hat{S}_a(\bar{T}_1) = \frac{T_1}{\bar{T}_1}S_a(T_1), \text{ for } T_1 \geq 0.6 \text{ seconds} \tag{6-4}$$

$$\hat{S}_a(\bar{T}_1) = S_a(T_1), \text{ for } T_1 < 0.6 \text{ seconds} \tag{6-5}$$

Since the archetype buildings have identical structural properties in each orthogonal direction, $\bar{T}_1 = T_1$, and $\hat{S}_a(\bar{T}_1) = S_a(T_1)$ for all the archetype buildings.

Step 5. For regular, well-configured structures, assume a dispersion, β, of 0.6. For irregular structures, or structures with configuration issues that are otherwise unfavorable for good seismic performance, assume a dispersion, β, of 0.7, or higher. Since the archetype buildings are assumed to be regular, well-configured structures, $\beta = 0.6$.

If the building under consideration has been analyzed using nonlinear response history analysis, and the judgment-based collapse fragility is not in reasonable agreement with the number of collapses predicted at different ground shaking intensities, re-examination of the analysis results or the derived collapse fragility is recommended. In the case of archaic

construction (i.e., not currently permitted under ASCE/SEI 7-16), the median spectral acceleration value at collapse can be estimated on the basis of past experience, and a dispersion of $\beta = 0.6$, or higher, should be assumed.

6.5   Collapse Modes

In addition to determining the likelihood of collapse (i.e., collapse fragility), it is also necessary to describe: (1) the potential collapse mode(s), along with the probability of occurrence of each, given that collapse occurs; (2) the extent of collapse in each mode at each story in the form of collapse area ratios; and (3) the respective probabilities that people occupying the areas of potential collapse will become fatalities or experience serious injuries. Collapse modes define the ways in which a building would be expected to collapse, ranging from partial to complete collapse. Possible collapse modes include single-story collapse, multi-story collapse, or total collapse. Collapse floor area ratios indicate the portion of floor area at each level that will be subjected to debris from collapse of the levels above. In some cases, collapse of one story on top of another might be expected to result in a cascading collapse of the lower stories. This should be considered when generating collapse modes.

> Collapse area ratios indicate the percent of floor area at each level that is subject to collapse in each mode.

For example, a hypothetical 4-story building might be expected to experience five possible modes of collapse:

- Mode 1 – total collapse in all stories

- Mode 2 – collapse in the 1st story (i.e., collapse of floor 2 onto floor 1)

- Mode 3 – collapse in the 2nd story (i.e., collapse of floor 3 onto floor 2)

- Mode 4 – collapse in the 3rd story (i.e., collapse of floor 4 onto floor 3)

- Mode 5 – collapse in the 4th story (i.e., collapse of the roof onto floor 4).

The corresponding collapse modes are shown in Table 6-1. In this example, it has been assumed that each mode has an equal chance of occurring (i.e., each has a collapse mode probability of 0.2), and that collapse at one level does not cause a cascading effect in the levels below. Note that the sum of the conditional probabilities that each collapse mode will occur must be equal to 1.0.

For each collapse mode, the table also shows the collapse floor area ratio at each level. The collapsed floor area ratio identifies the total floor area that will be subjected to debris from the floors above. In this example, it has been assumed that if a story collapses, the entire floor level associated with that story will be subjected to debris, as indicated by a collapse area ratio of 1.0 in

the table. It is possible to indicate partial collapse within a story by specifying a collapse area ratio less than 1.0.

Table 6-1   Sample Collapse Modes, Collapse Floor Area Ratios, and Probabilities of Fatalities and Serious Injuries for a Hypothetical Building

Collapse Modes					
	Mode 1	**Mode 2**	**Mode 3**	**Mode 4**	**Mode 5**
Probability of Collapse Mode	0.2	0.2	0.2	0.2	0.2
Probability of Fatality	1.0	0.9	0.9	0.9	0.9
Probability of Serious Injury	0	0.1	0.1	0.1	0.1
Collapse Floor Area Ratios					
Roof	1.0	0	0	0	0
Floor 4	1.0	0	0	0	1.0
Floor 3	1.0	0	0	1.0	0
Floor 2	1.0	0	1.0	0	0
Floor 1	1.0	1.0	0	0	0

Collapse predicted by analysis will be sensitive to modeling assumptions, relative strengths between floor levels, and the frequency content, amplitude and duration of the input ground motions. In general, it is not possible to reliably determine the range of possible collapse modes that might occur in a building on the basis of a limited suite of analyses. Therefore, information obtained from analysis must be supplemented with judgment regarding the viability of each mode for a particular structure, the appropriate floor area ratio at each floor level for each mode, and the probability of occurrence of each mode, given that collapse occurs.

In addition, it is necessary to specify the likelihood that persons in areas affected by collapse will become fatalities or will incur serious injuries. Based on casualty data from past earthquakes, the likelihood of fatality or serious injury can be related to the type and quality of the construction of the building. Available historic data are not robust, and judgment is necessary in assigning these probabilities.

For example, data from past U.S. earthquakes suggest that most people occupying unreinforced masonry bearing wall buildings with wood floors and roofs survive a building collapse. In this type of construction, heavy debris falls away from the building rather than into it, and casualties most commonly occur as a result of falling hazards outside of the building.

Casualty rates for this type of construction might be on the order of 10% (i.e., 0.1) for fatalities and 30% (i.e., 0.3) for serious injuries. Conversely, collapse of reinforced concrete structures has typically resulted in significant numbers of fatalities among people occupying floors impacted by collapse. Casualty rates for reinforced concrete construction might be on the order of 90% (i.e., 0.9) for fatalities and 10% (i.e., 0.1) for serious injuries. Additional information can be found in FEMA P-58/BD-3.7.8, *Casualty Consequence Function and Building Population Model Development*, provided as part of *Volume 3 – Supporting Electronic Materials and Background Documentation*.

Chapter 7
Calculate Performance

7.1   Introduction

This chapter outlines the procedures that are used to calculate building performance in the assessment process. These include generation of simulated demands, assessment of collapse, determination of damage, and computation of losses in the form of casualties, repair cost, repair time, embodied energy and carbon, and unsafe placarding. Calculation procedures are presented for intensity-based assessment. Calculations for scenario-based assessments are performed in a similar manner. Calculations for time-based assessments are performed as a series of intensity-based assessments that are weighted based on frequency of occurrence.

To assess uncertainty and explore variability in building performance, this process would ideally involve performing a large number of structural analyses, using a large suite of input ground motions, and analytical models with properties that have been randomly varied. Models would include all structural and nonstructural components and systems, and would be able to explicitly predict damage to each component of each system as it occurs. The results of each single analysis would represent one possible outcome, and the results of the large suite (thousands) of analyses would produce a smoothed distribution for probabilistic evaluation of earthquake consequences.

Given the current state of modeling capability, such an approach would be impractical for implementation in practice. Instead, a Monte Carlo procedure is used to assess a range of possible outcomes given a limited set of inputs. In this procedure, limited suites of analyses are performed to derive a statistical distribution of demands from a series of building response states for a particular intensity of motion. From this distribution, statistically consistent demand sets are generated representing a large number of possible building response states. These demand sets, together with fragility and consequence functions, are used to determine a building damage state and compute consequences associated with that damage.

Each unique performance outcome, in terms of a building damage state and consequences given one simulated demand set, is termed a realization. Many realizations are generated, each considering a single random combination of

> Performance calculation includes generation of simulated demands, assessment of collapse, determination of damage, and computation of losses.

> **Second Edition Update**
> Considerations for environmental impacts have been added.

> A Monte Carlo procedure is used to assess a range of possible outcomes given a limited set of inputs.

> Each realization represents one possible performance outcome. Many realizations are used to produce a distribution of losses for probabilistic assessment of earthquake performance.

possible values of each uncertain factor, to produce a distribution of losses for probabilistic assessment of earthquake performance. This approach, while lacking the precision of large suites of analyses explicitly assessing uncertainty and variability at each step in the process, is computationally efficient and better suited for practical use at this time.

The flowchart in Figure 7-1 illustrates the performance calculation process used to assess damage and consequences in each realization. The steps are described in the sections that follow.
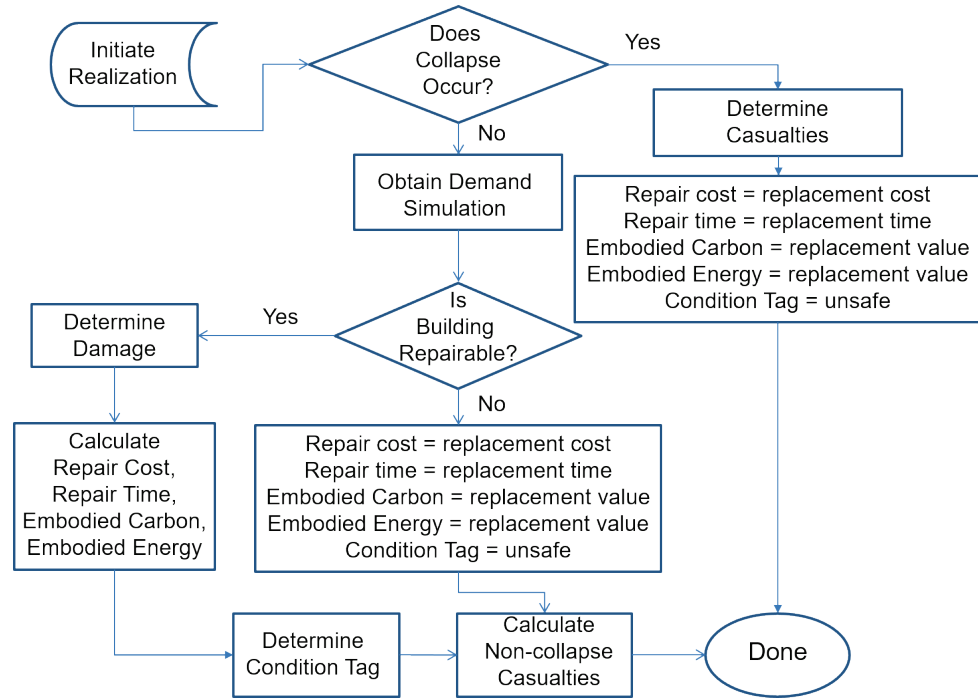
Figure 7-1   Flowchart for performance calculation in each realization.

7.2   Demand Simulation

> Generation of simulated demand sets occurs prior to initiation of realizations.

Not shown in the flowchart, and prior to the initiation of realizations, is the generation of simulated demand sets. For mathematical convenience, this step is conducted ahead of the actual realizations. Appendix G describes the process used to generate the hundreds to thousands of demand sets (one demand set is used per realization) needed to assess the distribution of possible building damage states for a ground motion intensity level. This process depends on whether nonlinear response history analysis or the simplified analysis procedure has been used to develop the set of initial demands.

7.2.1 Nonlinear Response History Analysis

Nonlinear response history analysis generates a suite of initial demand sets, one for each input ground motion. The results are assembled into a vector containing the values of each of the demand parameters (e.g., peak floor acceleration, peak floor velocity, peak story drift ratio, and residual story drift ratio at each level in each direction) for each analysis. These vectors are assembled into a matrix, with each row representing the results from one analysis, and each column representing the values of one demand parameter. The entries in the matrix are assumed to be a jointly lognormal distribution, and are manipulated to compute a vector of median demands (assumed to be the median vector derived from the suite of analyses), variances (or dispersion), and a correlation matrix that indicates how each demand parameter varies with respect to the other demand parameters in the set.

> Nonlinear response history analysis produces a suite of initial demand vectors, assembled into a matrix.

Once this manipulation has occurred, the terms of the diagonal dispersion matrix are augmented using a square-root-sum-of-squares approach to account for additional modeling uncertainty and ground motion uncertainty (in the case of scenario-based assessments). The resulting simulated demand sets will be statistically consistent with the initial demand set, but will more closely represent the range of possible responses that the building could experience at a particular ground motion intensity level. Figure 7-2 illustrates the potential variation in simulated displacement demands associated with nonlinear response history analysis of a hypothetical structure. The resulting response profile can vary in amplitude and shape from simulation to simulation.
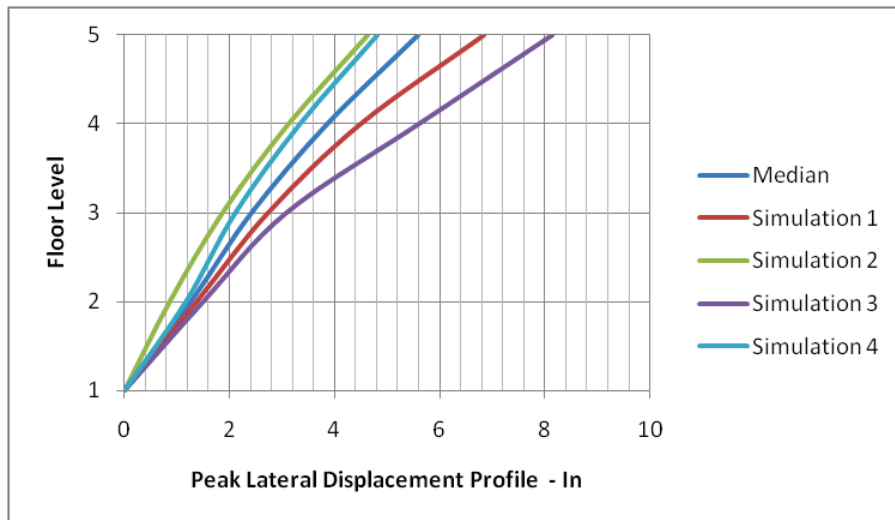
Figure 7-2 Potential variability in simulated drift demands associated with nonlinear response history analysis of a hypothetical building.

7.2.2 Simplified Analysis

Simplified analysis produces a single set of median demands and default estimates of dispersion associated with each demand parameter.

The simplified analysis procedure results in a single vector of estimated median values of each demand parameter (e.g., peak floor acceleration, peak floor velocity, peak story drift ratio, and residual story drift ratio at each level in each direction). It also utilizes default estimates of the dispersion associated with each parameter.

For each realization, a number between 1 and 100 is randomly generated, representing the percentile, within the lognormal distribution, for determination of demands for this realization using the default estimate of dispersion for each response quantity. This approach assumes that the building maintains the same response profile at a given intensity of ground motion, but with different amplitude. If one value of simulated demand is higher than the median by a particular measure, all are equally higher. In essence, it is assumed that there is perfect correlation between the various demands when using the simplified analysis procedure.

Figure 7-3 illustrates the potential variation in simulated displacement demands associated with simplified analysis of a hypothetical structure. The resulting response profile can vary in amplitude, but not shape. Use of the simplified analysis will result in more uniformity in response than nonlinear response history analysis, which is a less realistic treatment of potential variability.
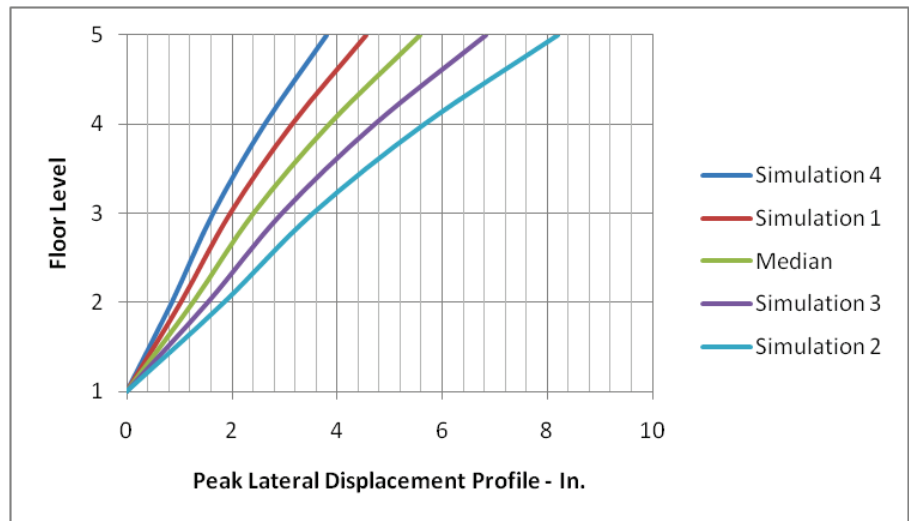
Figure 7-3   Potential variability in simulated drift demands associated with simplified analysis of a hypothetical building.

7.3   Realization Initiation

Each realization initiates with determination of the time of day, and day of the year at which the earthquake is assumed to occur. This information is

used, together with the population model, to determine the number of people present in the building in a given realization.

7.4   Collapse Determination

For each realization, a determination is made as to whether or not collapse has occurred. The possibility of collapse is assessed using the collapse fragility function described in Chapter 6. Figure 7-4 shows a collapse fragility function for a hypothetical building.
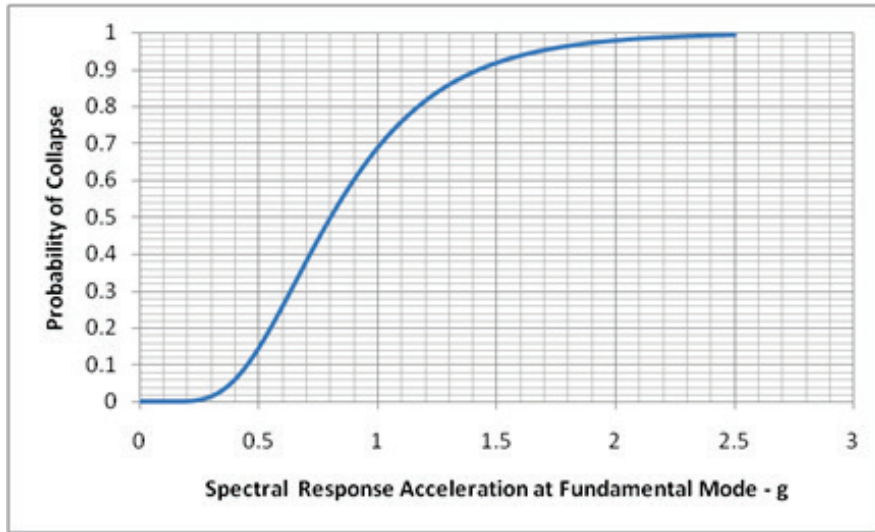
Figure 7-4   Collapse fragility function for a hypothetical building.

As an example, at a ground motion intensity level with a spectral acceleration of 0.5 g at the fundamental period of the building, Figure 7-4 indicates that there is a 15% probability of collapse. To determine if collapse has occurred in each realization, a number between 1 and 100 is randomly generated. If the random number is less than or equal to the value of conditional probability of collapse factored by 100 (i.e., $0.15 \times 100 = 15$), collapse is deemed to occur in this realization. If the number is greater than 15, collapse is deemed not to occur.

7.4.1   Collapse Mode

As described in Chapter 6, a building can collapse in one of several modes ranging from partial collapse to total collapse. Given that collapse is predicted to occur, the mode of collapse must be determined to estimate casualties. Development of the collapse fragility function includes identification of the possible collapse modes and the conditional probability of occurrence of each mode, given that collapse occurs, as well as the fraction of each floor subject to collapse debris.

> For each realization, a determination is made as to whether or not collapse has occurred.

The collapse mode probabilities are assembled into an array ranging from 1 to 100, with n_i sequential numbers assigned to each mode, where n_i is the conditional probability of occurrence for mode "i," factored by 100. To determine which collapse mode has occurred in a realization, a number between 1 and 100 is randomly generated. The range of the array in which this number falls indicates the collapse mode that has occurred.

For example, if a two story building has three potential collapse modes, consisting of first story collapse (50% probability), second story collapse (25% probability), and complete collapse (25%), these probabilities would be used to construct the array. Numbers 1 through 50 would be assigned to collapse mode 1; numbers 51 to 75 would be assigned to collapse mode 2; and numbers 76 to 100 would be assigned to collapse mode 3. A random number of 64 would indicate that collapse mode 2 occurred in this realization.

7.4.2 Casualties

Using a random number generator and a time-dependent population model appropriate for the building occupancy, along with the randomly generated day and time, the number of people present in the area of collapse is determined. Given that collapse has occurred and the collapse mode has been determined, the number of casualties is estimated based on the building population assumed present at the time of the realization, the associated fraction of floor area at each level subject to collapse, and additional building-specific casualty information.

For each collapse mode, user-defined mean fatality and injury rates are assigned. Based on building type and limited data from past earthquakes, these rates describe the percent of occupants that will suffer fatality or injury in an area impacted by collapse. These probabilities are factored by the ratio of floor area subject to debris, and the population present in the building, to estimate the resulting injuries and fatalities in each realization.

7.4.3 Repair Cost, Repair Time, and Embodied Energy and Carbon

Given that collapse has occurred, repair cost, repair time, and embodied energy and carbon for the realization are set equal to the building replacement values.

7.5 Damage Calculation

If collapse has not occurred, the damage sustained by each component is calculated. To determine damage for each realization in which collapse has

not occurred, one vector of simulated demands is obtained, and a damage state is determined utilizing the fragility functions assigned to each performance group. The overall building damage state for the realization is the aggregate of the damage states in each performance group.

Random number generation is used to determine the damage state for each component based on the assigned fragility function. For correlated damage states, each component in a performance group is assumed to have the same damage state, and the process is performed only one time for the performance group. For uncorrelated damage states, each component in a performance group can have a different damage state, and the process must be performed n times, where n is the number of components in the group.

> For correlated damage states, every element in a performance group is assumed to have the same damage state. For uncorrelated damage states, each element in a performance group can have a different damage state.

7.5.1 Sequential Damage States

Sequential damage states must occur in sequential order, with one state occurring before another is possible. Each sequential damage state represents a progression to higher levels of damage as demand increases. Figure 7-5 illustrates hypothetical fragility functions for three sequential damage states and a hypothetical realization demand of 0.25 g.
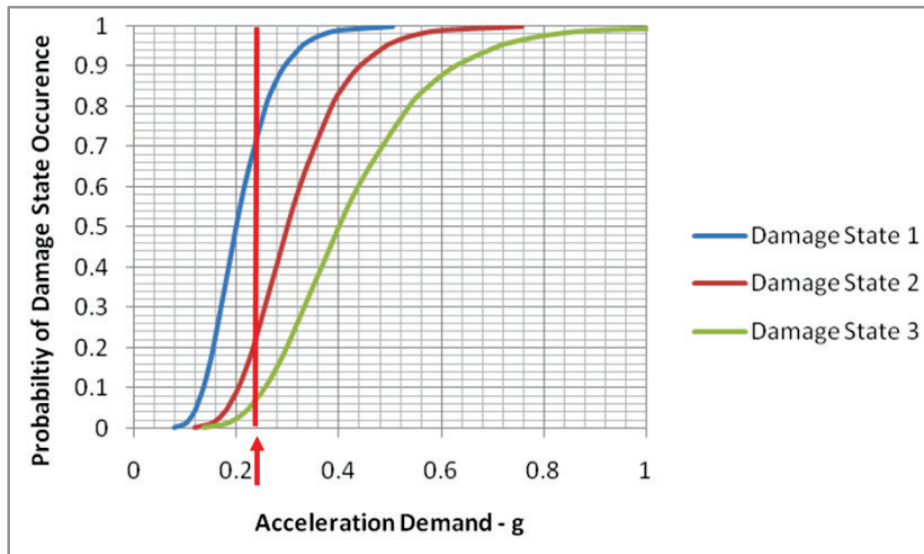
Figure 7-5   Hypothetical fragility functions for three sequential damage states.

Each sequential damage state is assigned a range of numbers. For example, DS1 ranging from ($P_1 \times 100$) to ($P_2 \times 100$), and DS2 ranging from ($P_2 \times 100 + 1$) to ($P_3 \times 100$), where P_i is the inverse probability of incurring damage state "i" at the demand level for the realization, as indicated by the fragility assigned to the performance group. A random number below ($P_1 \times 100$)

indicates that no damage has occurred; a random number between ($P_i \times 100$) and ($P_{i+1} \times 100$) indicates damage state P_i has occurred.

In this example, the probability of not incurring DS1 or higher is $P_1 = 1 - 0.75 = 0.25$; the probability of not incurring DS2 or higher is $1 - P_2 = 1 - 0.23 = 0.77$; and the inverse probability of not incurring DS3 is $P_3 = 1 - 0.06 = 0.94$. Therefore, the range of numbers assigned to no damage would be 1 to 25; the range assigned to DS1 would be 26 to 77; the range assigned to DS2 would be 78 to 94; and the range assigned to DS3 would be 95 to 100. A random number of 97 would indicate that a component has incurred DS3 for the realization.

When two or more sequential damage states have different dispersions, the fragility curves may cross, especially at the tails. In such cases, the probabilities are adjusted to avoid nonsensical negative probabilities of occurrence. For example, if the curve for DS2 crossed the curve for DS1 at a probability of 0.1 (which corresponds to an acceleration of 0.13 g), the probability of incurring DS1 is set equal to 0 for levels of acceleration less than 0.13 g, and the probability of incurring DS2 is obtained directly from the fragility curve for DS2.

7.5.2 Mutually Exclusive Damage States

Mutually exclusive damage states exist when the occurrence of one damage state precludes the occurrence of another damage state. Each mutually exclusive damage state must have a conditional probability of occurrence, given that the component is damaged, and the sum of the conditional probabilities must add up to 1.0.

Mutually exclusive damage states are each assigned a range of numbers, with DS1 assigned a range from 1 to (P(DS_1)×100); DS2 assigned a range from (P(DS_1) ×100+1) to (P(DS_1) +P(DS_2)) × 100, and so on. A random number is then generated between 1 and 100, and the range in which it falls determines the type of damage that occurs in the realization.

For example, if a hypothetical component that has three mutually exclusive damage states, DS1, DS2 and DS3, with conditional probabilities of occurrence equal to 20%, 30% and 50%, respectively, the range of numbers assigned to DS1 would be 1 to 20; the range assigned to DS2 would be 21 to 50; and the range assigned to DS3 would be 51 to 100. A random number of 42 would indicate that a component has incurred DS2 for the realization.

7.5.3 Simultaneous Damage States

Simultaneous damage states involve a series of potential damage states that are independent and unrelated in that they can occur, but need not necessarily occur, at the same time. Each simultaneous damage state is assigned a conditional probability of occurrence, given that the component is damaged. To identify the occurrence of damage, an initial random number is selected to determine whether damage has occurred or not. If the random number is less than the probability of incurring damage, then damage of some type is deemed to occur in the realization.

Given that damage has occurred, a second random number is selected for each possible damage state to determine if one or more of the simultaneous damages states have occurred. Unless one of the possible damage states has a conditional probability of occurrence equal to 1.0, there will be some small possibility that the random number generation will determine none of the simultaneous damage states has occurred. When this happens, the process is repeated until at least one damage state is deemed to occur for the realization.

7.6 Loss Calculation

If collapse has not occurred, losses are calculated based on the damage sustained by each component and the consequence functions assigned to each performance group. The aggregate of the losses in each performance group is the overall performance outcome for the realization.

In each realization, calculated losses include consideration of economies of scale and efficiencies in construction for repair actions at the performance group level. However, in aggregating losses to determine the overall performance outcome, global efficiencies of scale are not taken into account at the realization level.

A determination is made as to whether or not the building is repairable. The maximum residual drift ratio is used, together with a building repair fragility, to determine if repair is practicable. As with collapse determination, a random number generator is used to select an integer between 1 and 100. If this number is equal to or less than the probability of irreparability, as determined by the building repair fragility at the residual drift ratio for the realization, then the building is deemed irreparable for that realization. If the building is deemed irreparable, then the computed repair costs, repair times, and embodied energy and carbon are discarded and the total replacement cost, replacement times, and embodied energy and carbon are assigned to the realization.

> If the maximum residual drift ratio renders a building irreparable, then the computed repair costs and repair times are discarded and the total replacement cost and replacement times are assigned to the realization.

Loss distributions are developed by repeating the calculation of damage and loss for a large number of realizations, and sorting the values in ascending (or descending) order to enable the calculation of the probability that total loss will be less than a specific value for a given intensity of shaking. For example, if loss calculations are performed for 1,000 realizations, and the realizations are assembled in ascending order, the repair cost with a 90% chance of exceedance will be the repair cost calculated for the realization with the 100th largest cost, as 90% of the realizations will have had a higher computed cost.

Figure 7-6 shows a hypothetical cumulative loss distribution of repair costs for an intensity-based or scenario-based assessment. In the figure, each point represents the repair cost determined in a single realization. The smooth curve is a lognormal distribution that has been fitted to the data.
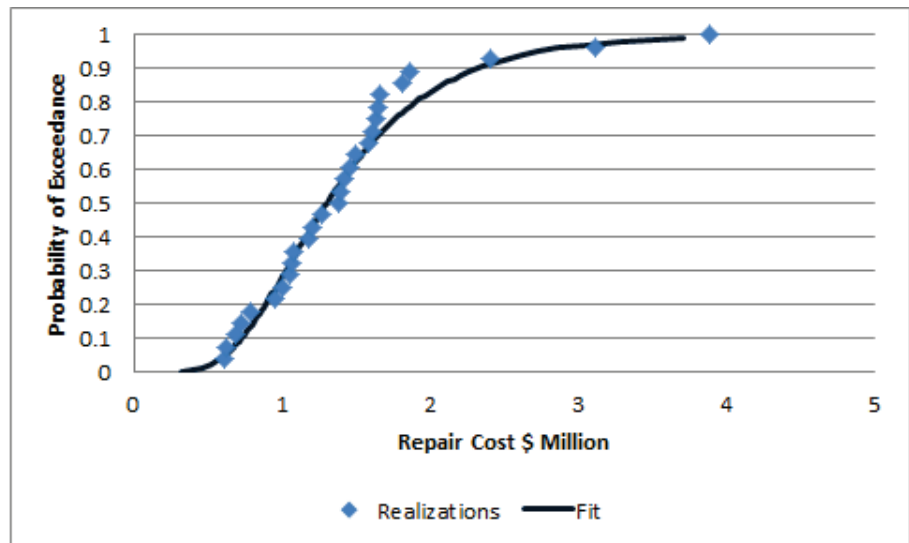
Figure 7-6   Hypothetical cumulative loss distribution of repair costs for an intensity-based or scenario-based assessment.

Any value of total loss can also be de-aggregated into the losses associated with a specific performance group by summing, on a realization basis, the sources of the loss. Figure 7-7 shows a hypothetical de-aggregation of repair costs across six performance groups. Results for other consequences can be similarly de-aggregated. Casualties can be de-aggregated across different building collapse modes, as well as those caused by falling hazards associated with different performance groups.

7.6.1   Unsafe Placard Loss Calculation

For each realization, and for each performance group with damage states that can result in unsafe placarding, a determination is made as to the number of components within a performance group that would need to be damaged to

trigger posting of an unsafe placard. The damage state calculated for each
component is evaluated to determine if the triggering percentage has been
exceeded for the group. If the number of components damaged to a given
damage state exceeds the triggering percentage in any performance group,
the building is assigned an unsafe placard. The probability of obtaining an
unsafe placard is then calculated as the number of realizations in which an
unsafe placard is assigned, divided by the total number of realizations for the
particular intensity.
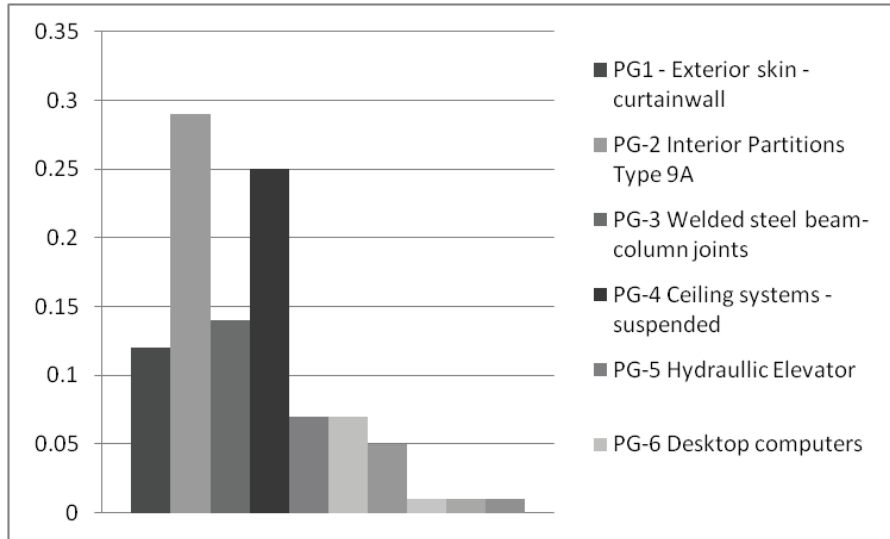
Figure 7-7   Hypothetical de-aggregation of repair costs by performance
                    group.

7.7   Time-Based Assessments

Time-based assessments produce a loss curve of the type shown in Figure
7-8, which plots the total value of a loss (e.g., repair cost, repair time, or
casualties), as a function of the annual rate of exceeding that loss. The curve
shown in Figure 7-8 is constructed using the results of a series of intensity-
based assessments that are weighted based on the frequency of occurrence, as
indicated by a seismic hazard curve for the site.

Figure 7-9 shows a representative seismic hazard curve, where the annual
frequency of exceeding earthquake intensity, $\lambda(e)$, is plotted against the
earthquake intensity, e. Typically, earthquake intensity is measured as
spectral acceleration at the first mode period of the building.

The hazard curve for the site is used with Equation 7-1 to calculate the
annual probability that the loss, L, will exceed a value, l:

$$P(L > l) = \int_{\lambda} P(L > l | E = e) \, d\lambda(e) \qquad\qquad (7\text{-}1)$$

where the term $P\left(L > l \middle| E = e\right)$ is the loss curve obtained from an intensity-based assessment for intensity, e.
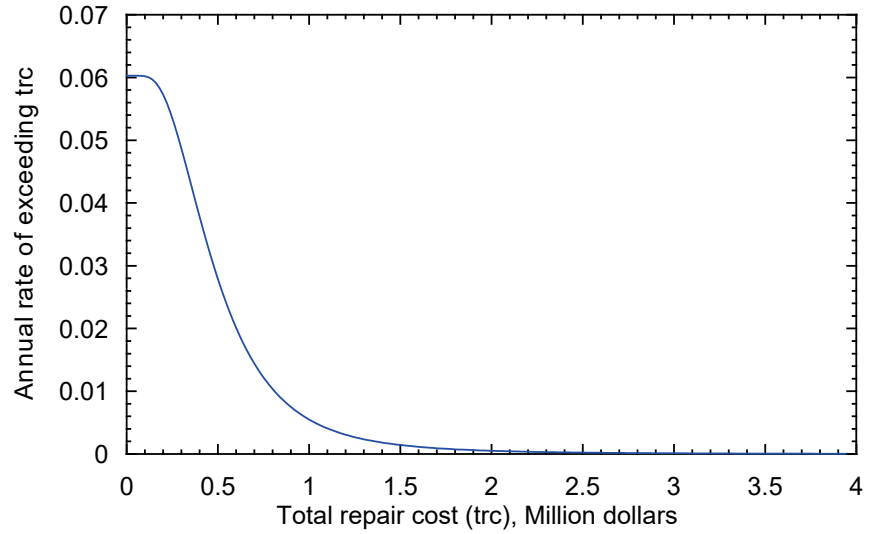
Figure 7-8　　Distribution of mean annual total repair cost.
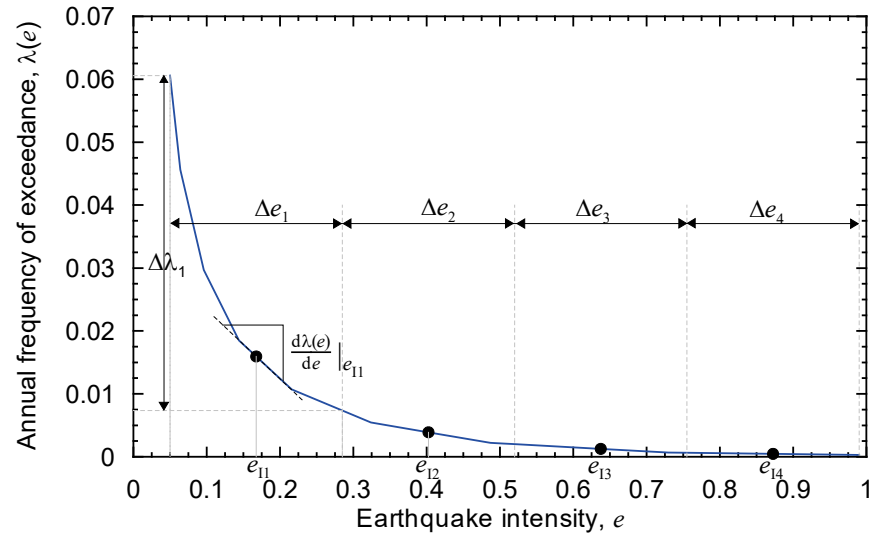
Figure 7-9　　Seismic hazard curve and intervals used for time-based loss calculations.

Equation 7-1 is solved by numerical integration. To perform this integration, the spectral range of interest is divided into n intervals, Δe_i. The spectral range of interest will typically range from a very low intensity, resulting in no damage, to a very high intensity, resulting in a high likelihood of collapse. The midpoint intensity in each interval is e_{Ii}, and the annual frequency of occurrence for earthquakes with an intensity in the range of Δe_i is $\Delta\lambda_i$, where the parameters are as defined in Figure 7-9, for $n = 4$. Note that in most time-based assessments, a larger number of intensities, n, will typically be necessary.

The intensity at e_{I1} is assumed to represent all earthquake shaking in the interval Δe_i. The number of intensities, n, required to implement time-based assessments will vary, and will depend on the slope of the hazard curve and the ability of the structure to survive a wide range of ground shaking intensities. An intensity-based assessment is performed at each of the midpoint intensities, e_{I1} through e_{In}. The product of the n intensity-based assessments is n loss curves of the type shown in Figure 7-10.
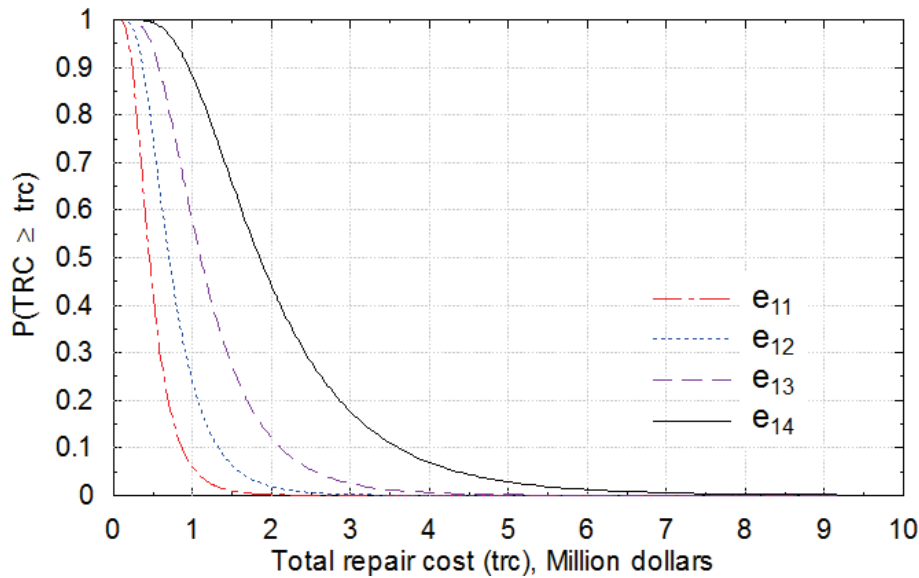
Figure 7-10   Cumulative probability distributions of total repair cost for a hypothetical building at four ground motion intensities.

The annual probability of occurrence, $\Delta\lambda_i$, for shaking intensity e_{Ij}, is calculated from the seismic hazard curve as the difference between the annual frequencies of exceedance at each end of the interval, Δe_i. Figure 7-10 is constructed by: (1) multiplying each loss curve by the annual frequency of occurrence in the interval corresponding to the earthquake intensity used to construct the curve; and (2) summing the annual frequencies for a given value of the loss.

Chapter 8

Decision Making

8.1 Introduction

Performance assessment can provide useful information for many decisions associated with real property. These include:

- Demonstrating equivalence of alternative design approaches.

- Selecting appropriate design criteria for new buildings.

- Determining if an existing building constitutes an acceptable risk for a particular planned use, whether or not it should be upgraded, and if so, to what level.

- Performing benefit-cost studies to determine a reasonable investment for improved seismic resistance in a building.

- Determining whether or not insurance is a cost-effective risk management technique.

This chapter illustrates how data obtained from performance assessments can be used to aid in the planning and design decision-making process.

8.2 Code Equivalence

For many years, building codes have permitted alternative designs and construction techniques that do not conform to the prescriptive seismic design criteria contained within the code. This permission is subject to the building official's satisfaction that the proposed design or construction technique is capable of providing performance that is equivalent to what is expected of code-conforming buildings. The performance assessment process can be used to demonstrate that an alternative design is capable of providing equivalent performance.

Commentary to Section 1.3 of ASCE/SEI 7-10, *Minimum Design Loads for Buildings and Other Structures* (ASCE, 2010), establishes the intended minimum safety-related seismic performance of building structures conforming to any of four Risk (or Occupancy) Categories. This performance is quantified in terms of acceptable probabilities of collapse, given that a structure is subjected to Maximum Considered Earthquake (MCE) shaking. The procedures of Chapter 6 can be used to assess collapse

> **Second Edition Update**
> The FEMA P-58 methodology was used to asses the performance of code-conforming buildings in terms of FEMA P-58 performance metrics. Results are presented in FEMA P-58, Volume 5.

> Code safety-related seismic performance is quantified in terms of acceptable probabilities of collapse, given MCE shaking.

behavior and to develop a collapse fragility for a specific building or alternative design. This can be used to determine directly, the probability of collapse given MCE shaking, a specific earthquake scenario of interest, or considering all earthquake hazards affecting a site on a time-basis.

It is envisioned that future building codes will likely include quantitative criteria that address performance issues in a broader context and more direct manner. Rather than considering the probability of collapse alone, it is possible that future codes could set safety-related goals in terms of the risk of casualties, rather than collapse. It is also possible that additional performance measures, such as the potential for loss of beneficial use, and damage to critical functionality-related equipment might be considered and quantified. With criteria so defined, intensity-based assessment procedures can be used to indicate probable building performance for Design Earthquake shaking or MCE shaking, as defined in the building code, or for any other target response spectrum.

<div style="float:left; border:1px solid; background:#aee0f5; padding:8px; width:200px;">
Intensity-based assessments can be used to indicate probable building performance for Design Earthquake shaking or MCE shaking, as defined in the building code.
</div>

8.3 Use of Scenario-Based Assessment Results

Scenario-based assessments evaluate the probable performance of a building assuming that it is subjected to an earthquake scenario consisting of a specific magnitude earthquake occurring at a specific location relative to the building site. Scenario-based assessments can be useful to decision-makers with buildings that are located close to a major active fault, and who believe that a particular magnitude earthquake might occur on this fault within a time period that is meaningful to them, often ranging from 10 to 30 years.

<div style="float:left; border:1px solid; background:#aee0f5; padding:8px; width:200px;">
Scenario-based assessments can be useful to decision-makers with buildings located close to major active faults.
</div>

Scenario-based assessments will provide direct information regarding the probable repair costs for such an occurrence, the potential for life loss, and the potential for long term loss of use. These impacts are quantified in the form of performance curves indicating the probability that losses will exceed a certain value, over the full range of possible values. Decision-makers may be uncomfortable with, or unable to use this type of probabilistic-based information, and might want a more specific answer regarding how big the losses could be. One way to provide this type of information is in the form of an expected performance, together with possible upper and lower bounds.

<div style="float:left; border:1px solid; background:#aee0f5; padding:8px; width:200px;">
Probabilistic results can be communicated in the form of an expected performance, together with possible upper and lower bounds
</div>

Expected performance can be mathematically derived from performance curves through numerical integration. Figure 8-1 illustrates this process, showing a scenario-based performance curve for a hypothetical performance measure. In the figure, the performance curve has been divided into five stripes, each with an equal probability of occurrence of 20%, given that the earthquake scenario has occurred. The probability of occurrence is equal to

the difference between the probabilities of non-exceedance at each end of the stripe. Within each stripe, the central value of the performance measure has been identified by reading horizontally from the middle of the stripe, and then reading vertically from the intersection point on the performance curve. The expected performance can be taken as the mean value of the performance measure, $\overline{PM}$, given by:

$$\overline{PM} = \sum_{i=1}^{k} P(i) PM_i \qquad (8\text{-}1)$$
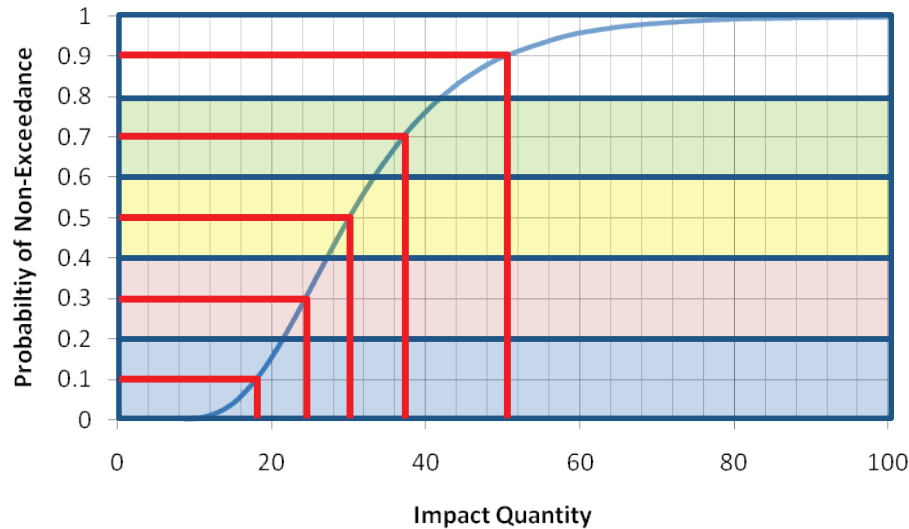
Figure 8-1   Hypothetical scenario-based peformance curve and striping for numerical integration of the mean value of a performance measure.

where $P(i)$ is the probability of occurrence for performance measure values within stripe i; PM_i is the central value of the performance measure for stripe i; and k is the number of stripes. For the case illustrated in the figure, the mean value, $\overline{PM}$, is given by 0.2 (19 + 24 +30 + 38 + 50) = 32. It should be noted that this value is slightly larger than the median value (i.e., the value corresponding to 50% probability of non-exceedance), which in this case has a value of 30. As the skew in a distribution increases, so does the difference between the mean and median values, with the mean being larger than the median. Any number of stripes can be used in the numerical integration process, and the stripes do not need to be uniform in size (i.e., the probability of occurrence need not be equal for each stripe). As the number of stripes increases, the accuracy of numerical integration also increases.

An alternative method of determining the mean value is to assume that the performance curve is approximated by a lognormal distribution, with median value, PM_{50}, and dispersion, β. The median value is the value with a 50%

probability of non-exceedance (i.e., the value exceeded 50% of the time), which is 30. The dispersion, β, can be approximated as:

$$\beta = 0.43\left(\frac{PM_{50}}{PM_{10}} - 0.782\right)$$ (8-2)

where, PM_{50} and PM_{10} are the 50th and 10th percentile values from the loss curve. The mean value can then be determined as:

$$\overline{PM} = PM_{50}e^{\beta^2/2}$$ (8-3)

where all terms are as previously defined. For the performance curve of Figure 8-1, these equations yield $\beta = 0.34$ and $\overline{PM} = 31.8$, which compares well with the value of 32 computed by numerical integration.

When providing expected (or mean) performance to decision-makers, it is also important to provide bounds on this performance so there is some understanding of the chance that performance will be superior or inferior to the mean. Often, PM_{10} (i.e., the value that is not exceeded 10% of the time) and PM_{90} (i.e., the value that is not exceeded 90% of the time) are appropriate bounds to communicate along with the mean.

8.4   Use of Time-Based Assessment Results

> Time-based assessments provide the average annual value of a performance measure, which is useful in cost-benefit analyses.

Time-based assessments evaluate the probable performance of a building over a specified period of time (e.g., 1 year, 30 years, or 50 years) considering all earthquakes that could occur in that time period, and the probability of occurrence associated with each earthquake. Time-based assessments can be used to provide the average annual value of a performance measure. Average annual values are useful in benefit-cost studies, and for determining reasonable insurance premiums on a property.

The average annual value of a performance measure is the mean value obtained from a time-based performance curve, such as that shown in Figure 8-2. It can be derived by numerical integration using Equation 8-1, as described for scenario-based performance curves in the previous section. For the hypothetical annual performance curve shown in Figure 8-2, the computed mean annual value of the performance measure is 0.2 (0.05 + 0.07 + 0.1 + 0.14 + 0.19) = 0.11 per year. If, for example, the performance measure was casualties, this value would indicate an average annual casualty rate of 0.11. If the performance measure was repair cost (in millions of dollars), this would indicate an average annual repair cost of $110,000.
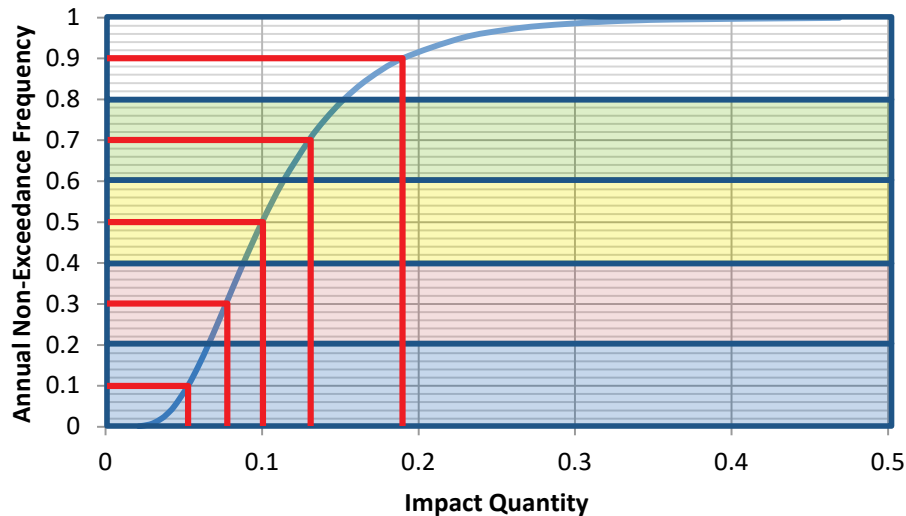
Figure 8-2   Hypothetical annual performance curve and striping for numerical integration of the mean annual value of a performance measure.

Earthquake losses, however, do not occur in annual increments. Over a period of many years, the average annual loss should approximate the total loss in a period of time, divided by the number of years in that period. If the performance measure is repair cost, the average annual repair cost is a reasonable measure of the insurance premium that a decision-maker might pay to insure against possible future earthquake repair costs. If the performance measure is expanded to include probable costs associated with loss of use, this can also indicate a reasonable value of insurance premiums to cover occupancy interruption costs.

> Average annual repair costs are a good measure of the insurance premium that a decision-maker might pay to insure against possible future earthquake repair costs.

Average annual values of a performance measure can also be an input to benefit-cost studies used to determine a reasonable investment for improved seismic resistance in a building. Benefit-cost studies involve a comparison between the net present value of average annual costs that are avoided through enhanced seismic resistance, versus the costs associated with providing the enhanced seismic resistance. The net present value, NPV, of a stream of equal annual future expenditures (or avoided expenditures) is given by:

> Net present value of average annual costs can be used to perform benefit-cost studies.

$$NPV = A \left\{ \frac{1 - \dfrac{1}{(1+i)^t}}{i} \right\} \qquad (8\text{-}4)$$

where A is a stream of equal annual expenditures (or avoided expenditures), t is the period of time in years, and i is the internal rate of return (or interest rate). The value of i represents the interest rate one would expect to pay if

capital was borrowed from others, or it represents the rate of return on investment that would be expected.

For decisions regarding property with an anticipated life of more than 40 years, the average annual cost (or savings) can be considered an annuity with an infinite term. In this case, Equation 8-4 reduces to the simpler form:

$$NPV = \frac{A}{i} \qquad (8\text{-}5)$$

As an example, consider a hypothetical company with operations in a single building in an earthquake-prone region. A performance assessment of the existing building indicates that it poses negligible risk for casualties, but potential earthquake damage could result in average annual repair costs of $150,000, and an average annual repair time of 5 days. Costs associated with each day of downtime are estimated to be $100,000 in lost profit.

The cost for seismic upgrade of the building, including design fees and internal costs, is estimated to be $3,000,000. A performance assessment of the upgraded building indicates that average annual repair costs will be reduced to $50,000, and the average annual repair time will be reduced to 3 days. The internal rate of return on investment is assumed to be 7%. Time-based assessment results can be used to determine if the upgrade is a reasonable investment if the company expects to remain in the building for 10 years, or if it expects to remain in the building indefinitely.

The average annual benefit of performing the upgrade is the average annual avoided repair cost ($150,000 - $50,000 = $100,000) plus the avoided loss in profit per year ((5 days - 3 days) × ($100,000) = $200,000), which results in a total reduction in average annual loss equal to $300,000. The net present value of the avoided average annual loss over a 10-year period and an indefinite period are given by:

$$NPV_{10\ years} = \$300,000 \left[\frac{1 - \dfrac{1}{1.07^{10}}}{0.07} \right] = \$2,108,000 \qquad (8\text{-}6)$$

$$NPV_{indefinite} = \frac{\$300,000}{0.07} = \$4,290,000 \qquad (8\text{-}7)$$

Since the net present value of losses avoided over a 10-year period is less than the cost of the seismic upgrade, there is not an economic benefit for this upgrade over a 10-year return period. However, if the company anticipated remaining in the building indefinitely, there would be a net benefit for investing in the upgrade.

In the above example, it is possible, although unlikely, that within 10 years of deciding not to upgrade the building, a damaging earthquake could occur resulting in real losses that are substantially in excess of the $3,000,000 cost of the upgrade.

Risk-averse decision-makers might want to avoid the realistic possibility of such a scenario. They might prefer to base decisions on a loss with a specific anticipated probability of occurrence, or return period, such as 10-year, 50-year, or 100-year losses. Time-based assessments can be used to provide this type of information.

Return period is the reciprocal of the annual frequency of exceedance. Thus, if a decision-maker is interested in a 50-year loss, one could read from the time-based performance curve the loss at an annual probability of exceedance of 1/50 years = 2%, and determine the 50-year loss directly. A risk-averse decision-maker might be willing to invest an amount up to the value of this loss in the form of seismic upgrades to avoid incurring the loss at some future point during the time period.

> Time-based assessments provide a means to determine the maximum loss likely to occur within in a specified time period.

8.5 Probable Maximum Loss

Many commercial lenders and real estate investors use a measure of seismic risk known as Probable Maximum Loss (PML). Such decision-makers will either not invest in a property, or will require the purchase of earthquake insurance, when the projected PML exceeds a certain threshold value, which is often 20%.

> Intensity-based assessments can be used to determine Probable Maximum Loss and other scenario loss measures used in real estate investment decisions.

ASTM E-2026, *Standard Guide for Seismic Risk Assessment of Buildings* (ASTM, 2007a) and ASTM E-2557, *Standard Practice for Probable Maximum Loss (PML) Evaluations for Earthquake Due-Diligence Assessments* (ASTM, 2007b) set standard procedures for seismic evaluations and the development of PMLs for use by the financial industry. These standards define several different measures including:

- **Scenario Expected Loss (SEL).** Scenario Expected Loss represents the mean repair cost, expressed as a percentage of building replacement value, for a particular intensity of ground motion, typically defined as a ground motion having a 475-year return period.

- **Scenario Upper Loss (SUL).** Scenario Upper Loss represents the 90th percentile repair cost, expressed as a percentage of building replacement value, for a particular intensity of ground motion, typically defined as a ground motion having a 475-year return period.

- **Probable Loss (PL).** Probable Loss represents the loss having a specific probability of exceedance, over a specified number of years.

Both Scenario Expected Loss and Scenario Upper-Bound Loss values can be determined by performing intensity-based assessments for response spectra having the specified return period. The Scenario Expected Loss is obtained by computing the mean repair cost for the assessment. The Scenario Upper Loss is determined directly from the performance curve for repair cost at the 90th percentile loss.

Probable loss can be derived directly from a time-based assessment using an appropriate return period for the assessment. The return period for a loss, P_R, can be derived from the desired probability of exceedance, P_{EY}, in Y years, using the formula:

$$P_R = \frac{-Y}{ln(1 - P_{EY})} \tag{8-8}$$

Once the return period for the loss is known, it is possible to compute the annual frequency of exceedance of the loss, as $1/P_R$, and then determine the corresponding probable loss for the frequency of exceedance directly from the annual performance curve.

Appendix A
Probability, Statistics, and Distributions

A.1   Introduction

This appendix provides a brief tutorial on probability and statistics including methods of expressing probabilities in the form of statistical distributions. It is intended to provide readers that are unfamiliar with these topics the basic information necessary for understanding the procedures used to account for uncertainties in performance assessment. Interested readers can obtain additional information in textbooks on probability and statistics, and structural reliability theory, such as Benjamin and Cornell (1970).

A.2   Statistical Distributions

Statistical distributions are mathematical representations of the probability of experiencing a specific outcome given a set of possible outcomes. The set representing all possible outcomes is termed a *population*. There are generally two broad types of populations considered in statistical studies. The first is a finite population of discrete outcomes, and the second is an infinite population of possible outcomes. Each is discussed separately, below.

A.2.1   Finite Populations and Discrete Outcomes

A *finite population* of outcomes occurs when each possible outcome has a discrete value representing one of a finite number of possible occurrences. Consider the classic case of a coin tossed in the air to determine an outcome. One of two possible outcomes will occur each time the coin is tossed. One is that the coin will land "heads-up" and the other is that it will land "heads-down." Which way the coin will land on a given toss is a function of many factors, including which way the coin is held before the toss, the technique used to toss the coin, how hard or high the coin is tossed, how much rotation it is given, and how it lands. It is not possible to precisely simulate each of these factors, and therefore, the occurrence of a "heads-up" or "heads-down" outcome in a given coin toss appears to be a random phenomenon that is not predictable. There is an equal chance that the coin will land "heads-up" or

"heads-down," and it is not known which way the coin will land before the toss is made.

If a coin is tossed in the air one time, there are two possible outcomes. These two outcomes ("heads-up" and "heads-down") completely define all possibilities for a single coin toss and, therefore, the probability that the coin will land either "heads-up" or "heads-down" is 100%. In essence, this illustrates the total probability theorem in that the sum of the probabilities of all possible outcomes will be 100%, also expressed as 1.0.

The probability that the coin will land "heads-up" is 50%, or 0.5. The probability that it will land "heads-down" is the inverse of this, calculated as one minus the probability of "heads-up," $1 - 0.5 = 0.5$, or 50%.

If a coin is tossed in the air many times, a "heads-up" outcome would be expected in half of the tosses, and a "heads-down" outcome would be expected in the other half. This does not mean that every second toss of the coin will have a "heads-up" outcome. Several successive "heads-up" or "heads-down" outcomes might occur; however, over a large number of tosses, there should be approximately the same number of each possible outcome.

A.2.2   Combined Probabilities

A *combined probability* is the probability of experiencing a specific combination of two or more independent outcomes. The combined probability of two independent events ($A + B$) is calculated as the product of the probability of outcome A and the probability of outcome B:

$$P(A + B) = P(A) \times P(B) \qquad\qquad \text{(A-1)}$$

To illustrate this, if a coin is tossed into the air two times, there is a 50% chance that the coin will land "heads-up" each time. The chance that the coin will land "heads-up" both times is calculated, using Equation A-1, as the probability of landing "heads-up" the first time (0.5) multiplied by the probability that it will land "heads-up" the second time (0.5), or $(0.5 \times 0.5) = 0.25$, or 25%.

This probability means that if a coin is tossed into the air twice in succession a large number of times, and record the number of "heads-up" outcomes, in each pair of tosses, approximately 25% of the total number of pairs of tosses will have two successive "heads-up" outcomes. This does not mean that every fourth time a pair of coin tosses is made two successive "heads-up" outcomes will occur. There is some possibility that two successive "heads-up" outcomes could occur several times in a row, and there is also a

possibility that more than four pairs of coin tosses will need to be made to obtain an outcome of two "heads-up" in any of the pairs of tosses. However, over a very large number of pairs of tosses, 25% of the pairs should be successive "heads-up" outcomes.

If a coin is tossed into the air three times, there is again a 50% chance on each toss that the coin will land "heads-up." The probability that the coin will land "heads-up" all three times is the probability that it will land "heads-up" the first two times (0.25) multiplied by the probability that it will land "heads-up" the third time (0.5), or (0.25 × 0.5) = 0.125, or 12.5%. If this exercise is repeated with four coin tosses, the probability that all four will land "heads-up" will be the probability that the first three tosses will land "heads-up" (0.125) times the probability that the fourth toss will land "heads-up" or (0.125 × 0.5 = 0.0625) or 6.25%. That is, there is approximately a 6% chance that on four coin tosses there will be four successive "heads-up" outcomes.

A.2.3   Mass Distributions

A *probability mass distribution* is a plot of the probability of occurrence of each of the possible outcomes in a finite population of discrete outcomes, such as a coin landing either "heads-up" or "heads-down" a specified number of times in N throws.

In the case of four coin tosses, there is a 6.25% chance that all four coin tosses will land "heads-up." There is also a 6.25% chance that all four coin tosses will land "heads-down," which is the same as no tosses landing "heads-up." The chance that three of the four coin tosses will land "heads-up" is equal to the combined chance of any of the following series of outcomes: "T-H-H-H"; "H-T-H-H"; "H-H-T-H" or "H-H-H-T," where "H" indicates "heads-up" and "T" indicates "heads-down." The chance of each of these series of outcomes is equal to (0.5 × 0.5 × 0.5 × 0.5) = 0.0625, or 6.25%. Therefore, the chance of exactly three out of four tosses landing "heads-up" is equal to the chance of "T-H-H-H," plus the chance of "H-T-H-H," plus the chance of "H-H-T-H," plus the chance of "H-H-H-T," or 0.0625 + 0.0625 + 0.0625 + 0.0625 = 0.25, or 25%. Similarly, the probability that exactly three of the four tosses will be "heads-down," or that only one of the tosses will land "heads-up," is also 25%. Similar approaches can be used to show that the probability of exactly half of the tosses landing "heads-up" is 37.5%.

Figure A-1 shows a probability mass distribution for the chance of obtaining zero, one, two, three, or four "heads-up" outcomes in four coin tosses. The

horizontal axis is potential outcome, and the vertical axis is the probability of that outcome. For example, the plot shows the chance that all four tosses will land "heads-up" is 0.06, the chance that three of the four tosses will land "heads-up" is 0.25, and the chance that exactly half of the tosses will land "heads-up" is 0.375.
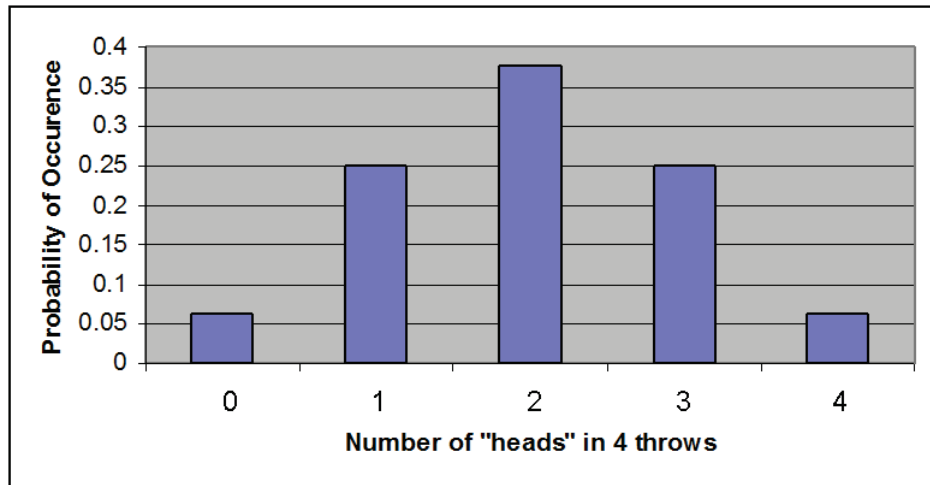
Figure A-1   Probability mass distribution indicating the probability of the number of "heads-up" outcomes in four successive coin tosses.

The probability of having not more than one "heads-up" outcome in four tosses is calculated as the sum of the probability of zero "heads-up", plus the probability of one "heads-up," which is 0.0625 + 0.25 = 0.3125, or 31.25%. Another way to say this is that the *probability of non-exceedance* for one "heads-up" in four coin tosses is 31.25%. The inverse of this is the cumulative probability of more than one "heads-up," which is 1 − 0.3125 = 68.75%. This could also be called the *probability of exceedance* of one "heads-up" in four tosses.

A.2.4   Infinite Populations and Continuous Distributions

The distribution of possible "heads-up" outcomes from a series of coin tosses is a finite population of discrete outcomes. In contrast, for many situations the range of possible outcomes is not finite or discrete, but rather a *continuous distribution* of an infinite number of possibilities.

One example of a continuous distribution is the possible compressive strength obtained from concrete cylinder tests taken from concrete using the same mix design. Such a distribution will have the form shown in Figure A-2, where the observed dispersion in strength can be attributed to minor variability in the relative proportions of cement and water, the strength of aggregates, the techniques used to cast and cure the cylinders, and other factors. There are an infinite number of possible outcomes for the strength of

any particular cylinder test. Such a plot is termed a *probability density function*.
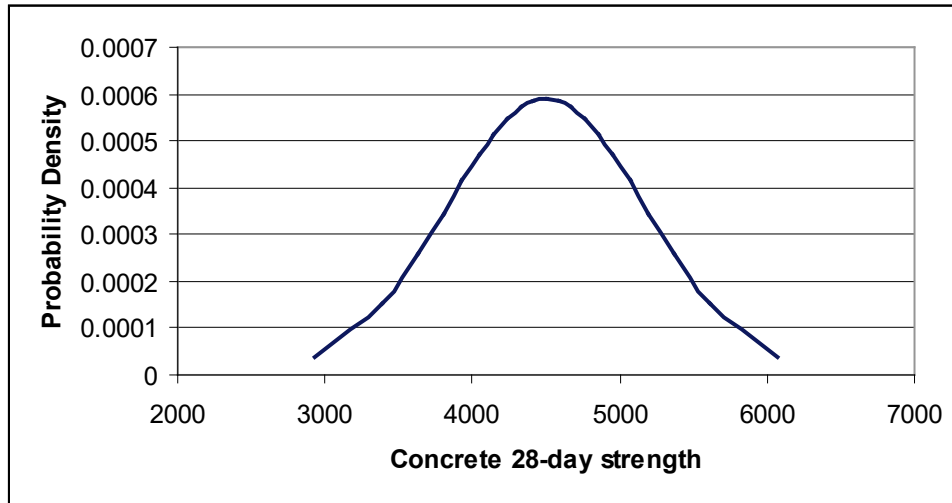
Figure A-2   Probability density function of possible concrete cylinder strengths for a hypothetical mix design.
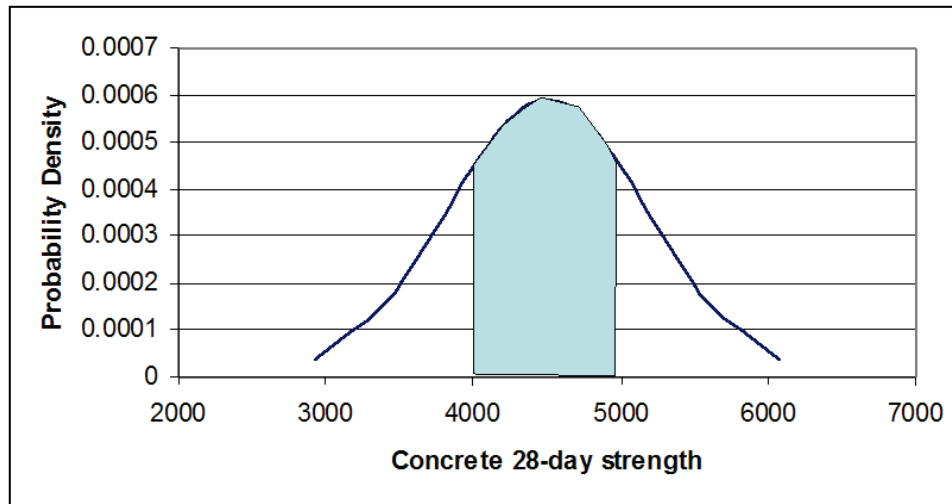
Figure A-3   Area under a probability density function indicating the probability that a member of the population will have a value within a defined range.

The area under a probability density function between any two points along the horizontal axis gives the probability that the value of any one member of the population will be within the range defined by the two points on the axis. In Figure A-3, the probability that a single cylinder test will have a compressive strength that is greater than 4,000 psi, but less than or equal to 5,000 psi, is given by the shaded area under the curve between 4000 psi and 5000psi, which in this case is equal to 54%. That is, there is a 54% chance

that any cylinder test in this population will have a compressive strength between 4,000 psi and 5,000 psi.

A.3   Common Forms of Distributions

A.3.1   Normal Distributions

The probability density function illustrated in Figure A-2 has a special set of properties known as a normal distribution. In a *normal distribution* the *median* outcome, which is the outcome that is exceeded 50% of the time, is also equal to the *mean* or average outcome, which is the total value of all possible outcomes, divided by the number of possible outcomes. In the concrete cylinder test example above, the median outcome is a compressive strength of 4,500 psi. The average strength of all cylinders tested is also 4,500 psi.

Normal distributions are also symmetric. That is, there is an equal probability of having a value at a defined measure above the mean (e.g., 1,000 psi above, or 5,500 psi), as there is of having a value at the same defined measure below the mean (e.g., 1,000 psi below, or 3,500 psi).

Two parameters uniquely define the characteristics of a normal distribution, namely, the mean value $\overline{x}$ and standard deviation, σ. Equation A-2 and Equation A-3 define these values for a random variable x (e.g., compressive strength of concrete as measured by cylinder testing):

$$\overline{x} = \frac{\sum\limits_{i=1}^{N} x_i}{N} \tag{A-2}$$

$$\sigma = \sqrt{\frac{1}{N-1}\sum\limits_{i=1}^{N}\left(x_i - \overline{x}\right)^2} \tag{A-3}$$

where N is the size of the population. If a parameter is normally distributed, having mean value, $\overline{x}$, and standard deviation, σ, it is possible to determine the value, x, of an outcome with a specific probability of exceedance, based on the number of standard deviations that the value lies away from the mean, $\overline{x}$. The number of standard deviations above or below the mean at a specified probability of exceedance is sometimes termed the *Gaussian variate*. Standard tables are available that provide the Gaussian variate. For example, there is a 97.7% chance that the value of any single outcome, x, will be greater than $\overline{x} - 2\sigma$, an 84.1% chance that the value will be greater than $\overline{x} - \sigma$, a 50% chance it will be greater than $\overline{x}$, a 15.8% chance it will be greater than $\overline{x} + \sigma$, and a 2.3% chance that it will be greater than $\overline{x} + 2\sigma$. Tables that provide values of the Gaussian variate are called *Gaussian tables*.

A.3.2 Cumulative Probability Functions

Figure A-4 plots probability density functions for different coefficients of variation. An alternative means of plotting probability distributions is the form of a cumulative probability function. Figure A-5 plots cumulative probability functions for the same normally distributed populations shown in Figure A-4. In both series of plots it can be observed that the larger the coefficient of variation, the greater the amount of scatter in the values of the possible outcomes.
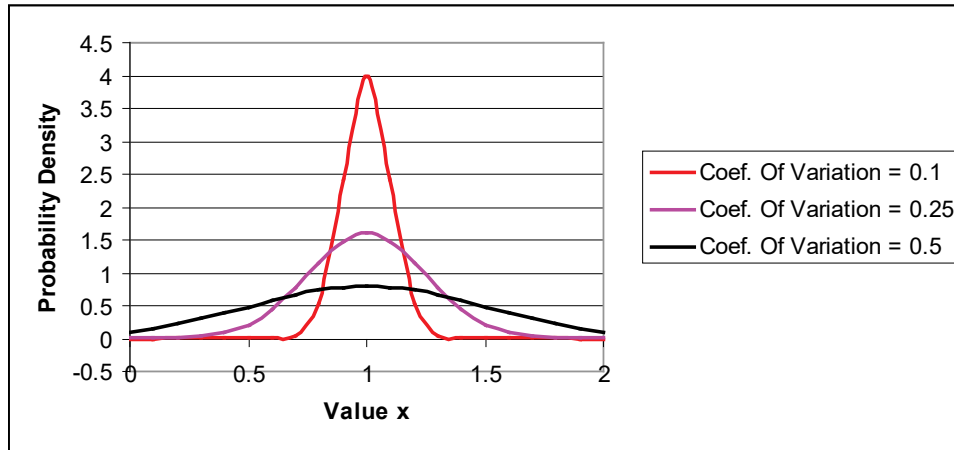
Figure A-4   Probability density plots of normal distributions with a mean value of 1.0 and coefficients of variation of 0.1, 0.25, and 0.5.
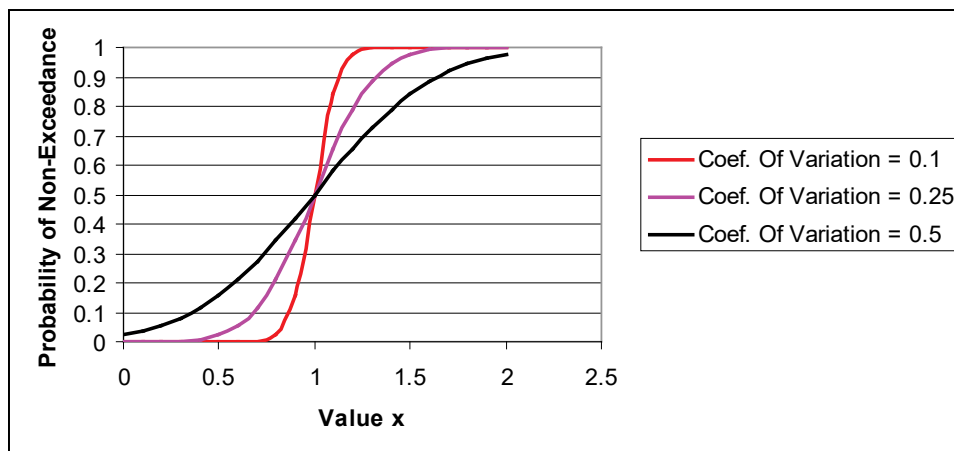
Figure A-5   Cumulative probability plots of normal distributions with a mean value of 1.0 and coefficients of variation of 0.1, 0.25, and 0.5.

Cumulative probability functions are obtained by integrating over the probability density function to determine the area under the curve between the lowest possible value of x and the specified value of x. A *cumulative probability function* gives the probability that an outcome in the population of possible outcomes will have a value that is less than or equal to the

specified value of *x*. This probability is sometimes termed the *probability of non-exceedance*. Table A-1 indicates representative values of the Gaussian variate for several commonly referenced probabilities of non-exceedance.

Table A-1   Values of the Gaussian Variate in Normal Distributions for Common Probabilities of Non-Exceedance

Probability of Non-Exceedance	Number of Standard Deviations below the Mean	Probability of Non-Exceedance	Number of Standard Deviations above the Mean
.02	-2.00	.60	0.25
.05	-1.64	.70	0.52
.10	-1.28	.80	0.84
.158	-1.00	.84	1.00
.20	-0.84	.90	1.28
.30	-0.52	.95	1.64
.40	-0.25	.98	2.00
.50	0.00		

A.3.3   Lognormal Distributions

Although normal distributions represent some random variables well, they do not represent all variables well. Some variables have skewed distributions. In skewed distributions, the mean value, $\bar{x}$, will be greater than or less than the median value. In structural reliability applications, such as performance assessment, it is common to use a specific type of skewed distribution known as a lognormal distribution. The skew inherent in lognormal distributions can reasonably represent the distributions observed in many structural engineering phenomena, such as the distribution of strength in laboratory test specimens.

A lognormal distribution has the property that the natural logarithm of the values of the population, ln(*x*), are normally distributed. The mean and the median of the natural logarithms of the population have the same value, equal to ln(θ), where θ is the median value. The standard deviation of the natural logarithms of the population, $\sigma_{\ln(x)}$, is called the dispersion, and is represented by the symbol, β. For relatively small values of dispersion, the value of β is approximately equal to the coefficient of variation for the population. Together, the values of median, θ, and dispersion, β, completely define the lognormal distribution for a population.

Figure A-6 plots probability density functions for three lognormally distributed populations having a median value of 1.0 and dispersions of 0.1,

0.25 and 0.5. Figure A-7 plots cumulative probability functions for the same lognormally distributed populations shown in Figure A-6.
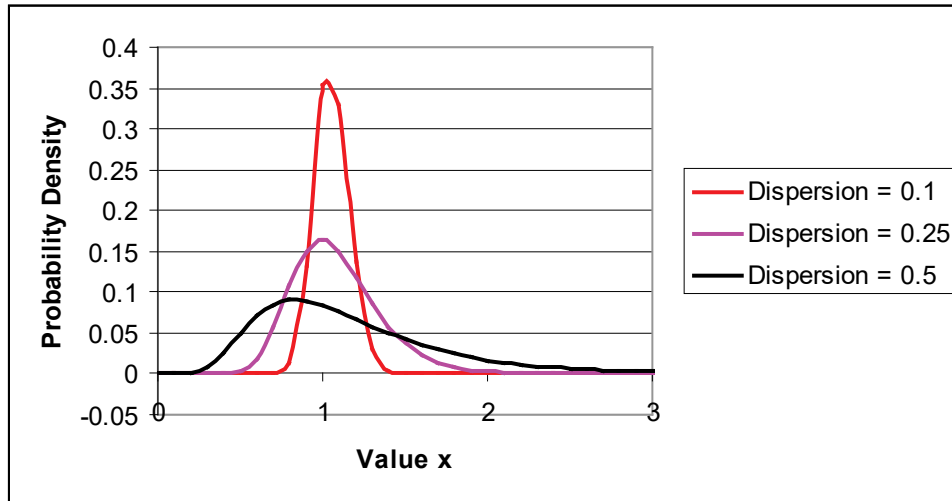
Figure A-6   Probability density plots of lognormal distributions with a median value of 1.0 and dispersions of 0.1, 0.25, and 0.5.
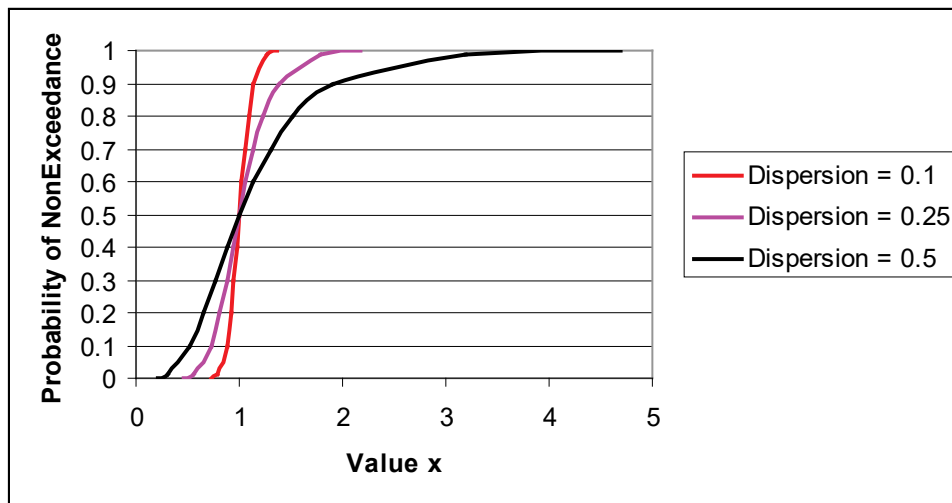
Figure A-7   Cumulative probability plots of lognormal distributions with a median value of 1.0 and dispersions of 0.1, 0.25, and 0.5.

In both series of plots, it can be observed that for small values of the dispersion, the distribution approaches the shape of the normal distribution. As the dispersion increases, the lognormal distribution becomes more and more skewed. This skew is such that extreme values above the median are substantially more probable than extreme values below the median, and there is zero probability of incurring a negative value in the distribution (because the natural logarithm of a negative number is positive).

Consider the distribution of possible actual yield strengths of various steel components, all conforming to a specific ASTM specification and grade. Since a random variable like yield strength cannot take on values less than zero, a lognormal distribution with a median value and dispersion could be used to describe the variation in possible steel strengths. In this example, the median value of actual yield strengths will be substantially higher than the minimum specified value, which is intended to have a very low probability of non-exceedance by any steel component conforming to the specification (i.e., the actual yield strength of any one component in the population should have a high probability of exceeding the minimum specified yield strength of the ASTM specification).

The seismic performance assessment methodology uses lognormal distributions to represent many uncertain factors that affect performance including: (1) the distributions of intensity for a scenario earthquake; (2) the values of response parameters given an intensity; (3) the probability of incurring a damage state as a function of a response parameter, herein termed a fragility; and (4) the probability of incurring a specific level of consequences in terms of casualties, repair costs, repair time or other impacts, given the occurrence of a damage state. These lognormal distributions are derived in a variety of ways:

- Intensity distributions are obtained based on statistical analysis of actual ground motion data recorded from past earthquakes, and represented in the form of equations known as attenuation relationships or ground motion prediction equations.

- Response parameter distributions are obtained by performing suites of structural analyses for multiple ground motion recordings and using these results to generate large numbers of statistically consistent simulated demand sets considering modeling uncertainty and ground motion uncertainty.

- Fragility distributions are obtained primarily through laboratory testing or observation of actual damage in past earthquakes.

- Loss distributions are obtained through performing multiple calculations of loss, and varying the factors that affect the loss.

Regardless of how they are derived, these distributions are represented by the median value, θ, and dispersion, β.

The mean, m_Y, and standard deviation, σ_Y, of a lognormal distribution, Y, can be calculated from θ_Y and β_Y as follows:

$$m_Y = \theta_Y \exp\left(\frac{\beta_Y^2}{2}\right) \qquad\qquad (A\text{-}4)$$

$$\sigma_Y^2 = m_Y^2 \left[\exp\left(\beta_Y^2\right) - 1\right] \qquad\qquad (A\text{-}5)$$

The coefficient of variation, V_Y, is given by:

$$V_Y = \frac{\sigma_Y}{m_Y} = \sqrt{\exp(\beta_Y^2) - 1} \qquad\qquad (A\text{-}6)$$

Many common spreadsheet applications have embedded functions that will automatically solve lognormal distribution problems. For example, in Excel, the LOGNORMDIST function will determine the cumulative probability of non-exceedance of any value in a population Y, based on input of the value, y, the natural logarithm of the median, $\ln(\theta_Y)$, and the dispersion, β_Y. The Excel input is of the form =LOGNORMDIST (y, $\ln(\theta_Y)$, β_Y). Similarly, the LOGINV function can be used to determine the value of y, at a given cumulative probability of non-exceedance, based on the desired probability, p, which must be less than 1.0, the natural logarithm of the median $\ln(\theta_Y)$, and the dispersion, β_Y. The Excel input is of the form =LOGINV (y, $\ln(\theta_Y)$, β_Y).

A.4   Probabilities over Time

Sometimes it is convenient to express the probability of the occurrence of an event conditioned on a specific period of time, such as a single year, the length of a lease, or the length of a mortgage loan. The probability that an event will occur in a single year is termed the *annual probability*. If the annual probability of the occurrence of an event, P_1, is known, it is possible to convert this into the probability, P_N, of the event occurring over any arbitrary length of time, N, using the formula:

$$P_N = 1 - \left(1 - P_1\right)^N \qquad\qquad (A\text{-}7)$$

Appendix B
Ground Shaking Hazards

B.1　Introduction

This appendix presents supplemental information on characterization of ground shaking hazards and an alternate procedure for scaling ground motions for scenario-based assessments.

B.2　Ground Motion Prediction Equations

Ground motion prediction equations, sometimes termed attenuation relationships, relate ground motion parameters to the magnitude of an earthquake, distance between the site and the fault rupture, and other parameters (e.g., soil type and rupture directivity). Models have been established for many ground motion parameters including peak horizontal acceleration, velocity, displacement, and corresponding spectral terms.

Ground motion prediction equations are developed primarily by statistical evaluation of large sets of ground motion data. Relationships have been developed for different regions of the United States (and other countries) and different fault types (e.g., strike-slip, dip-slip, and subduction faults).

Ground motion predictive equations generally return a geometric mean, S_g, of two horizontal spectral ordinates. For a given pair of horizontal earthquake histories with spectral ordinates, S_x and S_y, the geometric mean is $S_{gm} = \sqrt{S_x S_y}$. Because the functional form of the attenuation relationship involves the natural log of the ground motion parameter, the geometric mean of the ordinates (which is equivalent to the arithmetic mean of the logs of the ordinates) is used instead of the arithmetic mean to characterize the pair of histories.

Table B-1 presents selected models for North American ground motion prediction. These models all use moment magnitude, M_W, to define earthquake magnitude, but many use different definitions of site-to-source distance and other parameters. Figure B-1 defines some of the distance parameters used.

In 2014, a new set of ground motion prediction equations (Next Generation Attenuation Relationships for Western U.S, NGA-West2) were developed and used in the development of the seismic design maps in ASCE/SEI 7-16.

These new equations can be downloaded from the PEER Ground Motion Database, available at http://peer.berkeley.edu/ngawest2/ (last accessed March 15, 2018).

Table B-1   Ground Motion Prediction Models

Model	Calculated[1]	Site Conditions[2]	Variables[3]	T_n (seconds)	r (km)	M_W[4]
Western North America (WNA)						
Abrahamson and Silva, 2008	PHA, PHV, S_{ah}	$180 \leq V_{S30} \leq 2000$[5]	$M, r_{rup}, r_{jb}, V_{S30}, F, H, B$			5–8.5
Boore and Atkinson, 2008	PHA, PHV, S_{ah}	$180 \leq V_{S30} \leq 1300$	M, r_{jb}, V_{S30}, F			5–8
Campbell and Bozorgnia, 2008	PHA, PHV, S_{ah}	$150 \leq V_{S30} \leq 1500$	$M, r_{rup}, r_{jb}, V_{S30}, F, H, B$	0–10	0–200	4–8.5 (s) 4–8 (r) 4–7.5 (n)
Chiou and Youngs, 2008	PHA, PHV, S_{ah}	$150 \leq V_{S30} \leq 1500$	$M, r_{rup}, r_{jb}, V_{S30}, F, H, B$			4–8.5 (s) 4–8 (r,n)
Idriss, 2008	PHA, S_{ah}	$V_{S30} > 900$; $450 \leq V_{S30} \leq 900$	M, r_{rup}, F			4.5–8[5]
Central and Eastern North America (CENA)						
Atkinson and Boore, 1997	PHA, S_{ah}	Rock	M, r_{hypo}	0–2	10–300	4–9.5
Campbell, 2003	PHA, S_{ah}	Hard Rock	M, r_{rup}	0–4	1–1000	5–8.2
Toro et al., 1997	PHA, S_{ah}	Rock	M, r_{jb}	0–2	1–100	5–8
Subduction Zones						
Atkinson and Boore, 2003	PHA, S_{ah}	Rock to Poor Soil	M, r_{hypo}	0–3	10–300	5.5–8.3
Youngs et al., 1997	PHA, S_{ah}	Rock, Soil	M, r_{rup}, F, H	0–4	0–100	4–9.5

Notes: [1] PHA = peak horizontal ground acceleration; PHV = peak horizontal ground velocity; S_{ah} = horizontal spectral acceleration

[2] V_{S30} = average shear wave velocity in the upper 30 meters of sediments (m/s)

[3] r_{rup} = closest distance to the rupture surface; r_{jb} = closest horizontal distance to the vertical projection of the rupture; r_{hypo} = hypocentral distance; M = magnitude; F = fault type; H = hanging wall; B = three-dimensional basin response

[4] s = strike-slip faulting; r = reverse faulting; n = normal faulting

[5] Ranges are not specified but are estimated based on the datasets (Abrahamson and Silva, 2008; Idriss, 2008)
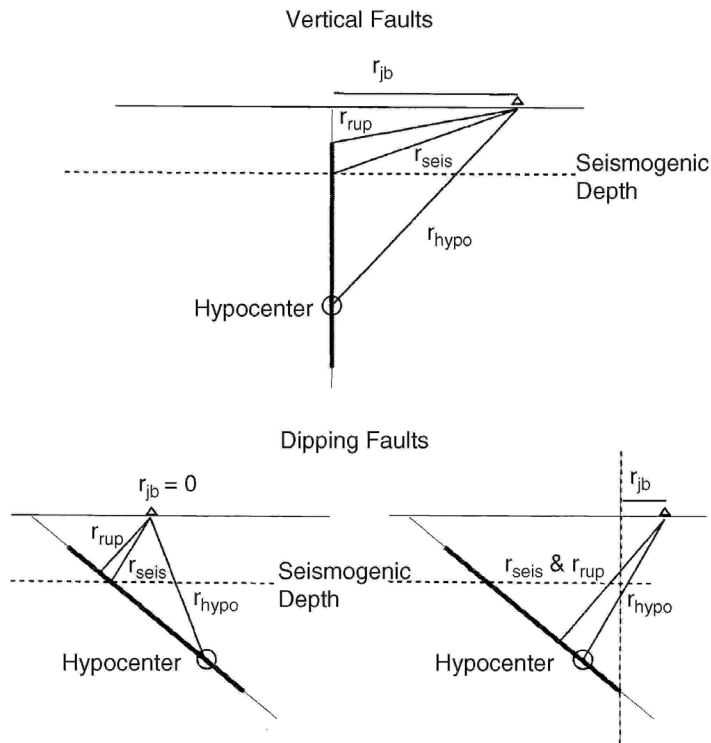
Figure B-1   Site-to-source distance definitions (Abrahamson and Shedlock, 1997).

B.3   Fault Rupture Directivity and Maximum Direction Shaking

Rupture directivity causes spatial variation in the amplitude and duration of ground motions in the vicinity of a fault. Propagation of rupture towards a site produces larger amplitudes of shaking, and shorter duration of strong-motions, than average directivity conditions at periods longer than 0.6 seconds. Somerville et al. (1997) developed modifications to the Abrahamson and Silva (1997) ground motion prediction equations to account for these variations. These and other equations at that time were constructed using strong motion databases that included few near-fault records, so spectral demands associated with near-fault shaking were not adequately represented.

Somerville et al. (1997) identified fault rupture directivity parameters θ and X for strike-slip faults, and ϕ and Y for dip-slip faults, as shown in Figure B-2. Ground motion parameters used to characterize directivity include: (1) *amplitude factor*, which is the bias in average horizontal response spectrum acceleration with respect to Abrahamson and Silva (1997); and (2) *fault-normal/average amplitude*, which is the ratio of fault normal to average (directivity) horizontal response spectrum acceleration. Bounds were set on the range of applicability of the directivity model.
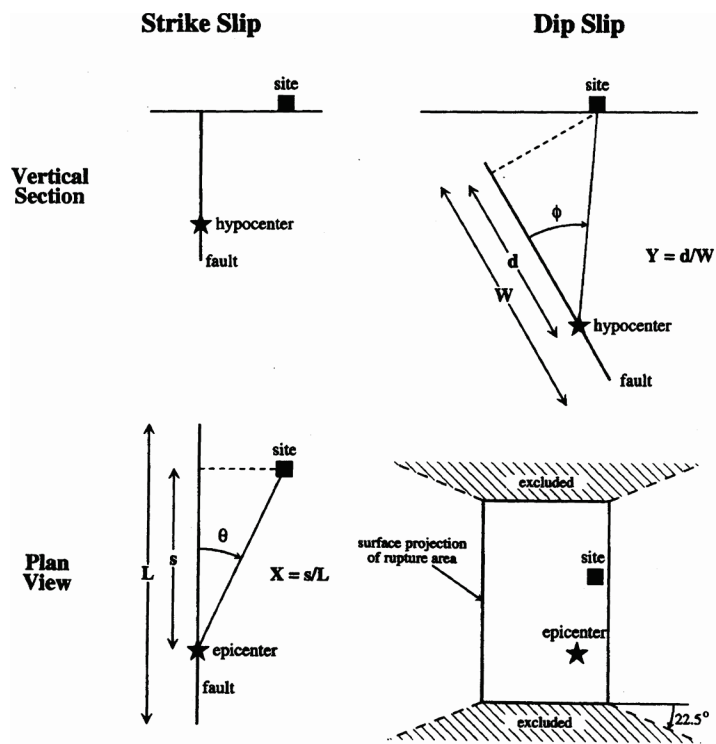
Figure B-2   Fault rupture directivity parameters (Somerville et al., 1997).

Next-Generation Attenuation (NGA) relationships for the Western United States were developed using a database that included many near-fault ground motion recordings. These relationships predict geomean spectral demand of recorded near-fault motions well, with little bias (Huang et al., 2008a, 2008b). Huang et al. (2008a, 2008b) also reported the median and 84th percentile ratios of maximum and minimum direction spectral demand to NGA-calculated geomean spectral demand for average directivity (i.e., all near-fault records) in the forward directivity region.

B.4   Probabilistic Seismic Hazard Assessment

Performance assessment can utilize site-specific characterization of ground shaking associated with different probabilities of exceedance. Such characterizations are routinely performed using probabilistic seismic hazard assessment (PSHA), described in the sections that follow, based on information from Kramer (1996), McGuire (2004) and Bozorgnia and Bertero (2004).

B.4.1   Probabilistic Seismic Hazard Assessment Calculations

In probabilistic seismic hazard assessment, probability distributions are determined for the magnitude of each possible earthquake on each source, $f_M(m)$, the location of each earthquake in or along each source, $f_R(r)$, and the

prediction of the response parameter of interest $P(\text{pga} > \text{pga}' \mid m,r)$. Kramer (1996) describes this as a four-step process enumerated below and depicted in Figure B-3:
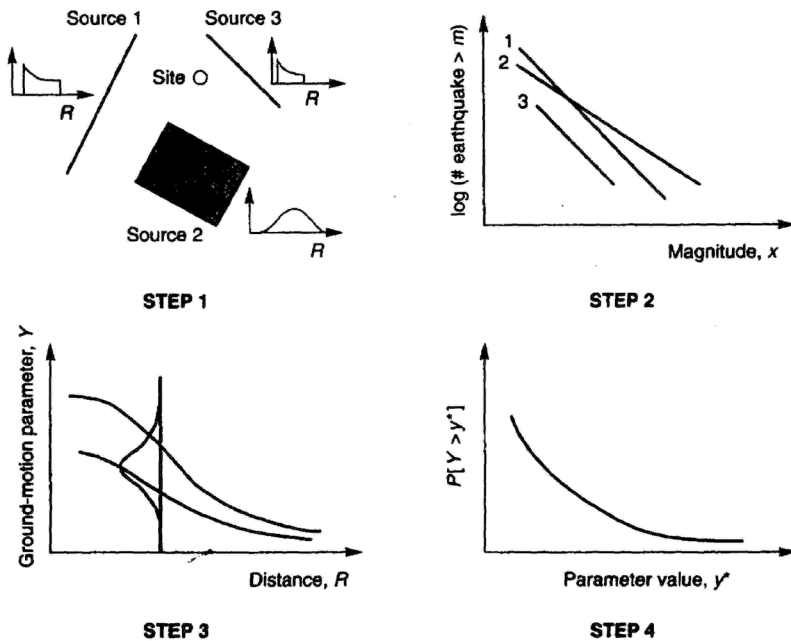
Figure B-3   Steps in probabilistic seismic hazard assessment (Kramer, 1996).

1. Identify and characterize geometry and potential M_W for all earthquake sources capable of generating significant shaking (i.e., $M_W \geq 4.5$) at the site. Develop the probability distribution of rupture locations within each source. Combine this distribution with the source geometry to obtain the probability distribution of source-to-site distance for each source.

2. Develop a distribution of earthquake occurrence for each source using a recurrence relationship. This distribution can be random or time-dependent.

3. Using predictive models, determine the ground motion produced at the site (including uncertainty) for earthquakes of any possible magnitude, occurring at any possible point, in each source zone.

4. Combine the uncertainties in earthquake location, size, and ground motion prediction to obtain the probability that the ground motion parameter of interest (e.g., peak horizontal ground acceleration, spectral acceleration) will be exceeded in a particular time frame (i.e., 10% chance of exceedance in 50 years).

Earthquake Source Characterization

Characterization of an earthquake source (there can be many sources for some sites) requires consideration of the spatial characteristics of the source, the distribution of earthquakes within that source, the distribution of earthquake size within that source, and the distribution of earthquakes over time. Each of these characteristics involves some degree of uncertainty, which is explicitly addressed in the process.

Spatial Uncertainty

Earthquake source geometries are typically characterized as shown in Figure B-4. Source zone geometries include: (1) point sources (e.g., volcanoes); (2) two-dimensional areal sources (e.g., a well-defined fault plane); and, (3) three-dimensional volumetric sources (e.g., areas where earthquake mechanisms are poorly defined such as the Central and Eastern United States). These representations can have varying levels of accuracy.

| (a) | (b) | (c) |
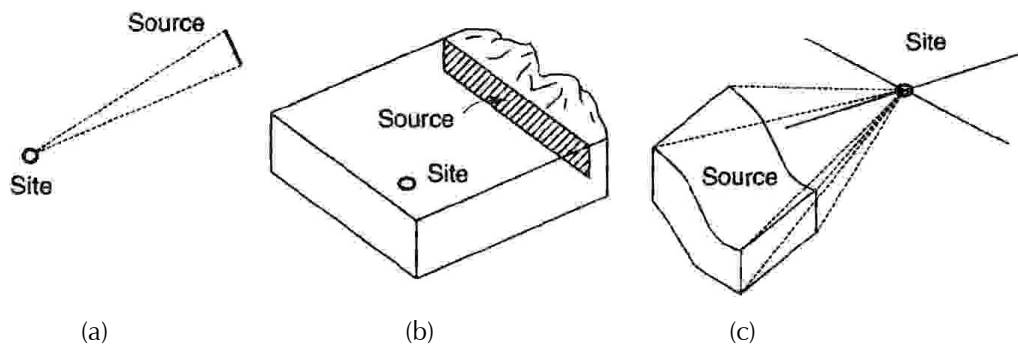
Figure B-4   Source zone geometries: (a) point sources; (b) two-dimensional areal sources; and (c) three-dimensional volumetric sources (Kramer, 1996).

Because attenuation relationships and other predictive models express ground motion parameters in terms of a measure of the source-to-site distance, the spatial uncertainty must be described with respect to the appropriate distance parameter. Uncertainty in source-to-site distance can be described by a probability density function, as shown in Figure B-5.

For a point source, the distance R is r_s. The probability that $R = r_s$ is 1.0, and the probability that $R \neq r_s$ is 0. For more complex source zones, it is easier to evaluate $f_R(r)$ by numerical integration. For example, the source zone in Figure B-5c is broken up into a large number of discrete elements of the same area. A histogram that approximates $f_R(r)$ can be constructed by tabulating the values of R that correspond to the center of each element.
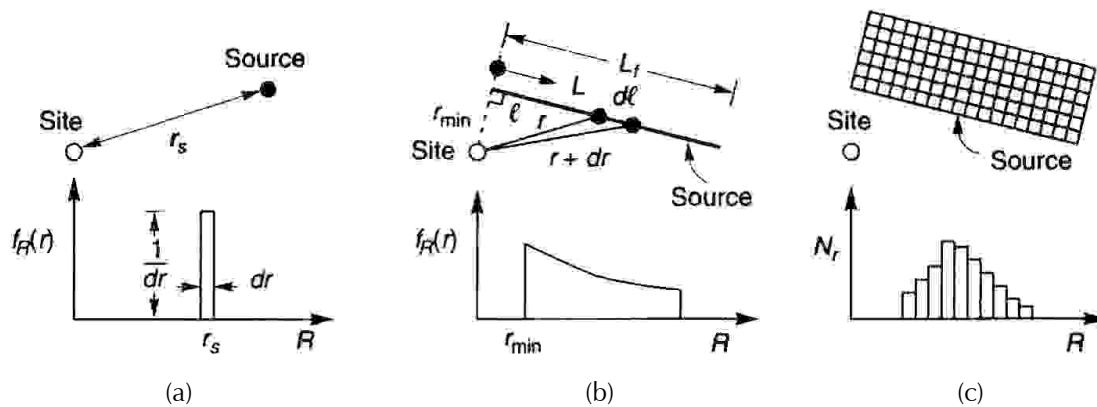
Figure B-5   Variations in site-to-source distance for three source zone geometries (Kramer, 1996).

Size Uncertainty

Recurrence laws describe the distribution of probable earthquake size over a period of time. One basic assumption is that past recurrence rates for a source are appropriate for the prediction of future seismicity. The best known recurrence law, Gutenberg and Richter (1944), is based on data collected from Southern California earthquakes over a period of years. Data were plotted according to the number of earthquakes that exceeded different magnitudes during that time period. The number of exceedances of each magnitude was divided by the length of the time period used to assemble the data, defining the mean annual rate of exceedance, λ_m, of an earthquake of magnitude, m. The reciprocal of the mean annual rate of exceedance for a particular magnitude is termed the return period for earthquakes exceeding that magnitude. Gutenberg-Richter (1944) plotted the logarithm of the annual rates of exceedance against magnitude and obtained the following linear regression relationship:

$$\log \lambda_m = a - bm \qquad\qquad (\text{B-1})$$

where λ_m is as defined above, 10^a is the mean annual number of earthquakes with magnitude greater than or equal to magnitude m, and b describes the relative likelihood of large and small earthquakes. As the value of b increases, the number of larger magnitude earthquakes decreases relative to the number of smaller magnitude earthquakes. The mean rate of small magnitude earthquakes is often under-predicted because historical records are used to supplement the instrumental records, and larger magnitude events dominate the historical record.

The Guttenberg-Richter recurrence law was originally developed from regional data, and not for specific source zones. Paleoseismic studies over the past 30 years have indicated that individual points on faults (or fault segments) tend to move approximately the same distance in successive

earthquakes. This suggests that faults repeatedly generate earthquakes of a similar size (within 0.5 magnitude), known as characteristic earthquakes, at or near their maximum capable magnitude. Geological evidence indicates that characteristic earthquakes occur more frequently than would be implied by extrapolation of the recurrence law from high exceedance rates (of low magnitude events) to low exceedance rates (of high magnitude events), resulting in a more complex recurrence law than that given in Equation B-1.

Attenuation Relationships

Scatter or randomness in the results obtained from predictive models is inevitable because of differences in site condition, path of travel, and fault rupture mechanics associated with the data set, and a lack of certainty as to the precise values of these parameters for any specific site. Scatter can be characterized by confidence limits, or by the standard deviation of the predicted parameter.

The probability that a ground motion parameter Y exceeds a certain value y for an earthquake of magnitude, m, occurring at a distance, r, is given by:

$$P[Y > y | m, r] = 1 - F_y(y) = 1 - \Phi\left(\frac{\ln y - \ln \theta}{\beta}\right) \tag{B-2}$$

where $F_Y(y)$ is the value of the cumulative distribution function of Y at m and r, which is assumed to be lognormal in form; θ is the median value of Y; and β is the dispersion. Figure B-6 illustrates the conditional probability of exceeding a particular value of a ground motion parameter for a given combination of m and r.
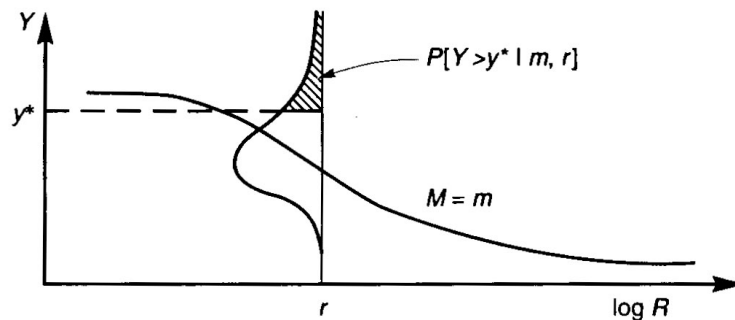
Figure B-6   Illustration of the conditional probability of exceeding a ground motion parameter (Kramer, 1996).

Temporal Uncertainty

The distribution of earthquake occurrence with time must be computed (or assumed) to calculate the probabilities of different earthquake magnitudes occurring in a given time period. Earthquakes are assumed to occur

randomly with time, and the assumption of random occurrence permits the use of simple probability models.

The temporal occurrence of earthquakes is commonly described as a Poisson process, which is a process that yields values of a random variable describing the number of occurrences of a particular event during a given time interval (or spatial region). In a Poisson process, the number of occurrences in one time interval are independent of the number that occur in any other time interval; the probability of occurrence during a very short time interval is proportional to the length of the time interval; and the probability of more than one occurrence in a very short time interval is negligible. Events in a Poisson process occur randomly, with no memory of the time, size, or location of any preceding events. Cornell and Winterstein (1988) showed that the Poisson model is useful for probabilistic hazard analysis unless the hazard is dominated by a single source zone that produces characteristic earthquakes, and the time since the previous significant event exceeds the average time between events.

In a Poisson process, the probability of a random variable, N, representing the number of occurrences of a particular event in a given time period is given by:

$$P[N = n] = \frac{\mu^n e^{-\mu}}{n!}$$
(B-3)

where μ is the average number of occurrences of the event in the time period. To characterize the temporal distribution of earthquake recurrence for probabilistic seismic hazard analysis, the Poisson probability is normally expressed as:

$$P[N = n] = \frac{(\lambda t)^n e^{-\lambda t}}{n!}$$
(B-4)

where λ is the average rate of recurrence of the event, and t is the time period. When the event is the exceedance of a particular earthquake magnitude, the Poisson model can be combined with a suitable recurrence law to predict the probability of at least one exceedance in a period of t years by:

$$P[N \geq 1] = 1 - e^{-\lambda_m t}$$
(B-5)

Probability Computations and Seismic Hazard Curves

Seismic hazard curves identify the annual frequency of exceedance of different values of a selected ground motion parameter. Development of seismic hazard curves involves probabilistic calculations that combine the

uncertainties in earthquake size, location, and frequency for each potential earthquake source that could impact shaking at the site.

Seismic hazard curve calculations are straightforward once the uncertainties in earthquake size, location, and frequency are established, but much bookkeeping is involved. The probability of exceeding a particular value y of a ground motion parameter, Y, is calculated for one possible source location, and then multiplied by the probability of that magnitude earthquake occurring at that particular location. The calculation is then repeated for all possible magnitudes and locations, and the probabilities of each are summed to compute the $P[Y > y]$ at the site. A summary of this process based on Kramer (1996) and McGuire (2004) is presented below.

For a given earthquake occurrence, the probability that a ground motion parameter, Y, will exceed a particular value y can be computed using the total probability theorem (Benjamin and Cornell, 1970) as:

$$P[Y > y] = P[Y > y | \mathbf{X}]P[\mathbf{X}] = \int P[Y > y | \mathbf{X}] f_x(\mathbf{X}) \, dx \qquad \text{(B-6)}$$

where $\mathbf{X}$ is a vector of random variables that influence Y. In most cases, the quantities in $\mathbf{X}$ are limited to the magnitude, M, and distance, R. Assuming that M and R are independent, the probability of exceedance can be written as:

$$P[Y > y] = \iint P[Y > y | m,r] f_M(m) f_R(r) \, dm \, dr \qquad \text{(B-7)}$$

where $P[Y > y | m,r]$ is obtained from the predictive relationship, and $F_M(m)$ and $f_R(r)$ are the probability density functions for magnitude and distance, respectively.

If the site is in a region of N_s potential earthquake sources, each of which has an average threshold rate of exceedance $v_i = \exp(\alpha_i - \beta_i m)$, the total average exceedance rate for the region is given by:

$$\lambda_y = \sum_{i=1}^{N_s} P[Y > y | m,r] f_{Mi}(m) f_{Ri}(r) \, dm \, dr \qquad \text{(B-8)}$$

This equation is typically solved by numerical integration. One simple approach described by Kramer (1996) is to divide the possible ranges of magnitude and distance into N_M and N_R segments, respectively. The average exceedance rate can then be calculated using the multi-level summation:

$$\lambda_y = \sum_{i=1}^{N_s} \sum_{j=1}^{N_m} \sum_{k=1}^{N_R} v_i P[Y > y | m_j, r_k] f_{Mi}(m_j) f_{Ri}(r_k) \Delta m \, \Delta r$$

$$= \sum_{i=1}^{N_s} \sum_{j=1}^{N_m} \sum_{k=1}^{N_R} v_i P[Y > y | m_j, r_k] P[M = m_j] P[R = r_k]$$

(B-9)

where:

$$m_j = m_0 + (j - 0.5)(m_{max} - m_0) / N_M$$

$$\Delta r = (r_{max} - r_{min}) / N_r$$

$$r_k = r_{min} + (k - 0.5)(r_{max} - r_{min}) / N_R$$

$$\Delta m = (m_{max} - m_0) / N_M$$

The above statement is equivalent to assuming that each source is capable of generating only N_M different earthquakes of magnitude, m_i, at only N_R different source-to-site distances of, r_k. The accuracy of this method increases with smaller segments and, thus, larger values of N_M and N_R.

Figure B-7 presents a sample seismic hazard curve for peak ground acceleration at a site in Berkeley, California. The figure shows contributions to the annual frequency of exceedance from nine different seismic sources.
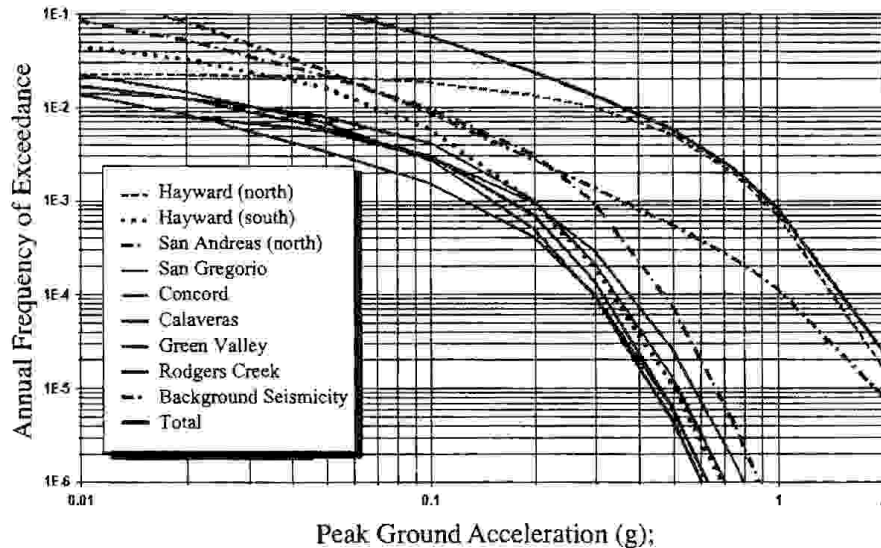
Figure B-7   Sample seismic hazard curve for Berkeley, California (McGuire, 2004).

Exceedance probabilities in a selected time period can be computed using seismic hazard curves combined with the Poisson model. The probability of exceedance for a value, y, in a time period, T, is:

$$P[Y_T > y] = 1 - e^{-\lambda_y T}$$

(B-10)

As an example, the probability that a peak horizontal ground acceleration of 0.10 g will be exceeded in a 50-year time period for a site characterized by the hazard curve in Figure B-7 is:

$$P[\text{PHA} > 0.1g \text{ in 50 years}] = 1 - e^{-\lambda_y T} = 1 - e^{-(0.060)(50)} = 0.950 = 95\% \qquad \text{(B-11)}$$

where $\lambda_y = 0.06$ is read from the curve in the figure corresponding to the total for all nine sources. An alternative, often made, computation is the value of the ground motion parameter corresponding to a particular probability of exceedance in a given time period. For example, the acceleration that has a 10% probability of exceedance in a 50-year time period would be the acceleration corresponding to an annual frequency of exceedance calculated by rearranging Equation B-10:

$$\lambda_y = -\frac{\ln(1 - P[Y_T > y])}{T} = -\frac{\ln(1 - 0.10)}{50} = 0.00211 \qquad \text{(B-12)}$$

Using the hazard curve from Figure B-7 for all nine sources, the corresponding zero-period spectral acceleration is approximately 0.75 g.

Hazard curves can be developed for specific periods of oscillation (0.2 s and 1.0 s are widely used periods), and the above calculations for probability of exceedance can be extended across the spectral domain. This permits development of probabilistic estimates of spectral demands for different probabilities of exceedance or return periods. Hazard curves have been developed for many different response quantities and characterizations of earthquake ground motion.

B.4.2 Inclusion of Rupture Directivity Effects

If the building site is located within 20 km of an active fault capable of generating an earthquake with magnitude M_w 6.5 or greater, rupture directivity effects should be considered. Average rupture directivity effects can be included directly in probabilistic seismic hazard analysis if the attenuation relationships are: (1) constructed using a database of recorded ground motions that include directivity effects (i.e., the NGA relationships described previously); or (2) corrected to account for rupture directivity in a manner similar to that described by Somerville et al. (1997) and Abrahamson (2000). The ratio of median maximum demand to geomean demand in the near-fault region is period-dependent, and can be as large as 2.0 (Huang et al., 2008a, 2008b).

B.4.3 Deaggregation of Seismic Hazard Curves and Epsilon

Probabilistic seismic hazard analysis enables calculation of annual rates of exceedance of ground motion parameters (e.g., spectral acceleration at a

selected period) at a particular site based on aggregating the risks from all possible source zones. Therefore, the computed rate of exceedance for a given parametric intensity value is not associated with any particular earthquake magnitude, m, or distance, r.

For a given building site and hazard curve, it is possible to establish the combinations of magnitude, distance, and source that contribute most to particular values of an intensity. This process is termed deaggregation (or disaggregation). Hazard deaggregation requires expression of the mean annual rate of exceedance as a function of magnitude and distance in the form:

$$\lambda_y(m_j, r_k) = P[M = m_j]P[R = r_k]\sum_{i=1}^{N_s} v_i P[Y > y | m_j, r_k] \qquad \text{(B-13)}$$

McGuire (2004) provides detailed information on hazard deaggregation.

Figure B-8 shows sample deaggregation results for horizontal spectral acceleration at periods of 0.2 s and 1.0 s for a site in the Western United States, for a 2% probability of exceedance in 50 years. Similar results can be obtained from the USGS *Unified Hazard Tool* (https://earthquake.usgs.gov /hazards/interactive/, last accessed March 15, 2018). Figure B-8b shows contributions to the 1-second uniform hazard spectral ordinate as a function of moment magnitude and distance. Approximately 50% of the total 1-second seismic demand can be ascribed to a M_W 7.8 earthquake at a distance of 14 km. The [M, r] pair that dominates the 1-second spectral demand at this site is, therefore, [7.8, 14].

Figure B-8 also introduces another important ground motion variable, termed epsilon, ε. Epsilon can be defined as:

$$\varepsilon = \frac{\ln S_a - \ln \theta}{\beta} \qquad \text{(B-14)}$$

where all variables vary as a function of period; S_a is the computed spectral acceleration for a given probability of exceedance (e.g., 2%) in a specified time period (e.g., 50 years) equal to 0.829 g in this instance at a period of 1 second; θ is the median value of spectral acceleration computed by an appropriate attenuation relationship for the dominant [M, r] pair equal to [7.8, 14] in this instance); and β is the dispersion in the attenuation relationship. In this example, and using the modal [M, r, ε] triple, ε ranges between 1 and 2, meaning that less than 15% of moment magnitude 7.8 earthquakes at a distance of 14 km would produce geomean spectral demands in excess of 0.829 g.
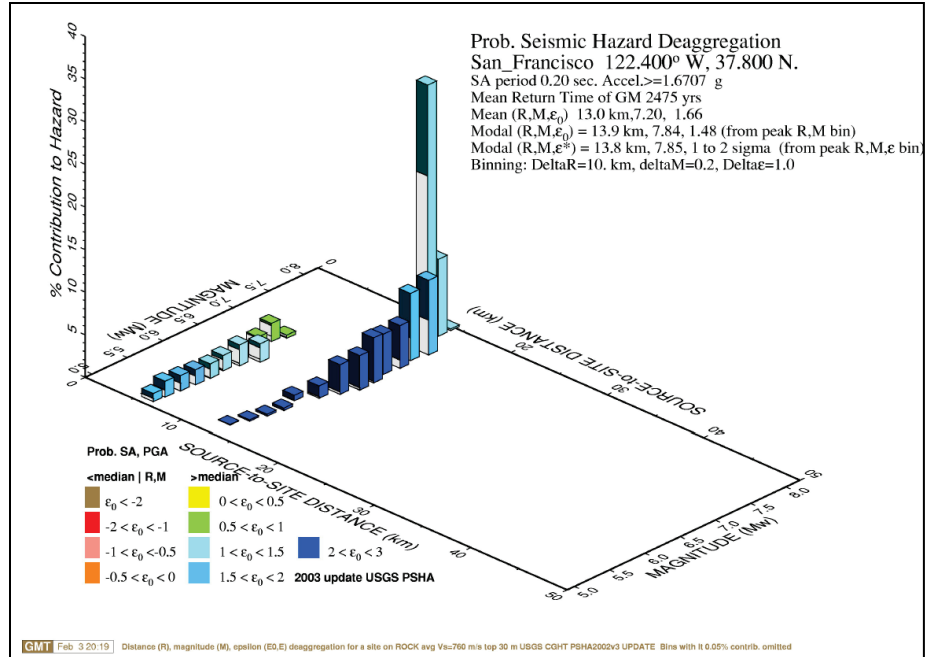
(a) 0.2 second deaggregation
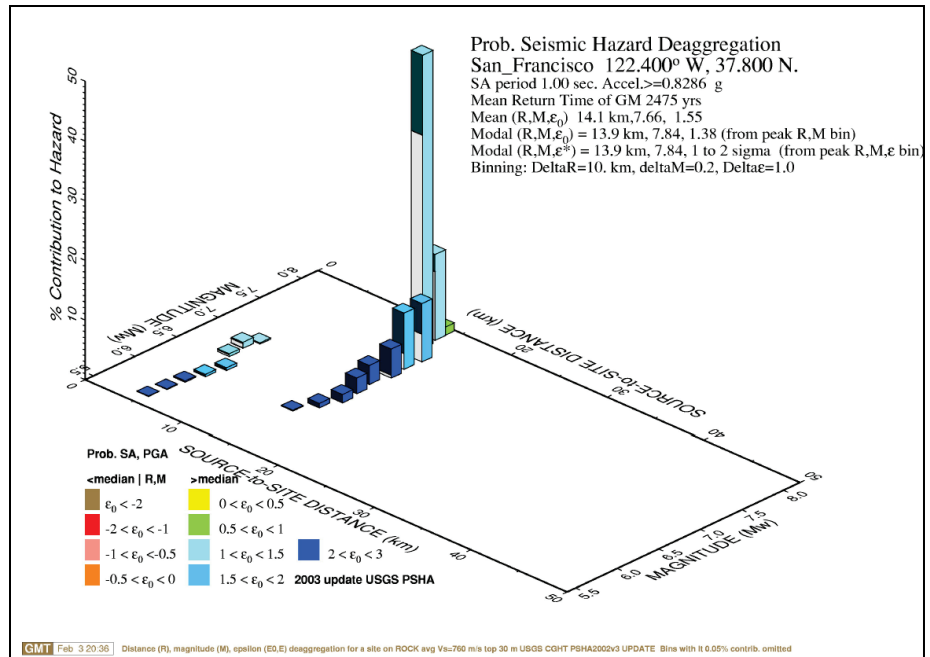
(b) 1.0 second deaggregation

Figure B-8   Sample deaggregation of a hazard curve from USGS.

Baker and Cornell (2005 and 2006) observed that ε is an indicator of spectral shape, with positive (or negative) values of ε at a given period tending to indicate a relative peak (or valley) in the acceleration response spectrum at that period. Figure B-9 illustrates these trends using six bins of 20 ground motions defined by $\varepsilon \geq 2.25$, $-0.06 \leq \varepsilon \leq 0.06$ and $\varepsilon \leq -2.25$, respectively,

at periods of 0.8 (Figure B-9a) and 0.3 second (Figure B-9b). The relative peak (or valley) in the spectra for the $+\varepsilon\,(-\varepsilon\,)$ bin of j motions at the two periods is clearly evident. No relative peak or valley at the reference periods is associated with the ε–neutral bin.
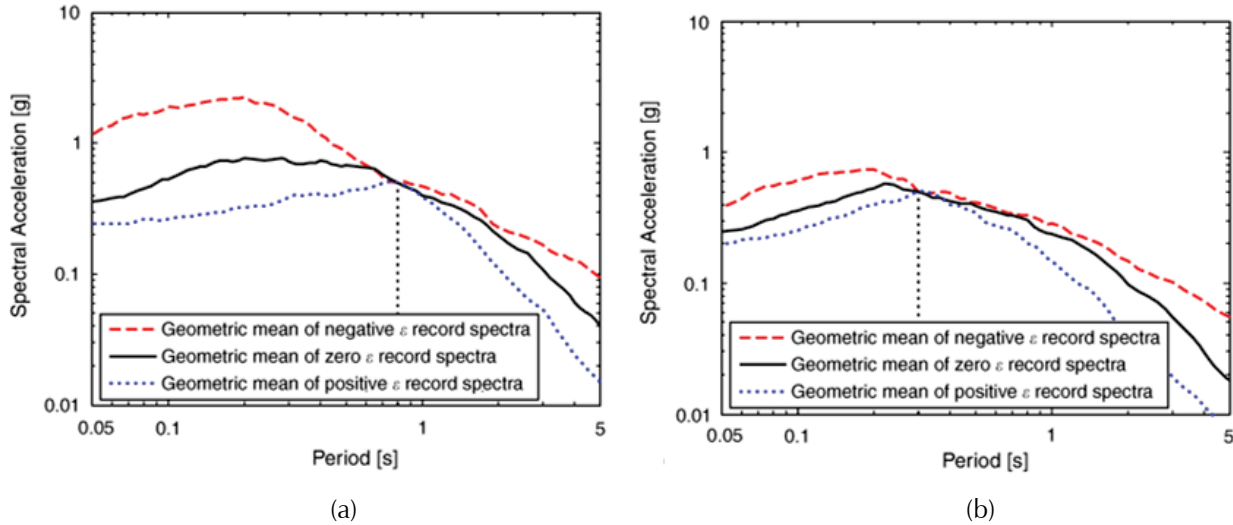
Figure B-9   Sample geometric-mean response spectra for negative-, zero- and positive-ε record sets, with each record scaled to: (a) $S_a(0.8\ \text{s}) = 0.5$ g; and (b) $S_a(0.3\ \text{s}) = 0.5$ g (Baker and Cornell 2006).

B.4.4 Conditional Mean Spectrum and Spectral Shape

Ordinates of uniform hazard spectra are each associated with the same annual frequency of exceedance. Building code and seismic design provisions for nonlinear response history analysis recommend scaling ground motions to match a target uniform hazard spectrum over a wide period range. Although this is convenient for design, and likely conservative, such scaling procedures have the following limitations:

- If the spectral ordinates of the uniform hazard spectrum are governed by multiple scenario events, the spectral shape will not be representative of any of the governing events, regardless of the return period (Baker and Cornell, 2006).

- For earthquake shaking with long return periods, the spectral ordinates of uniform hazard spectra are typically associated with high values of ε (greater than 1) across a wide range of periods (Harmsen, 2001). For the case in which the geomean spectral ordinate of a ground motion pair matches the uniform hazard spectrum ordinate at a given period, the geomean spectral ordinates are likely to be less than the uniform hazard spectrum at other periods. The geomean spectra for the $+\varepsilon$ record sets in Figure B-9 support this observation.

Baker and Cornell (2005, 2006) introduced the Conditional Mean Spectrum (CMS) which considers the correlation of spectral demands (represented by values of ε) at different periods, to address these limitations. Conditional Mean Spectra estimate the median geomean spectral acceleration response of a pair of ground motions given an $[M, r]$ pair and a target spectral ordinate, $\bar{S}_a(T_1)$, from which ε_T is back-calculated using an appropriate attenuation relationship. Baker and Cornell (2005) used the following equation to generate conditional mean spectra:

$$CMS_{\bar{S}_a(T_1)}(T_2) = \theta(M,r,T_2) \cdot \exp\left[\beta(M,r,T_2) \cdot \rho_{\varepsilon(T_1),\varepsilon(T_2)} \cdot \varepsilon_{T_1}\right] \quad \text{(B-15)}$$

where $CMS_{\bar{S}_a(T_1)}(T_2)$ is the ordinate of the spectrum at period T_2 given that the spectral demand at T_1 is $\bar{S}_a(T_1)$; $\theta(M,r,T_2)$ and $\beta(M,r,T_2)$ are the median and logarithmic standard deviation of spectral acceleration at T_2 computed using a ground motion attenuation relationship for the $[M, r]$ pair of interest; ε_T is the value of ε associated with $\bar{S}_a(T_1)$; and $\rho_{\varepsilon(T_1),\varepsilon(T_2)}$ is the correlation coefficient for ε between T_1 and T_2.

Baker and Jayaram (2008) developed a model for $\rho_{\varepsilon(T_1),\varepsilon(T_2)}$ using the NGA ground motion database (https://ngawest2.berkeley.edu/):

$$\begin{aligned}
&\text{if } T_{max} < 0.109 & \rho_{\varepsilon(T_1),\varepsilon(T_2)} = C_2 \\
&\text{else if } T_{min} > 0.109 & \rho_{\varepsilon(T_1),\varepsilon(T_2)} = C_1 \\
&\text{else if } T_{max} < 0.109 & \rho_{\varepsilon(T_1),\varepsilon(T_2)} = \min(C_2, C_4) \\
&\text{else} & \rho_{\varepsilon(T_1),\varepsilon(T_2)} = C_4
\end{aligned} \quad \text{(B-16)}$$

where: $T_{min} = \min(T_1, T_2)$, $T_{max} = \max(T_1, T_2)$, and

$$C_1 = 1 - \cos\left(\frac{\pi}{2} - 0.366\ln\left(\frac{T_{max}}{\max(T_{min}, 0.11)}\right)\right) \quad \text{(B-17)}$$

$$C_2 = \begin{cases} 1 - 0.105\left(1 - \dfrac{1}{1 + e^{100T_{max}-5}}\right)\left(\dfrac{T_{max} - T_{min}}{T_{max} - 0.01}\right), & \text{if } T_{max} < 0.2 \text{ sec} \\ 0, & \text{otherwise} \end{cases} \quad \text{(B-18)}$$

$$C_3 = \begin{cases} C_2 \text{ if } T_{max} < 0.11 \text{ sec} \\ C_1 \text{ if } T_{max} \geq 0.11 \text{ sec} \end{cases} \quad \text{(B-19)}$$

$$C_4 = C_1 + 0.5(\sqrt{C_3} - C_3)\left(1 + \cos\left(\frac{\pi T_{min}}{0.11}\right)\right) \quad \text{(B-20)}$$

Conditional Mean Spectra can be constructed using the following procedure:

1. Determine the value of $\bar{S}_a(T_1)$ from the probabilistic seismic hazard analysis at the desired mean annual frequency of exceedance.

2. Deaggregate the hazard at $\bar{S}_a(T_1)$ and identify the modal $[M, r, \varepsilon]$ triple.

3. Select an appropriate ground motion attenuation relationship.

4. Generate the spectrum using Equations B-15 through B-20 and the selected attenuation relationship for the $[M, r, \varepsilon]$ triple of Step 2.

5. Amplitude scale the spectrum to recover $\bar{S}_a(T_1)$.

As an illustration, consider the deaggregation results of Figure B-8b for a site in San Francisco. As presented in Figure B-8b, the value of $\bar{S}_a(T_1)$ is 0.83 g for a return period of 2,475 years, and the modal $[M, r, \varepsilon]$ triple for the hazard is [7.8, 14 km, 1 to 2]. In this example, $\varepsilon = 1.5$ (taken as the midpoint of 1 and 2), and the Chiou and Youngs (2008) NGA relationship was selected. Figure B-10 presents the results of Steps 4 and 5 using dotted and solid lines, respectively (if $\varepsilon = 2$ is used in Step 4, the scale factor for Step 5 is 1). The figure also presents the uniform hazard spectrum for this site at a return period of 2475 years. Except at period T_1, the ordinates of the uniform hazard spectrum are greater than those of the scaled Conditional Mean Spectrum.

The Conditional Mean Spectrum can be refined to also consider uncertainty in each spectral acceleration value at periods other than $\bar{S}_a(T_1)$. This is done because the probabilities associated with the target spectrum are associated only with $\bar{S}_a(T_1)$, and real ground motions with the target $\bar{S}_a(T_1)$ also have variability. Baker and Cornell (2005) computed the conditional standard deviation of spectral accelerations as follows:

$$\beta_{\overline{S_a(T_1)}=x}(T_2) = \beta(M, r, T_2)\sqrt{1 - \rho^2_{\varepsilon(T_1), \varepsilon(T_2)}} \tag{B-21}$$

where $\beta_{\overline{S_a(T_1)}=x}(T_2)$ is the conditional dispersion in $S_a(T_2)$ given $\bar{S}_a(T_1)$ and the other variables are as defined above. The target spectrum computed using Equation B-15 and Equation B-21 has been termed a Conditional Spectrum (Abrahamson and Al Atik, 2010), because, unlike the Conditional Mean Spectrum, it is not just a mean value. Figure B-11 shows the Conditional Spectrum corresponding to the Conditional Mean Spectrum plotted in Figure B-10. Methods and software tools are available to find ground motions that match a target mean and standard deviation (Jayaram et al., 2011).
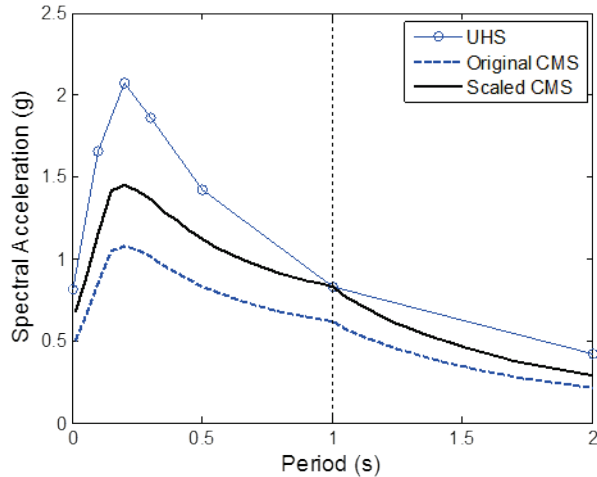
Figure B-10   Uniform Hazard Spectrum with 2% probability of exceedance in 50 years, Conditional Mean Spectrum, and scaled Conditional Mean Spectrum for a rock site in San Francisco.
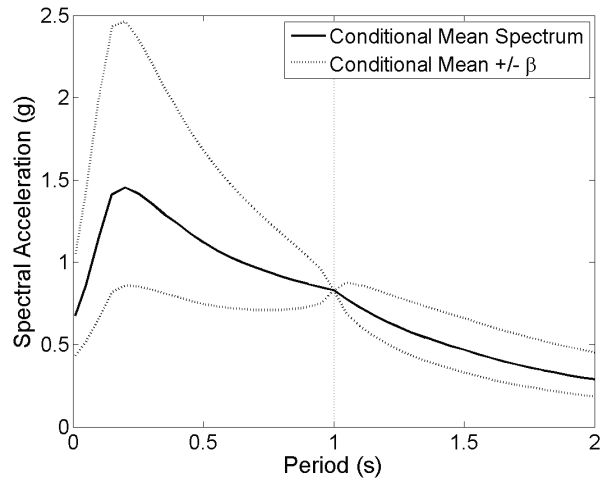
Figure B-11   Conditional Spectrum for $S_a(1s)$ with 2% probability of exceedance in 50 years for a rock site in San Francisco.

B.5   Vertical Earthquake Shaking

Vertical response spectra can be generated using ground motion prediction equations for vertical ground shaking parameters and probabilistic seismic hazard analysis to determine ordinates of spectral response at the desired annual frequencies of exceedance. This technique is discussed in Gülerce and Abrahamson (2011).

This section presents simplified procedures that can be used to generate vertical response spectra from horizontal spectra for the same site using approximate relationships between typical vertical and horizontal spectra. Extracted from FEMA P-750, *NEHRP Recommended Seismic Provisions for*

New Buildings and Other Structures (FEMA, 2009a), these procedures can be used for most buildings where important periods of vertical response are less than or equal to 1.0 second. For buildings with important periods of vertical response in excess of 1.0 second, site-specific analysis should be conducted.

B.5.1 Procedure for Site Classes A, B, and C

For structural periods less than or equal to 1.0 second, the vertical response spectrum can be constructed by scaling the corresponding ordinates of the horizontal response spectrum, S_a, as follows:

- For periods less than or equal to 0.1 second, the vertical spectral acceleration, S_v, can be taken as

$$S_v = S_a \qquad \text{(B-22)}$$

- For periods between 0.1 and 0.3 second, the vertical spectral acceleration, S_v, can be taken as

$$S_v = (1 - 1.048[\log(T) + 1])S_a \qquad \text{(B-23)}$$

- For periods between 0.3 and 1.0 second, the vertical spectral acceleration, S_v, can be taken as

$$S_v = 0.5 S_a \qquad \text{(B-24)}$$

B.5.2 Procedure for Site Classes D and E

For structural periods less than or equal to 1.0 second, the vertical response spectrum can be constructed by scaling the corresponding ordinates of the horizontal response spectrum, S_a, as follows:

- For periods less than or equal to 0.1 second, the vertical spectral acceleration, S_v, can be taken as

$$S_v = \eta S_a \qquad \text{(B-25)}$$

- For periods between 0.1 and 0.3 second, the vertical spectral acceleration, S_v, can be taken as

$$S_v = (\eta - 2.1(\eta - 0.5)[\log(T) + 1])S_a \qquad \text{(B-26)}$$

- For periods between 0.3 and 1.0 second, the vertical spectral acceleration, S_v, can be taken as

$$S_v = 0.5 S_a \qquad \text{(B-27)}$$

In Equations B-25 through B-27, η can be taken as 1.0 for $S_s \leq 0.5\,\text{g}$; 1.5 for $S_s \leq 1.5\,\text{g}$; and $(1 + 0.5(S_s - 0.5))$ for $0.5\,\text{g} \leq S_s \leq 1.5\,\text{g}$.

B.6   Soil-Structure Interaction

Structural response to earthquake shaking is affected by the dynamic interactions of the soil-structure system. Soil-structure interaction involves foundation flexibility, kinematic interaction, and foundation damping. Soil-structure interaction analysis includes direct or indirect (simplified) simulation of the system to prescribed free-field input motions, which are typically imposed as bedrock motions.

Approaches to soil-structure interaction analysis are illustrated in Figure B-12. Typical structural analysis assumes a rigid base (Figure B-12a) and neglects the effects of soil-structure interaction. Input motions at the base of the foundation are derived using code-based procedures assuming the soil classification at the site.

Use of fixed-base models can overestimate demands on stiff seismic-force-resisting systems (e.g., reinforced concrete shear walls, steel braced frames) because the response of such systems is sensitive to small base rotations and translations that occur as a result of foundation flexibility. Relatively flexible systems (e.g., moment-resisting frames) are less sensitive to foundation movement, and are often not significantly affected by soil-structure interaction.
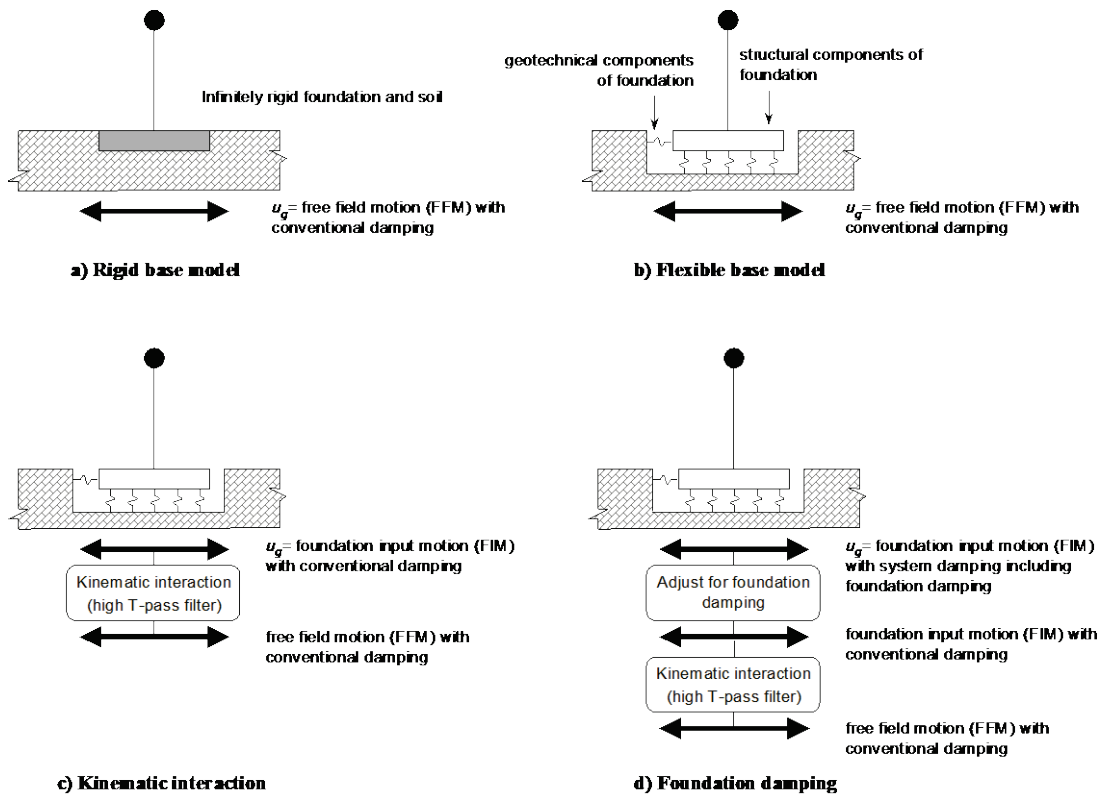
Figure B-12   Analysis for soil-structure interaction (FEMA, 2005).

B.6.1 Direct Analysis

Soil-structure interaction can be directly analyzed using finite-element models that represent the soil as discretized solid finite elements. Soil elements can either use equivalent linear properties, or full nonlinear representation. Direct analysis can explicitly address foundation flexibility, kinematic interaction, and foundation damping effects. Solution of the kinematic interaction problem is often difficult without customized finite element codes because typical codes cannot account for wave inclination and wave incoherence effects, both of which can be important.

Response history analysis requires the development of a three-dimensional numerical model of the soil-foundation-structure system. Stress-strain or constitutive models (linear, nonlinear or equivalent linear) for the soils in the model should be developed based on test data. Appropriate and consistent frequency-dependent stiffness and damping matrices should be developed for the boundaries of the soil in the numerical model.

B.6.2 Simplified Analysis

Simplified procedures for including the effects of soil-structure interaction in response analysis are based on FEMA 440, *Improvement of Nonlinear Static Seismic Analysis Procedures* (FEMA, 2005). More guidance on detailed procedures that can be used, together with example applications of these procedures, is provided in NIST GCR 12-917-21, *Soil-Structure Interaction for Building Structures* (NIST, 2012).

Foundation Flexibility

Figure B-12b illustrates the incorporation of foundation flexibility into the numerical model of a building. Current procedures, such as ASCE/SEI 41-06, *Seismic Rehabilitation of Existing Buildings* (ASCE, 2007) partially address foundation flexibility effects by providing guidance on the stiffness and strength of the soil components of the soil-foundation-structure system.

Numerical simulation including foundation flexibility provides global response predictions that include elastic and inelastic deformations in the soil-foundation system. These deformations are sometimes referred to as inertial effects. Inclusion of inertial effects can provide significantly different and more accurate response predictions than fixed base assumptions. Also, foundation response and failures (e.g., rocking, soil bearing failure, pier/pile slip) can be explicitly evaluated using such an approach. However, incorporation of foundation flexibility alone does not capture the reduction in shaking demand that occurs, relative to the free-field

motion, due to kinematic interaction or foundation damping effects, as described below.

Kinematic Interaction

Kinematic interaction, illustrated in Figure B-12c, is a result of relatively stiff foundation elements within soil stratum that causes foundation input motions to deviate from free-field motions. The effects on superstructure response are strongly period-dependent, being maximized at short periods. They can be visualized as a filter applied to the high-frequency components of the free-field ground motion. Kinematic effects include base slab averaging and embedment effects:

- **Base slab averaging.** Ground motion shaking is spatially variable. In the absence of a foundation, each point within a building footprint, would experience somewhat different shaking at the same instant in time. Placement of a structure and foundation across these spatially variable motions produces an averaging effect, and the overall motion experienced by the building is less than the localized maxima that would have occurred in the free-field, particularly at short periods. Base slab averaging occurs to some extent in virtually all buildings. The slab averaging effect occurs at the foundation level for mats or spread footings interconnected by either grade beams or reinforced concrete slabs. Even if a laterally stiff foundation system is not present, averaging can occur at the first elevated level of buildings with rigid diaphragms. Base slab averaging effects should be neglected in buildings with disconnected foundation elements and flexible floor and roof diaphragms.

- **Embedment effects.** Embedment effects are associated with the reduction of ground motion with depth into a soil stratum. Embedment effects should not be considered for buildings without basements, even if the footings are embedded. Embedment effects tend to be significant when the depth of embedment is greater than about 10 feet.

Simplified procedures are available (FEMA, 2005; NIST, 2012) to reduce the free field motion to a foundation input motion in response to kinematic interaction effects. A ratio-of-response-spectra factor can be used, which is the ratio of the response spectral ordinates imposed on the foundation (i.e., the foundation input motion) to the free-field spectral ordinates. The 5% damped free-field spectrum is multiplied by the product of the period-dependent reduction factors for base-slab averaging and embedment to derive the foundation input motion spectrum. Since the embedment computation is dependent on the peak horizontal ground acceleration, the computation must

be repeated for every level of hazard considered for the performance and loss assessment.

The resulting foundation input motion can be applied to a fixed-base model or combined with a flexible-base model. Kinematic effects tend to be important for buildings with relatively short fundamental periods (e.g., less than 0.5 second), large plan dimensions, and embedded basements.

Foundation Damping

Figure B-12d illustrates foundation damping effects that are another result of inertial interaction. Foundation damping results from the relative movements of the foundation and free-field soil. It is associated with radiation of energy away from the foundation and hysteretic damping within the soil. The result is an effective decrease in the spectral ordinates of ground motion experienced by the structure. Foundation damping effects tend to be greatest for stiff structural framing systems (e.g., reinforced concrete shear walls, steel braced frames) and relatively soft foundation soils (e.g., Site Classes D and E).

Simplified procedures are available (FEMA, 2005; NIST, 2012) to assess foundation damping. In these procedures, foundation radiation damping reduces the ordinates of the 5% damped acceleration response spectrum used as the basis for selecting and scaling ground motions. Hysteretic damping in the soil should be captured directly through the use of nonlinear soil springs.

B.7　Alternative Procedure for Hazard Characterization to Explicitly Consider Ground Motion Dispersion in Nonlinear Response History Analysis

Scenario-based assessments consider uncertainty in spectral demand. Ground motion intensity is assumed to be lognormally distributed with median value θ, and dispersion, β. In Chapter 5, ground motion dispersion is indirectly considered in the modeling uncertainty assumed in response calculation. This section presents an alternative procedure for ground motion selection in conjunction with nonlinear response history analysis that can be used to explicitly consider ground motion dispersion. If this procedure is selected, assumptions for modeling uncertainty used in response calculation must be adjusted accordingly.

Eleven values of spectral acceleration at each user-selected interval are used to characterize the distribution of seismic demand for scenario-based assessments as follows:

$$S_{ai} = \theta e^{\beta \eta_i} \quad \text{for } i = 1, 11 \tag{B-28}$$

where S_{ai} is the ith target spectral acceleration at a given period, and values of η_i are listed in Table B-2.

Table B-2   Values of η_i for Generating a Distribution of $S_{ai}(T)$

i	η_i	i	η_i	i	η_i
1	-1.69	5	-0.23	9	0.75
2	-1.10	6	0	10	1.10
3	-0.75	7	0.23	11	1.69
4	-0.47	8	0.47		

Figure B-13 illustrates this process for a scenario earthquake having a median spectral acceleration of 0.3 g and dispersion of 0.4. The figure shows the cumulative probability distribution represented by this median and dispersion, along with 11 equally spaced intervals, each having a probability of occurrence of 9.09%.
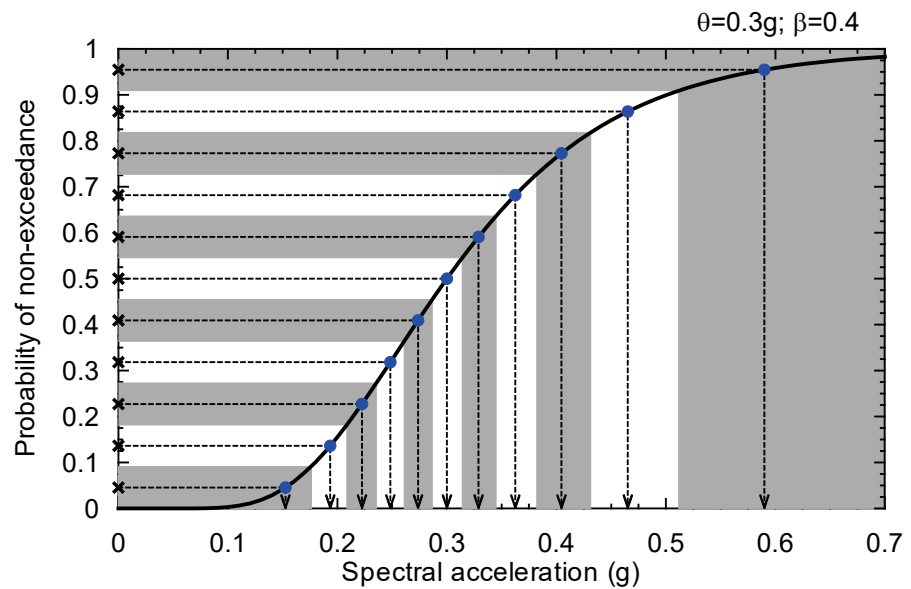
Figure B-13   Cumulative probability distribution for a scenario earthquake divided into 11 intervals with an equal probability of occurrence.

For each horizontal stripe, the central or midpoint value of the probability of non-exceedance is shown by the symbol "✘" with values of 4.55%, 13.64%, 22.73%, 31.82%, 40.91%, 50%, 59.09%, 68.18%, 77.27%, 86.36%, and 95.45%. A dashed horizontal line extends across the plot from the vertical axis to the cumulative distribution function, and then vertically down to the horizontal axis, where spectral acceleration values of 0.153 g, 0.193 g, 0.222 g, 0.248 g, 0.274 g, 0.300 g, 0.329 g, 0.362 g, 0.405 g, 0.465 g and 0.590 g, respectively, can be read.

The values of spectral acceleration, S_{a1} to S_{a11}, characterize the distribution of spectral acceleration shown in the figure and can be obtained from the following equation:

$$S_{ai} = \theta \cdot e^{\beta \cdot \Phi^{-1}(P_i)} \qquad \text{(B-29)}$$

where Φ^{-1} is the inverse standardized normal distribution, and P_i is the midpoint cumulative probability for region i. The values for η_i in Table B-2 are calculated from $\Phi^{-1}(P_i)$ for 11 target spectral accelerations. Alternatively, these values can be generated using an Excel worksheet and the function LOGINV $(p, \ln(\theta), \beta)$, where $p = (0.04545 \ldots.. 0.9545)$, $\ln(0.3) = -1.204$ is the mean, and $\beta = 0.4$ is the dispersion.

Identical to the procedures involving a Uniform Hazard Spectrum, users must specify a period range (T_{max}, T_{min}) for scaling pairs of ground motions. The characterization of the earthquake hazard can involve the following steps:

1. Select the magnitude and site-to-source distance for the scenario event.

2. Select an appropriate attenuation relationship(s) for the region, site soil type, and source characteristics.

3. Establish the period range (T_{max}, T_{min}) for scaling pairs of ground motions.

4. Determine the median spectral acceleration demands, θ, and the corresponding dispersions, β, in the period range (T_{max}, T_{min}) using the attenuation relationship(s) of Step 2.

5. Establish 11 target spectra, $S_{ai}(\bar{T})$, $i = 1.11$, using the medians and dispersions from Step 4 and Equation B-29 in the period range (T_{max}, T_{min}).

6. Select 11 pairs of ground motions.

7. Construct a geomean spectrum for each pair of ground motions.

8. For each target spectrum of Step 5, scale a pair of motions such that for each period in the range (T_{max}, T_{min}), the geomean spectrum matches the response spectrum $S_{ai}(T)$.

9. Repeat Step 8 for the remaining 10 spectra.

This procedure will result in 11 pairs of earthquake histories to represent the potential range of intensities associated with the scenario.

Step 8 in this procedure requires the selection of pairs of motions in Step 6 with geomean spectra in the period range (T_{max}, T_{min}) that are similar in shape to the target spectra of Step 5. If appropriate pairs of motions are

unavailable, an alternative to Steps 7, 8 and 9 is to spectrally match pairs of motions to the target spectra of Step 5, with each component in a pair matched to the same target spectrum.

A refinement to the above procedure involves the use of Conditional Mean Spectra and the effective fundamental period, $\overline{T}$, as defined in Chapter 4. Steps 4 through 9 above are altered as follows:

1. Determine the median spectral acceleration demand, θ, and the corresponding dispersion, β, at effective fundamental period $\overline{T}$, using the attenuation relationship(s) of Step 2.

2. Compute 11 target values of spectral acceleration, $S_{ai}(\overline{T})$, $i = 1..11$, using the medians and dispersions from Step 3.

3. Generate Conditional Mean Spectra, CMS$_i$, for the 11 target values of $S_{ai}(\overline{T})$ given magnitude and distance from Step 1 and η from Section B.7.

4. Select 11 pairs of ground motions, p_i, $i = 1..11$, such that the shape of the geomean spectrum for p_i is similar to that of the CMS$_i$ of Step 5 over a user-specified period range, which must include T_1^X and T_1^Y.

5. Amplitude scale the geomean spectral acceleration of the two components of p_i to $S_{ai}(\overline{T})$.

6. Repeat Step 8 for the remaining 10 spectra.

Similarly, spectral matching of pairs of motions can be used in lieu of selecting pairs of ground motions with geomean spectral shapes that are similar to CMS$_i$.

Appendix C

Residual Drift

C.1   Introduction

Residual drift (i.e., permanent set) is an important consideration in judging the post-earthquake safety of a building and the economic feasibility of repair. Modest levels of residual drift can require costly and difficult adjustments to certain nonstructural components (e.g., re-alignment of elevator rails and building facades), and can also lead to concerns that a building is unsafe for post-earthquake inspection or repair. Larger residual drifts can result in attempts to straighten the structural frame, or implementation of other measures intended to improve the stability of the system. Residual drifts can become large enough to seriously jeopardize structural stability in aftershocks, and render the building uneconomical to repair (i.e., the cost of repair is comparable to the cost of replacing the building).

Research has shown that residual drifts predicted by nonlinear response-history analysis are highly variable and sensitive to modeling assumptions. Key factors include the post-yield hardening/softening slope and unloading response. Also, residual drift can be larger for near-fault records with forward directivity pulses or long-duration records that cause many cycles of significant inelastic response. Accurate statistical simulation of residual drift requires advanced nonlinear response-history analyses, with a large number of ground motions and careful attention to the cyclic hysteretic response of the models and numerical accuracy of the solution.

Since the requirements for direct simulation of residual drift are computationally complex and not practical for general implementation, equations were developed to estimate residual drift as a function of the peak transient response of the structure. This appendix provides background information on the basis for the recommended relationships.

C.2   Past Research on Prediction of Residual Drift

Analytical studies by Riddell and Newmark (1979) and Mahin and Bertero (1981) first identified some of the key behavioral aspects associated with calculating residual drift. Recent studies, including MacRae and Kawashima (1997), MacRae (1994), Christopoulos et al. (2003), Christopoulos and

Pampanin (2004), Pampanin et al. (2003), and Ruiz-Garcia and Miranda (2005, 2006), have confirmed that residual drifts are largely dependent on the following parameters: (1) magnitude of peak transient inelastic drifts; (2) lateral strength of the structure relative to earthquake demand; (3) inelastic post-yield stiffness; (4) cyclic unloading response; (5) pulses in the ground motions; and (6) duration of ground shaking. The effects of these parameters are interrelated, and some are implicitly accounted for in the assessment of story drift. It is desirable that analytical models for residual drift account for variations in post-yield stiffness and cyclic unloading response because these parameters are structural parameters that can be influenced in design. For example, assessment of residual drift should differentiate between conventional structures and systems that employ self-centering devices that are designed to minimize residual drift.

Figure C-1 presents a schematic plot of peak story drift ratio versus ground motion intensity, relating predicted peak transient drift and residual drift under increasing intensity. Point "a" in the figure corresponds to the onset of inelastic response, below which residual drift does not occur. Point "c" corresponds to collapse of the structure, where residual and transient responses converge. Point "b" corresponds to the region between these two limits, where the residual drift is shown as some fraction of the transient drift.
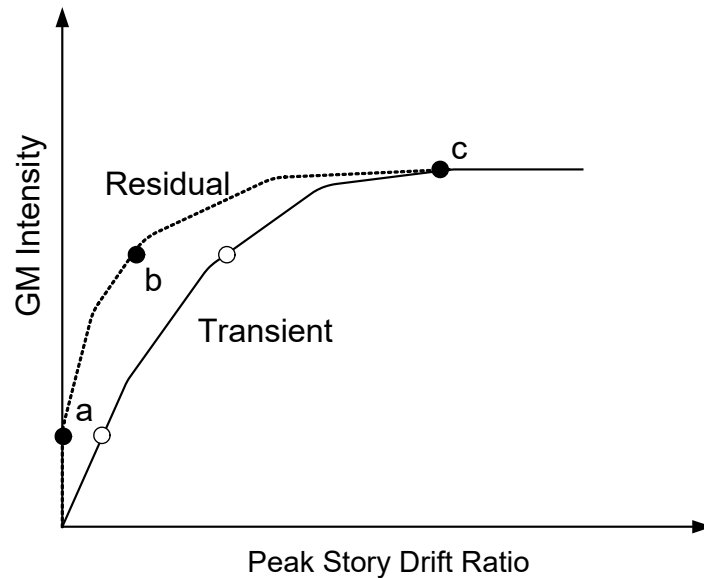
Figure C-1   Plot of peak story drift ratio versus ground motion intensity, relating predicted peak transient drift and residual drift ratios.

The figure indicates that the ratio between residual drift and transient drift is not constant, but it may be reasonable to treat this ratio as a constant. Much

of the existing literature to date has evaluated residual drift at intermediate levels of response, sometimes distinguishing between the degree of inelasticity by varying the strength of the structure, either by adjusting the strength using a response modification factor or by adjusting the transient story ductility demand.

The characteristics of unloading behavior can have a significant impact on residual displacements. Figure C-2 presents load versus deflection plots representing the types of unloading behaviors that have been identified as important in prior research. These studies have consistently shown that residual displacements are largest in elastic-plastic (EP) systems, due to their tendency to preserve the inelastic displacements upon unloading. This is in contrast to general inelastic (GI) response, where pinching or other effects lead to smaller unloading stiffness. Most recently, researchers have been examining the benefits of so-called self-centering (SC) systems, which are specifically designed with unloading characteristics (e.g., restoring forces) intended to minimize (or potentially eliminate) residual displacements. There are also structural behavioral characteristics, such as foundation rocking, which have natural self-centering tendencies.
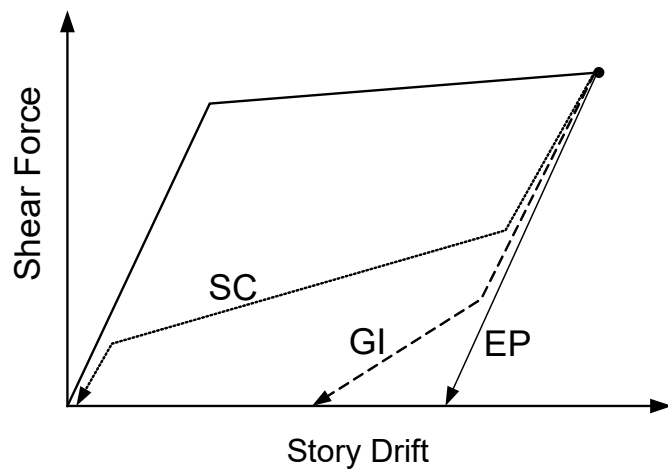
Figure C-2   Idealized unloading response characteristics for elastic-plastic (EP), general inelastic (GI), and self-centering (SC) systems.

Due to the variety of approaches and parameters addressed by various researchers, it is difficult to generalize the results of all prior research. However, important overall results and observations from key analytical studies can be summarized as follows:

- MacRae and Kawashima (1997) investigated residual displacements in single-degree-of-freedom bilinear oscillators with a focus on bridge design, where the presence of residual displacements was cited as a

major factor in bridge closures and replacement. They proposed a model to estimate residual displacements as a function of the peak inelastic displacement, unloading properties of the inelastic oscillator, and a statistical coefficient based on nonlinear response history analyses. In an illustrative example, they predicted residual displacements equal to about 0.16 times the maximum transient displacement. According to their proposed model, the residual displacement ratio could be deaggregated into the following product, $0.16 = 0.67 \times 0.9 \times 0.27$, where 0.67 is the ratio of plastic to total drift (equal to the sum of the elastic and plastic drift), 0.9 represents the effect of reduced unloading stiffness, and 0.27 is a statistical parameter accounting for inelastic dynamic response. The specific value of 0.27 represents the mean plus one standard deviation from a range of analyses for systems with modest strain hardening and a ductility demand ratio of 4.

- Christopoulos et al. (2003) conducted analyses of single-degree-of-freedom models with a primary emphasis on characterizing the effects of post-yield hardening stiffness and hysteretic unloading behavior on response. The models were generally representative of modern ductile moment frame buildings, ranging in height from 4 to 20 stories, designed with base shear yield ratios, V_y/W, ranging from 0.26 to 0.11, respectively. They applied ground motions to represent both design and maximum earthquakes. Maximum drift ratios observed in their analyses were in the range of 2% to 3%. Analyses of elastic-plastic (EP) models with zero hardening had residual displacements ranging from 0.1 to 0.4 times the peak inelastic transient displacements. These ratios reduced to 0.1 to 0.2 for systems with 5% strain-hardening, and increased up to 0.7 for systems with 5% strain-softening (i.e., –5 % hardening). The largest residual displacements and peak transient ductilities (up to 5 times yield) were observed in a 4-story building with strain-softening (approximate period equal to1 second). Comparable analyses using a general inelastic model (i.e., Takeda model) had significantly smaller residual drifts, ranging between 0.07 to 0.12 times peak transient drifts for systems with zero or positive strain-hardening, and 0.10 to 0.15 times peak transient drifts for systems with strain-softening. In related studies of multi-degree-of-freedom models (Pampanin et al., 2003), residual drifts were on the order of 0.05 to 0.25 times the total transient drift, depending on post-yield hardening and hysteretic modeling assumptions.

- Ruiz-Garcia and Miranda (2005, 2006) conducted an extensive parametric study of single- and multi-degree-of-freedom systems with the goal to characterize probabilistic residual drift hazard curves. They generally expressed their results in terms of a parameter, C_r, relating

residual drift to elastic spectral displacement. For consistency with other prior research studies, this parameter would need to be modified to account for the difference between peak inelastic transient displacement and elastic spectral displacement. Presumably, this adjustment is close to unity when the equal displacement approximation is expected to be applicable (i.e., in long period systems dominated by single mode behavior under small to moderate displacements). For elastic-plastic models with periods greater than 1 second, and elastic demand to yield strength ratios of $R = 1.5$ to 6, they reported median values of $C_r = 0.25$ to 0.5. This ratio increased to $C_r = 0.8$ for oscillators with periods between 0.5 and 1 second, and became even larger for smaller periods. Since the ratio is conditioned on elastic spectral displacement, the large amplification at small periods is probably a reflection of the amplification between elastic and inelastic transient displacements that occurs in the short period range. For stiffness-degrading systems, the median value of C_r reduced to about 0.1 to 0.3. They also reported dispersion in C_r of about 0.8, which was fairly constant across various periods and building strengths.

C.3   Model to Calculate Residual Drift

Based on the results of prior analytical studies, the following set of equations were developed to relate residual story drift, Δ_r, to story drift, Δ:

$$\begin{aligned}
\Delta_r &= 0 & &\text{for } \Delta \leq \Delta_y \\
\Delta_r &= 0.3\left(\Delta - \Delta_y\right) & &\text{for } \Delta_y < \Delta < 4\Delta_y \\
\Delta_r &= \left(\Delta - 3\Delta_y\right) & &\text{for } \Delta \geq 4\Delta_y
\end{aligned} \qquad \text{(C-1)}$$

where Δ_y is the story drift at yield. These equations were calibrated such that at a ductility ratio of 4, the ratio of residual drift to peak transient drift is 0.23. At ductility ratios of 2 and 6, the ratios of residual drift to peak transient drift are 0.15 and 0.5, respectively. Ultimately, as the collapse point is reached, residual drift and peak story drift will converge. The relationship between these equations is illustrated in Figure C-3.

The equations apply to typical building systems. They are intentionally simplistic due to a lack of physical data for validation of modeling of residual displacements and the analytical complexity necessary to obtain significant improvement in residual drift estimates. The equations do not distinguish between many of the behavioral characteristics known to affect residual drift. For example, where previous studies of idealized models have shown a correlation between post-yield stiffness and residual drift, this is not directly reflected in the equations. Characteristics like post-yield stiffness are,

however, considered in the overall process to the extent that they impact story drift calculations upon which residual drift estimates are based.
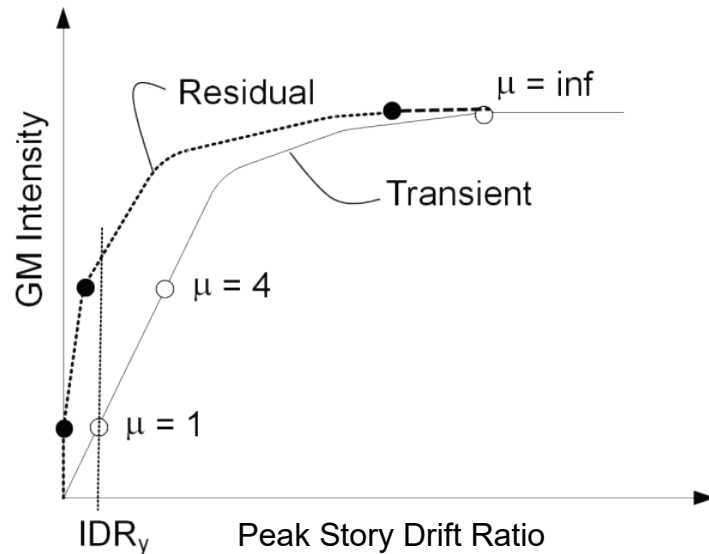
Figure C-3   Idealized model to estimate residual drift from transient story drift.

To illustrate how the equations work, consider a steel moment frame with a yield drift ratio of 1%. At 3% total drift, the predicted residual drift ratio would be 0.6%, or about 0.20 times the peak transient drift ratio. At 5% total drift, the predicted residual drift ratio would be about 1.9%, or about 0.38 times the peak transient drift ratio. At 7% total drift (approaching the collapse point), the residual drift ratio would be about 3.9%, or 0.56 times the peak transient drift ratio.

Per Ruiz-Garcia and Miranda (2005, 2006), the dispersion on residual drift estimates is about 0.8. Alternative ways to consider this dispersion in a performance assessment include: (1) calculate the median residual drift demand fragility using Equation C-1 based on the median transient and yield drift ratios, and then apply a dispersion of 0.8; or (2) calculate the residual drift probability based on integration of the conditional probability of residual drift and the transient drift. In the latter case, the dispersion on the conditional probability of residual drift should be reduced by the record-to-record variability in the transient drift.

C.4   Damage States for Residual Drift

Table C-1 identifies four damage states (DS_i) associated with residual drift. These damage states range from the onset of damage to nonstructural components to near-collapse of the structure. The proposed median story drifts (residual drift as a percentage of story height) are approximate and

based on a combination of judgment and limits previously suggested in Table C1-3 of FEMA 356, *Prestandard and Commentary for the Seismic Rehabilitation of Buildings* (FEMA, 2000b). For DS4, limits on residual drift expressed in terms of the design shear force are intended to cover cases in regions of low seismicity where the destabilizing effects of *P*-delta might dominate at smaller drift ratios than the values noted.

Table C-1 Damage States for Residual Story Drift Ratio

Damage State	Description	Residual Story Drift Ratio Δ/h [(1)]
DS1	No structural realignment is necessary for structural stability; however, the building may require adjustment and repairs to nonstructural and mechanical components that are sensitive to building alignment (e.g., elevator rails, curtain walls, and doors).	0.2% (equal to the maximum out-of-plumb tolerance typically permitted in new construction)
DS2	Realignment of structural frame and related structural repairs required to maintain permissible drift limits for nonstructural and mechanical components and to limit degradation in structural stability (i.e., collapse safety)	0.5%
DS3	Major structural realignment is required to restore margin of safety for lateral stability; however, the required realignment and repair of the structure may not be economically and practically feasible (i.e., the structure might be at total economic loss).	1%
DS4	Residual drift is sufficiently large that the structure is in danger of collapse from earthquake aftershocks (note: this performance point might be considered as equal to collapse, but with greater uncertainty).	High Ductility Systems $4\% < 0.5V_{design}/W$ Moderate Ductility Systems $2\% < 0.5V_{design}/W$ Limited Ductility Systems $1\% < 0.5V_{design}/W$

Notes: [(1)] *h* is the story height.

Further work is needed to establish appropriate parameters to describe the uncertainty in these limits and loss functions to define the direct economic loss and downtime losses associated with these damage states. For example, DS1 may require repairs to nonstructural components that may not otherwise be damaged, except for the need to realign components. Similarly, depending on the type of system, DS2 may require extensive structural repairs beyond those evident from the assessment of structural component damage.

The relationship between transient and residual drift demands, per Equation C-1, can be combined with the information in Table C-1 to relate these

damage states to story drifts. Through the yield drift, Δ_y, the relationship between the residual drift damage states and peak transient drift will depend on the stiffness of the system. Some example relationships are summarized in Table C-2, which are based on the assumed yield drift ratios noted.

Table C-2 Sample Transient Story Drift Ratios, Δ / h, associated with Damage State Definitions for Residual Drift

Sample Framing System	Δ_y / h	Δ / h			
		DS1[1]	DS2[1]	DS3[1]	DS4[2]
Steel ductile moment resisting frame	1%	1.5%	2.7%	4.1%	7.1%
Reinforced concrete shear wall	0.5%	1%	2.2%	2.6%	3.6%
Timber shear wall	1%	1.5%	2.7%	4.1%	5.1%

Notes: [1] $\Delta_r / h = 0.2\%$, 0.5% and 1.0% for DS1, DS2 and DS3, respectively.

 [2] $\Delta_r / h = 4\%$, 2% and 2% for steel moment resisting frames, reinforced concrete shear walls, and timber shear walls, respectively.

Appendix D

Component Fragility Specifications

D.1 Summary of Provided Fragility Specifications

Fragility specifications are detailed descriptions of potential component damage states, fragility functions, and consequence functions. Table D-1 provides a summary listing of structural and nonstructural component fragility specifications provided as part of the methodology. The table is organized by general system type, and includes the fragility group classification number, a description of the type of components included in the fragility group, and the number of sub-categories available for each component type. The fragility classification numbers are based on NISTIR 6389, *UNIFORMAT II Elemental Classification for Building Specifications, Cost Estimating and Cost Analysis* (NIST, 1999). The sub-categories have been developed to differentiate between components with:

- different vulnerability to damage (e.g., code compliance, details of construction, braced versus unbraced systems, and anchored versus unanchored equipment); and

- different repair, life-safety, or occupancy consequences associated with damage (e.g., gypsum wallboard repairs consisting of patch and paint versus replacement of ceramic tile).

Differences in structural vulnerability are generally related to compliance with ductile detailing requirements in material design standards for special, intermediate, or ordinary systems. Differences in nonstructural system vulnerability are generally related to bracing and anchorage and the governing code at the time of installation.

Differences in consequence functions are generally related to repair costs, which are a function of the quantity of material damaged. For example, fragility specifications for low aspect ratio concrete shear walls include sub-categories for the following wall thicknesses:

- less than 8 inches thick

- 8 to 16 inches thick

- 16 to 24 inches thick

The relative difficulty in accessing or conducting repairs and the quality of finish materials also affect repair costs. For each of the above low aspect ratio wall thicknesses, for example, additional sub-categories have been developed to account for differences in repair costs related to panel height, considering panels that are:

- Less than 15 feet tall

- 16 to 24 feet tall

- 25 to 40 feet tall

Similar logic for other structural and nonstructural components and systems expands the list to more than 700 individual fragility specifications. Each fragility specification includes a description of the component, a description of the possible damage states, the logical interrelationship between the damage states, the demand parameter used to determine damage state occurrence, the consequence functions associated with each damage state, and a quality rating for the specification. The quality rating is an indication of the reliability of the data and procedures used in the development of the fragility.

All vulnerable structural components, nonstructural components, and contents are assigned a fragility specification and categorized into fragility groups and performance groups. Procedures for selecting appropriate fragility specifications for individual building components, along with procedures for creating user-defined, building-specific fragility specifications, are provided in *Volume 2 – Implementation Guide*. Details including the specific attributes of each fragility specification are provided in *Volume 3 – Supporting Electronic Materials*, accessible through the Fragility Manager in the *Performance Assessment Calculation Tool* (PACT), or viewed directly in the *Fragility Database* (Excel workbook), or the *Fragility Specification* (PDF file).

> **Second Edition Update**
> Fragility and consequence data for selected components have been updated.

This Second Edition includes fragilities for the following new structural and nonstructural components:

- Wall partitions, metal studs with gypsum wallboard (FEMA P-58-3, BD-3.9.32)

- Acoustical tile or lay-in panel suspended ceilings (FEMA P-58-3, BD-3.9.31)

- Concrete link beams

- Buckling-restrained braced frames

- Concrete flat slabs

Additional changes to the fragility and consequence information are documented in: (1) FEMA P-58-3 *FEMAP-58_UpdatestoFragilitiesMemo* PDF file and (2) *FEMAP-58_LinebyLineComparisonofFragilityDB.xls*, an Excel Workbook presenting a line-by-line comparison of current fragility database versus versions published prior to September 2016. Please note that due to these changes, a building model developed with a previous version of PACT may cause an error.

Table D-1   List of Provided Fragility Specifications

General System Description	Fragility Classification Number	Component Description	Number of Sub-Categories
Miscellaneous Structural Steel Components/ Connections	B1031.001	Bolted shear tab gravity connections	1
	B1031.011	Steel column base plates	3
	B1031.021	Welded column splices	3
Structural Steel Special Concentrically Braced Frames	B1033.001	Special Concentrically Braced Frame with wide flange (WF) braces, balanced design criteria, chevron brace	3
	B1033.002	Special Concentrically Braced Frame with WF braces, balanced design criteria, single diagonal	3
	B1033.003	Special Concentrically Braced Frame with WF braces, balanced design criteria, X Brace	3
	B1033.011	Special Concentrically Braced Frame with hollow structural section (HSS) braces, balanced design criteria, chevron brace	3
	B1033.012	Special Concentrically Braced Frame with HSS braces, balanced design criteria, single diagonal	3
	B1033.013	Special Concentrically Braced Frame with HSS braces, balanced design criteria, X Brace	3
	B1033.021	Special Concentrically Braced Frame with HSS braces, tapered gusset plates, design to AISC minimum standard, chevron brace	3
	B1033.022	Special Concentrically Braced Frame with HSS braces, tapered gusset plates, design to AISC minimum standard, single diagonal	3

Table D-1   List of Provided Fragility Specifications (continued)

General System Description	Fragility Classification Number	Component Description	Number of Sub-Categories
Structural Steel Special Concentrically Braced Frames (cont'd)	B1033.023	Special Concentrically Braced Frame with HSS braces, tapered gusset plates, design to AISC minimum standard, X Brace	3
	B1033.031	Special Concentrically Braced Frame, design to AISC minimum standards, chevron brace	3
	B1033.032	Special Concentrically Braced Frame, design to AISC minimum standards, single diagonal	3
	B1033.033	Special Concentrically Braced Frame, design to AISC minimum standards, X Brace	3
	B1033.041	Special Concentrically Braced Frame with double angle braces, chevron brace	3
	B1033.042	Special Concentrically Braced Frame with double angle braces, single diagonal	3
	B1033.043	Special Concentrically Braced Frame with double angle braces, X Brace	3
Structural Steel Concentrically Braced Frames	B1033.051	Ordinary Concentrically Braced Frame with compact braces, chevron brace	3
	B1033.052	Ordinary Concentrically Braced Frame with compact braces, single diagonal	3
	B1033.053	Ordinary Concentrically Braced Frame with compact braces, X Brace	3
	B1033.061	Ordinary Concentrically Braced Frame, brace design to ductile slenderness limits, chevron brace	3
	B1033.062	Ordinary Concentrically Braced Frame, brace design to ductile slenderness limits, single diagonal	3
	B1033.063	Ordinary Concentrically Braced Frame, brace design to ductile slenderness limits, X Brace	3
	B1033.071	Braced frame, design for factored loads, no additional seismic detailing, chevron brace	3
	B1033.072	Braced frame, design for factored loads, no additional seismic detailing, single diagonal	3

Table D-1   List of Provided Fragility Specifications (continued)

General System Description	Fragility Classification Number	Component Description	Number of Sub-Categories
Structural Steel Concentrically Braced Frames (cont'd)	B1033.073	Braced frame, design for factored loads, no additional seismic detailing, X Brace	3
	B1033.101	Buckling-Restrained Brace (BRB), chevron brace	3
	B1033.111	Buckling-Restrained Brace (BRB), single diagonal	3
Structural Steel Moment Frames	B1035.001	Post-Northridge Reduced Beam Section (RBS) connection with welded web, beam one side	2
	B1035.011	Post-Northridge RBS connection with welded web, beam both sides	2
	B1035.021	Post-Northridge welded steel moment connection other than RBS, beam one side	2
	B1035.031	Post-Northridge welded steel moment connection other than RBS, beam both sides	2
	B1035.041	Pre-Northridge Welded Unreinforced Flange-Bolted (WUF-B) beam-column joint, beam one side	2
	B1035.051	Pre-Northridge WUF-B beam-column joint, beam both sides	2
Structural Steel Eccentrically Braced Frames	B1035.061	Eccentrically Braced Frame shear link, no floor beams	2
	B1035.062	Eccentrically Braced Frame shear link, with floor beams	2
Reinforced Concrete Special Moment Frames	B1041.001a	ACI 318 Special Moment Frame (SMF), beam one side	3
	B1041.001b	ACI 318 SMF, beam both sides	3
	B1041.011a	Moment frame with SMF-conforming beam and column flexural and confinement reinforcement but weak joints, beam one side	3
	B1041.011b	Moment frame with SMF-conforming beam and column flexural and confinement reinforcement but weak joints, beam both sides	3
Reinforced Concrete Intermediate Moment Frames	B1041.021a	ACI 318 Intermediate Moment Frame (IMF), beam one side	3
	B1041.021b	ACI 318 IMF, beam both sides	3

Table D-1   List of Provided Fragility Specifications (continued)

General System Description	Fragility Classification Number	Component Description	Number of Sub-Categories
Reinforced Concrete Ordinary Moment Frames	B1041.031a	ACI 318 Ordinary Moment Frame (OMF) with weak joints and beam flexural response, beam one side	3
	B1041.031b	ACI 318 OMF with weak joints and beam flexural response, beam both sides	3
	B1041.041a	ACI 318 OMF with weak joints and column flexural response, beam one side	3
	B1041.041b	ACI 318 OMF with weak joints and column flexural response, beam both sides	3
	B1041.051a	ACI 318 OMF with weak beams and weak joints, beam flexural or shear response, beam one side	3
	B1041.051b	ACI 318 OMF with weak beams and weak joints, beam flexural or shear response, beam both sides	3
	B1041.061a	ACI 318 OMF with weak columns, beam one side	3
	B1041.061b	ACI 318 OMF with weak columns, beam both sides	3
	B1041.071a	ACI 318 OMF with weak columns and high axial load, beam one side	3
	B1041.071b	ACI 318 OMF with weak columns and high axial load, beam both sides	3
Reinforced Concrete Non-Conforming Moment Frames	B1041.081a	Non-conforming Moment Frame (MF) with weak joints and beam flexural response, beam one side	3
	B1041.081b	Non-conforming MF with weak joints and beam flexural response, beam both sides	3
	B1041.091a	Non-conforming MF with weak joints and column flexural response, beam one side	3
	B1041.091b	Non-conforming MF with weak joints and column flexural response, beam both sides	3
	B1041.101a	Non-conforming MF with weak beams and strong joints, beam one side	3
	B1041.101b	Non-conforming MF with weak beams and strong joints, beam both sides	3
	B1041.111a	Non-conforming MF with weak columns, beam one side	3

General System Description	Fragility Classification Number	Component Description	Number of Sub-Categories
Reinforced Concrete Non-Conforming Moment Frames (cont'd)	B1041.111b	Non-conforming MF with weak columns, beam both sides	3
	B1041.121a	Non-conforming MF with weak columns and strong joints, beam both sides	3
	B1041.121b	Non-conforming MF with weak columns and strong joints, beam one side	3
	B1041.131a	Non-conforming MF with inadequate development of reinforcing, beam one side	3
	B1041.131b	Non-conforming MF with inadequate development of reinforcing, beam both sides	3
Reinforced Concrete Shear Walls	B1042.001a	Concrete link beam, diagonally reinforced	6
	B1042.002a	Concrete link beam, conventionally reinforced	6
	B1044.001	Rectangular low aspect ratio concrete walls, less than 8" thick	3
	B1044.011	Rectangular low aspect ratio concrete walls, 8" to 16"	3
	B1044.021	Rectangular low aspect ratio concrete walls, 18" to 24" thick	3
	B1044.031	Low-rise reinforced concrete walls with return flanges, less than 8" thick	3
	B1044.041	Low-rise reinforced concrete walls with return flanges, 8" to 16" thick	3
	B1044.051	Low-rise reinforced concrete walls with return flanges, 17" to 24" thick	3
	B1044.061	Low-rise reinforced concrete walls with boundary columns, less than 8" thick	3
	B1044.071	Low-rise reinforced concrete walls with boundary columns, 8" to 16" thick	3
	B1044.081	Low-rise reinforced concrete walls with boundary columns, 17" to 24" thick	3
	B1044.091	Slender reinforced concrete walls, 12" thick	3
	B1044.101	Slender reinforced concrete walls, 18" thick	3
	B1044.111	Slender reinforced concrete walls, 30" thick	3

Table D-1   List of Provided Fragility Specifications (continued)

General System Description	Fragility Classification Number	Component Description	Number of Sub-Categories
Reinforced Concrete Flat Slabs	B1049.001	Reinforced concrete flat slab, columns without shear reinforcing	6
	B1049.011	Reinforced concrete flat slab, columns with shear reinforcing	2
	B1049.021	Post-tensioned concrete flat slab, columns without shear reinforcing	4
	B1049.031	Post-tensioned concrete flat slab, columns with shear reinforcing	2
	B1049.041	Reinforced concrete flat slab with drop panel or drop capital, columns without shear reinforcing	4
Reinforced Masonry Ordinary Walls	B1051.001	Ordinary reinforced masonry walls with partially grouted cells, 4" to 6" thick, shear dominated	2
	B1051.003	Ordinary reinforced masonry walls with partially grouted cells, 4" to 6" thick, flexure dominated	2
	B1051.011	Ordinary reinforced masonry walls with partially grouted cells, 8" to 12'" thick, shear dominated	2
	B1051.013	Ordinary reinforced masonry walls with partially grouted cells, 8" to 12" thick, flexure dominated	2
	B1051.021	Ordinary reinforced masonry walls with partially grouted cells, 16" thick, shear dominated	2
	B1051.023	Ordinary reinforced masonry walls with partially grouted cells, 16" thick, flexure dominated	2
Reinforced Masonry Special Walls	B1052.001	Special reinforced masonry walls with fully grouted cells, 8" or 12" thick, shear dominated	2
	B1052.003	Special reinforced masonry walls with fully grouted cells, 8" to 12" thick, flexure dominated	2
	B1052.011	Special reinforced masonry walls with fully grouted cells, 16" thick, shear dominated	2
	B1052.013	Special reinforced masonry walls with fully grouted cells, 16" thick, flexure dominated	2
Cold-Formed Steel Walls	B1061.001a	Cold-formed steel walls with structural sheathing, interior, with gypsum wallboard	3
	B1061.001b	Cold-formed steel walls with structural sheathing, exterior, with stucco on one side	3

Table D-1   List of Provided Fragility Specifications (continued)

General System Description	Fragility Classification Number	Component Description	Number of Sub-Categories
Light-Framed Wood Walls	B1071.001	Light-framed wood walls with structural panel sheathing and gypsum wallboard	2
	B1071.011	Light-framed wood walls with structural panel sheathing and stucco	2
	B1071.031	Light-framed wood walls with diagonal let-in bracing	1
Exterior Walls	B1071.041	Full-height wood studs with gypsum wallboard	1
	B2011.001a	Cold-formed steel walls with structural sheathing and gypsum wallboard	3
	B2011.001b	Cold-formed steel walls with structural sheathing, stucco on one side	3
	B2011.101	Light-framed wood walls with structural panel sheathing and gypsum wallboard	2
	B2011.102	Light-framed wood walls with structural panel sheathing and stucco	2
	B2011.131	Light-framed wood walls with diagonal let-in bracing	1
Exterior Precast Concrete Wall Panels	B2011.201a	Precast concrete panels with user-specified in-plane and out-of-plane connection capacity	2
Exterior Glazing	B2022.001	Generic curtain walls	3
	B2022.011	Midrise stick-built curtain walls	28
	B2023.001	Generic storefronts	2
	B2023.011	Storefronts	15
Tile Roofs	B3011.011	Concrete tile roof, tiles secured and code compliant	1
	B3011.012	Clay tile roof, tiles secured and code compliant	1
	B3011.013	Concrete tile roof, unsecured tiles	1
	B3011.014	Clay tile roof, unsecured tiles	1
Masonry Chimneys	B3031.001a	Unreinforced masonry chimney, repairs including replacement with masonry	3
	B3031.002a	Unreinforced masonry chimney, repairs including replacement with framing	3

Table D-1   List of Provided Fragility Specifications (continued)

General System Description	Fragility Classification Number	Component Description	Number of Sub-Categories
Masonry Parapets	B3041.001	Unreinforced and unbraced masonry parapet	1
Stairs	C2011.001a	Prefabricated steel stair	2
	C2011.011a	Precast concrete stair assembly	2
	C2011.021a	Monolithic cast-in-place and precast concrete stair	4
	C2011.031a	Hybrid steel and concrete stair assembly	2
Wall Partitions and Finishes	C1011.001a	Wall partition, metal studs with gypsum wallboard	4
	C1011.011a	Wall partition, wood studs with gypsum wallboard	1
	C3011.001a	Wall partition finish, gypsum wallboard and wallpaper	4
	C3011.002a	Wall partition finish, gypsum wallboard and ceramic tile	4
	C3011.003a	Wall partition finish, high-end marble or wood panel	4
Floors	C3021.001a	Generic floor covering, damage caused by floor flooding due to pipe failure	16
	C3027.001	Raised access floors, non-seismically rated and seismically rated	2
Ceilings	C3032.001a	Suspended ceilings, with and without lateral support	12
Pendant Lighting	C3034.001	Independent pendant lighting, non-seismically rated and seismically rated	2
Elevators	D1014.011	Traction elevator	2
	D1014.021	Hydraulic elevator	2
Piping	D2021.011a	Cold or hot potable water piping	14
	D2022.011a	Heating hot water piping	14
	D2031.011b	Sanitary waste piping	12
	D2051.011a	Chilled water piping	15
	D2061.011a	Steam piping	10
Chillers	D3031.011a	Chiller, unanchored and not vibration isolated	4
	D3031.012a	Chiller, vibration isolated but not restrained	12

Table D-1 List of Provided Fragility Specifications (continued)

General System Description	Fragility Classification Number	Component Description	Number of Sub-Categories
Chillers (cont'd)	D3031.013a	Chiller, hard anchored, or vibration isolated and restrained	12
Cooling Towers	D3031.021a	Cooling tower, unanchored and not vibration isolated	4
	D3031.022a	Cooling tower, vibration isolated but not restrained	12
	D3031.023a	Cooling tower, hard anchored, or vibration isolated and restrained	12
Compressors	D3032.011a	Compressor, unanchored and not vibration isolated	4
	D3032.012a	Compressor, vibration isolated but not restrained	12
	D3032.013a	Compressor, hard anchored, or vibration isolated and restrained	12
HVAC Distribution	D3041.001a	HVAC in-line fan, independently supported, with vibration isolators	4
	D3041.002a	HVAC in-line fan, independently supported, without vibration isolators	4
	D3041.011a	HVAC galvanized sheet metal ducting	8
	D3041.021a	HVAC stainless steel ducting	8
	D3041.031a	HVAC drops and diffusers in suspended ceilings	2
	D3041.032a	HVAC drops and diffusers without ceilings	4
	D3041.041a	Variable Air Volume (VAV) box with in-line coil	2
	D3041.101a	HVAC fan, unanchored and not vibration isolated	1
	D3041.102a	HVAC fan, vibration isolated but not restrained	3
	D3041.103a	HVAC fan, hard anchored, or vibration isolated and restrained	3
Air Handling Units	D3052.011a	Packaged air handling unit, unanchored and not vibration isolated	4
	D3052.013a	Packaged air handling unit, hard anchored, or vibration isolated and restrained	12
Control Panels	D3067.011a	Control panel, unanchored and not vibration isolated	1
	D3067.012a	Control panel, hard anchored, or vibration isolated and restrained	3

Table D-1   List of Provided Fragility Specifications (continued)

General System Description	Fragility Classification Number	Component Description	Number of Sub-Categories
Fire Sprinkler Water Piping	D4011.021a	Fire sprinkler horizontal mains and branch lines, old style victaulic / thin wall steel	4
	D4011.031a	Fire sprinkler drops into unbraced ceilings	6
	D4011.053a	Fire sprinkler drops into braced ceilings	4
	D4011.071a	Fire sprinkler drops, no ceilings	4
Transformers	D5011.011a	Transformer/primary service, unanchored and not vibration isolated	4
	D5011.013a	Transformer/primary service, hard anchored, or vibration isolated and restrained	12
Motor Control Centers	D5012.013a	Motor control center, unanchored and not vibration isolated	1
	D5012.013b	Motor control center, hard anchored, or vibration isolated and restrained	3
Low Voltage Switchgear	D5012.021a	Low voltage switchgear, unanchored and not vibration isolated	4
	D5012.023a	Low voltage switchgear, hard anchored, or vibration isolated and restrained	12
Distribution Panel	D5012.031a	Distribution panel, unanchored and not vibration isolated	4
	D5012.033a	Distribution panel, hard anchored, or vibration isolated and restrained	12
Battery Racks	D5092.011a	Battery rack, unanchored and not vibration isolated	1
	D5092.013a	Battery rack, hard anchored, or vibration isolated and restrained	3
Battery Chargers	D5092.021a	Battery charger, unanchored and not vibration isolated	1
	D5092.023a	Battery charger, hard anchored, or vibration isolated and restrained	3
Diesel Generators	D5092.031a	Diesel generator, unanchored and not vibration isolated	4
	D5092.032a	Diesel generator, vibration isolated but not restrained	12
	D5092.033a	Diesel generator, hard anchored, or vibration isolated and restrained	12

Table D-1   List of Provided Fragility Specifications (continued)

General System Description	Fragility Classification Number	Component Description	Number of Sub-Categories
Miscellaneous Contents	E2022.001	Modular office workstations	1
	E2022.010	Unsecured fragile objects on shelves	4
	E2022.020	Home entertainment and desktop electronic equipment	4
	E2022.102a	Bookcases	10
	E2022.112a	Vertical filing cabinets	4
	E2022.124a	Lateral filing cabinets	4
	F1012.001	Steel storage racks	1

Appendix E
Population Models

E.1   Population Models

Population models are used to determine the distribution of people within a building envelope, and the variability of this distribution over time of day and day of the year. Population models include a definition of the peak population, which is the number of people likely to be present at times of peak occupancy, and the fraction of this peak population likely to be present at other times. In this appendix, population models are provided for the following occupancies:

- Commercial Office

- Education (K-12) – typical elementary, middle school, and high school classrooms

- Healthcare – general in-patient hospitals

- Hospitality – hotels and motels

- Multi-Unit Residential – also applicable to single-family detached housing, with some modification

- Research Laboratories

- Retail – shopping malls and department stores

- Warehouse

Peak population values for each occupancy are defined Chapter 3. Table E-1 presents a series of daily population models for different occupancies in terms of the fraction of the peak population present in a building at different times of day for weekdays and weekends. Figures E-1 through E-5 plot the variation in population versus time of day, as depicted in Table E-1.

Table E-2 presents the monthly variation in population, relative to the daily population model for weekdays and weekends for each occupancy. Monthly variations are used to characterize the effects of holidays by prorating weekday populations considering the number of holidays per month and the total number of weekdays, on average, for that month.

Table E-1   Default Variation in Population by Time of Day and Day of Week, Relative to Expected Peak Population for Different Occupancies

Time of Day	Commercial Office		Education - Elementary Schools		Education - Middle Schools		Education - High Schools		Healthcare	
	Week-days	Week-ends	Week-days	Week-ends	Week-days	Week-ends	Week-days	Week-ends	Week-days	Week-ends
12:00 AM	0%	0%	0%	0%	0%	0%	0%	0%	40%	40%
1:00 AM	0%	0%	0%	0%	0%	0%	0%	0%	40%	40%
2:00 AM	0%	0%	0%	0%	0%	0%	0%	0%	40%	40%
3:00 AM	0%	0%	0%	0%	0%	0%	0%	0%	40%	40%
4:00 AM	0%	0%	0%	0%	0%	0%	0%	0%	40%	40%
5:00 AM	0%	0%	0%	0%	0%	0%	0%	0%	40%	40%
6:00 AM	0%	0%	0%	0%	5%	0%	5%	0%	40%	40%
7:00 AM	25%	0%	5%	0%	50%	0%	50%	0%	40%	40%
8:00 AM	50%	5%	100%	2%	100%	2%	100%	2%	40%	40%
9:00 AM	75%	5%	100%	2%	100%	2%	100%	2%	60%	50%
10:00 AM	100%	5%	100%	2%	100%	2%	100%	2%	80%	65%
11:00 AM	100%	5%	100%	2%	100%	2%	100%	2%	100%	80%
12:00 PM	50%	5%	100%	2%	100%	2%	100%	2%	100%	80%
1:00 PM	50%	5%	100%	2%	100%	2%	100%	2%	100%	80%
2:00 PM	100%	5%	100%	2%	100%	2%	100%	2%	100%	80%
3:00 PM	100%	5%	50%	2%	100%	2%	100%	2%	100%	80%
4:00 PM	75%	5%	5%	2%	50%	2%	50%	2%	100%	80%
5:00 PM	50%	5%	5%	2%	25%	2%	25%	2%	100%	80%
6:00 PM	25%	0%	5%	0%	5%	0%	5%	0%	100%	80%
7:00 PM	0%	0%	0%	0%	0%	0%	0%	0%	100%	80%
8:00 PM	0%	0%	0%	0%	0%	0%	0%	0%	80%	65%
9:00 PM	0%	0%	0%	0%	0%	0%	0%	0%	60%	50%
10:00 PM	0%	0%	0%	0%	0%	0%	0%	0%	40%	40%
11:00 PM	0%	0%	0%	0%	0%	0%	0%	0%	40%	40%

Table E-1 Default Variation in Population by Time of Day and Day of Week, Relative to Expected Peak Population for Different Occupancies (continued)

Time of Day	Hospitality		Multi-Unit Residential		Research Laboratories		Retail		Warehouse	
	Week-days	Week-ends	Week-days	Week-ends	Week-days	Week-ends	Week-days	Week-ends	Week-days	Week-ends
12:00 AM	100%	100%	100%	100%	10%	10%	0%	0%	0%	0%
1:00 AM	100%	100%	100%	100%	10%	10%	0%	0%	0%	0%
2:00 AM	100%	100%	100%	100%	10%	10%	0%	0%	0%	0%
3:00 AM	100%	100%	100%	100%	10%	10%	0%	0%	0%	0%
4:00 AM	100%	100%	100%	100%	10%	10%	0%	0%	0%	0%
5:00 AM	100%	100%	100%	100%	10%	10%	0%	0%	0%	0%
6:00 AM	100%	100%	80%	100%	25%	25%	0%	0%	0%	0%
7:00 AM	80%	100%	60%	100%	25%	25%	0%	0%	25%	0%
8:00 AM	70%	100%	40%	100%	50%	25%	5%	5%	50%	2%
9:00 AM	50%	75%	20%	75%	75%	25%	10%	10%	100%	2%
10:00 AM	50%	50%	20%	50%	100%	25%	20%	25%	100%	2%
11:00 AM	50%	25%	20%	50%	100%	25%	40%	50%	100%	2%
12:00 PM	50%	25%	20%	50%	50%	25%	60%	75%	100%	2%
1:00 PM	50%	25%	20%	50%	50%	25%	60%	100%	100%	2%
2:00 PM	50%	25%	25%	50%	100%	25%	60%	100%	100%	2%
3:00 PM	50%	25%	30%	50%	100%	25%	60%	100%	100%	2%
4:00 PM	50%	25%	35%	50%	75%	25%	60%	100%	100%	2%
5:00 PM	50%	25%	50%	50%	50%	25%	60%	100%	100%	2%
6:00 PM	50%	25%	67%	50%	25%	25%	60%	75%	50%	0%
7:00 PM	50%	25%	84%	50%	25%	25%	60%	50%	25%	0%
8:00 PM	50%	50%	100%	50%	10%	10%	40%	25%	0%	0%
9:00 PM	50%	50%	100%	75%	10%	10%	20%	10%	0%	0%
10:00 PM	100%	100%	100%	100%	10%	10%	5%	5%	0%	0%
11:00 PM	100%	100%	100%	100%	10%	10%	0%	0%	0%	0%
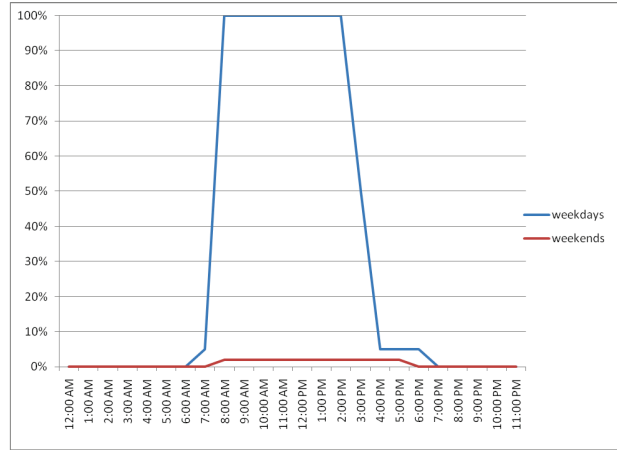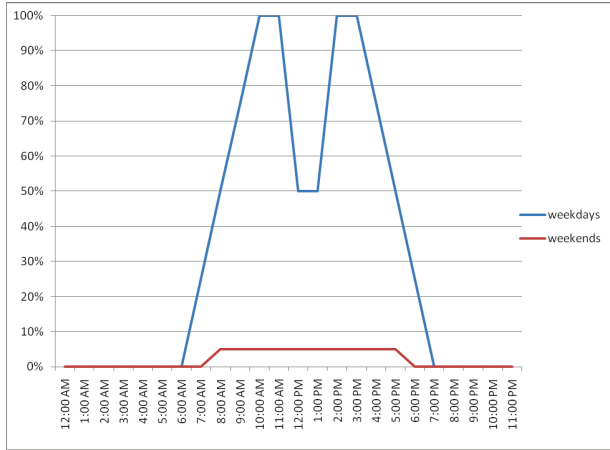
(a) Commercial office

(b) Education – elementary school

Figure E-1   Plot of default variation in population (relative to expected peak population) by time of day for: (a) Commercial Office; and (b) Education – Elementary School occupancies.
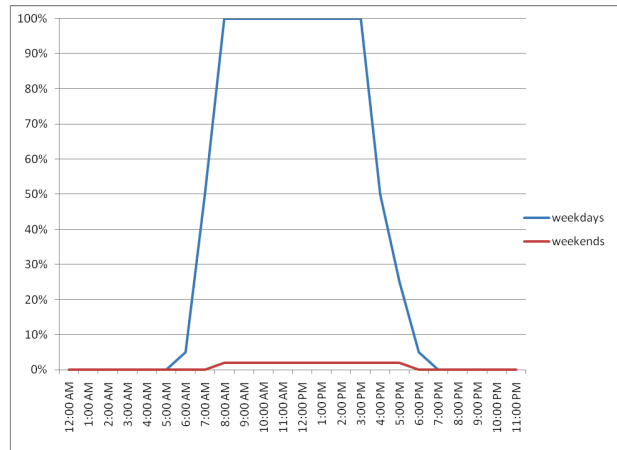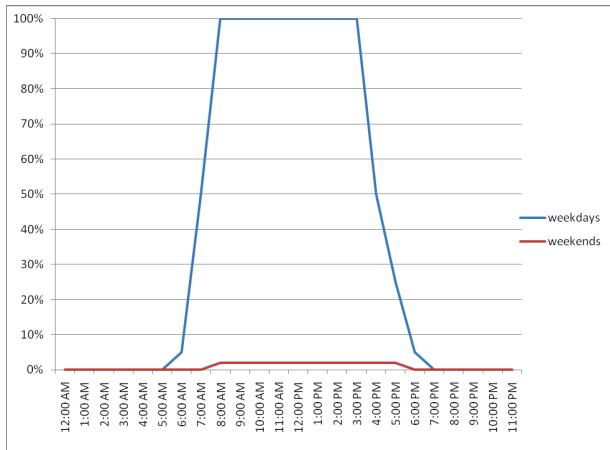
(a) Education – middle school

(b) Education – high school

Figure E-2   Plot of default variation in population (relative to expected peak population) by time of day for: (a) Education – Middle School; and (b) Education – High School occupancies.
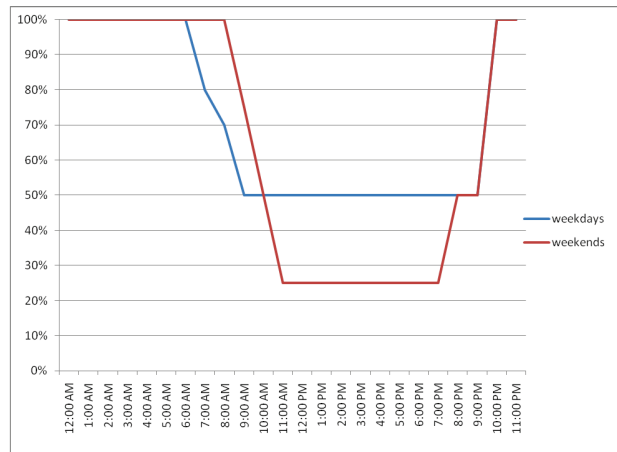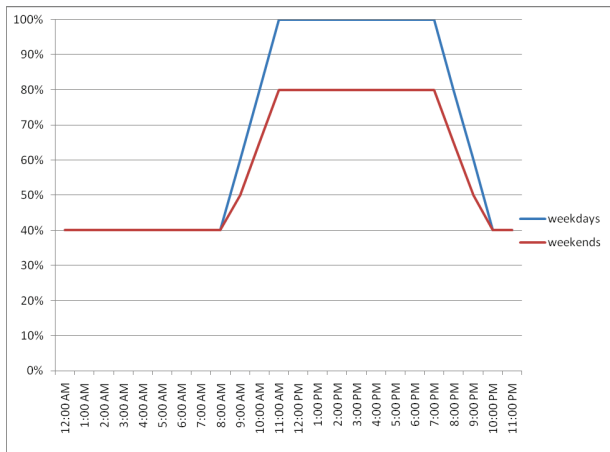
(a) Healthcare

(b) Hospitality

Figure E-3   Plot of default variation in population (relative to expected peak population) by time of day for: (a) Healthcare; and (b) Hospitality occupancies.
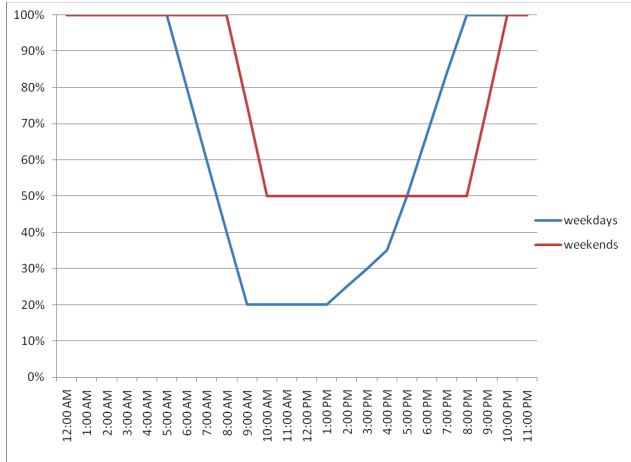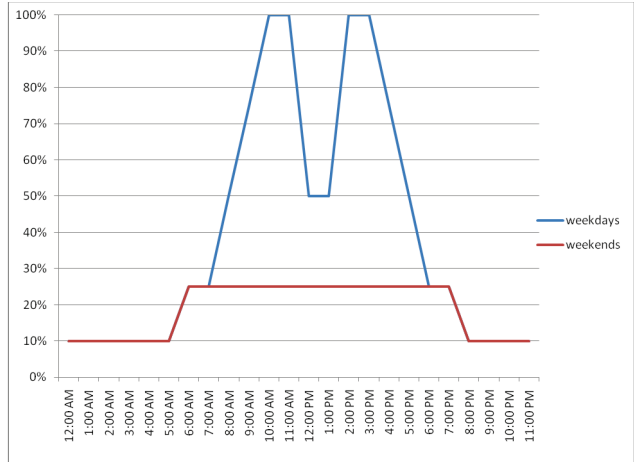
(a) Multi-Unit Residential   (b) Research

Figure E-4   Plot of default variation in population (relative to expected peak population) by time of day for: (a) Multi-Unit Residential; and (b) Research occupancies.
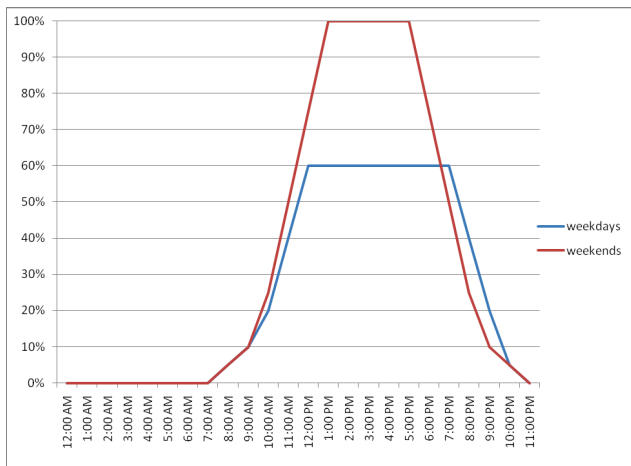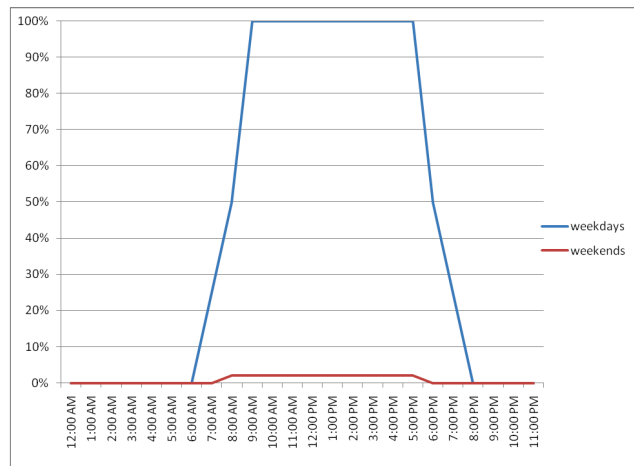
(a) Retail   (b) Warehouse

Figure E-5   Plot of default variation in population (relative to expected peak population) by time of day for: (a) Retail; and (b) Warehouse occupancies.

Table E-2 Default Variation in Population by Month, Relative to the Daily Population Model for Different Occupancies

Month	Commercial Office		Education - Elementary Schools		Education - Middle Schools		Education - High Schools		Healthcare	
	Week-day	Week-end	Week-day	Week-end	Week-day	Week-end	Week-day	Week-end	Week-day	Week-end
Jan.	91%	100%	73%	100%	73%	100%	73%	100%	100%	100%
Feb.	95%	100%	90%	100%	90%	100%	90%	100%	100%	100%
March	100%	100%	100%	100%	100%	100%	100%	100%	100%	100%
April	100%	100%	77%	100%	77%	100%	77%	100%	100%	100%
May	95%	100%	95%	100%	95%	100%	95%	100%	100%	100%
June	100%	100%	77%	100%	77%	100%	77%	100%	100%	100%
July	95%	100%	0%	100%	0%	100%	0%	100%	100%	100%
Aug.	100%	100%	0%	100%	0%	100%	0%	100%	100%	100%
Sept.	95%	100%	95%	100%	95%	100%	95%	100%	100%	100%
Oct.	100%	100%	95%	100%	95%	100%	95%	100%	100%	100%
Nov.	95%	100%	81%	100%	81%	100%	81%	100%	100%	100%
Dec.	95%	100%	64%	100%	64%	100%	64%	100%	100%	100%

Month	Hospitality		Multi-Unit Residential		Research Laboratories		Retail		Warehouse	
	Week-day	Week-end	Week-day	Week-end	Week-day	Week-end	Week-day	Week-end	Week-day	Week-end
Jan.	100%	100%	100%	100%	91%	100%	95%	100%	91%	100%
Feb.	100%	100%	100%	100%	95%	100%	100%	100%	95%	100%
March	100%	100%	100%	100%	100%	100%	100%	100%	100%	100%
April	100%	100%	100%	100%	100%	100%	100%	100%	100%	100%
May	100%	100%	100%	100%	95%	100%	100%	100%	95%	100%
June	100%	100%	100%	100%	100%	100%	100%	100%	100%	100%
July	100%	100%	100%	100%	95%	100%	95%	100%	95%	100%
Aug.	100%	100%	100%	100%	100%	100%	100%	100%	100%	100%
Sept.	100%	100%	100%	100%	95%	100%	100%	100%	95%	100%
Oct.	100%	100%	100%	100%	100%	100%	100%	100%	100%	100%
Nov.	100%	100%	100%	100%	95%	100%	95%	100%	95%	100%
Dec.	100%	100%	100%	100%	95%	100%	95%	100%	95%	100%

Appendix F

Normative Quantities

F.1   Normative Quantities

Normative quantities are an estimate of the components and contents likely to be present in a building of a specific occupancy on a gross square foot (gsf) basis. They can be used to provide an approximate inventory of the type and quantity of typical components found in typical buildings. Normative quantity values for 10th, 50th, and 90th percentile quantities were developed based on data from surveys of 3,000 typical buildings across various occupancies. Normative quantity units of measurement are consistent with the basic units of measure used to determine repair cost and repair time consequences in the fragility specifications.

Table F-1 through Table F-8 summarize normative quantity information provided for the following occupancies:

- Commercial Office

- Education (K-12) – typical elementary, middle school, and high school classrooms

- Healthcare – general in-patient hospitals, medical equipment excluded

- Hospitality – hotels and motels

- Multi-Unit Residential – also applicable to single-family detached housing, with some modification

- Research – special purpose laboratory equipment excluded

- Retail – shopping malls and department stores

- Warehouse – inventory excluded

Information in these tables is utilized in a companion *Normative Quantity Estimation Tool*, which is an Excel workbook designed to assist in estimating quantities of components and contents for building performance modeling provided as part of *Volume 3 – Supporting Electronic Materials and Background Documentation*.

Table F-1   Normative Quantities for Commercial Office Occupancies

Component Type	Unit of Measurement	10th Percentile Quantity	50th Percentile Quantity	90th Percentile Quantity
Gross area	SF	10,000	85,000	1,103,000
Volume	CF per 1 gsf	10.300	13.600	18.000
Cladding				
Gross wall area	SF per 1 gsf	0.380	0.645	1.200
Windows or glazing area	100 SF per 1 gsf	8.0E-04	3.0E-03	6.0E-03
Roof area – total	SF per 1 gsf	0.025	0.270	1.300
Interior partition length	100 LF per 1 gsf	7.0E-04	1.0E-03	1.2E-03
Ceramic tile floors	SF per 1 gsf	0.020	0.042	0.104
Ceramic tile walls	100 LF per 1 gsf	3.6E-05	7.6E-05	1.9E-04
Ceilings				
Ceiling - lay in tile percentage	%		90%	
Ceiling - gypsum board percentage	%		5%	
Ceiling - exposed percentage	%		3%	
Ceiling - other (high end) percentage	%		2%	
Stairs	FL per 1 gsf	8.0E-05	1.0E-04	1.2E-04
Elevators	EA per 1 gsf	1.5E-05	2.8E-05	7.9E-05
Plumbing				
Plumbing fixtures	EA per 1 gsf	5.0E-04	1.1E-03	2.6E-03
Piping				
Cold domestic water piping – 2 ½ inch diameter or smaller	1,000 LF per 1 gsf	2.0E-05	4.2E-05	1.0E-04
Cold domestic water piping – greater than 2 ½ diameter	1,000 LF per 1 gsf	1.0E-05	1.5E-05	2.0E-05
Hot domestic water piping – 2 ½ inch diameter or smaller	1,000 LF per 1 gsf	4.0E-05	8.4E-05	2.1E-04
Hot domestic waster piping – greater than 2 ½ diameter	1,000 LF per 1 gsf	2.0E-05	3.0E-05	4.0E-05
Gas supply piping	1,000 LF per 1 gsf	1.0E-05	1.5E-05	2.0E-05
Sanitary waste piping	1,000 LF per 1 gsf	3.0E-05	5.7E-05	1.2E-04
HVAC				
Chiller capacity	TN per 1 gsf	2.5E-03	2.9E-03	3.3E-03
Cooling tower capacity	TN per 1 gsf	2.5E-03	2.9E-03	3.3E-03
Boiler capacity	BTU per 1 gsf	30.000	45.000	60.000

Table F-1 Normative Quantities for Commercial Office Occupancies (continued)

Component Type	Unit of Measurement	10th Percentile Quantity	50th Percentile Quantity	90th Percentile Quantity
Air handling units	CFM per 1 gsf	0.500	0.700	0.900
Fans	CFM per 1 gsf	0.000	0.000	0.000
HVAC ducts – 6 sq. ft. or larger	1,000 LF per 1 gsf	1.5E-05	2.0E-05	2.5E-05
HVAC ducts – less than 6 sq. ft.	1,000 LF per 1 gsf	5.0E-05	7.5E-05	9.0E-05
HVAC in-line drops and diffusers	EA per 1 gsf	6.0E-03	9.0E-03	2.0E-02
HVAC in-line coils	EA per 1 gsf	3.0E-03	5.0E-03	6.0E-03
VAV boxes	EA per 1 gsf	1.0E-03	2.0E-03	4.0E-03
Piping				
Steam and chilled water piping – 2 ½ inch diameter or smaller	1,000 LF per 1 gsf	0.0E+00	0.0E+00	5.0E-06
Steam and chilled water piping – greater than 2 ½ diameter	1,000 LF per 1 gsf	0.0E+00	0.0E+00	5.0E-06
Heating water piping – 2 ½ inch diameter or smaller	1,000 LF per 1 gsf	0.0E+00	5.0E-06	1.0E-05
Heating water piping – greater than 2 ½ diameter	1,000 LF per 1 gsf	0.0E+00	5.0E-06	1.0E-05
Electrical				
Electrical load	W per 1 gsf	6.000	16.200	27.000
Electrical distribution conduits	LF per 1 gsf	7.0E-02	2.0E-01	4.0E-01
Electrical distribution – cable trays	LF per 1 gsf	0.0E+00	2.0E-02	5.0E-02
Wall mounted switchgear	EA per 1 gsf	1.0E-04	1.5E-04	2.0E-04
Lighting fixtures – lay in fluorescent	EA per 1 gsf	1.0E-02	1.5E-02	2.0E-02
Lighting fixtures – stem hung fluorescent	EA per 1 gsf	1.0E-02	1.5E-02	2.0E-02
Standby generators	KVA per 1 gsf	0.0E+00	0.0E+00	0.0E+00
Fire protection				
Sprinkler piping	20 LF per 1 gsf	8.5E-03	1.0E-02	1.1E-02
Sprinkler drops	EA per 1 gsf	7.0E-03	9.0E-03	1.2E-02

Table F-2   Normative Quantities for Education (K-12) Occupancies

Component Type	Unit of Measurement	10th Percentile Quantity	50th Percentile Quantity	90th Percentile Quantity
Gross area	SF	3,100	36,400	218,900
Volume	CF per 1 gsf	10.400	13.370	19.200
Cladding				
Gross wall area	SF per 1 gsf	0.380	0.750	1.700
Windows or glazing area	100 SF per 1 gsf	3.0E-04	1.1E-03	2.9E-03
Roof area - total	SF per 1 gsf	0.150	0.680	1.280
Interior partition length	100 LF per 1 gsf	3.0E-04	5.6E-04	9.8E-04
Ceramic tile floors	SF per 1 gsf	0.024	0.079	0.166
Ceramic tile walls	100 LF per 1 gsf	4.4E-05	1.4E-04	3.0E-04
Ceilings				
Ceiling - lay in tile percentage	%		95%	
Ceiling - gypsum board percentage	%		3%	
Ceiling - exposed percentage	%		2%	
Ceiling - other (high end) percentage	%		0%	
Stairs	FL per 1 gsf	6.0E-05	7.0E-05	9.0E-05
Elevators	EA per 1 gsf	9.0E-06	2.0E-05	1.3E-04
Plumbing				
Plumbing fixtures	EA per 1 gsf	6.1E-04	2.0E-03	4.2E-03
Piping				
Cold domestic water piping – 2 ½ inch diameter or smaller	1,000 LF per 1 gsf	2.0E-05	3.0E-05	4.0E-05
Cold domestic water piping – greater than 2 ½ diameter	1,000 LF per 1 gsf	1.0E-05	1.5E-05	2.0E-05
Hot domestic water piping – 2 ½ inch diameter or smaller	1,000 LF per 1 gsf	4.0E-05	6.0E-05	8.0E-05
Hot domestic waster piping – greater than 2 ½ diameter	1,000 LF per 1 gsf	2.0E-05	3.0E-05	4.0E-05
Gas supply piping	1,000 LF per 1 gsf	2.0E-05	4.0E-05	4.5E-05
Sanitary waste piping	1,000 LF per 1 gsf	3.0E-05	4.5E-05	6.0E-05
HVAC				
Chiller capacity	TN per 1 gsf	0.0E+00	0.0E+00	2.5E-03
Cooling tower capacity	TN per 1 gsf	0.0E+00	0.0E+00	2.5E-03
Boiler capacity	BTU per 1 gsf	30.000	45.000	60.000
Air handling units	CFM per 1 gsf	0.000	0.000	0.600

Table F-2   Normative Quantities for Education (K-12) Occupancies (continued)

Component Type	Unit of Measurement	10th Percentile Quantity	50th Percentile Quantity	90th Percentile Quantity
HVAC ducts – 6 sq. ft. or larger	1,000 LF per 1 gsf	0.0E+00	0.0E+00	1.5E-05
HVAC ducts – less than 6 sq. ft.	1,000 LF per 1 gsf	0.0E+00	5.0E-05	8.0E-05
HVAC in-line drops and diffusers	EA per 1 gsf	0.0E+00	5.0E-03	8.0E-03
HVAC in-line coils	EA per 1 gsf	0.0E+00	0.0E+00	1.5E-03
VAV boxes	EA per 1 gsf	0.0E+00	0.0E+00	1.5E-03
Fan coil units	EA per 1 gsf	2.0E-03	4.0E-03	0.0E+00
Piping				
Steam and chilled water piping - 2 ½ inch diameter or smaller	1,000 LF per 1 gsf	0.0E+00	0.0E+00	5.0E-06
Steam and chilled water piping – greater than 2 ½ diameter	1,000 LF per 1 gsf	0.0E+00	5.0E-06	1.0E-05
Heating water piping – 2 ½ inch diameter or smaller	1,000 LF per 1 gsf	0.0E+00	2.5E-05	4.0E-05
Heating water piping – greater than 2 ½ diameter	1,000 LF per 1 gsf	0.0E+00	5.0E-06	1.0E-05
Electrical				
Electrical load	W per 1 gsf	7.000	18.800	23.000
Electrical distribution conduits	LF per 1 gsf	1.0E-01	2.0E-01	3.0E-01
Electrical distribution – cable trays	LF per 1 gsf	0.0E+00	0.0E+00	0.0E+00
Wall mounted switchgear	EA per 1 gsf	1.0E-04	1.5E-04	2.0E-04
Lighting fixtures – lay in fluorescent	EA per 1 gsf	1.0E-02	1.5E-02	1.7E-02
Lighting fixtures – stem hung fluorescent	EA per 1 gsf	1.0E-02	1.5E-02	1.7E-02
Standby generators	KVA per 1 gsf	0.0E+00	0.0E+00	0.0E+00
Fire protection				
Sprinkler piping	20 LF per 1 gsf	7.5E-03	9.0E-03	1.0E-02
Sprinkler drops	EA per 1 gsf	6.0E-03	8.0E-03	1.0E-02

Table F-3   Normative Quantities for Healthcare Occupancies

Component Type	Unit of Measurement	10th Percentile Quantity	50th Percentile Quantity	90th Percentile Quantity
Gross area	SF	20,000	127,700	1,515,000
Volume	CF per 1 gsf	13.000	15.750	18.000
Cladding				
Gross wall area	SF per 1 gsf	0.260	0.500	1.000
Windows or glazing area	100 SF per 1 gsf	4.0E-04	1.4E-03	3.1E-03
Roof area - total	SF per 1 gsf	0.090	0.290	1.050
Interior partition length	100 LF per 1 gsf	7.5E-04	1.1E-03	1.4E-03
Ceramic tile floors	SF per 1 gsf	0.035	0.071	0.159
Ceramic tile walls	100 LF per 1 gsf	6.2E-05	1.3E-04	2.9E-04
Ceilings				
Ceiling - lay in tile percentage	%		80%	
Ceiling - gypsum board percentage	%		8%	
Ceiling - exposed percentage	%		8%	
Ceiling - other (high end) percentage	%		4%	
Stairs	FL per 1 gsf	7.0E-05	8.0E-05	1.0E-04
Elevators	EA per 1 gsf	1.2E-05	2.8E-05	9.8E-05
Plumbing				
Plumbing fixtures	EA per 1 gsf	1.2E-03	2.4E-03	5.3E-03
Piping				
Cold domestic water piping – 2 ½ inch diameter or smaller	1,000 LF per 1 gsf	8.0E-05	1.1E-04	1.3E-04
Cold domestic water piping – greater than 2 ½ diameter	1,000 LF per 1 gsf	3.0E-05	4.0E-05	5.0E-05
Hot domestic water piping – 2 ½ inch diameter or smaller	1,000 LF per 1 gsf	1.6E-04	2.2E-04	2.6E-04
Hot domestic waster piping – greater than 2 ½ diameter	1,000 LF per 1 gsf	6.0E-05	8.0E-05	1.0E-04
Gas supply piping	1,000 LF per 1 gsf	5.0E-06	1.0E-05	1.5E-05
Sanitary waste piping	1,000 LF per 1 gsf	1.1E-04	1.5E-04	1.8E-04
Process piping - 2 ½ inch diameter or smaller	1,000 LF per 1 gsf	1.2E-04	1.6E-04	2.0E-04
Process piping – greater than 2 ½ diameter	1,000 LF per 1 gsf	4.0E-05	6.0E-05	7.0E-05
Acid waste piping	1,000 LF per 1 gsf	4.0E-05	6.0E-05	7.0E-05

Table F-3   Normative Quantities for Healthcare Occupancies (continued)

Component Type	Unit of Measurement	10th Percentile Quantity	50th Percentile Quantity	90th Percentile Quantity
HVAC				
Chiller capacity	TN per 1 gsf	2.9E-03	3.3E-03	3.7E-03
Cooling tower capacity	TN per 1 gsf	2.9E-03	3.3E-03	3.7E-03
Boiler capacity	BTU per 1 gsf	40.000	50.000	65.000
Air handling units	CFM per 1 gsf	0.800	1.000	1.250
Fans	CFM per 1 gsf	0.800	1.000	1.250
HVAC ducts – 6 sq. ft. or larger	1,000 LF per 1 gsf	2.5E-05	3.5E-05	4.0E-05
HVAC ducts – less than 6 sq. ft.	1,000 LF per 1 gsf	5.0E-05	7.5E-05	9.0E-05
HVAC in-line drops and diffusers	EA per 1 gsf	1.6E-02	2.0E-02	2.2E-02
HVAC in-line coils	EA per 1 gsf	3.0E-03	5.0E-03	6.0E-03
VAV boxes	EA per 1 gsf	3.0E-03	5.0E-03	6.0E-03
Piping				
Steam and chilled water piping – 2 ½ inch diameter or smaller	1,000 LF per 1 gsf	0.0E+00	2.0E-05	1.5E-05
Steam and chilled water piping – greater than 2 ½ diameter	1,000 LF per 1 gsf	2.0E-05	3.0E-05	2.5E-05
Heating water piping – 2 ½ inch diameter or smaller	1,000 LF per 1 gsf	6.0E-05	8.0E-05	1.0E-04
Heating water piping – greater than 2 ½ diameter	1,000 LF per 1 gsf	2.0E-05	3.0E-05	3.5E-05
Electrical				
Electrical load	W per 1 gsf	14.000	23.100	35.600
Electrical distribution conduits	LF per 1 gsf	3.0E-01	5.0E-01	6.0E-01
Electrical distribution – cable trays	LF per 1 gsf	0.0E+00	4.0E-02	7.5E-02
Wall mounted switchgear	EA per 1 gsf	2.0E-04	4.0E-04	5.0E-04
Lighting fixtures – lay in fluorescent	EA per 1 gsf	1.0E-02	1.5E-02	1.7E-02
Lighting fixtures – stem hung fluorescent	EA per 1 gsf	1.0E-02	1.5E-02	1.7E-02
Standby generators	KVA per 1 gsf	3.5E-03	5.0E-03	1.5E-02
Fire protection				
Sprinkler piping	20 LF per 1 gsf	1.0E-02	1.1E-02	1.3E-02
Sprinkler drops	EA per 1 gsf	1.0E-02	1.2E-02	1.4E-02

Table F-4   Normative Quantities for Hospitality Occupancies

Component Type	Unit of Measurement	10th Percentile Quantity	50th Percentile Quantity	90th Percentile Quantity
Gross area	SF			
Volume	CF per 1 gsf	9.000	11.000	14.000
Cladding				
Gross wall area	SF per 1 gsf	0.300	0.350	0.500
Windows or glazing area	100 SF per 1 gsf	7.0E-04	1.2E-03	1.7E-03
Roof area - total	SF per 1 gsf	0.600	0.200	0.060
Interior partition length	100 LF per 1 gsf	5.5E-04	6.0E-04	8.0E-04
Ceramic tile floors	SF per 1 gsf	0.120	0.160	0.240
Ceramic tile walls	100 LF per 1 gsf	2.2E-04	2.9E-04	4.3E-04
Ceilings				
Ceiling - lay in tile percentage	%		15%	
Ceiling - gypsum board percentage	%		70%	
Ceiling - exposed percentage	%		8%	
Ceiling - other (high end) percentage	%		7%	
Stairs	FL per 1 gsf	9.0E-05	1.1E-04	1.2E-04
Elevators	EA per 1 gsf	1.4E-05	1.5E-05	4.0E-05
Plumbing				
Plumbing fixtures	EA per 1 gsf	3.0E-03	4.0E-03	6.0E-03
Piping				
Cold domestic water piping – 2 ½ inch diameter or smaller	1,000 LF per 1 gsf	6.0E-05	8.0E-05	1.2E-04
Cold domestic water piping – greater than 2 ½ diameter	1,000 LF per 1 gsf	1.0E-05	1.5E-05	2.0E-05
Hot domestic water piping – 2 ½ inch diameter or smaller	1,000 LF per 1 gsf	1.2E-04	1.6E-04	2.4E-04
Hot domestic waster piping – greater than 2 ½ diameter	1,000 LF per 1 gsf	2.0E-05	3.0E-05	4.0E-05
Gas supply piping	1,000 LF per 1 gsf	2.0E-05	4.0E-05	4.5E-05
Sanitary waste piping	1,000 LF per 1 gsf	7.0E-05	9.5E-05	1.4E-04
HVAC				
Chiller capacity	TN per 1 gsf	0.0E+00	0.0E+00	2.0E-03
Cooling tower capacity	TN per 1 gsf	0.0E+00	0.0E+00	2.0E-03
Boiler capacity	BTU per 1 gsf	30.000	45.000	50.000
Air handling units	CFM per 1 gsf	0.000	0.000	0.600

Table F-4   Normative Quantities for Hospitality Occupancies (continued)

Component Type	Unit of Measurement	10th Percentile Quantity	50th Percentile Quantity	90th Percentile Quantity
HVAC ducts – 6 sq. ft. or larger	1,000 LF per 1 gsf	0.0E+00	0.0E+00	1.5E-05
HVAC ducts – less than 6 sq. ft.	1,000 LF per 1 gsf	0.0E+00	5.0E-05	8.0E-05
HVAC in-line drops and diffusers	EA per 1 gsf	4.0E-03	8.0E-03	1.2E-02
HVAC in-line coils	EA per 1 gsf	0.0E+00	0.0E+00	1.5E-03
VAV boxes	EA per 1 gsf	0.0E+00	0.0E+00	1.5E-03
Fan coil units	EA per 1 gsf	4.0E-03	6.0E-03	0.0E+00
Piping				
Steam and chilled water piping - 2 ½ inch diameter or smaller	1,000 LF per 1 gsf	0.0E+00	0.0E+00	5.0E-06
Steam and chilled water piping – greater than 2 ½ diameter	1,000 LF per 1 gsf	0.0E+00	0.0E+00	5.0E-06
Heating water piping - 2 ½ inch diameter or smaller	1,000 LF per 1 gsf	0.0E+00	5.0E-06	1.0E-05
Heating water piping – greater than 2 ½ diameter	1,000 LF per 1 gsf	0.0E+00	5.0E-06	1.0E-05
Electrical				
Electrical load	W per 1 gsf	6.000	11.000	15.000
Electrical distribution conduits	LF per 1 gsf	0.0E+00	2.0E-01	3.0E-01
Electrical distribution – cable trays	LF per 1 gsf	0.0E+00	0.0E+00	0.0E+00
Wall mounted switchgear	EA per 1 gsf	1.0E-04	1.5E-04	2.0E-04
Lighting fixtures – lay in fluorescent	EA per 1 gsf	0.0E+00	0.0E+00	4.0E-03
Lighting fixtures – stem hung fluorescent	EA per 1 gsf	0.0E+00	0.0E+00	4.0E-03
Standby generators	KVA per 1 gsf	0.0E+00	0.0E+00	0.0E+00
Fire protection				
Sprinkler piping	20 LF per 1 gsf	1.0E-02	1.1E-02	1.3E-02
Sprinkler drops	EA per 1 gsf	1.0E-02	1.2E-02	1.4E-02

Table F-5   Normative Quantities for Multi-Unit Residential Occupancies

Component Type	Unit of Measurement	10th Percentile Quantity	50th Percentile Quantity	90th Percentile Quantity
Gross area	SF	5,000	34,000	582,200
Volume	CF per 1 gsf	7.440	10.460	14.500
Cladding				
Gross wall area	SF per 1 gsf	0.320	0.770	1.300
Windows or glazing area	100 SF per 1 gsf	6.0E-04	1.5E-03	3.0E-03
Roof area - total	SF per 1 gsf	0.090	0.320	1.000
Interior partition length	100 LF per 1 gsf	7.0E-04	1.2E-03	1.6E-03
Ceramic tile floors	SF per 1 gsf	0.108	0.212	0.340
Ceramic tile walls	100 LF per 1 gsf	1.9E-04	3.8E-04	6.1E-04
Ceilings				
Ceiling - lay in tile percentage	%		0%	
Ceiling - gypsum board percentage	%		95%	
Ceiling - exposed percentage	%		5%	
Ceiling - other (high end) percentage	%		0%	
Stairs	FL per 1 gsf	1.0E-04	1.2E-04	1.4E-04
Elevators	EA per 1 gsf	7.0E-06	3.4E-05	8.0E-05
Plumbing				
Plumbing fixtures	EA per 1 gsf	2.7E-03	5.3E-03	8.5E-03
Piping				
Cold domestic water piping - 2 ½ inch diameter or smaller	1,000 LF per 1 gsf	5.4E-05	1.1E-04	1.7E-04
Cold domestic water piping – greater than 2 ½ diameter	1,000 LF per 1 gsf	1.0E-05	1.5E-05	2.0E-05
Hot domestic water piping - 2 ½ inch diameter or smaller	1,000 LF per 1 gsf	1.1E-04	2.1E-04	3.4E-04
Hot domestic waster piping – greater than 2 ½ diameter	1,000 LF per 1 gsf	2.0E-05	3.0E-05	4.0E-05
Gas supply piping	1,000 LF per 1 gsf	2.0E-05	4.0E-05	4.5E-05
Sanitary waste piping	1,000 LF per 1 gsf	6.4E-05	1.2E-04	1.9E-04
HVAC				
Chiller capacity	TN per 1 gsf	0.0E+00	0.0E+00	2.0E-03
Cooling tower capacity	TN per 1 gsf	0.0E+00	0.0E+00	2.0E-03
Boiler capacity	BTU per 1 gsf	30.000	45.000	60.000
Air handling units	CFM per 1 gsf	0.000	0.000	0.600

Table F-5   Normative Quantities for Multi-Unit Residential Occupancies (continued)

Component Type	Unit of Measurement	10th Percentile Quantity	50th Percentile Quantity	90th Percentile Quantity
HVAC ducts – 6 sq. ft. or larger	1,000 LF per 1 gsf	0.0E+00	0.0E+00	1.5E-05
HVAC ducts – less than 6 sq. ft.	1,000 LF per 1 gsf	0.0E+00	5.0E-05	8.0E-05
HVAC in-line drops and diffusers	EA per 1 gsf	4.0E-03	8.0E-03	1.2E-02
HVAC in-line coils	EA per 1 gsf	0.0E+00	0.0E+00	1.5E-03
VAV boxes	EA per 1 gsf	0.0E+00	0.0E+00	1.5E-03
Fan coil units	EA per 1 gsf	2.0E-03	4.0E-03	0.0E+00
Piping				
Steam and chilled water piping - 2 ½ inch diameter or smaller	1,000 LF per 1 gsf	0.0E+00	0.0E+00	5.0E-06
Steam and chilled water piping – greater than 2 ½ diameter	1,000 LF per 1 gsf	0.0E+00	0.0E+00	5.0E-06
Heating water piping - 2 ½ inch diameter or smaller	1,000 LF per 1 gsf	0.0E+00	5.0E-06	1.0E-05
Heating water piping – greater than 2 ½ diameter	1,000 LF per 1 gsf	0.0E+00	5.0E-06	1.0E-05
Electrical				
Electrical load	W per 1 gsf	8.300	11.400	19.500
Electrical distribution conduits	LF per 1 gsf	0.0E+00	2.0E-01	3.0E-01
Electrical distribution – cable trays	LF per 1 gsf	0.0E+00	0.0E+00	0.0E+00
Wall mounted switchgear	EA per 1 gsf	1.0E-04	1.5E-04	2.0E-04
Lighting fixtures – lay in fluorescent	EA per 1 gsf	0.0E+00	0.0E+00	4.0E-03
Lighting fixtures – stem hung fluorescent	EA per 1 gsf	0.0E+00	0.0E+00	4.0E-03
Standby generators	KVA per 1 gsf	0.0E+00	0.0E+00	0.0E+00
Fire protection				
Sprinkler piping	20 LF per 1 gsf	1.0E-02	1.1E-02	1.3E-02
Sprinkler drops	EA per 1 gsf	1.0E-02	1.2E-02	1.4E-02

Table F-6   Normative Quantities for Retail Occupancies

Component Type	Unit of Measurement	10th Percentile Quantity	50th Percentile Quantity	90th Percentile Quantity
Gross area	SF	25,000	40,000	90,000
Volume	CF per 1 gsf	18.000	20.000	23.000
Cladding				
Gross wall area	SF per 1 gsf	0.250	0.300	0.400
Windows or glazing area	100 SF per 1 gsf	4.0E-04	6.0E-04	8.0E-04
Roof area - total	SF per 1 gsf	0.700	0.500	0.300
Interior partition length	100 LF per 1 gsf	6.0E-05	1.0E-04	1.2E-04
Ceramic tile floors	SF per 1 gsf	0.040	0.060	0.072
Ceramic tile walls	100 LF per 1 gsf	7.2E-05	1.1E-04	1.3E-04
Ceilings				
Ceiling - lay in tile percentage	%		90%	
Ceiling - gypsum board percentage	%		3%	
Ceiling - exposed percentage	%		2%	
Ceiling - other (high end) percentage	%		5%	
Stairs	FL per 1 gsf	5.0E-05	1.0E-04	1.2E-04
Elevators	EA per 1 gsf	5.0E-05	1.0E-04	1.2E-04
Plumbing				
Plumbing fixtures	EA per 1 gsf	1.0E-03	1.5E-03	1.8E-03
Piping				
Cold domestic water piping - 2 ½ inch diameter or smaller	1,000 LF per 1 gsf	2.0E-05	3.0E-05	4.0E-05
Cold domestic water piping – greater than 2 ½ diameter	1,000 LF per 1 gsf	1.0E-05	1.5E-05	2.0E-05
Hot domestic water piping - 2 ½ inch diameter or smaller	1,000 LF per 1 gsf	4.0E-05	6.0E-05	8.0E-05
Hot domestic waster piping – greater than 2 ½ diameter	1,000 LF per 1 gsf	2.0E-05	3.0E-05	4.0E-05
Gas supply piping	1,000 LF per 1 gsf	2.0E-05	4.0E-05	4.5E-05
Sanitary waste piping	1,000 LF per 1 gsf	3.0E-05	4.5E-05	6.0E-05
HVAC				
Chiller capacity	TN per 1 gsf	0.0E+00	0.0E+00	2.5E-03
Cooling tower capacity	TN per 1 gsf	0.0E+00	0.0E+00	2.5E-03
Boiler capacity	BTU per 1 gsf	30.000	45.000	60.000
Air handling units	CFM per 1 gsf	0.000	0.000	0.600

Table F-6   Normative Quantities for Retail Occupancies (continued)

Component Type	Unit of Measurement	10th Percentile Quantity	50th Percentile Quantity	90th Percentile Quantity
Fans	CFM per 1 gsf	0.000	0.000	15.000
HVAC ducts – 6 sq. ft. or larger	1,000 LF per 1 gsf	0.0E+00	5.0E-05	8.0E-05
HVAC ducts – less than 6 sq. ft.	1,000 LF per 1 gsf	0.0E+00	5.0E-06	8.0E-06
HVAC in-line drops and diffusers	EA per 1 gsf	0.0E+00	0.0E+00	1.5E-03
HVAC in-line coils	EA per 1 gsf	0.0E+00	0.0E+00	1.5E-03
VAV boxes	EA per 1 gsf	2.0E-03	4.0E-03	0.0E+00
Piping				
Steam and chilled water piping - 2 ½ inch diameter or smaller	1,000 LF per 1 gsf	0.0E+00	0.0E+00	5.0E-06
Steam and chilled water piping – greater than 2 ½ diameter	1,000 LF per 1 gsf	0.0E+00	5.0E-06	1.0E-05
Heating water piping - 2 ½ inch diameter or smaller	1,000 LF per 1 gsf	0.0E+00	2.5E-05	4.0E-05
Heating water piping – greater than 2 ½ diameter	1,000 LF per 1 gsf	0.0E+00	5.0E-06	1.0E-05
Electrical				
Electrical load	W per 1 gsf	7.000	18.800	23.000
Electrical distribution conduits	LF per 1 gsf	1.0E-01	2.0E-01	3.0E-01
Electrical distribution – cable trays	LF per 1 gsf	0.0E+00	0.0E+00	0.0E+00
Wall mounted switchgear	EA per 1 gsf	1.0E-04	1.5E-04	2.0E-04
Lighting fixtures – lay in fluorescent	EA per 1 gsf	1.0E-02	1.5E-02	1.7E-02
Lighting fixtures – stem hung fluorescent	EA per 1 gsf	1.0E-02	1.5E-02	1.7E-02
Standby generators	KVA per 1 gsf	0.0E+00	0.0E+00	0.0E+00
Fire protection				
Sprinkler piping	20 LF per 1 gsf	7.5E-03	9.0E-03	1.0E-02
Sprinkler drops	EA per 1 gsf	6.0E-03	8.0E-03	1.0E-02

Table F-7   Normative Quantities for Warehouse Occupancies

Component Type	Unit of Measurement	10th Percentile Quantity	50th Percentile Quantity	90th Percentile Quantity
Gross area	SF			
Volume	CF per 1 gsf	20.000	28.000	40.000
Cladding				
Gross wall area	SF per 1 gsf	0.200	0.220	0.300
Windows or glazing area	100 SF per 1 gsf	0.0E+00	1.0E-05	2.0E-05
Roof area - total	SF per 1 gsf	1.000	1.000	1.000
Interior partition length	100 LF per 1 gsf	3.0E-05	3.0E-05	4.0E-05
Ceramic tile floors	SF per 1 gsf	0.001	0.002	0.004
Ceramic tile walls	100 LF per 1 gsf	2.2E-06	4.3E-06	7.2E-06
Ceilings				
Ceiling - lay in tile percentage	%		5%	
Ceiling - gypsum board percentage	%		5%	
Ceiling - exposed percentage	%		90%	
Ceiling - other (high end) percentage	%		0%	
Stairs	FL per 1 gsf	0.0E+00	0.0E+00	0.0E+00
Elevators	EA per 1 gsf	0.0E+00	0.0E+00	0.0E+00
Plumbing				
Plumbing fixtures	EA per 1 gsf	3.0E-05	6.0E-05	1.0E-04
Piping				
Cold domestic water piping - 2 ½ inch diameter or smaller	1,000 LF per 1 gsf	2.4E-06	4.8E-06	8.0E-06
Cold domestic water piping – greater than 2 ½ diameter	1,000 LF per 1 gsf	1.0E-05	1.5E-05	2.0E-05
Hot domestic water piping - 2 ½ inch diameter or smaller	1,000 LF per 1 gsf	4.8E-06	9.6E-06	1.6E-05
Hot domestic waster piping – greater than 2 ½ diameter	1,000 LF per 1 gsf	2.0E-05	3.0E-05	4.0E-05
Gas supply piping	1,000 LF per 1 gsf	1.0E-05	1.5E-05	2.0E-05
Sanitary waste piping	1,000 LF per 1 gsf	1.2E-05	2.0E-05	2.8E-05
HVAC				
Chiller capacity	TN per 1 gsf	0.0E+00	0.0E+00	2.0E-03
Cooling tower capacity	TN per 1 gsf	0.0E+00	0.0E+00	2.0E-03
Boiler capacity	BTU per 1 gsf	10.000	15.000	20.000
Air handling units	CFM per 1 gsf	0.000	0.200	0.400

Table F-7   Normative Quantities for Warehouse Occupancies (continued)

Component Type	Unit of Measurement	10th Percentile Quantity	50th Percentile Quantity	90th Percentile Quantity
Fans	CFM per 1 gsf	0.000	0.000	0.300
HVAC ducts – 6 sq. ft. or larger	1,000 LF per 1 gsf	0.0E+00	0.0E+00	1.0E-05
HVAC ducts – less than 6 sq. ft.	1,000 LF per 1 gsf	0.0E+00	4.0E-05	6.0E-05
HVAC in-line drops and diffusers	EA per 1 gsf	2.0E-03	3.0E-03	5.0E-03
HVAC in-line coils	EA per 1 gsf	0.0E+00	0.0E+00	1.0E-03
VAV boxes	EA per 1 gsf	0.0E+00	0.0E+00	1.0E-03
Piping				
Steam and chilled water piping - 2 ½ inch diameter or smaller	1,000 LF per 1 gsf	0.0E+00	0.0E+00	5.0E-06
Steam and chilled water piping – greater than 2 ½ diameter	1,000 LF per 1 gsf	0.0E+00	0.0E+00	5.0E-06
Heating water piping - 2 ½ inch diameter or smaller	1,000 LF per 1 gsf	0.0E+00	5.0E-06	1.0E-05
Heating water piping – greater than 2 ½ diameter	1,000 LF per 1 gsf	0.0E+00	5.0E-06	1.0E-05
Electrical				
Electrical load	W per 1 gsf	4.000	6.000	12.000
Electrical distribution conduits	LF per 1 gsf	2.0E-02	1.0E-01	1.5E-01
Electrical distribution – cable trays	LF per 1 gsf	0.0E+00	0.0E+00	0.0E+00
Wall mounted switchgear	EA per 1 gsf	5.0E-05	8.0E-05	1.0E-03
Lighting fixtures – lay in fluorescent	EA per 1 gsf	0.0E+00	0.0E+00	0.0E+00
Lighting fixtures – stem hung fluorescent	EA per 1 gsf	1.0E-02	1.5E-02	2.0E-02
Standby generators	KVA per 1 gsf	0.0E+00	0.0E+00	0.0E+00
Fire protection				
Sprinkler piping	20 LF per 1 gsf	4.5E-03	5.5E-03	6.5E-03
Sprinkler drops	EA per 1 gsf	6.0E-03	8.0E-03	1.0E-02

Table F-8   Normative Quantities for Research Occupancies

Component Type	Unit of Measurement	10th Percentile Quantity	50th Percentile Quantity	90th Percentile Quantity
Gross area	SF	35,000	96,000	330,000
Volume	CF per 1 gsf	13.000	16.000	20.000
Cladding				
Gross wall area	SF per 1 gsf	0.400	0.520	1.100
Windows or glazing area	100 SF per 1 gsf	7.0E-04	1.5E-03	4.3E-03
Roof area - total	SF per 1 gsf	1.050	0.245	0.110
Interior partition length	100 LF per 1 gsf	6.0E-04	8.5E-04	1.1E-03
Ceramic tile floors	SF per 1 gsf	0.010	0.028	0.080
Ceramic tile walls	100 LF per 1 gsf	1.8E-05	5.0E-05	1.4E-04
Ceilings				
Ceiling - lay in tile percentage	%		85%	
Ceiling - gypsum board percentage	%		5%	
Ceiling - exposed percentage	%		8%	
Ceiling - other (high end) percentage	%		2%	
Laboratory casework	LF per 1 gsf	0.0E+00	2.2E-02	4.0E-02
Fume hoods	EA per 1 gsf	0.0E+00	9.0E-04	1.9E-03
Stairs	FL per 1 gsf	8.0E-05	1.0E-04	1.2E-04
Elevators	EA per 1 gsf	1.3E-05	1.7E-05	1.0E-04
Plumbing				
Plumbing fixtures				
Domestic	EA per 1 gsf	2.5E-04	7.0E-04	2.0E-03
Lab	EA per 1 gsf	7.0E-05	2.7E-04	3.0E-03
Piping				
Cold domestic water piping - 2 ½ inch diameter or smaller	1,000 LF per 1 gsf	4.0E-05	6.0E-05	8.0E-05
Cold domestic water piping – greater than 2 ½ diameter	1,000 LF per 1 gsf	1.0E-05	2.0E-05	3.0E-05
Hot domestic water piping - 2 ½ inch diameter or smaller	1,000 LF per 1 gsf	8.0E-05	1.2E-04	1.6E-04
Hot domestic waster piping – greater than 2 ½ diameter	1,000 LF per 1 gsf	2.0E-05	4.0E-05	6.0E-05
Gas supply piping	1,000 LF per 1 gsf	5.0E-06	1.0E-05	1.5E-05
Sanitary waste piping	1,000 LF per 1 gsf	5.0E-05	8.0E-05	1.1E-04

Table F-8   Normative Quantities for Research Occupancies (continued)

Component Type	Unit of Measurement	10th Percentile Quantity	50th Percentile Quantity	90th Percentile Quantity
Process piping - 2 ½ inch diameter or smaller	1,000 LF per 1 gsf	3.0E-04	4.0E-04	5.0E-04
Process piping – greater than 2 ½ diameter	1,000 LF per 1 gsf	1.0E-04	1.5E-04	1.8E-04
Acid waste piping	1,000 LF per 1 gsf	1.0E-04	1.5E-04	1.8E-04
HVAC				
Chiller capacity	TN per 1 gsf	2.9E-03	3.3E-03	3.7E-03
Cooling tower capacity	TN per 1 gsf	2.9E-03	3.3E-03	3.7E-03
Boiler capacity	BTU per 1 gsf	55.000	65.000	75.000
Air handling units	CFM per 1 gsf	1.000	1.250	1.500
Fans	CFM per 1 gsf	1.000	1.250	1.500
HVAC ducts – 6 sq. ft. or larger	1,000 LF per 1 gsf	3.5E-05	5.0E-05	7.0E-05
HVAC ducts – less than 6 sq. ft.	1,000 LF per 1 gsf	8.0E-05	1.0E-04	1.2E-04
HVAC in-line drops and diffusers	EA per 1 gsf	1.3E-02	1.6E-02	2.0E-02
HVAC in-line coils	EA per 1 gsf	1.3E-03	2.0E-03	2.5E-03
VAV boxes	EA per 1 gsf	0.0E+00	3.0E-04	5.0E-04
Pressure dependent air valves (phoenix type boxes)	EA per 1 gsf	6.0E-03	1.0E-02	1.2E-02
Piping				
Steam and chilled water piping - 2 ½ inch diameter or smaller	1,000 LF per 1 gsf	0.0E+00	1.0E-05	1.5E-05
Steam and chilled water piping – greater than 2 ½ diameter	1,000 LF per 1 gsf	1.5E-05	2.0E-05	2.5E-05
Heating water piping - 2 ½ inch diameter or smaller	1,000 LF per 1 gsf	6.0E-05	8.0E-05	1.0E-04
Heating water piping – greater than 2 ½ diameter	1,000 LF per 1 gsf	2.0E-05	3.0E-05	3.5E-05
Electrical				
Electrical load	W per 1 gsf	14.500	22.800	48.800
Electrical distribution conduits	LF per 1 gsf	3.0E-01	5.0E-01	6.0E-01
Electrical distribution – cable trays	LF per 1 gsf	0.0E+00	4.0E-02	7.5E-02
Wall mounted switchgear	EA per 1 gsf	1.0E-03	3.0E-03	4.0E-03
Lighting fixtures – lay in fluorescent	EA per 1 gsf	1.0E-02	1.5E-02	1.7E-02
Lighting fixtures – stem hung fluorescent	EA per 1 gsf	1.0E-02	1.5E-02	1.7E-02

Table F-8   Normative Quantities for Research Occupancies (continued)

Component Type	Unit of Measurement	10th Percentile Quantity	50th Percentile Quantity	90th Percentile Quantity
Standby generators	KVA per 1 gsf	3.5E-03	5.0E-03	1.5E-02
Fire protection				
Sprinkler piping	20 LF per 1 gsf	9.0E-03	1.0E-02	1.1E-02
Sprinkler drops	EA per 1 gsf	8.0E-03	1.0E-02	1.3E-02

Appendix G

Generation of Simulated Demands

G.1 Introduction

The methodology uses a Monte Carlo procedure to calculate the distribution of probable losses for each ground motion intensity or earthquake scenario. In this process, a large number of earthquake realizations (hundreds to thousands) are developed. Each realization represents one possible building performance outcome in response to earthquake shaking, and each realization requires a unique set of demands (e.g., peak floor accelerations, story drift ratios, story velocities) to determine damage states and resulting consequences.

Rather than requiring a large number of structural analyses to develop these demands, the results from a limited suite of analyses are mathematically transformed into a large series of simulated demand sets. This appendix describes the algorithms used to transform the demands developed from a limited number of structural analyses into the larger number of simulated demand sets used to calculate performance.

G.2 Nonlinear Response History Analysis

When nonlinear response history analysis is used, results from structural analyses are assembled into a matrix with each row representing the responses obtained from a particular analysis, and each column containing the peak value of a particular demand parameter at a specified location in the building (e.g., peak floor acceleration at the third floor in the east-west direction) obtained from that analysis. This demand matrix is considered to be representative of a jointly lognormal distribution. Mathematical manipulation is performed to determine a median value for each parameter based on the analysis results, and also a covariance matrix that indicates the relationship of each parameter to the others in the set. Then a large number of simulated demand vectors are mathematically generated using a random number selection process, the median values, and the covariance matrix. The required minimum number of nonlinear analyses depends on many factors, including the required accuracy of the loss calculation; the dynamic properties of the building and number of stories; and, the characteristics of

the ground motion. In this appendix, 11 analyses are used for the purposes of illustration.

G.2.1 Algorithm

Yang (Yang et al., 2006; Yang et al., 2009) developed the original algorithm used to generate simulated demands. The algorithm was extended to address the effects of modeling uncertainty, β_m and ground motion uncertainty, β_{gm}, on demand distribution.

Let m represent the number of response analyses performed at an intensity level, or scenario. For each analysis, the peak absolute value of each demand parameter is assembled into a row vector with n entries, where n is the number of demand parameters. The m row vectors are catenated to form an $m \times n$ matrix (m rows $\times$ n columns, which is m analyses $\times$ n demand parameters), with each column representing m values of one demand parameter.

Denote the matrix of demand parameters, $\mathbf{X}$. The entries in $\mathbf{X}$ are assumed to be jointly lognormal. The natural logarithm of each entry in $\mathbf{X}$ is computed to form an $m \times n$ matrix $\mathbf{Y}$. The entries in $\mathbf{Y}$ are assumed to be jointly normal and can be characterized by a $1 \times n$ mean vector, $\mathbf{M_Y}$, containing the means of the natural logarithms of each demand and an $n \times n$ covariance matrix, $\Sigma_{\mathbf{YY}}$.

A vector of natural logarithm of demand parameters, $\mathbf{Z}$, can be generated with the same statistical distribution as $\mathbf{Y}$ using a vector of uncorrelated standard normal random variables, $\mathbf{U}$, with a mean of $\mathbf{0}$, which is vector of zeroes, and a covariance of $\mathbf{I}$ as shown in Equation G-1, where $\mathbf{A}$ and $\mathbf{B}$ are matrices of constant coefficients that linearly transforms $\mathbf{U}$ to $\mathbf{Z}$.

$$\mathbf{Z} = \mathbf{AU} + \mathbf{B} = \mathbf{L}_{np}\mathbf{D}_{pp}\mathbf{U} + \mathbf{M_Y} \qquad (G\text{-}1)$$

In Equation G-1, p is the rank of the covariance matrix $\Sigma_{\mathbf{YY}}$, obtained by counting the number nonzero eigenvalues of $\Sigma_{\mathbf{YY}}$. If $\Sigma_{\mathbf{YY}}$ is full-rank, then $p = n$. The rank of $\Sigma_{\mathbf{YY}}$ may not be full (i.e., $p \leq n$) for two reasons: (1) the number of analyses m is less than or equal to the number of demand variables n, a common situation; or (2) one or more vectors of peak demands obtained from analyses are a linear combination of other analysis vectors. In either case, a non-full-rank covariance matrix can be interpreted as a condition of insufficient data for generating the covariance matrix. For example, using 11 analyses ($m = 11$) to assess to develop simulated demands for an 8-story planar frame building would result in 11 demand vectors, each having 8 entries representing peak story drift ratios, and 9 entries representing peak

accelerations at the floor levels of the building (i.e., 1st floor, 2nd floor, …8th floor, roof) resulting in a 17×17 ($n = 8 + 9 = 17$) covariance matrix that is not-full-rank with $p = 10$.

PACT utilizes Equation G-1 to generate the demand parameter vector, $\mathbf{Z}$. This equation can handle both full-rank and non-full-rank Σ_{YY}. In Equation G-1, $\mathbf{D}_{pp}$ is a $p \times p$ matrix obtained by partitioning the square-root of eigenvalues of covariance matrix Σ_{YY}, denoted as $\mathbf{D}_Y$, which is an $n \times n$ matrix. As mentioned earlier, p is the rank of Σ_{YY}, therefore, if Σ_{YY} is full rank, $p = n$; and if Σ_{YY} is not-full-rank, then $p < n$. Similarly, matrix $\mathbf{L}_{np}$ is an $n \times p$ matrix obtained by partitioning the $n \times n$ eigenvector matrix of Σ_{YY}, denoted as $\mathbf{L}_Y$.

The effect of modeling uncertainty, β_m and ground motion uncertainty, β_{gm}, in estimation of losses is implemented in the process for estimation of $\mathbf{Z}$. Once the covariance matrix of observations, Σ_{YY}, is generated, it is decomposed into two matrices: (1) a variance matrix; and (2) a correlation coefficient matrix. The variance matrix consists of variance of each demand parameter, and is inflated with β_m and β_{gm} using a square-root-sum-of-squares technique. A new covariance matrix is assembled using the original correlation coefficient matrix and the inflated variance matrix. The process of estimation of $\mathbf{Z}$ using Equation G-1 then continues, as illustrated in Figure G-1.

Where:
X – is the matrix of analytically determined demands (observations)
Y – is the natural logarithm of X
$\mathbf{M_Y}$ – is the mean demand vector
Σ_{YY} – is the covariance matrix of demand vector
Z – is the natural logarithm of realizations
W – is the matrix of statistically determined demands
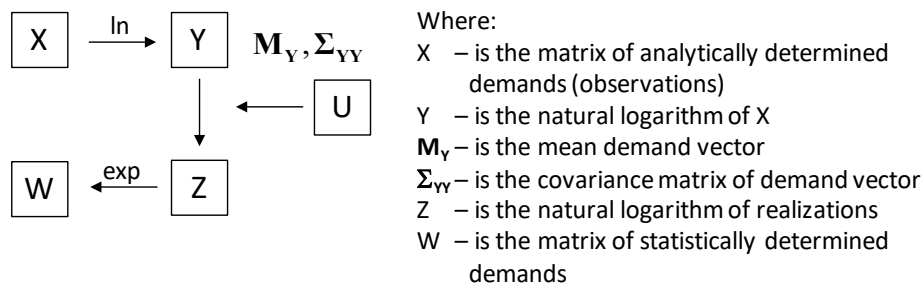
Figure G-1   Generation of simulated vectors of correlated demand parameters (adapted from Yang et al., 2006).

One simulated demand is generated by: (1) computing $\mathbf{M_Y}$, and Σ_{YY} from the matrix of the logarithms of the analysis results $\mathbf{Y}$; (2) updating Σ_{YY} for modeling uncertainty; (3) populating $\mathbf{U}$ by random sampling each demand parameter on a distribution with a mean of $\mathbf{0}$ and a covariance matrix of $\mathbf{I}$; (4) computing $\mathbf{Z}$ per equation G-1; and (5) taking the exponential of every entry in $\mathbf{Z}$ to recover the vector of simulated demand parameters $\mathbf{W}$. N vectors of $\mathbf{U}$ are required for the N simulations using one vector per simulation. The process is computationally efficient because $\mathbf{M_Y}$ and Σ_{YY} are computed just once for each intensity of shaking.

G.2.2   Sample Application of the Algorithm

This section illustrates the process described above for a sample 3-story, planar building. In this example, 7 demand parameters ($n = 7$), 3 story drift ratios (δ_1, δ_2, δ_3) and 4 floor accelerations (a_1, a_2, a_3, a_4), are used to assess performance. N is selected as 10000. Eleven analyses ($m = 11$) are performed. Although not considered in this example, residual drift ratios and floor velocities are included in the actual implementation of the methodology. Table G-1 presents the demand parameter matrix $\mathbf{X}$ of 11 rows (one per analysis) × 7 columns (one per demand parameter) for this example. Modeling uncertainty, record-to-record variability, and ground motion variability are set aside to simplify the presentation. Because $m > n$, the covariance matrix of observations is full-rank, therefore $p = n = 7$.

G.2.2.1   Generation of Realizations Using Full-Rank Covariance Matrices

To visually illustrate the process of drawing realizations using observed data, consider the matrix $\mathbf{X} = [\mathbf{X}_1, \mathbf{X}_2 ......\mathbf{X}_7]$ in Table G-1, with 7 columns (vectors) of demand, with 11 entries (rows) per vector. Joint probability distributions can be developed for pairs of vectors. For example: (1) between $\mathbf{X}_1$ (first story drift ratio) and $\mathbf{X}_3$ (third story drift ratio); and (2) between $\mathbf{X}_4$ (ground floor acceleration) and $\mathbf{X}_7$ (roof acceleration). In Figure G-2, the black solid circles show the relationship between $\mathbf{X}_1$ and $\mathbf{X}_3$, and $\mathbf{X}_4$ and $\mathbf{X}_7$, constructed using the data of Table G-1. $\mathbf{X}_1$ and $\mathbf{X}_3$ are weakly correlated, while $\mathbf{X}_4$ and $\mathbf{X}_7$ are strongly correlated.

Table G-1   Matrix of Analytically Determined Demand Parameters, X

	Δ_1 (%)	Δ_2 (%)	Δ_3 (%)	a_1 (g)	a_2 (g)	a_3 (g)	A_r (g)
1	1.26	1.45	1.71	0.54	0.87	0.88	0.65
2	1.41	2.05	2.43	0.55	0.87	0.77	0.78
3	1.37	1.96	2.63	0.75	1.04	0.89	0.81
4	0.97	1.87	2.74	0.55	0.92	1.12	0.75
5	0.94	1.8	2.02	0.40	0.77	0.74	0.64
6	1.73	2.55	2.46	0.45	0.57	0.45	0.59
7	1.05	2.15	2.26	0.38	0.59	0.49	0.52
8	1.40	1.67	2.1	0.73	1.50	1.34	0.83
9	1.59	1.76	2.01	0.59	0.94	0.81	0.72
10	0.83	1.68	2.25	0.53	1.00	0.9	0.74
11	0.96	1.83	2.25	0.49	0.90	0.81	0.64

(a) $\mathbf{X}_1$ and $\mathbf{X}_3$ (b) $\mathbf{X}_4$ and $\mathbf{X}_7$
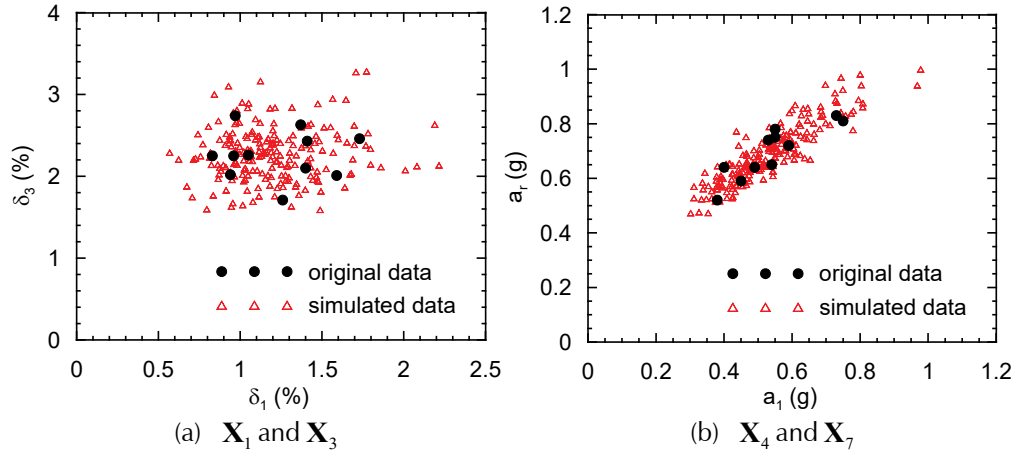
Figure G-2   Plots illustrating the correlation relationship between demand parameters.

A joint probability density function of the type shown in Figure G-3 can be constructed for any pair of vectors given two means, two variances, a covariance, and type of distribution (e.g., normal or log-normal). This figure presents the joint probability density functions for $\mathbf{X}_1$ and $\mathbf{X}_3$, and $\mathbf{X}_4$ and $\mathbf{X}_7$ constructed using the data of Table G-2, hereafter termed the original data.

(a) $\mathbf{X}_1$ and $\mathbf{X}_3$ (b) $\mathbf{X}_4$ and $\mathbf{X}_7$
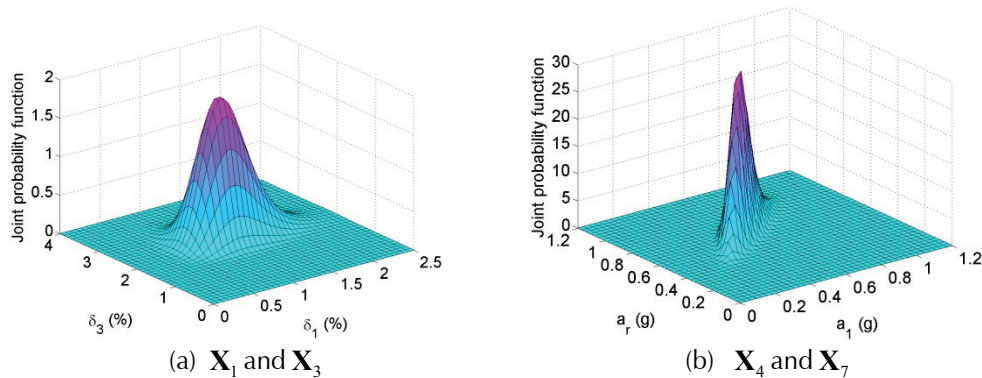
Figure G-3   Joint probability density functions.

The entries in matrix $\mathbf{X}$ are assumed to be jointly lognormal. The log of each entry in $\mathbf{X}$ is used to construct the entries in matrix $\mathbf{Y}$, which are now assumed to be jointly normal. Table G-2 presents the entries in $\mathbf{Y}$; the last row in the table contains the mean of each column vector in $\mathbf{Y}$ representing the mean vector $\mathbf{M}_\mathbf{Y}$ of Equation G-1. Table G-3 presents the covariance matrix $\Sigma_{\mathbf{YY}}$ of $\mathbf{Y}$. Table G-4 presents the diagonal matrix of the square root of eigenvalues of $\Sigma_{\mathbf{YY}}$, denoted as $\mathbf{D}_\mathbf{Y}$. All diagonal terms in $\mathbf{D}_\mathbf{Y}$ are positive, showing that $\Sigma_{\mathbf{YY}}$ is full-rank.

Table G-2   Natural Logarithm of Demand Parameters, Y

	δ_1	δ_2	δ_3	a_1	a_2	a_3	a_r
1	0.231	0.372	0.536	-0.616	-0.139	-0.128	-0.431
2	0.344	0.718	0.888	-0.598	-0.139	-0.261	-0.248
3	0.315	0.673	0.967	-0.288	0.039	-0.117	-0.211
4	-0.030	0.626	1.008	-0.598	-0.083	0.113	-0.288
5	-0.062	0.588	0.703	-0.916	-0.261	-0.301	-0.446
6	0.548	0.936	0.900	-0.799	-0.562	-0.799	-0.528
7	0.049	0.765	0.815	-0.968	-0.528	-0.713	-0.654
8	0.336	0.513	0.742	-0.315	0.405	0.293	-0.186
9	0.464	0.565	0.698	-0.528	-0.062	-0.211	-0.329
10	-0.186	0.519	0.811	-0.635	0.000	-0.105	-0.301
11	-0.041	0.604	0.811	-0.713	-0.105	-0.211	-0.446
μ_y	0.179	0.625	0.807	-0.634	-0.131	-0.222	-0.370

Table G-3   Covariance Matrix, Σ_{YY}, of Demand Parameters, Y

	1	2	3	4	5	6	7
1	0.059	0.012	-0.001	0.020	-0.001	-0.015	0.005
2	0.012	0.022	0.013	-0.011	-0.025	-0.034	-0.008
3	-0.001	0.013	0.018	0.004	-0.003	-0.003	0.004
4	0.020	-0.011	0.004	0.046	0.048	0.049	0.027
5	-0.001	-0.025	-0.003	0.048	0.070	0.078	0.033
6	-0.015	-0.034	-0.003	0.049	0.078	0.099	0.037
7	0.005	-0.008	0.004	0.027	0.033	0.037	0.021

Table G-4   Diagonal Matrix, D_Y, of the Square Root of Eigenvalues of Σ_{YY}

0.007	0.000	0.000	0.000	0.000	0.000	0.000
0.000	0.046	0.000	0.000	0.000	0.000	0.000
0.000	0.000	0.060	0.000	0.000	0.000	0.000
0.000	0.000	0.000	0.070	0.000	0.000	0.000
0.000	0.000	0.000	0.000	0.169	0.000	0.000
0.000	0.000	0.000	0.000	0.000	0.273	0.000
0.000	0.000	0.000	0.000	0.000	0.000	0.471

Table G-5   Matrix $\mathbf{L_Y}$ for the Sample Problem

-0.209	0.026	0.098	0.329	-0.294	0.866	-0.026
0.639	0.104	0.487	0.066	0.490	0.230	-0.216
-0.578	0.150	-0.122	0.121	0.778	0.087	-0.019
0.316	0.262	-0.551	-0.472	0.140	0.369	0.386
-0.266	0.078	0.654	-0.434	-0.032	0.030	0.552
0.191	0.202	-0.037	0.679	0.028	-0.185	0.652
0.081	-0.922	-0.071	0.014	0.216	0.131	0.271

All of the matrices required to generate the correlated vectors have been constructed. The next step in the process is to compute the 7×1 vector $\mathbf{U}$ of uncorrelated standard normal random variables, with a mean of $\mathbf{0}$ and a covariance matrix of $\mathbf{I}$. In this example, the **randn** function in Matlab is used, but any random generation algorithm can be used. This process is repeated 9999 times to construct the 10000 simulations. The next step involves taking the exponential of each value in the 7×10000 matrix to recover the demand parameters. Table G-6 presents the first 10 simulations of the 10000.

Table G-6   Matrix of Simulated Demand Parameters (First 10 Vectors of 10000)

	δ_1 (%)	δ_2 (%)	δ_3 (%)	a_1 (g)	a_2 (g)	a_3 (g)	a_r (g)
1	0.886	1.927	1.770	0.282	0.528	0.435	0.464
2	1.259	1.992	2.614	0.585	0.860	0.841	0.765
3	1.373	1.784	2.019	0.612	1.172	0.918	0.698
4	1.136	2.394	2.989	0.461	0.661	0.645	0.716
5	1.428	1.518	1.699	0.491	0.779	0.831	0.691
6	1.019	1.782	2.358	0.553	0.929	0.891	0.710
7	1.441	2.141	2.307	0.501	0.786	0.644	0.620
8	1.032	1.720	1.967	0.449	0.892	0.842	0.671
9	0.993	1.766	2.316	0.501	0.936	0.991	0.758
10	1.513	2.039	2.071	0.460	0.691	0.590	0.615

As a last step, the statistics of the simulated demands should be compared with those of the demands calculated by response history analysis. A rigorous comparison of the analytical and simulated demands is achieved by computing the ratios of the mean vectors and the covariance matrices. Table G-7 presents ratios of elements of mean simulated response vector to elements of mean response history response vector. All values are close to 1.0. Table G-8 presents similar ratios of element covariance matrices

obtained from realizations and observations covariance matrices. Again, all values are close to 1.0. The data in Table G-7 and Table G-8 indicate that the simulated vectors of demand have the same underlying statistics as those of the original demand vectors.

Table G-7 Ratio of Simulated to Original Logarithmic Means

δ_1	δ_2	δ_3	a_1	a_2	a_3	a_r
0.9895	0.9967	0.9977	1.0001	0.9836	0.9913	0.9991

Table G-8 Ratio of Entries in Simulated and Original Σ_{YY} Matrices

0.999	1.022	0.718	1.000	1.058	1.044	1.008
1.022	1.006	1.015	0.973	0.993	0.997	0.955
0.718	1.015	1.016	1.047	0.975	0.947	1.064
1.000	0.973	1.047	0.996	0.993	0.986	0.991
1.058	0.993	0.975	0.993	0.989	0.989	0.986
1.044	0.997	0.947	0.986	0.989	0.993	0.983
1.008	0.955	1.064	0.991	0.986	0.983	0.991

G.2.2.2 Generation of Realizations Using Non-Full-Rank Covariance Matrices

This section illustrates the process and approximations involved in a case where the covariance matrix of demand parameters is non-full-rank, using the same example considered in the previous section. In this illustration, it is assumed that only five analyses ($m = 5$) are performed. In this case $m < n$, therefore the covariance matrix of observations is non-full-rank. Table G-9 shows the natural logarithm of these five analyses, which are the first five out of eleven used in the previous example (Table G-2). This matrix of demand parameters is denoted as $\mathbf{Y}'$. The last row in Table G-9 tabulates the mean of each column vector in $\mathbf{Y}'$ representing the mean vector $\mathbf{M}_{Y'}$ of Equation G-1. Table G-10 presents the covariance matrix $\Sigma_{Y'Y'}$ of $\mathbf{Y}'$. Table G-11 presents the diagonal matrix $\mathbf{D}_{Y'}$ of square root of eigenvalues of $\Sigma_{Y'Y'}$. Only the last four diagonal terms in $\mathbf{D}_Y$ are positive, indicating that $\Sigma_{Y'Y'}$ is non-full-rank, and $p = 4$.

The matrix $\mathbf{D}_{pp}$ in Equation G-1, is a 4×4 matrix. It is shaded in gray in Table G-11, and separately illustrated in Table G-12. In the same fashion, the matrix of eigenvectors of $\Sigma_{Y'Y'}$, denoted as $\mathbf{L}_{Y'}$, is shown in Table G-13, where the shaded area corresponds to matrix $\mathbf{L}_{np}$ in (G-1) and is separately shown in Table G-14. The matrix $\mathbf{L}_{np}$ in this example is a 7×4 matrix.

Table G-9   Natural Logarithm of Demand Parameters, Y′

	δ_1	δ_2	δ_3	a_1	a_2	a_3	a_r
1	0.231	0.372	0.536	-0.616	-0.139	-0.128	-0.431
2	0.344	0.718	0.888	-0.598	-0.139	-0.261	-0.248
3	0.315	0.673	0.967	-0.288	0.039	-0.117	-0.211
4	-0.030	0.626	1.008	-0.598	-0.083	0.113	-0.288
5	-0.062	0.588	0.703	-0.916	-0.261	-0.301	-0.446
μ_y	0.159	0.595	0.820	-0.603	-0.117	-0.139	-0.325

Table G-10   Covariance Matrix, $\Sigma_{Y'Y'}$, of Demand Parameters, Y′

	1	2	3	4	5	6	7
1	0.037	0.004	0.001	0.029	0.011	-0.008	0.011
2	0.004	0.018	0.022	0.008	0.004	-0.002	0.011
3	0.001	0.022	0.039	0.022	0.013	0.015	0.018
4	0.029	0.008	0.022	0.049	0.024	0.015	0.019
5	0.011	0.004	0.013	0.024	0.012	0.009	0.009
6	-0.008	-0.002	0.015	0.015	0.009	0.026	0.005
7	0.011	0.011	0.018	0.019	0.009	0.005	0.012

Table G-11   Matrix $D_{Y'}$ for the Sample Problem

0.000	0.000	0.000	0.000	0.000	0.000	0.000
0.000	0.000	0.000	0.000	0.000	0.000	0.000
0.000	0.000	0.000	0.000	0.000	0.000	0.000
0.000	0.000	0.000	0.056	0.000	0.000	0.000
0.000	0.000	0.000	0.000	0.176	0.000	0.000
0.000	0.000	0.000	0.000	0.000	0.222	0.000
0.000	0.000	0.000	0.000	0.000	0.000	0.331

Table G-12   Matrix D_{pp} for the Sample Problem

0.056	0.000	0.000	0.000
0.000	0.176	0.000	0.000
0.000	0.000	0.222	0.000
0.000	0.000	0.000	0.331

Table G-13 Matrix $L_{Y'}$ for the Sample Problem

0.215	-0.154	0.034	-0.577	0.180	-0.667	0.345
-0.152	-0.267	-0.696	0.002	0.560	0.241	0.223
0.485	0.118	0.414	-0.081	0.294	0.532	0.450
0.072	0.402	-0.278	0.472	-0.281	-0.242	0.629
-0.135	-0.808	0.287	0.346	-0.178	-0.030	0.308
-0.043	-0.110	-0.278	-0.533	-0.658	0.387	0.207
-0.818	0.254	0.327	-0.188	0.157	0.058	0.309

Table G-14 Matrix L_{np} for the Sample Problem

-0.577	0.180	-0.667	0.345
0.002	0.560	0.241	0.223
-0.081	0.294	0.532	0.450
0.472	-0.281	-0.242	0.629
0.346	-0.178	-0.030	0.308
-0.533	-0.658	0.387	0.207
-0.188	0.157	0.058	0.309

Given matrices D_{pp}, L_{np}, and $M_{Y'}$, Equation G-1 is used to generate realizations based on the five analyses. In this process U is a 4×1 vector of uncorrelated standard normal random variables, with a mean of 0 and a covariance matrix of I. The fact that only a vector of 4 random numbers are used to draw a vector of seven demand parameters for one realization shows how insufficient data can affect drawing realizations. By repeating this exercise 9999 times, 10000 realizations are generated per Equation G-1 to create the 7×10000 matrix Z. Finally, the exponential of Z is obtained as W. Table G-15 presents the first 10 simulations of W.

Table G-16 and Table G-17 presents ratios of mean simulated response to mean response history analysis results, and ratios of the simulated to response history covariance matrix elements. The data in Table G-16 and Table G-17 indicate that the simulated vectors of demand have similar underlying statistics to those of the original demand vectors, but with less precision than when a larger number of analyses were performed, as was the case with a full-rank matrix, where $m = 11$.

Table G-15 Matrix of Simulated Demand Parameters (First 10 Vectors of 10000)

	δ_1 (%)	δ_2 (%)	δ_3 (%)	a_1 (g)	a_2 (g)	a_3 (g)	a_r (g)
1	1.122	1.751	2.185	0.582	0.926	0.845	0.703
2	0.981	1.979	2.578	0.478	0.849	0.907	0.727
3	1.409	1.798	2.106	0.590	0.903	0.778	0.734
4	1.024	2.147	3.374	0.694	1.043	1.119	0.839
5	1.287	1.661	2.169	0.590	0.915	0.988	0.729
6	1.808	2.159	2.812	0.726	0.982	0.878	0.897
7	1.190	1.668	1.855	0.490	0.832	0.744	0.660
8	1.014	1.790	2.505	0.530	0.895	1.069	0.728
9	1.092	1.748	1.928	0.427	0.781	0.737	0.653
10	0.890	2.006	2.745	0.479	0.863	0.968	0.729

Table G-16 Ratio of Simulated to Original Logarithmic Means

δ_1	δ_2	δ_3	a_1	a_2	a_3	a_r
1.003	1.000	0.999	1.001	1.003	1.005	1.001

Table G-17 Ratio of Entries in Simulated and Original $\Sigma_{Y'Y'}$ Matrices

1.001	0.925	0.662	0.991	0.986	1.013	0.983
0.925	0.982	0.981	0.958	0.964	0.980	0.976
0.662	0.981	0.977	0.956	0.961	0.964	0.970
0.991	0.958	0.956	0.979	0.976	0.942	0.972
0.986	0.964	0.961	0.976	0.975	0.951	0.970
1.013	0.980	0.964	0.942	0.951	0.967	0.944
0.983	0.976	0.970	0.972	0.970	0.944	0.973

G.2.3 Matlab Code

The Matlab macro below can be used to generate correlated simulated vectors of demand parameters. The vectors of demand parameters established by response history analysis, EDP.txt file, should have the same construction as Table G-1; that is, one demand parameter per column, one analysis per row. The file beta.txt includes a $2 \times n$ matrix where the values in the two rows are for β_m and β_{gm}, respectively, and those in each column are for each demand parameter.

For intensity-based and time-based assessments, the user should input dispersions for analysis and modeling for each demand parameter, and set the dispersion for ground motion equal to zero. For scenario-based assessments

using the procedures of Chapter 5, the user should input for dispersions for analysis, modeling, and ground motion for each demand parameter.

Example Matlab Code:

```
% Develop underlying statistics of the response history analysis
clear;
num_realization = 10000;

% loading information: EDP, epistemic variability,
EDPs =load('EDP.txt');
B=load('beta.txt');%matrix for dispersions βm and βgm ,

% taking natural logarithm of the EDPs.  Calling it lnEDPs
lnEDPs=log(EDPs); % Table G-2, or Table G-9
[num_rec num_var]=size(lnEDPs);

% finding the mean matrix of lnEDPs.  Calling it lnEDPs_mean
 lnEDPs_mean=mean(lnEDPs); % last row in Table G-2, or Table G-9
 lnEDPs_mean=lnEDPs_mean';

% finding the covariance matrix of lnEDPs.  Calling it lnEDPs_cov
 lnEDPs_cov=cov(lnEDPs); % Table G-3, or Table G-10

% finding the rank of covariance matrix of lnEDPs.  Calling it
% lnEDPs_cov_rank
 lnEDPs_cov_rank=rank(lnEDPs_cov);

 % inflating the variances with epistemic variability
sigma = sqrt(diag(lnEDPs_cov)); % sqrt first to avoid under/overflow
sigmap2 = sigma.*sigma;

 R = lnEDPs_cov ./ (sigma*sigma');
B=B';
sigmap2=sigmap2+(B(:,1).* B(:,1)); % Inflating variance for βm
sigmap2=sigmap2+(B(:,2).* B(:,2)); % Inflating variance for βgm
sigma=sqrt(sigmap2);
sigma2=sigma*sigma';
 lnEDPs_cov_inflated=R.*sigma2;

 % finding the eigenvalues eigenvectors of the covariance matrix.
Calling
 % them D2_total and L_total
 [L_total D2_total]=eig(lnEDPs_cov_inflated);  % Table G-5, Table G-
13
  D2_total=eig(lnEDPs_cov_inflated);

 % Partition L_total to L_use.  L_use is the part of eigenvector matrix
 % L_total that corresponds to positive eigenvalues
```

```
 if lnEDPs_cov_rank >= num_var
    L_use =L_total; % Table G-5
 else
    L_use =(L_total(:,num_var- lnEDPs_cov_rank+1:num_var));
%Table G-13
 end
% Partition the D2_total to D2_use.  D2_use is the part of eigenvalue
%vector D2_total that corresponds to positive eigenvalues
 if lnEDPs_cov_rank >= num_var
    D2_use =D2_total;
 else
    D2_use =D2_total(num_var- lnEDPs_cov_rank+1:num_var);
 end

 % Find the square root of D2_use and call is D_use.
 D_use =diag((D2_use).^0.5); %Table G-4, or Table G-12

 % Generate Standard random numbers
 if lnEDPs_cov_rank >= num_var
    U = randn(num_realization,num_var) ;
 else
    U = randn(num_realization, lnEDPs_cov_rank) ;
 end
 U = U' ;

 % Create Lambda = D_use .  L_use
 Lambda = L_use * D_use ;

 % Create realizations matrix
 Z = Lambda * U + lnEDPs_mean * ones(1,num_realization) ;

 lnEDPs_sim_mean=mean(Z');
 lnEDPs_sim_cov=cov(Z');

 A=lnEDPs_sim_mean./lnEDPs_mean'; %Table G-7, or Table G-16
 B=lnEDPs_sim_cov./lnEDPs_cov; %Table G-8, or Table G-17

 W=exp(Z);

%end
```

G.3   Simplified Analysis

When the simplified analysis procedure is used, only a single analysis is
performed for each intensity level or scenario. The results of this analysis
are transformed into estimated median demands, which are then associated
with a judgmentally determined dispersion for use in simulated demand
generation.

For performance assessment using the simplified analysis procedure, PACT internally generates a set of N statistically consistent demand vectors, given the single column vector of demand parameters, $\{\theta\}$ and a value of the dispersion, β, using the following two-step procedure:

1. N values of z are randomly generated, where z is normally distributed with a mean value of 0 and a standard deviation of 1.0.

2. $\{\theta\}\exp(z\beta)$ is computed for each value of z.

Each vector computed using Step 2 is used to generate one value of loss.

Appendix H
Fragility Development

H.1   Introduction

This appendix provides quantitative procedures for developing the median, θ, and dispersion, β, for fragility functions based on various levels of available data. The procedures can be used for structural and nonstructural components, elements, and systems.

H.1.1   Fragility Function Definition

Fragility functions are statistical distributions used to indicate the probability that a component, element, or system will be damaged as a function of a single predictive demand parameter, such as story drift or floor acceleration. Fragility functions take the form of lognormal cumulative distribution functions, having a median value, θ, and logarithmic standard deviation, or dispersion, β. The mathematical form for such a fragility function is:

$$F_i(D) = \Phi\left(\frac{\ln(D/\theta_i)}{\beta_i}\right) \qquad \text{(H-1)}$$

where $F_i(D)$ is the conditional probability that the component will be damaged to damage state "i" (or more severe damage state) as a function of a demand parameter, D; Φ denotes the standard normal (Gaussian) cumulative distribution function; θ_i denotes the median value of the probability distribution; and β_i denotes the logarithmic standard deviation. Both θ and β are established for each component type and damage state using one of the methods presented in Section H.2.

For sequential damage states, the conditional probability that a component will be damaged to damage state "i," given that it experiences demand, D, is:

$$P[i|D] = F_{i+1}(D) - F_i(D) \qquad \text{(H-2)}$$

where $F_{i+1}(D)$ is the conditional probability that the component will be damaged to damage state "i+1" or a more severe state, and $F_i(D)$ is as previously defined. Note that, when β_{i+1} is greater than β_i, the fragilities functions are crossing, and Equation H-2 can produce a negative probability at some levels of D, which is meaningless. This condition is addressed in Section H.3.4.

Figure H-1 shows the form of a typical lognormal fragility function when plotted in the form of a cumulative distribution function, and illustrates the calculation of the probability that a component will be in damage state "i" at a particular level of demand, d.

(a)

(b)
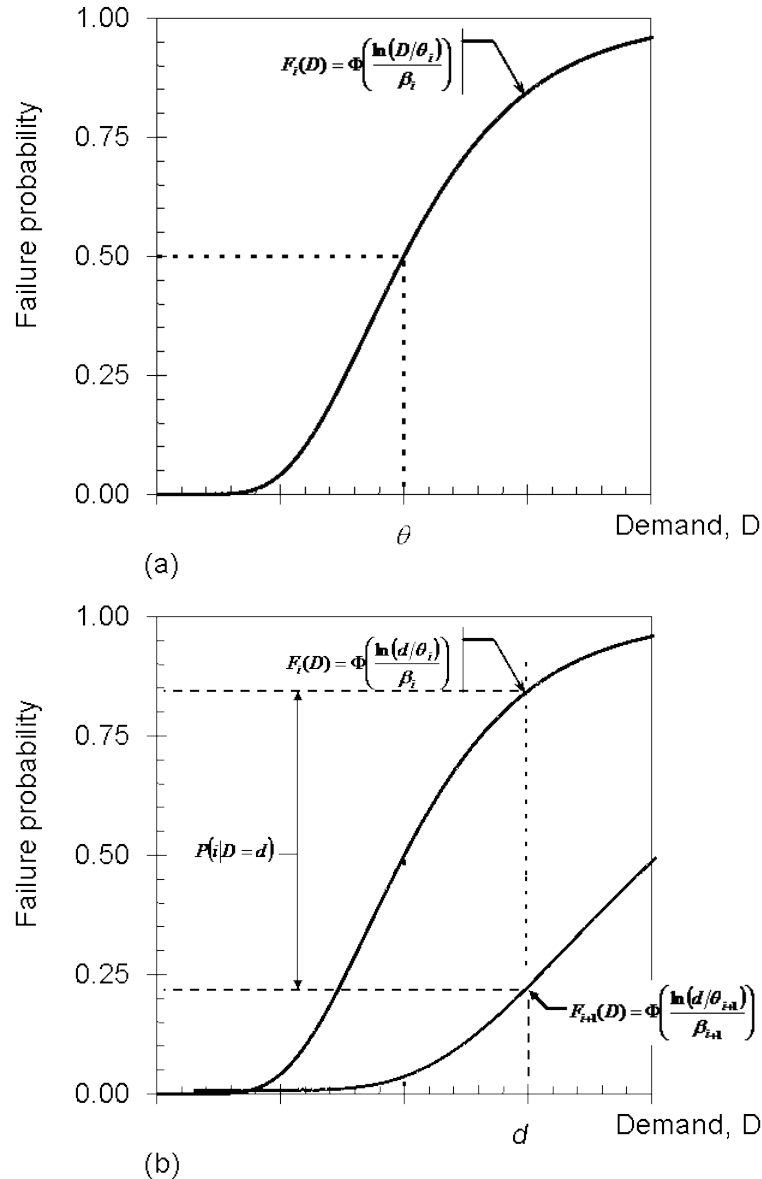
Figure H-1   Illustration of: (a) typical lognormal fragility function; and (b) evaluation of individual damage-state probabilities.

The dispersion, β, represents uncertainty in the actual value of demand, D, at which a damage state is likely to initiate. This uncertainty is the result of variability in the quality of construction and installation of components in a building, as well as variability in the loading history that a component might experience before it fails. When fragility parameters are determined on the basis of a limited set of test data, two contributors to uncertainty should be

considered. The first of these, termed β_r, represents the random variability that is observed in the test data from which the fragility parameters are determined. The second, termed β_u, represents uncertainty that the tests represent actual conditions of installation and loading, or uncertainty that the available data are an adequate sample size to accurately represent the true random variability. The total dispersion, β, is computed as:

$$\beta = \sqrt{\beta_r^{\,2} + \beta_u^{\,2}} \qquad\qquad\qquad \text{(H-3)}$$

The following minimum values of uncertainty, β_u, are recommended:

- A minimum value of $\beta_u = 0.25$ should be used if any of the following apply:

  o   Test data are available for five (5) or fewer specimens.

  o   In an actual building, a component can be installed in a number of different configurations, but all specimens were tested with the same configuration.

  o   All specimens were subjected to the same loading protocol.

  o   Actual behavior of the component is expected to be dependent on two or more demand parameters (e.g., simultaneous drift in two orthogonal directions), but specimens were loaded using only one demand parameter.

- Otherwise, a value of $\beta_u = 0.10$ may be used.

H.1.2   Methods of Derivation

Fragility functions are best derived from a large quantity of test data that investigate the behavior of the component of interest at varying levels of demand. FEMA 461, *Interim Testing Protocols for Determining the Seismic Performance Characteristics of Structural and Nonstructural Components* (FEMA, 2007), provides recommended procedures for laboratory testing intended to develop fragility data.

Because testing is expensive and time consuming, there are limited data presently available for use as a basis to develop fragility functions for most building components. The procedures in this appendix provide guidance for deriving values of the median, θ, and dispersion, β, for fragility functions given the following varying levels of available data:

- **Actual Demand Data.** Data are available from m individual specimen tests, and each tested specimen experienced the damage state of interest at a known value of demand, D.

- **Bounding Demand Data.** Test data or earthquake experience data are available from m individual specimen tests, but the damage state of interest only occurred in some specimens. For the other specimens, testing was terminated before the damage state of interest occurred, or the earthquake did not result in damage to the specimens. The maximum demand, D_i, that each specimen was subjected to is known, but this maximum demand may not be the demand at which the damage state initiated.

- **Capable Demand Data.** Test data or earthquake experience data are available from m individual specimen tests, but the damage state of interest did not occur in any of the specimens. The maximum demand, D_i, that each specimen was subjected to is known.

- **Derivation.** No data are available, but it is possible to model the behavior and analytically estimate the level of demand at which the damage state of interest will occur.

- **Expert Opinion.** No data are available and analysis of the behavior is not feasible, but one or more knowledgeable individuals can offer an opinion as to the level of demand at which damage is likely to occur, based on experience or engineering judgment.

Additionally, Section H.2.6 provides guidance for updating existing fragility functions as more data become available (e.g., from additional testing).

H.1.3 Documentation

Each fragility function should be accompanied by documentation of data sources and procedures used so that others can evaluate the quality of the resulting fragility parameters. As a minimum, documentation should include:

- **Applicability.** Description of the type of component addressed, including any limitations on the type of installation to which the fragility applies.

- **Specimen types.** Description of the specimens used to establish the fragility, including the number of specimens examined, their locations, and the specific details of the specimen fabrication, construction, mounting, and installation.

- **Demand parameters and application of loads.** Description of the loading protocol or characteristics of earthquake motion applied to each specimen; identification of the demand parameters examined that might be most closely related to failure probability, and how demand is

calculated or inferred from the loading protocol or excitation; indication of whether or not the reported demand quantities are the value at which damage occurred, or the maxima to which each specimen was subjected.

- **Damage states.** Description of each damage state, including the physical damage observed and any force-deformation quantities recorded, quantitative definition of damage states in terms of the repairs required, and possible casualty or unsafe placard consequences.

- **Observation summary, analysis method, and results.** Tabular or graphical listing of specimens, demand parameters, and damage states identifying the method(s) used to derive fragility parameters; summary of the resulting fragility function parameters, θ and β; and results of tests to establish fragility function quality, including sample calculations.

H.2   Derivation of Fragility Parameters

H.2.1   Actual Demand Data

When data are available from a suitable series of tests, and the damage state of interest was initiated at a known value of the demand, d_i, for each tested specimen, the median value of the demand at which the damage state is likely to initiate, θ, is given by the equation:

$$\theta = e^{\left(\frac{1}{M}\sum_{i=1}^{M}\ln d_i\right)} \tag{H-4}$$

where:

M = total number of specimens tested

d_i = demand in test "i" at which the damage state was first observed to occur.

The value of the random dispersion, β_r, is given by:

$$\beta_r = \sqrt{\left(\frac{1}{M-1}\sum_{i=1}^{M}\left(\ln\left(d_i/\theta\right)\right)^2\right)^2} \tag{H-5}$$

where M, d_i, and θ are as defined above.

If one or more of the values of d_i appear to be significantly above or below the bulk of the data, the procedure for outliers specified in Section H.3.2 should be applied. The resulting fragility parameters should be tested using the goodness-of-fit test specified in Section H.3.3. If the test passes at the 5% significance level, the fragility parameters are deemed acceptable.

Example: Determine the parameters θ and β from a series of 10 tests, all of which produced the damage state of interest. The damage state initiated at story drift ratios of: 0.9, 0.9, 1.0, 1.1, 1.1, 1.2, 1.3, 1.4, 1.7, and 2 percent.

Test #	Demand di	ln(di)	ln(di/θi)	ln(di/θi)^2
1	0.9	-0.10536	-0.30384	0.092321
2	0.9	-0.10536	-0.30384	0.092321
3	1	0	-0.19848	0.039396
4	1.1	0.09531	-0.10317	0.010645
5	1.1	0.09531	-0.10317	0.010645
6	1.2	0.182322	-0.01616	0.000261
7	1.3	0.262364	0.063881	0.004081
8	1.4	0.336472	0.137989	0.019041
9	1.7	0.530628	0.332145	0.11032
10	2	0.693147	0.494664	0.244692
Σ		1.984833		0.623723

$$\theta = e^{\left(\frac{1}{M}\sum_{i=1}^{M} \ln d_i\right)} = e^{\left(\frac{1}{10}(1.9848)\right)} = 1.22$$

$$\beta_r = \sqrt{\frac{1}{M-1}\sum_{i=1}^{M}\left(\ln\left(\frac{d_i}{\theta}\right)\right)^2} = \sqrt{\frac{1}{(10-1)}(0.6237)} = 0.26$$

H.2.2 Bounding Demand Data

When data are available from a suitable series of tests, but the damage state of interest was initiated in only some of the specimens, bounding demand data can be used to derive fragility parameters. For each specimen "i," it is necessary to know the maximum value of the demand, d_i, to which the specimen was subjected, and whether or not the damage state of interest occurred in the specimen.

The data should be divided into a series of N bins. It is suggested, but not essential, that N be taken as the largest integer that is less than or equal to the square root of M, where M is the total number of specimens available (this will usually result in an appropriate number of approximately equally sized sets). To divide the specimens into bins, data should be sorted in order of ascending maximum demand value, d_i, for each test, then divided into N groups of approximately equal size. Each group "j" will have M_j specimens, where:

$$\sum_{i=1}^{N} M_j = M \tag{H-6}$$

The average value of the maximum demand for each bin of specimens is:

$$\bar{d}_j = \frac{1}{M_j}\sum_{k=1}^{M_j} d_k \tag{H-7}$$

The natural logarithm of d_j (i.e., $\ln(d_j)$) is taken as the value of x_j. Determine the number of specimens within each bin in which the damage state of interest was achieved, m_j, and the inverse standard normal distribution, y_j, of the failed fraction of specimens in the bin as:

$$y_j = \Phi^{-1}\left(\frac{m_j + 1}{M_j + 1}\right) \tag{H-8}$$

This is also the number of standard deviations above the mean that the stated fraction lies, assuming a mean value, $\mu = 0$ and a standard deviation, $\sigma = 1$, and can be determined using the "normsinv" function in an Excel worksheet, or by referring to standard Gaussian tables for normal distributions.

A straight line is fit to the data points, x_j and y_j, using a least-squares approach. The straight line will have the form:

$$y = bx + c \tag{H-9}$$

where, b is the slope of the line and c is the y-intercept. The slope b is given by:

$$b = \frac{\sum\limits_{i=1}^{M}(x_j - \bar{x})(y_j - \bar{y})}{\sum\limits_{i=1}^{M}(x_j - \bar{x})^2} \tag{H-10}$$

$$\bar{x} = \frac{1}{M}\sum\limits_{j=1}^{M}x_j \tag{H-11}$$

$$\bar{y} = \frac{1}{M}\sum\limits_{j=1}^{M}y_j \tag{H-12}$$

Determine the value of the random dispersion, β_r as:

$$\beta_r = \frac{1}{b} = \frac{\sum\limits_{i=1}^{M}(x_j - \bar{x})}{\sum\limits_{i=1}^{M}(x_j - \bar{x})(y_j - \bar{y})} \tag{H-13}$$

and the value of the median, θ, as:

$$\theta = e^{-c\beta_r} = e^{(\bar{x} - \bar{y}\beta_r)} \tag{H-14}$$

Example: Consider the damage statistics shown in the figure below depicting the hypothetical performance of motor control centers (MCCs) observed after various earthquakes in 45 facilities. Each stack of boxes represents data from one facility. Each box represents one specimen and several damage states are recorded. Crosshatched boxes represent MCCs that experienced a noticeable earthquake effect, such as shifting on their supports, but remained operable. Black boxes represent MCCs that were found to be inoperable following an earthquake. Calculate the fragility function using *PGA* as the demand parameter, binning at halfway points between the *PGA* values shown in the figure.
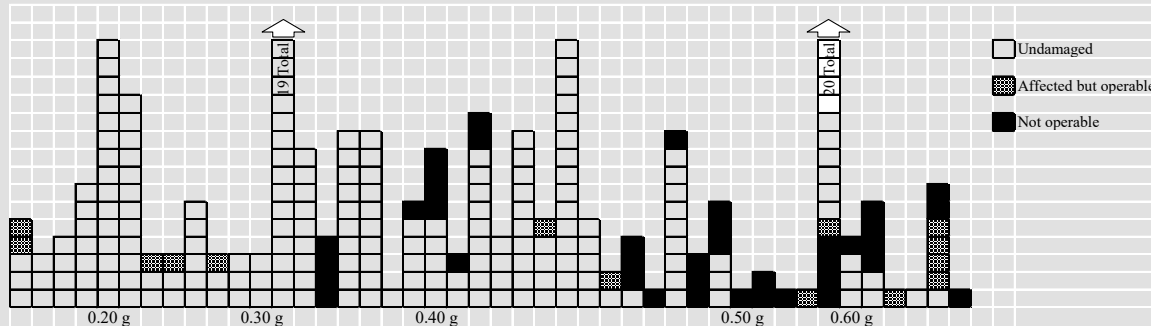
Figure H-2   Hypothetical observed earthquake damage data for motor control centers.

The number of bins, N, and lower bound demands, a_j, are dictated by the available data. N is taken as 5 with lower bounds of a_j = 0.15g, 0.25g, 0.35g, 0.45g, and 0.55g respectively. The damage state of interest is loss of post-earthquake functionality (black boxes in the figure). Values of M_j and m_j are determined by counting all boxes (M_j) and black boxes (m_j) in each bin, and are shown in the table below. The value of M is the summation: $\Sigma M_j = 260$. Values x_j and y_j are calculated as $x_j = \ln(\bar{d}_j)$, and $y_j = \Phi^{-1}((m_j+1)/(M_j+1))$. Average values are calculated as: $\bar{x} = -0.99$, $\bar{y} = -1.05$. For each bin, the values of $x_j - \bar{x}$ and $y_j - \bar{y}$ are shown in the table.

Table H-1   Example Solution Data

j	$a_j(g)$	$\bar{r}_j(g)$	M_j	m_j	x_j	y_j	$x_j - \bar{x}$	$y_j - \bar{y}$	$(x_j - \bar{x})^2$	$(x_j - \bar{x})(y_j - \bar{y})$
1	0.15	0.2	52	0	-1.61	-2.08	-0.623	-1.031	0.388	0.642
2	0.25	0.3	48	4	-1.20	-1.27	-0.217	-0.223	0.047	0.049
3	0.35	0.4	84	8	-0.92	-1.25	0.070	-0.202	0.005	-0.014
4	0.45	0.5	35	15	-0.69	-0.14	0.294	0.907	0.086	0.266
5	0.55	0.6	41	12	-0.51	-0.50	0.476	0.549	0.226	0.261
$\Sigma =$			**260**		**-4.93**	**-5.23**			**0.753**	**1.204**
	Average=				-0.99	-1.05				

Then, β and θ are calculated as:

$$\beta_r = \frac{\sum_{j=1}^{N}(x_j - \bar{x})^2}{(x_j - \bar{x})(y_j - \bar{y})} = \frac{0.753}{1.204} = 0.63$$

$$\theta = e^{(\bar{x} - \bar{y}\beta_r)} = e^{(-0.99 + 1.05(0.63))} = e^{(-0.329)} = 0.72g$$

H.2.3 Capable Demand Data

When data are available from a suitable series of tests, but the damage state of interest was not initiated in any of the specimens, capable demand data can be used to estimate fragility functions. For each specimen "i," it is necessary to know the maximum value of the demand, d_i, to which the specimen was subjected, and whether or not the specimen experienced any damage or distress.

From the M specimen tests, the maximum demand experienced by each specimen, d_{max}, and the minimum demand experienced by any of the specimens that exhibited damage, d_{min}, must be determined. The value, d_a, is taken as the smaller of d_{min} or $0.7d_{max}$. If none of the specimens in any of the tests exhibited any sign of damage or distress, the value of d_m can be taken as d_{max}. If one or more of the specimens exhibited some type of damage or distress, d_m is taken as:

$$d_m = \frac{d_{max} + d_a}{2} \tag{H-15}$$

Determine the subjective failure probability, S, at d_m as:

$$S = \frac{0.5M_C + 0.1M_B}{M_A + M_B + M_C} \tag{H-16}$$

where M_A is the number of specimens that did not exhibit damage or distress, but that were loaded with demands, $d_i \geq d_a$; M_B is the number of specimens that exhibited damage or distress, but did not appear to be initiating or on the verge of initiating the damage state of interest; and M_C is the number of specimens that appeared to be on the verge of initiating the damage state of interest. Determine the median, θ, as:

$$\theta = d_m e^{-0.4z} \tag{H-17}$$

where z is determined from Table H-2 based on the value of M_A and S. The logarithmic standard deviation is taken as $\beta = 0.4$.

Table H-2   Values of Parameter, z, Given M_A and S

Conditions	z
$M_A \geq 3$ and $S = 0$	-2.326
$M_A < 3$ and $S \leq 0.075$	-1.645
$0.075 < S \leq 0.15$	-1.282
$0.15 < S \leq 0.3$	-0.842
$S > 0.3$	-0.253

Example: Determine the parameters θ and β from 10 specimen tests. Five of the specimens had maximum imposed drift ratio demands of 1% with no observable signs of distress. Three of the specimens had maximum imposed drift ratio demands of 1.5% and exhibited minor distress, but did not appear to be at or near initiation of the damage state of interest. Two of the specimens had maximum imposed drift ratio demands of 2%, and did not exhibit the damage state of interest during the test, but appeared to be about to initiate such damage. From the data provided, $d_{max} = 2\%$; $d_{min} = 1.5\%$; d_a is the smaller of $0.7d_{max}$ or d_{min}, which is $0.7(2\%) = 1.4\%$; $M_A = 0$; $M_B = 3$; and $M_C = 2$.

$$d_m = \frac{d_{max} + d_a}{2} = \frac{2\% + 1.4\%}{2} = 1.7\%$$

$$S = \frac{0.5M_C + 0.1M_B}{M_A + M_B + M_C} = \frac{0.5(2) + 0.1(3)}{0 + 3 + 2} = 0.26$$

From Table H-1, z is -0.842. Therefore,

$$\theta = d_m e^{-0.4z} = 1.7\% e^{-0.4(-0.842)} = 2.4\%$$

and β is taken as 0.4.

H.2.4 Derivation

Where no test data are available, there are two methods available for analytical derivation of fragility parameters. The first uses a single calculation of the probable capacity and a default value of the logarithmic standard deviation. The second uses Monte Carlo analysis to explore the effect of variation in material strength, construction quality, and other random variables on the resulting capacity calculation.

- **Single calculation.** The capacity of the component, Q, is calculated in terms of a demand parameter, d, using average material properties, dimensions, and estimates of workmanship. Resistance factors are taken as unity, and any conservative bias that exists in code equations, if such equations are used, should be removed. The logarithmic standard deviation is taken as $\beta = 0.4$. The median capacity, θ, is taken as:

$$\theta = 0.92Q \qquad \text{(H-18)}$$

- **Monte Carlo simulation.** All factors that are important to predicting capacity and are also uncertain (e.g., material strength, cross section dimensions, member straightness, and workmanship) are identified. A median value and dispersion for each of these random variables is estimated. Sufficient analyses are conducted by randomly selecting the values of each of these variables in accordance with their estimated

distribution properties, and the capacity is calculated each time. The median value of the capacity is determined as the capacity that is exceeded in 50% of the calculations. The random logarithmic standard deviation, β_r, is taken as the standard deviation of the natural logarithm of the calculated capacity values. Equation H-3 is used to determine the total logarithmic standard deviation, β, assuming a value of $\beta_u = 0.25$.

H.2.5 Expert Opinion

Where no test data exist, and calculation of probable capacity is not feasible, expert opinion can be used to determine approximate fragility parameters. One or more experts with professional experience in the design or post-earthquake damage observation of the component of interest are selected. Advice is solicited using a format similar to the example shown.

Note the suggested inclusion of representative images, which should be recorded with the responses. If an expert refuses to provide estimates or limits them to certain conditions, either narrow the component definition accordingly and iterate, or ignore that expert's response and analyze the remaining ones.

Calculate the median value, θ, as:

$$\theta = \frac{\sum_{i=1}^{N} w_i^{1.5} \theta_i}{\sum_{i=1}^{N} w_i^{1.5}} \tag{H-19}$$

where, N is the number of experts providing an opinion; θ_i is expert "i's" opinion as to the median value, and w_i is expert "i's" level of expertise, on a 1-5 scale.

Calculate the lower bound value for the capacity as:

$$d_l = \frac{\sum_{i=1}^{N} w_i^{1.5} d_{li}}{\sum_{i=1}^{N} w_i^{1.5}} \tag{H-20}$$

where, d_{li} is expert "i's" opinion as to the lower bound value and other terms are as previously defined. The value of the logarithmic standard deviation, β, is taken as:

$$\beta = \frac{\ln(\theta / d_l)}{1.28} \tag{H-21}$$

If this calculation produces an estimate of β that is less than 0.4, either justify the β, or take β as having a value of 0.4 and recalculate θ as:

$$\theta = 1.67d_l \qquad \text{(H-22)}$$

Example: Solicitation of Expert Opinion

Objective. This form solicits judgment about the values of a demand parameter, *D,* at which a particular structural or nonstructural component experiences a particular damage state. Judgment is needed because relevant empirical and/or analytical data are currently unavailable or are impractical to acquire at this time.

Definitions. Please provide judgment regarding the damageability of the component of interest, including relevant damage states and a corresponding demand parameter that best correlates with the anticipated damage. Images of a representative sample of the component and damage state may be attached.

Component name:_____

Component definition:_____

Damage state name:_____

Damage state definition:_____

Relevant Demand Parameter:_____

Definition of Demand Parameter:_____

Uncertainty/Personal Bias. Uncertainty is to be expected. Because of variability in design, construction, installation, inspection, age, maintenance, and interaction with nearby components, there is likely no precise threshold level of demand that causes damage. Judgment should be based on the overall class of components in general, not any one particular instance, and not on cases in which the expert was personally involved in designing, constructing, checking, or reviewing.

Estimated Capacities. To account for expected uncertainties, please provide median and lower bound values of demand at which damage would be expected to occur:

Estimated median capacity:_____
Damage would occur at this level of demand in 5 cases out of 10; alternatively, in a single instance, there is an equal chance that the median estimate provided is too low or too high.

Estimated lower-bound capacity:_____
Damage would occur at this level of demand in 1 case out of 10; alternatively, in a single instance, there is a 10% chance that the estimate is too high. The lower bound should be judged carefully. Research shows that without careful thought, expert judgment of the lower bound tends to be too close to the median estimate. After an initial estimate is made, consider all conditions that might make the actual threshold for damage lower (e.g., errors in design, construction, installation, deterioration, interaction with nearby components), and revise accordingly.

Expertise. On a scale of 1 to 5, where 1 means "no experience or expertise," and 5 means "very familiar and highly experienced," rate your experience and expertise with this component and its damageability.

Level of expertise:_____

Name:_____ Date:_____

H.2.6 Updating Fragility Functions with New Data

Fragility parameters for a component can be updated as additional data become available. Pre-existing and updated fragility parameters are termed θ, β, θ', and β', respectively. The additional data are assumed to be a set of M specimens with known maximum demands and known damage. It is not necessary that any of the specimens experienced the damage state of interest.

The revised median, θ', and logarithmic standard deviation, β', are calculated as:

$$\theta' = e^{\sum\limits_{j=1}^{5} w'_j \ln(d_j)} \tag{H-23}$$

$$\beta' = \sum\limits_{j=1}^{5} w'_j \beta_j \tag{H-24}$$

where:

$$w'_j = \frac{w_j \prod\limits_{i=1}^{M} L(i,j)}{\sum\limits_{j=1}^{5} w_j \prod\limits_{i=1}^{M} L(i,j)} \tag{H-25}$$

and $\prod$ denotes the product of the terms that follow. If specimen "i" did not experience the damage state of interest, then:

$$L(i,j) = 1 - \Phi\left(\frac{\ln(d_i/x_j)}{0.707 s \beta_j}\right) \tag{H-26}$$

If specimen "i" did experience the damage state of interest (or a more severe damage state), then:

$$L(i,j) = \Phi\left(\frac{\ln(d_i/x_j)}{0.707 s \beta_j}\right) \tag{H-27}$$

where:

$x_1 = x_4 = x_5 = \theta$

$x_2 = \theta e^{-1.22\beta}$

$x_3 = \theta e^{1.22\beta}$

$\beta_1 = \beta_2 = \beta_3 = \beta$

$\beta_4 = 0.64\beta$

$\beta_5 = 1.36\beta$

$w_1 = 1/3$

$w_2 = w_3 = w_4 = w_5 = 1/6$

H.3 Assessing Fragility Function Quality

The quality of fragility function parameters can be assessed using the procedures of this section.

H.3.1 Competing Demand Parameters

The behavior of some components may depend on several types of demands, for example in-plane and out-of-plane drift, or both drift and acceleration. It is not always clear which demand parameter is the best single predictor of component damage. If sufficient data are available, fragility functions for each relevant demand parameter should be developed. The fragility relationship with the lowest dispersion, β, should be selected.

H.3.2 Elimination of Outliers

When fragilities are determined on the basis of actual demand data, it is possible that one or more tests reported spurious values of demand, d_i, that reflect experimental errors rather than true demands at which the specimens failed. In cases where one or more values of d_i in the data set are obvious outliers from the bulk of the data, the data should be investigated for relevance to the component damage process, especially where $d_i << \theta$ for the outliers. If there is no indication that these data reflect a real recurring issue in the damage process, Peirce's criterion (Ross, 2003) should be applied to test and eliminate doubtful observations of d_i, as follows:

1. Calculate $\ln(\theta)$ and β of the complete data set.

2. Let D denote the number of doubtful observations, and let R denote the maximum distance of an observation from the body of the data, defined as:

$$R = \frac{\left|\ln(d) - \ln\theta\right|}{\beta} \qquad \text{(H-28)}$$

   where θ, β, and M are as previously defined, d is a measured demand. Values of R are as shown in Table H-3. Begin with the assumption that $D = 1$, even if there appears to be more than one doubtful observation.

3. Calculate the maximum allowable deviation: $\left|\ln(d) - \ln(\theta)\right|_{\text{max}}$. Note that this can include values for $d >> \theta$ and $d << \theta$.

4. For any suspicious measurement d_i, obtain $\left|\ln(d_i) - \ln(\theta)\right|$.

5. Eliminate the suspicious measurements if:
   $$\left|\ln(d_i) - \ln(\theta)\right| > \left|\ln(d) - \ln(\theta)\right|_{\text{max}}$$

6. If this results in the rejection of one measurement, assume $D = 2$, keeping the original values of θ and β, and go on to Step 8.

7. If more than one measurement is rejected in the above test, assume the next highest value of doubtful observations. For example, if two measurements are rejected in Step 5, assume $D = 3$, keeping the original values of θ and β as the process is continued.

8. Repeat Steps 2 through 5, sequentially increasing D until no additional data measurements are eliminated.

9. Obtain θ and β for the reduced data set as was done for the original data set.

Table H-3   Values of R for Applying Peirce's Criterion

M	D=1	D=2	D=3	D=4	D=5	D=6	D=7	D=8	D=9
3	1.1960								
4	1.3830	1.0780							
5	1.5090	1.2000							
6	1.6100	1.2990	1.0990						
7	1.6930	1.3820	1.1870	1.0220					
8	1.7630	1.4530	1.2610	1.1090					
9	1.8240	1.5150	1.3240	1.1780	1.0450				
10	1.8780	1.5700	1.3800	1.2370	1.1140				
11	1.9250	1.6190	1.4300	1.2890	1.1720	1.0590			
12	1.9690	1.6630	1.4750	1.3360	1.2210	1.1180	1.0090		
13	2.0070	1.7040	1.5160	1.3790	1.2660	1.1670	1.0700		
14	2.0430	1.7410	1.5540	1.4170	1.3070	1.2100	1.1200	1.0260	
15	2.0760	1.7750	1.5890	1.4530	1.3440	1.2490	1.1640	1.0780	
16	2.1060	1.8070	1.6220	1.4860	1.3780	1.2850	1.2020	1.1220	1.0390
17	2.1340	1.8360	1.6520	1.5170	1.4090	1.3180	1.2370	1.1610	1.0840
18	2.1610	1.8640	1.6800	1.5460	1.4380	1.3480	1.2680	1.1950	1.1230
19	2.1850	1.8900	1.7070	1.5730	1.4660	1.3770	1.2980	1.2260	1.1580
20	2.2090	1.9140	1.7320	1.5990	1.4920	1.4040	1.3260	1.2550	1.1900
>20	alnM + b								
a	0.4094	0.4393	0.4565	0.4680	0.4770	0.4842	0.4905	0.4973	0.5046
b	0.9910	0.6069	0.3725	0.2036	0.0701	-0.0401	-0.1358	-0.2242	-0.3079

H.3.3 Goodness-of-Fit Testing

Fragility parameters that are developed on the basis of actual demand data should be tested for goodness-of-fit (Lilliefors, 1967) in accordance with this section. Calculate:

$$D = \max_x \left| F_i(d) - S_M(d) \right| \tag{H-29}$$

where $S_M(d)$ denotes the sample cumulative distribution function

$$S_M(d) = \frac{1}{M} \sum_{i=1}^{M} H(d_i - d) \tag{H-30}$$

and H is taken as:

- 1.0 if $d_i - d$ is positive
- ½ if $d_i - d$ is zero
- 0 if $d_i - d$ is negative

If $D > D_{critical}$ from Table H-3, the fragility function fails the goodness-of-fit test. Use values at a significance level of $\alpha = 0.05$ in assigning a quality rating for a fragility function.

Table H-4   Critical Values for the Lilliefors Goodness-of-Fit Test

Significance Level	$D_{critical}$
$\alpha = 0.15$	$0.775 / (M^{0.5} - 0.01 + 0.85M^{-0.5})$
$\alpha = 0.10$	$0.819 / (M^{0.5} - 0.01 + 0.85M^{-0.5})$
$\alpha = 0.05$	$0.895 / (M^{0.5} - 0.01 + 0.85M^{-0.5})$
$\alpha = 0.025$	$0.995 / (M^{0.5} - 0.01 + 0.85M^{-0.5})$

H.3.4 Adjusting Fragility Functions that Cross

Some components will have two or more possible damage states, with a defined fragility function for each. For any two (cumulative lognormal) fragility functions i and j with medians $\theta_j > \theta_i$ and logarithmic standard deviations $\beta_i \neq \beta_j$, the fragility functions will cross at extreme values. When fragility functions cross, it is possible to get negative values of probability for being in damage state "i," which is meaningless. In such cases, the fragility functions can be adjusted using either of the following two methods:

- **Method 1.** Adjust the fragility functions such that:

$$F_i(D) = \max_j \left\{ \Phi\left(\frac{\ln(D/\theta_i)}{\beta_i} \right) \right\} \quad \text{for all } j \geq i \tag{H-31}$$

This method assures that the probability of failure for the damage state with the higher median value, $F_i(D_j)$, is never taken as less than the probability of failure for a damage state with a lower median value $F_i(D_i)$.

- **Method 2.** Establish values of θ and β for the various damage states independently. Calculate the average of the dispersion values for each of the damage states with crossing fragility curves as:

$$\beta_i' = \frac{1}{N}\sum_{i=1}^{N}\beta_i \qquad \text{(H-32)}$$

The average logarithmic standard deviation, β', is used as a replacement for the independently calculated values of dispersion. Using the average dispersion, an adjusted median value must be calculated for each of the crossing fragilities as:

$$\theta_i' = e^{\left(1.28(\beta'-\beta_i)+\ln\theta_i\right)} \qquad \text{(H-33)}$$

H.3.5 Fragility Function Quality Levels

Fragility functions should be assigned a quality level of high, medium, or low, in accordance with the criteria in Table H-4.

Table H-5   Criteria for Fragility Function Quality Levels

Quality	Method	Peer Reviewed[1]	Number of Specimens	Notes
High	Actual	Yes	≥ 5	Passes Lilliefors test at 5% significance level. Examine and justify: (a) differences greater than 20% in θ or β, compared with past estimates; and (b) any case of $\beta < 0.2$ or $\beta > 0.6$.
	Bounding	Yes	≥ 20	Examine and justify: (a) differences greater than 20% in θ or β, compared with past estimates; and (b) any case of $\beta < 0.2$ or $\beta > 0.6$.
	Update	Yes	≥ 6	Prior was at least moderate quality
Moderate	Actual		≥ 3	Examine and justify any case of $\beta < 0.2$ or $\beta > 0.6$.
	Bounding		≥ 16	Examine and justify any case of $\beta < 0.2$ or $\beta > 0.6$.
	Capable	Yes	≥ 6	
	Dreviation	Yes		
	Expert	Yes		At least 3 experts with experience rating ≥ 3
	Update		≥ 6	Prior was at least moderate quality
Low				All other cases

Notes: [1] Data and derivation published in a peer-reviewed journal.

Appendix I

Rugged Components

I.1 Rugged Components

Rugged components are components that are not susceptible to earthquake shaking-induced damage, or have very high thresholds for damage. High thresholds for damage include shaking intensities that are not likely to be encountered in typical building structures. Since rugged components are not directly damaged by earthquake shaking, they are not expected to contribute to earthquake impacts, and are not explicitly included in the building performance model. Estimates of building replacement cost and replacement time, however, must consider the presence of rugged components in the building.

Table I-1 provides a list of structural and nonstructural components that have been identified as rugged. This list was developed based on post-earthquake observations and laboratory testing. The table is organized by the general system description and classification numbering system used for fragility specifications, NISTIR 6389, *UNIFORMAT II Elemental Classification for Building Specifications, Cost Estimating and Cost Analysis* (NIST, 1999).

Because items identified in Table I-1 are considered rugged, fragility and consequence data have not been developed for these components. If such a component is determined to be vulnerable to damage (i.e., not rugged) in a particular building or assessment, user-defined fragilities and consequences must be developed to assess their impact on performance. Similarly, if a fragility specification associated with a vulnerable component is omitted from a building performance model, it has the same effect as considering that component to be rugged for the purposes of that assessment.

Table I-1   List of Rugged Components

General System Description	NISTIR Classification Number	Component Description
Foundations	A10	Spread footings, mat foundations, grade beams
Basement Construction	A20	Basement walls and slabs
Floor Construction	B101	Gravity-frame components of floor systems that do not participate in lateral resistance. This includes most floor framing and sheathing other than concrete slab-column frames
Roof Construction	B102	Gravity-frame components of roof systems that do not participate in lateral resistance. This includes most roof framing other than concrete slab-column frames. This also includes most diaphragm sheathing
Structural Steel	B103	Simple beam framing
Reinforced Concrete	B104	Floor and roof framing other than slab-column frames and beam-column frames
Cold-Formed Steel	B106	Horizontal floor and roof framing
Light-framed Wood	B107	Horizontal floor and roof framing
Roof Coverings	B301	Composite and built-up roofing systems (including flashing and insulation) except tile roofing on sloped surfaces.
Roof Openings	B302	Roof hatches and skylights
Floor Finishes	C302	Floor finishes, including carpeting, except when water leaks occur
Plumbing Fixtures	D201	Toilets, sinks, tubs, urinals
Rain Water Drainage	D204	Rain water leaders and gutters
Electrical Distribution Systems	D304	Conduits and raceways
Standpipes	D402	Wet and dry standpipes
Other Fire Protection Systems	D409	Smoke detectors, heat detectors, and alarm control systems
Lighting and Branch Wiring	D502	Lighting panels and wiring
Communications and Security	D503	Communications and security equipment
Commercial Equipment	E101	Commercial equipment (note: occupancy-specific equipment deemed fragile or important require user-defined fragility and consequence data for performance assessment)

Appendix J

Collapse Fragility Development Using Incremental Dynamic Analysis

J.1 Introduction

This appendix describes the use of incremental dynamic analysis (IDA) for development of collapse fragilities. Additional information on assessing structural collapse using incremental dynamic analysis techniques is provided in FEMA P-695, *Quantification of Building Seismic Performance Factors* (FEMA, 2009b).

J.2 Procedure

Incremental dynamic analysis (IDA) involves a large number of nonlinear response history analyses that are performed using ground motions that are systematically scaled to increasing earthquake intensities until collapse occurs. Incremental dynamic analysis yields a distribution of results at varying intensities that can be used to generate a collapse fragility.

In general, each ground motion pair is scaled to an initial intensity level, characterized by a common value of the geomean spectral response acceleration at the first mode period, $S_a(\overline{T})$. The structure is subjected to nonlinear response history analysis, using each of these ground motion pairs, and the number of analyses that produce collapse predictions is determined. Then, ground motion amplitudes are systematically incremented, and the process repeated, until 50% or more of the analyses at the intensity level result in collapse. The intensity at which 50% of the analyses predict collapse is taken as the median collapse intensity. A dispersion is fit to the collapse data and modified to account for other uncertainties. The basic steps in the procedure are as follows:

1. Construct a mathematical model representing the structure.

2. Select an appropriate suite of ground motion pairs that represent scenario events likely to result in collapse of the structure, considering the site seismic hazard.

3. Scale the ground motion suite such that the geomean spectral acceleration at the first mode period of the structure, $S_a(\bar{T})$, for each pair is at a value low enough for inelastic response to be negligible.

4. Analyze the mathematical model for each scaled ground motion pair and determine the maximum value of story drift.

5. Increment the intensity of the effective first mode spectral response acceleration, $S_a(\bar{T})$, to which each ground motion pair is scaled.

6. Analyze the structure for each incrementally scaled ground motion pair and record the maximum value of story drift.

7. Repeat Steps 5 and 6 above for each ground motion pair until the analysis:

    a. produces a very large increase in drift for a small increment in the value of intensity, indicating the onset of dynamic instability;

    b. results in numerical instability suggesting collapse;

    c. results in predicted demands on gravity-load carrying components that exceed their reliable capacities; or

    d. predicts drift levels that exceed the range of model validity.

8. Determine the value of spectral acceleration, $S_a(\bar{T})$ at which 50% of the ground motion pairs produce predictions of collapse. This value of $S_a(\bar{T})$ is taken as the median collapse capacity, $\hat{S}_a(\bar{T})$.

9. Determine a dispersion for the collapse fragility.

J.3   Mathematical Models

Three dimensional mathematical models should be used unless structural response is independent in each of two orthogonal directions. Additional guidance on modeling provided in Chapters 5 and 6 is also applicable.

J.4   Ground Motion Selection and Scaling

Ground motion selection and scaling can utilize uniform hazard spectra (UHS) or conditional mean spectra (CMS), described in Appendix B. In both cases, a sufficient number of ground motions should be used to provide stable estimates of median collapse capacity. In limited study, use of 11 pairs of motions, each rotated 90 degrees to produce a total of 22 motion sets, were found to be sufficient. For some structures, stable prediction of median collapse capacity may be possible with fewer motions.

Ground motions generated for response-history analysis as described in Chapter 4, which are at an intensity level that is approximately equal to the median collapse capacity, $\hat{S}_a(\overline{T})$, can also be used.

J.4.1 Uniform Hazard Spectrum

Ground motion pairs for incremental dynamic analysis based on a uniform hazard spectrum should be selected as follows:

1. Estimate the median collapse capacity, $\hat{S}_a(\overline{T})$, and the mean annual frequency of exceedance corresponding to $\hat{S}_a(\overline{T})$. For buildings that conform to the seismic design and detailing criteria contained in ASCE/SEI 7-10, $\hat{S}_a(\overline{T})$ can be estimated as approximately 3 times the value of the design level spectral ordinate at period, $\overline{T}$.

2. Develop a target uniform hazard spectrum consistent with the mean annual frequency of exceedance for $\hat{S}_a(\overline{T})$ estimated in Step 1.

3. Select an appropriate suite of ground motion pairs with geometric mean spectra that have a shape similar to the target uniform hazard spectrum.

If the estimate of median collapse capacity, $\hat{S}_a(\overline{T})$, in Step 1 is significantly different (i.e., larger or smaller) than the value computed from incremental dynamic analysis, a new uniform hazard spectrum should be determined for the mean annual frequency of exceedance corresponding to $\hat{S}_a(\overline{T})$ determined by analysis. If the shape of the new spectrum is significantly different from the target spectrum initially developed in Step 2, a new suite of motions should be selected to match the new spectrum, and the analyses repeated.

J.4.2 Conditional Mean Spectrum

Ground motion pairs for incremental dynamic analysis based on a conditional mean spectrum should be selected as follows:

1. Estimate the median collapse capacity, $\hat{S}_a(\overline{T})$, and the mean annual frequency of exceedance corresponding to $\hat{S}_a(\overline{T})$. For buildings that conform to the seismic design and detailing criteria contained in ASCE/SEI 7-10, $\hat{S}_a(\overline{T})$ can be estimated as approximately 3 times the value of the design level spectral ordinate at period, $\overline{T}$.

2. Deaggregate the seismic hazard at the mean annual frequency of exceedance (see Appendix B) to determine the magnitude and distance of characteristic events that dominate the hazard at this level of shaking.

3. Generate a conditional mean spectrum at period $\overline{T}$ for the $[M, r, \varepsilon]$ triple corresponding to the events selected in Step 2, using an appropriate

attenuation function (see Appendix B). Normalize the conditional mean spectrum so that the peak ordinate is equal to 1.0.

4. Select an appropriate suite of ground motions with geometric mean spectra that have a shape and period at peak spectral response that are similar to the target conditional mean spectrum.

If the estimate of median collapse capacity, $\hat{S}_a(\overline{T})$, in Step 1 is significantly different (i.e., larger or smaller) than the value computed from incremental dynamic analysis, a new conditional mean spectrum should be generated for the mean annual frequency of exceedance corresponding to $\hat{S}_a(\overline{T})$ determined by analysis. If the shape of the new spectrum is significantly different from the target spectrum initially developed in Step 3, a new suite of motions should be selected to match the new spectrum, and the analyses repeated.

J.5   Collapse Fragility Development

The amplitude of each ground motion pair should be incremented, and nonlinear response history analysis performed, until a measure of collapse is achieved. The median collapse capacity is taken as the value of $S_a(\overline{T})$ at which 50% of the ground motion pairs produce collapse, as measured by: numerical instability, simulated collapse, non-simulated collapse criteria, or excessive lateral drift for a small increase in $S_a(\overline{T})$.

Figure J-1 presents a collapse fragility plot constructed using the median and dispersion values obtained from incremental dynamic analysis results and the assumption of a lognormal distribution.
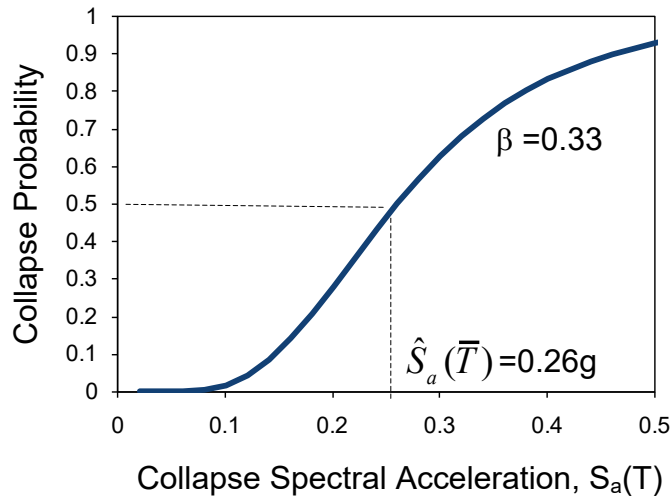
Figure J-1   Lognormal collapse fragility curve plotted using median and dispersion values from incremental dynamic analysis.

Note that the dispersion in Figure J-1, which is based on analysis of a mathematical model constructed using best estimate mechanical properties, does not include all sources of uncertainty. The following additional sources of uncertainty must also be considered in calculating the total dispersion to define the final collapse fragility curve:

- Variation in calculated story drift resulting from different ground motion records, $\beta_{a\Delta}$, (also termed analysis record-to-record uncertainty). Default values of $\beta_{a\Delta}$ are provided in Chapter 5, Table 5-6. Alternatively, a value of 0.45 can be used.

- Uncertainty due to ambiguity in building definition and construction quality, β_c. Values of β_c based on the level of building definition and construction quality assurance are provided in Chapter 5.

- Uncertainty associated with the quality and completeness of the nonlinear analysis model, β_q. Values of β_q based on the quality of the analytical model are provided in Chapter 5. Given that few component force-deformation models have been validated by large-scale experimental testing, β_q should typically have a value between 0.3 and 0.5.

Total dispersion can be estimated using Equation J-1 and the information above. Alternatively, a default total dispersion of 0.6 can be used to define the lognormal collapse fragility curve.

$$\beta = \sqrt{\beta_{a\Delta}^2 + (\beta_c^2 + \beta_q^2)} = \sqrt{\beta_{a\Delta}^2 + \beta_m^2} \qquad \text{(J-1)}$$

Appendix K
Sliding and Overturning

K.1   Introduction

This appendix provides the derivation and assumptions underlying procedures for calculation of fragility functions related to overturning and sliding of unanchored components. These procedures are based on Section 7.1, Section A.2, and Appendix B of ASCE/SEI 43-05, *Seismic Design Criteria for Structures, Systems, and Components in Nuclear Facilities* (ASCE, 2005).

The procedures cover only the development of fragility parameters for sliding and overturning damage states. In each case, users must determine the extent of damage that will result from the controlling behavior, and the consequences of that damage.

K.2   Overturning

Fragility functions for overturning are based on peak total floor velocity, V_{PT}, as the demand parameter. Fragility parameters include the median peak total floor velocity, $\hat{V}_{PT}$, at which overturning initiates, and a dispersion reflecting the uncertainty in this behavior mode.

Unanchored components are assumed to exhibit an oscillatory rocking behavior until a critical displacement is reached and the object becomes unstable. The critical displacement is represented in the form of a tipping angle, α, at which the center of mass of the component is located directly over the leading edge (or toe), as shown in Figure K-1.
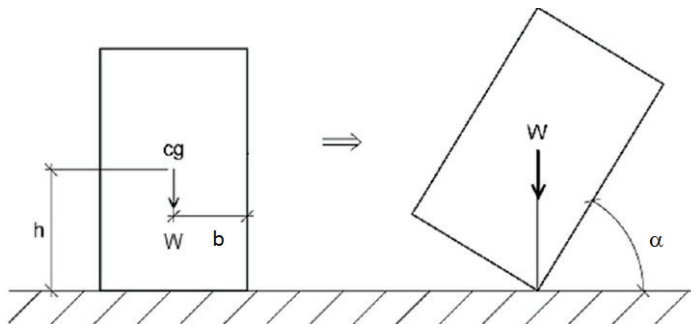
Figure K-1   Overturning of unanchored components.

Housner (1963) developed an expression for overturning failure of unanchored objects as a function of peak ground velocity:

$$PGV = 2gR\sqrt{(1-\cos\alpha)}$$ (K-1)

where PGV is the peak ground velocity at which overturning initiates, $R = \sqrt{b^2 + h^2}$, and the quantities α, b and h are as defined in Figure K-1.

The procedure, as adapted from ASCE 43-05, uses estimates of the component effective rocking frequency, f_r, and damping ratio, β_r, to express the probability of overturning occurrence as a function peak total floor velocity, V_{PT}, defined as the peak value of the sum of the ground velocity and the relative velocity between the ground and the floor level. It reflects a more detailed understanding of the dynamics associated with overturning instability, and provides general corroboration with Housner's equation for aspect ratios of typical concern. Key assumptions include the following:

- The relationship between peak ground velocity, PGV, and the component rocking frequencies and damping remain valid for use on elevated floor levels (i.e., above grade), with V_{PT} substituted for peak ground velocity.

- Overturning occurs about a single axis as a result of horizontal shaking in one direction. Simultaneous rocking about two axes is neglected, as are the effects of vertical acceleration.

- The component has a rectangular shape with height, $2h$, and width, $2b$.

- Component weight, W, is uniformly distributed.

From geometry, the critical tipping angle at which a component will become unstable is given by:

$$\alpha = \arctan\left(\frac{b}{h}\right)$$ (K-2)

The horizontal spectral acceleration that will tip the component to the critical angle, α, is determined by:

$$S_{aO} = \frac{2B}{\alpha}$$ (K-3)

where B is given by the equation:

$$B = \cos(\alpha) + \frac{b}{h}\sin(\alpha) - 1$$ (K-4)

The value of S_{aO} is used in the calculation of median peak total floor velocity, $\hat{V}_{PT}$. It is also used to determine whether sliding or overturning will be the controlling behavior mode. If the spectral acceleration that will tip the

component to the critical angle, S_{aO}, is greater than the coefficient of static friction, μ_S, then the component will be expected to slide rather than overturn. Conversely, if S_{aO} is less than μ_S, the component will be expected to overturn rather than slide.

The effective rocking frequency, f_r, and damping ratio, β_r, are determined by:

$$f_r = \frac{1}{2\pi}\sqrt{\frac{2gB}{C_3\alpha^2 h}} \tag{K-5}$$

$$\beta_r = \frac{\gamma}{\sqrt{4\pi^2 + \gamma^2}} \tag{K-6}$$

where:

$$C_3 = \frac{4}{3}\left(1+\left(\frac{b}{h}\right)^2\right) \tag{K-7}$$

$$\gamma = -2 * \ln\left(C_R\right) \tag{K-8}$$

$$C_R = 1 - \frac{2\left(\frac{b}{h}\right)^2}{C_3} \tag{K-9}$$

Spectral floor velocity, S_v, as a function of damping, β, is represented by the equation:

$$S_v\left(\beta\right) = V_{PT}D_{amp} \tag{K-10}$$

The spectral amplification factor is derived from Table 2 of Newmark and Hall (1982) assuming that the effective rocking frequency, f_r, falls within the constant velocity domain of the spectrum. This yields:

$$D_{amp} = 2.31 - 0.41 * \ln\left(100\beta_r\right) \tag{K-11}$$

Spectral velocity can be related to pseudo spectral acceleration using the relationship:

$$S_v\left(\beta\right) = \frac{S_a\left(f_r, \beta\right)}{2\pi f_r} \tag{K-12}$$

Substituting S_{aO} for $S_a(f_r, \beta)$ in Equation K-12, and setting Equation K-10 equal to Equation K-12, yields the median peak total floor velocity for overturning:

$$\hat{V}_{PT} = \frac{S_{aO}g}{2\pi f_r D_{amp}} \qquad \text{(K-13)}$$

Due to considerable uncertainty associated with this behavior mode and the assumptions underlying this derivation, a dispersion of 0.5 is recommended for this fragility.

K.3   Sliding

Unanchored components resting on surfaces with a static coefficient of friction, μ_S, that is less than the horizontal spectral acceleration that will tip the component to the critical angle, S_{aO}, are likely to slide rather than overturn. This procedure provides an estimate of the median peak total floor velocity at which the sliding displacement of an unanchored object will equal or exceed a limiting displacement. For sliding behaviors, users must determine a sliding displacement, δ, at which the component is likely to become damaged either by falling off a bearing surface or impacting an adjacent object.

Sliding displacement is a function of the square of peak total floor velocity, V_{PT}, and the dynamic coefficient of friction, μ_D, at the base. The procedure for estimating median V_{PT} is based on the reserve energy approach described in Section 7.1, Section A.1, and Appendix B of ASCE 43-05. It relies on the observation that peak sliding displacements tend to be related to the frequency associated with 10%-damped spectral velocity ordinates that are equal to or greater than twice the dynamic coefficient of friction, μ_D. The procedure additionally assumes the following:

- Spectral characteristics of motion, as characterized by response spectra, at elevated floor levels (i.e., above grade) are similar to shaking at the ground level, and the assumed relationships between critical sliding frequencies, 10% damped spectral velocity ordinates, and V_{PT} remain valid.

- The component aspect ratio and coefficient of friction are such that sliding, rather than overturning, is likely to occur.

- The effects of vertical shaking are neglected.

- For any floor response spectrum, the frequency at which the 10%-damped spectral acceleration equals or exceeds $2\mu_D$ is within the constant velocity domain of the spectrum.

- Damping associated with sliding can be approximated as 10% of critical, and the corresponding spectral velocity amplification factor, D_{amp} for 10%-damped behavior has a value of 1.37.

The sliding frequency f_s in the constant velocity domain of the response spectrum is related to spectral acceleration by the equation:

$$S_a = 2\pi f_s S_v \qquad \text{(K-14)}$$

Substituting $2\mu_D$ for the critical value of spectral acceleration at which sliding occurs, and using the relationship of Equation K-10:

$$2\mu_D = 2\pi f_s S_v = 2\pi f_s \left(1.37 V_{PT}\right) \qquad \text{(K-15)}$$

and:

$$2\pi f_s = \frac{2\mu_D g}{V_{PT}} \qquad \text{(K-16)}$$

From ASCE 43-05, sliding displacement can be approximated by:

$$\delta = \frac{2\mu g}{\left(2\pi f_s\right)^2} \qquad \text{(K-17)}$$

Substituting the expression from Equation K-16 for $2\pi f_s$ yields:

$$\delta = 2\mu_D g \left(\frac{1.37 V_{PT}}{2\mu_D g}\right)^2 \qquad \text{(K-18)}$$

Solving for V_{PT} yields the median peak total floor velocity for sliding:

$$\hat{V}_{PT} = \frac{\sqrt{2\mu_D g \delta}}{1.37} \qquad \text{(K-19)}$$

As with overturning, due to considerable uncertainty associated with this behavior mode and the assumptions underlying this derivation, a dispersion of 0.5 is recommended for this fragility.

Glossary

Definitions

Annual frequence of exceedance. The average number of times per year that an event having magnitude larger than a reference value is likely to occur (typically less than 1).

Annualized loss. The average value of loss, per year, over a period of many years.

Backbone curve. A component force-deformation relationship that envelopes either monotonic or cyclic loading response.

Building performance model. An organized collection of data necessary to define building assets that are at risk and vulnerable to the effects of earthquake shaking.

Capacity boundary. A component force-deformation relationship that represents the maximum strength that a component can develop at a given level of deformation; generally equal to the response of the component to monotonic loading.

Casualties. Loss of life, or serious injury requiring hospitalization.

Collapse floor area ratio. The portion of floor area at each level that is subject to collapse in each collapse mode.

Collapse fragility. A mathematical relationship that defines the probability of incurring structural collapse as a function of ground motion intensity.

Collapse mode(s). One or more ways in which a building would be expected to collapse, ranging from partial to complete collapse. Possible collapse modes include single-story collapse, multi-story collapse, or total collapse.

Component. One of many parts, both structural and nonstructural, that together comprise a building.

Conditional probability. The probability that an outcome will occur, given that a particular event occurs or condition exists.

Consequences. The losses resulting from earthquake damage in terms of potential casualties, repair and replacement costs, repair time, and unsafe placarding.

Consequence function. A relationship that indicates the potential distribution of losses as a function of damage state.

Core and shell replacement cost. The cost to replace the basic building structure, exterior enclosure, and mechanical, electrical, and plumbing infrastructure that is typically present in a building before tenant improvements are made, including costs associated with demolition of the damaged building and clearing the site of debris.

Correlation. A mathematical relationship that defines the extent to which the value of one parameter is dependent on the value of one or more other parameters.

Cyclic envelope. A component force-deformation relationship that envelopes the hysteretic behavior of a component in response to cyclic loading.

Damage state. For a particular component, or the building as a whole, a condition of damage associated with a unique set of consequences.

Decision-maker(s). An individual or group responsible for selecting the performance objectives for a performance-based design.

Demand. A parameter that is predictive of component or building damage states, including peak floor (or ground) acceleration, peak component deformation, peak (or residual) story drift, peak floor (or ground) velocity, or peak component force (or stress).

Discount rate. A factor used to indicate the time-dependent value of money in economic analyses.

Dispersion. A measure of uncertainty associated with prediction of the true value of a random, or otherwise uncertain, behavior.

Distribution. A mathematical function describing the statistical probability that elements in a set will have specific values.

Earthquake scenario. A specific earthquake event, defined by a magnitude and geographic location (distance) relative to a building site.

Floor acceleration. At a floor level, the acceleration of the center of mass relative to a fixed point in space.

Floor velocity. At a floor level, the velocity of the center of mass relative to a fixed point in space.

Fragility function. A mathematical relationship that defines the probability of incurring a damage state conditioned on the value of a single demand parameter.

Fragility group. A set of similar building components having the same potential damage characteristics in terms of fragility and consequence functions.

Fragility specification. A detailed description of potential component damage states, fragility functions, and consequence functions.

Fragility unit of measure. The basic unit used as a basis for defining quantities in a fragility group for the purposes of estimating damage and consequences. Components in a fragility group can be defined in individual units of "each," units of lineal feet (e.g., 1000 LF), units of square feet (e.g., 250 SF), or other units.

Geometric mean (geomean). In characterizing ground motion intensity, the square root of the product of the value of a ground motion parameter in each of two orthogonal directions (i.e., $\sqrt{xy}$).

Intensity. The severity of ground shaking as represented by a 5%-damped, elastic acceleration response spectrum, or the 5% damped spectral response acceleration at a specific natural period of vibration.

Intensity-based assessment. An assessment of the probable performance of a building subjected to a ground motion of a specified intensity.

Lognormal distribution. A distribution of values, characterized by a median value and dispersion, with the property that the natural logarithm of the values is normally distributed.

Mean. The average value of a parameter (or population of values). If the population of values is normally distributed, the mean will be equal to the median. If the distribution is skewed, the mean may be less than or greater than the median.

Mean recurrence interval. The average amount of time between expected repeat occurrences of an event (e.g., an earthquake scenario or loss), typically expressed in years.

Median. The value of an uncertain parameter (or population of values) that will be exceeded 50% of the time.

Mutually exclusive damage states. A series of related damage states in which the occurrence of any one type of damage will preclude the occurrence of another type of damage.

Net present value. For a particular discount rate, the present value of benefits that will be received in the future, less the associated costs of these benefits, considering the time-dependent value of money.

Normal distribution. A symmetric distribution described by a mean value and standard deviation. When plotted as a probability density function, a normal distribution has the shape of a bell curve.

Normative quantity. An estimate of the quantity of nonstructural components and contents likely to be present in a building of a specific occupancy on a gross square foot basis.

Nonstructural component. A building component that is not part of the structural system.

Performance. The probable damage and resulting consequences as a result of earthquake shaking or other hazards.

Performance function. A statistical distribution that indicates the probability that losses of a specified or smaller magnitude will be incurred as a result of future earthquakes.

Performance group. A subset of components described by a single fragility group that will experience the same demand in response to earthquake shaking.

Performance group quantity. The number of fragility units of measure present in a building, in the performance group under consideration.

Performance measure. A means of quantifying the consequences associated with earthquake shaking in terms that are meaningful to decision-makers. Performance measures include casualties, repair and replacement costs, repair time, and unsafe placarding.

Performance objective. An expectation as to the probable damage state and resulting consequences that a building may experience in future earthquakes.

Period. The time, in seconds, necessary for a structure to complete one cycle of motion in free vibration.

Probable Maximum Loss. The probable cost of repairing earthquake damage expressed as percentage of building replacement cost with a particular confidence of non-exceedance, conditioned on a particular earthquake return period.

Realization. One possible performance outcome for a particular earthquake scenario or intensity comprising a unique set of demands, damage states, and consequences.

Repair cost. The cost, in present dollars, necessary to restore a building to its pre-earthquake condition, or in the case of total loss, to replace the building with a new structure of similar construction.

Repair fragility. A mathematical relationship that defines the probability that a building will be considered irreparable as a function of residual drift ratio.

Repair time. The time, in weeks, necessary to repair a damaged building to its pre-earthquake condition.

Replacement cost. The cost, in present dollars, necessary to replace a building that has been damaged beyond the point of practicable repair, including costs associated with demolition and removal of debris.

Replacement time. The time, in weeks, necessary to replace a building that has been damaged beyond the point of practicable repair, including time associated with demolition and removal of debris.

Residual drift. The difference in permanent displacement between the center of mass of two adjacent floors as a result of earthquake shaking.

Residual drift ratio. Residual drift divided by story height.

Return on investment. The annual income that can be derived from an investment divided by the present value of the investment.

Return period. See mean recurrence interval.

Rugged. Not vulnerable to damage, or having a very high threshold for damage; alternatively, not considered significant for assessing seismic performance impacts.

Scenario-based assessment. An assessment of the probable performance of a building subjected to a specified earthquake scenario.

Scenario Expected Loss. A probable maximum loss with mean chance of occurrence.

Scenario Upper Loss. A probable maximum loss with a 10% chance of exceedance.

Seismic hazard curve. A plot of the annual frequency of exceedance of the possible values of a ground shaking intensity parameter.

Sequential damage states. A series of related component damage states that must occur in sequence following the occurrence of an initial damage state.

Simulated demands. A vector set of demands representing the building response in a particular realization, reflecting the correlation between the various response quantities predicted in the structural analyses and uncertainties inherent in structural response prediction.

Simultaneous damage states. A series of independent and unrelated component damage states that can occur, but need not necessarily occur, at the same time.

Stakeholder(s). An individual or group affected by the performance of a building, including building owners, lenders, insurers, tenants, and the general public.

Story drift. The instantaneous difference in lateral displacement between the center of mass of two adjacent floors.

Story drift ratio. Story drift divided by story height.

Structural component. A building component that is part of the intended gravity or seismic-force-resisting system, or that provides measurable resistance to earthquake shaking.

Structural system. A collection of structural components acting together in resisting gravity forces, seismic forces, or both.

Time-based assessment. An assessment of the probable performance of a building, considering all earthquake scenarios and the associated probability of occurrence of each, over a specified period of time.

Total loss threshold. A user-defined cap on the level of repair effort at which a building is likely to be replaced rather than repaired.

Total replacement cost. The cost to replace an entire building (core, shell, and tenant improvements) as it exists in its pre-earthquake condition, including costs associated with demolition of the damaged building and clearing the site of debris.

Unsafe placarding. A post-earthquake inspection rating that deems a building, or portion of a building, damaged to the point that entry, use, or occupancy poses immediate risk to safety. Unsafe placards are typically colored red.

Yield drift. The value of drift at which a structure reaches its effective yield strength.

Yield story drift. The value of story drift at which a story in a structure reaches its effective yield strength.

Yield story drift ratio. Yield story drift divided by story height.

Symbols

Notation

a_i^* in the simplified analysis method, estimated median peak floor acceleration at level "i"

b slope of a straight line fit to a series of data having x and y values

c y intercept of a straight line fit to a series of data having x and y values

d_i value of the demand at which a particular damage state was first observed to occur in specimen "i" in a series of m tests, or the maximum value of demand to which a specimen was subjected without occurrence of the damage state

$\overline{d}_j$ maximum demand experienced by a series of test specimens in bin "j"

d_{max} maximum demand, d, experienced by a specimen in a series of tests

d_{min} for a series of tests of specimens, the minimum value of demand, d, at which any specimen exhibited damage or distress

e_i in time-based assessment the mid-range intensity within an incremental range of intensities, Δe_i

f_r rocking frequency of an unanchored object, (hz)

f_s frequency associated with sliding of an unanchored object, (hz)

h building height (also designated as H)

h_i in the simplified procedure, the height of level "i" above the building base

i interest rate, or expected rate of return on money

k in the simplified procedure, a coefficient used to account for nonlinear mode shape

m_j number of specimens in bin "j" for which damage conforming to a particular damage state is observed

t period of years over which an investment decision is amortized

v_i^* in the simplified analysis method, estimated median peak floor velocity at level "i"

v_{si} reference floor velocity parameter used to determine estimated peak floor velocity in the simplified analysis procedure

w_j in simplified analysis, weight lumped at a structure's level "j"

x_j natural logarithm of $\overline{d}_j$

$\overline{x}$ mean value of a series of values, x_j

y_j inverse lognormal distribution value for the number of specimen tests that experienced a damage state in a bin "j" of specimen tests

$\overline{y}$ mean of the values of y_j

A amount of money that is earned or expended each year over a period of several years

B parameter used to calculate the critical tipping demand on an unanchored object

C_1 in the simplified analysis procedure, a coefficient used to account for the difference in displacement response between elastic and inelastic structures, assuming non-degrading inelastic behavior

C_2 in the simplified analysis procedure, a coefficient used to account for the effects of stiffness degradation on displacement response

C_3 coefficient used to determine the rocking capacity of an unanchored object

C_q coefficient that adjusts computed median strength capacity for construction quality

C_R coefficient used to determine the rocking capacity of an unanchored object

C_{sm} coefficient used to derive an approximate estimate of the fraction of total mass effective in first mode response

C_{vx} in the simplified analysis procedure, the fraction of the total pseudo lateral force, applied to level "x"

D_{amp} spectral velocity amplification factor

F_x in the simplified analysis procedure, the pseudo lateral force applied to level "x"

H total building height above the base; also, the height of a wall panel

M total number of test specimens for which test data is available and for which the damage state of interest occurred

M_A in a series of M tests, the number of specimens that did not experience any damage or distress but which experienced demands greater than or equal to a reference value, d_a

M_B in a series of M tests, the number of specimens that experienced some damage or distress but which did not experience the damage state of interest

M_j number of test specimens in a bin "j" of a series of tests

N total number of vulnerable stories in a building performance model

NPV net present value of a future stream of incomes or expenditures

PGA peak ground acceleration, (g)

PGV peak ground velocity, (in/sec)

PM_{10} value of a performance measure (e.g., repair cost) with a 10% chance of exceedance

PM_{50} median value of a performance measure (e.g., repair time) with a 50% of exceedance

PM_{90} value of a performance measure (e.g., casualties) with a 90% chance of exceedance

$\overline{PM}$ mean value of a performance measure, also known as the expected value or average value

$P(C)$ conditional probability of building collapse, given an intensity of shaking

$P(U_i)$ probability, for a given intensity or scenario, that damage sustained by components in performance group "i" will result in an unsafe placard

$P(U_T)$ total conditional probability, given a specific intensity of motion or earthquake scenario, that a building will receive an unsafe placard

P_{EY} probability of exceedance of an event in Y years

P_R mean return period for an event

R number of realizations in a performance assessment

R_n nominal resistance in accordance with load and resistance factor design (LRFD) specifications

S in the simplified analytical procedure, the ratio of elastic base shear force to the structure's yield shear strength

$S_a(T)$ spectral response acceleration at period T, (g)

$\hat{S}_a(T)$ median collapse capacity of a structure, measured in terms of spectral response acceleration at period T, (g)

$S_a{}^{max}$ for time-based assessment, the maximum spectral response acceleration at which performance is assessed, (g)

$S_a{}^{min}$ for time-based assessment, the minimum spectral response acceleration at which performance is assessed, (g)

S_{aD} effective value of design spectral acceleration at which a structure satisfies all applicable seismic design criteria of ASCE/SEI 7-10, (g)

S_{aO} spectral acceleration that will tip an unanchored object to a critical angle at which overturning instability will occur, (g)

$S_{gm}(T)$ geometric mean (geomean) spectral response acceleration at period T, (g)

$S_v(1)$ spectral velocity at a period of 1 second

T period of structural response, i.e., the amount of time that a structure in free vibration will take to complete one cycle of motion, (sec)

T_1 period of fundamental mode of vibration

T_1^X period of fundamental mode of translation along the horizontal X axis

T_1^Y period of fundamental mode of translation along the horizontal Y axis

$\overline{T}$ average of the periods of the fundamental mode of translation along each of two orthogonal building axes

T_{max} maximum period in a range of periods used to scale ground motions for nonlinear response history analysis

T_{min} minimum period in a range of periods used to scale ground motions for nonlinear response history analysis

V in the simplified analysis procedure, a pseudo lateral force used to estimate story drifts

V_s average shear wave velocity of soil soil in the upper 100 feet (30 meters)

V_{PT} peak total floor velocity at a floor level, in/sec

V_{yt} effective yield strength of a structure responding in the first mode

W_1 in simplified analysis, the first mode weight effective of a structure

Y number of years considered in a time-based assessment

α for an unanchored object, the critical tip angle at which the object will become unstable and overturn, radians

β measure of dispersion in the true value of a random parameter, also called uncertainty

β_a uncertainty associated with analysis record-to-record response variability

β_{aa} in the simplified analysis procedure, default record-to-record variability (dispersion) associated with floor acceleration response

β_{av} in the simplified analysis procedure, default record-to-record variability (dispersion) associated with floor velocity response

$\beta_{a\Delta}$ in the simplified analysis procedure, default record-to-record variability (dispersion) associated with story drift response

β_c modeling uncertainty associated with ambiguity in details of construction; also, the uncertainty associated with estimates of repair cost

β_C in calculation-based fragilities, uncertainty associated with the quality of installation (or construction) of a component

β_D uncertainty associated with the ability of a design equation to predict actual behavior when material strength is defined

β_{FA} in the simplified analysis procedure, the total dispersion associated with floor acceleration

β_{FV} in the simplified analysis procedure, the total dispersion associated with floor velocity

β_{gm} dispersion accounting for uncertainty in ground motion intensity as reflected in attenuation relationships

β_m modeling uncertainty associated with dispersion in the predicted response from structural analysis

β_M uncertainty in material strength

β_q modeling uncertainty associated with the quality and completeness of the nonlinear analysis model, considering component hysteretic modeling, estimates of damping, and the number of elements included in the model

β_r in a series of data used to establish fragility functions, the random variability evident in the data; also, the damping ratio for a rocking object (fraction of critical damping)

β_{SD} in the simplified analysis procedure, the total dispersion associated with story drift

β_u in a series of data used to establish fragility functions, a measure of uncertainty representing differences between the conditions inherent in the data set and actual conditions present in a real building

δ sliding displacement that will cause an unanchored component to hit another object, resulting in damage

δ_i peak displacement of floor "i" relative to the base

δ_r peak displacement of the roof relative to the base

δ_y component deformation at yield

γ factor used to determine effective damping for a rocking component

Δ_i in the simplified procedure, the uncorrected story drift ratio at level "i"

$\Delta_i{}^*$ estimated median peak story drift ratio at story "i"

Δ_r estimated median residual story drift ratio

Δe_i in time-based assessments, an incremental range of earthquake intensities

$\Delta \lambda_i$ in time-based assessments, the probability of occurrence in a period of time, for earthquake intensity in range Δe_i

Δ_y estimated story drift at development of yield strength

θ in lognormal distributions, the median value of demand

θ_{DS} in lognormal distributions, the median value of demand

λ mean annual frequency of exceedance of a ground motion parameter

μ ratio of component deformation at onset of damage, to component deformation at yield

μ_D kinetic coefficient of friction between an unanchored object and its resting surface

μ_S static coefficient of friction between an unanchored object and its resting surface

ϕ resistance factor, as specified in load and resistance factor design (LRFD) specifications

ϕ_{j1} in simplified analysis, the ordinate of the first mode deflection at floor level "j"

References

Abrahamson, N.A., 2000, "State of the practice of seismic hazard evaluation," *Proceedings*, GeoEng2000, Melbourne, Australia.

Abrahamson, N.A., and Al Atik, L., 2010, "Scenario spectra for design ground motions and risk calculation," *Proceedings*, 9th U.S. National and 10th Canadian Conference on Earthquake Engineering, Toronto, Canada.

Abrahamson, N.A., and Shedlock, K., 1997, "Overview," *Seismological Research Letters*, Vol. 68, No. 1, pp. 9-23.

Abrahamson, N.A., and Silva, W.J., 1997, "Empirical response spectral attenuation relations for shallow crustal earthquakes," *Seismological Research Letters*, Vol. 68, pp. 94-127.

Abrahamson, N.A., and Silva, W.J., 2008, "Summary of the Abrahamson & Silva NGA ground-motion relations," *Earthquake Spectra*, Vol. 24, No. 1, pp. 67-97.

ACI, 2014, *Building Code Requirements for Structural Concrete and Commentary*, ACI 318-14, American Concrete Institute, Farmington Hills, Michigan.

AISC, 2016a, *Seismic Provisions for Structural Steel Buildings*, ANSI/AISC 341-16, American Institute of Steel Construction, Chicago, Illinois.

AISC, 2016b, *Specification for Structural Steel Buildings*, ANSI/AISC 360-16, American Institute of Steel Construction, Chicago, Illinois.

ASCE, 2003, *Seismic Evaluation of Existing Buildings*, ASCE/SEI 31-03, American Society of Civil Engineers, Reston, Virginia.

ASCE, 2005, *Seismic Design Criteria for Structures, Systems, and Components in Nuclear Facilities,* ASCE/SEI 43-05, American Society of Civil Engineers, Reston, Virginia.

ASCE, 2007, *Seismic Rehabilitation of Existing Buildings*, ASCE/SEI 41-06, American Society of Civil Engineers, Reston, Virginia.

ASCE, 2010, *Minimum Design Loads for Buildings and Other Structures*, ASCE/SEI 7-10, American Society of Civil Engineers, Reston, Virginia.

ASCE, 2014, *Seismic Rehabilitation of Existing Buildings*, ASCE/SEI 41-13, American Society of Civil Engineers, Reston, Virginia.

ASCE, 2017, *Minimum Design Loads and Associated Criteria for Buildings and Other Structures*, ASCE/SEI 7-16, American Society of Civil Engineers, Reston, Virginia.

ASTM, 2007a, *Standard Guide for Seismic Risk Assessment of Buildings*, ASTM E2026-07, ASTM International, West Conshohocken, Pennsylvania.

ASTM, 2007b, *Standard Practice for Probable Maximum Loss (PML) Evaluations for Earthquake Due-Diligence Assessments*, ASTM E2557-07, ASTM International, West Conshohocken, Pennsylvania.

ASTM, 2011, *Standard Specification for Structural Steel Shapes*, ASTM A992-11, ASTM International, West Conshohocken, Pennsylvania.

ASTM, 2012, *Standard Specification for Carbon Structural Steel*, ASTM A36-12, ASTM International, West Conshohocken, Pennsylvania.

ASTM, 2013, *Standard Specification for Ready-Mixed Concrete*, ASTM C94-13, ASTM International, West Conshohocken, Pennsylvania.

ATC, 1992, *Guidelines for Cyclic Seismic Testing of Components of Steel Structures,* ATC-24 Report, Applied Technology Council, Redwood City, California.

ATC, 1996, *Seismic Evaluation and Retrofit of Concrete Buildings,* ATC-40 Report, Applied Technology Council, Redwood City, California.

ATC, 2002, *Proceedings of FEMA-Sponsored Workshop on Communicating Earthquake Risk*, ATC-58-1 Report, Applied Technology Council, Redwood City, California.

ATC, 2010, *Modeling and Acceptance Criteria for Seismic Design and Analysis of Tall Buildings*, PEER/ATC-72-1 Report, prepared by Applied Technology Council for Pacific Earthquake Engineering Research Center, Redwood City, California.

Atkinson, G., and Boore, D.M., 1997, "Some comparisons of recent ground motion relations," *Seismological Research Letters*, Vol. 68, pp. 24-40.

Atkinson, G., and Boore, D.M., 2003, "Empirical ground-motion relations for subduction zone earthquakes and their application to Cascadia and other regions," *Bulletin of the Seismological Society of America*, Vol. 93, pp. 1703-1729.

Baker, J., and Cornell, C.A., 2005, "A vector-valued ground motion intensity measure consisting of spectral acceleration and epsilon," *Earthquake Engineering and Structural Dynamics*, Vol. 34, No. 10, pp. 1193-1217.

Baker, J., and Cornell, C.A., 2006, "Spectral shape, epsilon and record selection," *Earthquake Engineering and Structural Dynamics*, Vol. 35, No. 9, pp. 1077-1095.

Baker, J., and Jayaram, N., 2008, "Correlation of spectral acceleration values from NGA ground motion models," *Earthquake Spectra*, Vol. 24, No. 1, pp. 299-318.

Benjamin, J., and Cornell, C.A., 1970, *Probability, Statistics, and Decision for Civil Engineers*, McGraw-Hill, New York, New York.

Boore, D.M., and Atkinson, G., 2008, "Ground-motion prediction equations for the average horizontal component of PGA, PGV, and 5%-damped SA at spectral periods between 0.01 s and 10.0 s," *Earthquake Spectra*, Vol. 24, pp. 99-138.

Bozorgnia, Y., and Bertero, V.V., 2004, *Earthquake Engineering: From Engineering Seismology to Performance-Based Earthquake Engineering*, CRC Press.

Campbell, K., 2003, "Prediction of strong-ground motion using the hybrid-empirical method and its use in the development of ground-motion (attenuation) relations in eastern North America," *Bulletin of the Seismological Society of America*, Vol., 93, pp. 1012-1033.

Campbell, K.W., and Bozorgnia, Y., 2008, "NGA ground motion model for the geometric mean horizontal component of PGA, PGV, PGD and 5% damped linear elastic response spectra for periods ranging from 0.01 to 10s," *Earthquake Spectra*, Vol. 24, No. 1, pp. 139-171.

Carnegie Mellon University Green Design Institute, 2008, *Economic Input-Output Life Cycle Assessment (EIO-LCA)*, Pittsburg, Pennsylvania. Available at: http://eiolca.net, last accesssed March 18, 2018.

Chiou, B.S.J., and Youngs, R.R., 2008, "Chiou-Youngs NGA ground motion relations for the geometric mean horizontal component of peak and spectral ground motion parameters," *Earthquake Spectra*, Vol. 24, pp. 173-215.

Christopoulos, C., Pampanin, S., and Priestley, M.J.N., 2003, "Performance-based seismic response of frame structures including residual deformations, Part I: single degree of freedom systems," *Journal of Earthquake Engineering*, Vol. 7, No. 1, pp. 97-118.

Christopoulos, C., and Pampanin, S., 2004, "Towards performance-based design of MDOF structures with explicit consideration of residual deformations," Invited Paper, *Indian Society for Earthquake Technologies (ISET) Journal of Earthquake Technology*, Special Issue on Performance-Based Design, Vol. 41, pp. 172-193.

Cornell, C.A., and Winterstein, S.R., 1988, "Temporal and magnitude dependence in earthquake recurrence models," *Bulletin of the Seismological Society of America*, Vol. 78, No. 4, pp. 1522-1537.

FEMA, 1997, *NEHRP Guidelines for the Seismic Rehabilitation of Buildings*, FEMA 273, prepared by the Applied Technology Council and the Building Seismic Safety Council, for the Federal Emergency Management Agency, Washington, D.C.

FEMA, 2000a, *Action Plan for Performance Based Seismic Design*, FEMA 349, prepared by the Earthquake Engineering Research Institute for the Federal Emergency Management Agency, Washington D.C.

FEMA, 2000b, *Prestandard and Commentary for the Seismic Rehabilitation of Buildings*, FEMA 356, prepared by the American Society of Civil Engineers for the Federal Emergency Management Agency, Washington D.C.

FEMA, 2005, *Improvement of Nonlinear Static Seismic Analysis Procedures*, FEMA 440, prepared by the Applied Technology Council for the Federal Emergency Management Agency, Washington, D.C.

FEMA, 2007, *Interim Testing Protocols for Determining the Seismic Performance Characteristics of Structural and Nonstructural Components*, FEMA 461, prepared by the Applied Technology Council for the Federal Emergency Management Agency, Washington, D.C.

FEMA, 2009a, *NEHRP Recommended Seismic Provisions for New Buildings and Other Structures,* FEMA P-750, prepared by the Building Seismic Safety Council for the Federal Emergency Management Agency, Washington, D.C.

FEMA, 2009b, *Quantification of Building Seismic Performance Factors*, FEMA P-695, prepared by Applied Technology Council for Federal Emergency Management Agency, Washington, D.C.

FEMA, 2009c, *Effects of Strength and Stiffness Degradation on Seismic Response*, FEMA P-440A, prepared by the Applied Technology Council for the Federal Emergency Management Agency, Washington, D.C.

FEMA, 2016, *Seismic Performance Assessment of Buildings, Volume 3 – Supporting Electronic Materials and Background Documentation, Second Edition*, FEMA P-58-3, prepared by the Applied Technology Council for the Federal Emergency Management Agency, Washington, D.C.

FEMA, 2018a, *Seismic Performance Assessment of Buildings, Volume 2 – Implementation Guide, Second Edition*, FEMA P-58-2, prepared by the Applied Technology Council for the Federal Emergency Management Agency, Washington, D.C.

FEMA, 2018b, *Seismic Performance Assessment of Buildings, Volume 3 – Supporting Electronic Materials and Background Documentation, Third Edition*, FEMA P-58-3, prepared by the Applied Technology Council for the Federal Emergency Management Agency, Washington, D.C.

FEMA, 2018c, *Seismic Performance Assessment of Buildings, Volume 4 – Methodology for Assessing Environmental Impacts,* FEMA P-58-4, prepared by the Applied Technology Council for the Federal Emergency Management Agency, Washington, D.C.

FEMA, 2018d, *Seismic Performance Assessment of Buildings, Volume 5 – Expected Seismic Performance of Code Conforming Buildings*, FEMA P-58-5, prepared by the Applied Technology Council for the Federal Emergency Management Agency, Washington, D.C.

FEMA, 2018e, *Guidelines for Performance-Based Seismic Design of Buildings*, FEMA P-58-6, prepared by the Applied Technology Council for the Federal Emergency Management Agency, Washington, D.C.

FEMA, 2018f, *Building the Performance You Need, A Guide to State-of-the-Art Tools for Seismic Design and Assessment*, FEMA P-58-7, prepared by the Applied Technology Council for the Federal Emergency Management Agency, Washington, D.C.

FEMA, 2018g, *Methodology for Environmental Impact Assessment*, FEMA P-58/BD-3.7.20, Technical Background Documentation, prepared by the Applied Technology Council for the Federal Emergency Management Agency, Washington, D.C.

FEMA, 2018h, *Updates to Fragilities*, FEMA P-58/BD-3.7.19, Technical Background Documentation, prepared by the Applied Technology Council for the Federal Emergency Management Agency, Washington, D.C.

Gülerce, Z., and Abrahamson, N.A., 2011, "Site-specific design spectra for vertical ground motion," *Earthquake Spectra*, Vol. 27, No. 4, pp. 1023-1047.

Gutenberg, R., and Richter, C.F., 1944, "Frequency of earthquakes in California," *Bulletin of the Seismological Society of America*, Vol. 34, pp. 185-188.

Harmsen, S.C., 2001, "Mean and modal ε in the deaggregation of probabilistic ground motion," *Bulletin of the Seismologic Society of America*, Vol. 91, No. 6, pp. 1537-1552.

Housner, G.W., 1963, "The behavior of inverted pendulum structures during earthquakes," *Bulletin of the Seismological Society of America*, Vol. 53, No. 2, pp. 403-417.

Huang, Y.-N., and Whittaker, A.S., 2012, "Calculation of peak ground velocity from 1-second spectral velocity," FEMA P-58/BD-3.7.5 Report, Applied Technology Council, Redwood City, California.

Huang, Y.-N., Whittaker, A.S., and Luco, N., 2008a, "Maximum spectral demands in the near-fault region," *Earthquake Spectra*, Vol. 24, No. 1, pp. 319-341.

Huang, Y.-N., Whittaker, A.S., and Luco, N., 2008b, *Performance assessment of conventional and base-isolated nuclear power plants for earthquake and blast loadings*, Technical Report MCEER-08-0019, Multidisciplinary Center for Earthquake Engineering Research, University at Buffalo, Buffalo, New York.

Huang, Y.-N., Whittaker, A.S., Luco, N., and Hamburger, R.O., 2011, "Selection and scaling of earthquake ground motions in support of performance-based design," *Journal of Structural Engineering*, Vol. 137, No. 3, pp. 311-321.

Ibarra, L.F., and Krawinkler, H.K., 2005, *Global Collapse of Frame Structures under Seismic Excitations,* PEER 2005/06 Report, Pacific Earthquake Engineering Research Center, Berkeley, California.

Idriss, I.M., 2008, "An NGA empirical model for estimating the horizontal spectral values generated by shallow crustal earthquakes," *Earthquake Spectra*, Vol. 24, No. 1, pp. 217-242.

Jayaram, N., Lin, T., and Baker, J.W., 2011, "A computationally efficient ground-motion selection algorithm for matching a target response spectrum mean and variance," *Earthquake Spectra*, Vol. 27, No. 3, pp. 797-815.

Kramer, S.L., 1996, *Geotechnical Earthquake Engineering*, Prentice Hall, Upper Saddle River, New Jersey.

Liel, A., Haselton, C., Deierlein, G., and Baker, J., 2009, "Incorporating modeling uncertainties in the assessment of seismic collapse risk of buildings," *Structural Safety*, Vol. 31, No. 2, pp. 197-211.

Lilliefors, H., 1967, "On the Kolmogorov-Smirnov test for normality with mean and variance unknown," *Journal of the American Statistical Association*, Vol. 62, No. 318, pp. 399-402.

MacRae, G.A., 1994, "P-delta effects on single-degree-of-freedom structures in earthquakes," *Earthquake Spectra*, Vol. 10, No. 3, pp. 539-568.

MacRae, G.A., and Kawashima, K., 1997, "Post-earthquake residual displacements of bilinear oscillators," *Earthquake Engineering & Structural Dynamics*, Vol. 26, No. 7, pp. 701-716.

Mahin, S.A., and Bertero, V.V., 1981, "An evaluation of inelastic seismic design spectra," *Journal of the Structural Division*, ASCE, Vol. 107, No. 9, pp. 1777-1795.

McGuire, R., 2004, *Seismic Hazard and Risk Analysis,* EERI Monograph, Earthquake Engineering Research Institute, Oakland, California.

Moehle, J., and Deierlein, G., 2004, "A Framework Methodology for Performance-Based Earthquake Engineering," *Proceedings*, 13th World Conference on Earthquake Engineering, Vancouver, British Columbia, Paper No. 679.

Newmark, N.M., and Hall, W.J., 1982, *Earthquake Spectra and Design*, Earthquake Engineering Research Institute, Oakland, California.

NIST, 1999, *UNIFORMAT II Elemental Classification for Building Specifications, Cost Estimating and Cost Analysis*, NISTIR 6389 Report, National Institute of Standards and Technology, Gaithersburg, Maryland.

NIST, 2010a, *Nonlinear Structural Analysis for Seismic Design: A Guide for Practicing Engineers*, GCR 10-917-5, prepared by the NEHRP Consultants Joint Venture, a partnership of the Applied Technology Council and the Consortium of Universities for Research in Earthquake Engineering, for the National Institute of Standards and Technology, Gaithersburg, Maryland.

NIST, 2010b, *Evaluation of the FEMA P-695 Methodology for Quantification of Building Seismic Performance Factors*, GCR 10-917-8, prepared by the NEHRP Consultants Joint Venture, a partnership of the Applied Technology Council and the Consortium of Universities for Research in Earthquake Engineering, for the National Institute of Standards and Technology, Gaithersburg, Maryland.

NIST, 2011, *Selecting and Scaling Earthquake Ground Motions for Performing Response-History Analyses*, GCR 11-917-15, prepared by the NEHRP Consultants Joint Venture, a partnership of the Applied Technology Council and the Consortium of Universities for Research in Earthquake Engineering, for National Institute of Standards and Technology, Gaithersburg, Maryland.

NIST, 2012, *Soil-Structure Interaction for Building Structures*, GCR 12-917-21, prepared by the NEHRP Consultants Joint Venture, a partnership of the Applied Technology Council and the Consortium of Universities for Research in Earthquake Engineering, for the National Institute of Standards and Technology, Gaithersburg, Maryland.

NIST, 2017a, *Recommended Modeling Parameters and Acceptance Criteria for Nonlinear Analysis in Support of Seismic Evaluation, Retrofit, and Design*, GCR 17-917-45, prepared by the Applied Technology Council for National Institute of Standards and Technology, Gaithersburg, Maryland.

NIST, 2017b, *Guidelines for Nonlinear Structural Analysis for Design of Buildings, Part I – General*, GCR 17-917-46v1, prepared by the Applied Technology Council for National Institute of Standards and Technology, Gaithersburg, Maryland.

NIST, 2017c, *Guidelines for Nonlinear Structural Analysis for Design of Buildings, Part IIa – Steel Moment Frames*, GCR 17-917-46v2, prepared by the Applied Technology Council for National Institute of Standards and Technology, Gaithersburg, Maryland.

NIST, 2017d, *Guidelines for Nonlinear Structural Analysis for Design of Buildings, Part IIb – Reinforced Concrete Moment Frames*, GCR 17-917-46v3, prepared by the Applied Technology Council for National Institute of Standards and Technology, Gaithersburg, Maryland.

Pampanin, S., Christopoulos, C., and Priestley, M.J.N., 2003, "Performance-based seismic response of frame structures including residual deformations, Part II: multidegree of freedom systems," *Journal of Earthquake Engineering*, Vol. 7, No. 1, pp. 119-147.

PEER, 2017, *Guidelines for Performance-Based Design of Tall Buildings*, PEER Report 2017/06 version 2.03, prepared by Tall Buildings Initiative Working Group, Pacific Earthquake Engineering Research Center, Berkeley, California.

Riddell, R., and Newmark, N.M., 1979, *Statistical Analysis of the Response of Nonlinear Systems Subjected to Earthquakes*, Structural Research Series No. 468 Technical report, Illinois University, Urbana-Champaign, Illinois.

Ross, S.M., 2003, "Peirce's criterion for the elimination of suspect experimental data," *Journal of Engineering Technology*, Vol. 20, No 2, pp. 38-41.

Ruiz-Garcia, J., and Miranda, E., 2005, *Performance-based assessment of existing structures accounting for residual displacements*, Technical Report No. 153, The John A. Blume Earthquake Engineering Center, Stanford University, Stanford, California.

Ruiz-Garcia, J., and Miranda, E., 2006, "Direct estimation of residual displacement from displacement spectral ordinates," *Proceedings of 8th U.S. National Conference on Earthquake Engineering*, Paper No. 1101, 10 pp.

Somerville, P.G., Smith, N.F., Graves, R.W., and Abrahamson, N.A., 1997, "Modification of empirical strong ground motion attenuation relations to include the amplitude and duration effects of rupture directivity," *Seismological Research Letters*, Vol. 68, No. 1, pp. 199-222.

TMS, 2016, *Building Code Requirements and Specification for Masonry Structures*, TMS 402, The Masonry Society, Longmont, Colorado.

Toro, G., Abrahamson, N.A., and Schneider, J., 1997, "Model of strong ground motion in eastern and central North America: Best estimates and uncertainties," *Seismological Research Letters*, Vol. 68, pp. 41-57.

Vamvatsikos, D., and Cornell, C.A., 2006, "Direct estimation of the seismic demand and capacity of oscillators with multi-linear static pushovers through IDA," *Earthquake Engineering and Structural Dynamics*, Vol. 35, Issue 9, pp. 1097-1117.

Yang, T.Y., Moehle, J., Stojadinovic, B., Der Kiureghian, A., 2006, "An application of PEER performance-based earthquake engineering methodology," *Proceedings*, 8th U.S. National Conference on Earthquake Engineering, San Francisco, California, Paper No. 1448.

Yang, T.Y., Moehle, J., Stojadinovic, B., and Der Kiureghian, A., 2009, "Seismic performance evaluation of facilities: methodology and implementation," *Journal of Structural Engineering*, Vol. 135, No. 10, pp. 1146-1154.

Youngs, R.R., Chiou, B.S.J., Silva, W.J., and Humphrey, J., 1997, "Strong ground motion attenuation relationships for subduction zone earthquakes," *Seismological Research Letters*, Vol. 68, No. 1, pp. 58-73.

Project Participants

SECOND EDITION PROJECT TEAM

Federal Emergency Management Agency

Mike Mahoney (Project Officer)
Federal Emergency Management Agency
400 C Street, SW
Washington, D.C. 20472

Robert D. Hanson (Technical Monitor)
Federal Emergency Management Agency
5885 Dunabbey Loop
Dublin, Ohio 43017

Applied Technology Council

Christopher Rojahn
Applied Technology Council
201 Redwood Shores Parkway, Suite 240
Redwood City, California 94065

Ayse Hortacsu (Project Manager)
Applied Technology Council
201 Redwood Shores Parkway, Suite 240
Redwood City, California 94065

Jon A. Heintz (Project Executive)
Applied Technology Council
201 Redwood Shores Parkway, Suite 240
Redwood City, California 94065

Project Management Committee

Ronald O. Hamburger (Project Technical Director)
Simpson Gumpertz & Heger, Inc.
100 Pine Street, Suite 1600
San Francisco, California 94111

John Gillengerten
1055 Rivermeade Dr.
Hebron, Kentucky 41048

William T. Holmes
Rutherford + Chekene
375 Beale Street, Suite 310
San Francisco, California 94105

John D. Hooper
Magnusson Klemencic Associates
1301 Fifth Avenue, Suite 3200
Seattle, Washington 98101

Stephen A. Mahin (deceased)
University of California, Berkeley
777 Davis Hall
Berkeley, California 94720

Jack P. Moehle
University of California, Berkeley
3444 Echo Springs Road
Lafayette, California 94549

Khalid Mosalam
University of California, Berkeley
Structural Engineering, Mechanics, and Materials
Civil and Environmental Engineering
723 Davis Hall
Berkeley, California 94720

Laura Samant
2547 Diamond Street
San Francisco, California 94131

Steven R. Winkel
The Preview Group, Inc.
2765 Prince Street
Berkeley, California 94705

Project Steering Committee

William T. Holmes
Rutherford + Chekene
375 Beale Street, Suite 310
San Francisco, California 94105

Lucy Arendt
St. Norbert College
100 Grant Street, Cofrin Hall, 310
De Pere, Wisconsin 54115

Deborah Beck
Beck Creative Strategies LLC
531 Main Street, Suite 313
New York, New York 10044

Christopher Deneff
FM Global Engineering Standards
270 Central Avenue
Johnston, Rhode Island 02919

H. John Price
9839 Caminito Rogelio
San Diego, California 92131

Jonathan C. Siu
City of Seattle, Dept. of Planning and
  Development
P.O. Box 34019
Seattle, Washington 98124

Jeffrey R. Soulages
Intel Corporation
2501 NW 229th Street MS: RA1-220
Hillsboro, Oregon 97124

Eric Von Berg
Newmark Realty Capital, Inc.
595 Market Street, Suite 2550
San Francisco, California 94105

Williston Warren (ATC Board Contact)
SESOL Inc.
1918 Santiago Drive, Suite A
Newport Beach, California 92660

Stakeholder Products Team

Laura Samant (Team Leader)
2547 Diamond Street
San Francisco, California 94131

David Mar
Mar Structural Design
2629 Seventh Street, Suite C
Berkeley, California 94710

Lori Peek
University of Colorado
Natural Hazards Center
Institute of Behavioral Sciences Building
1440 15th Street
Boulder, Colorado 80302

Maryann T. Phipps
Estructure
1144 65th Street
Oakland, California 94608

Sharyl Rabinovici
1720 Le Roy Ave.
Berkeley, California 94709

L. Thomas Tobin
Tobin & Associates
444 Miller Ave.
Mill Valley, California 94941

Performance Products Team

John Gillengerten (Team Leader)
1055 Rivermeade Dr.
Hebron, Kentucky 41048

David R. Bonneville
Degenkolb Engineers
375 Beale St., Suite 500
San Francisco, California 94105

Dominic Campi
Rutherford + Chekene
375 Beale Street, Suite 310
San Francisco, California 94105

Vesna Terzic
California State University, Long Beach
Department of Civil Engineering & Construction
  Engineering Management
Long Beach, California 90815

Products Update Team

John D. Hooper (Team Leader)
Magnusson Klemencic Associates
1301 Fifth Avenue, Suite 3200
Seattle, Washington 98101

Peter Morris
AECOM
2020 L Street
Sacramento, California 95811

Russell Larsen
Magnusson Klemencic Associates
1301 Fifth Avenue, Suite 3200
Seattle, Washington 98101

Stakeholder Products Consultants

Sandra L. Grabowski
Adler Enterprises LLC
4600 Miller Street
Wheat Ridge, Colorado 80033

Stacia Sydoriak
2049 Bronson St
Fort Collins, Colorado 80526

Jennifer Tobin-Gurley
University of Colorado
Natural Hazards Center
Institute of Behavioral Sciences Building
1440 15th Street
Boulder, Colorado 80302

Taline Mitten
Mar Structural Design
2629 Seventh Street Suite C
Berkeley, California 94710

Performance Products Consultants

Shreyash Chokshi
California State University, Long Beach
1250 Bellflower Blvd, VEC-129
Long Beach, California 90840

Abe Lynn
Degenkolb Engineers
375 Beale St., Suite 500
San Francisco, California 94105

Travis Chrupalo
Degenkolb Engineers
375 Beale St., Suite 500
San Francisco, California 94105

Daniel Saldana
California State University, Long Beach
1250 Bellflower Blvd, VEC-129
Long Beach, California 90840

Erica Hays
Degenkolb Engineers
375 Beale St., Suite 500
San Francisco, California 94105

Vinit M. Shah
California State University, Long Beach
1250 Bellflower Blvd, VEC-129
Long Beach, California 90840

Nirmal Kumawat
California State University, Long Beach
1250 Bellflower Blvd, VEC-129
Long Beach, California 90840

Udit S. Tambe
California State University, Long Beach
1250 Bellflower Blvd, VEC-129
Long Beach, California 90840

Duy Vu To
15662 Jefferson Street
Midway City, California 92655

Peny Villanueva
California State University, Long Beach
1250 Bellflower Blvd, VEC-129
Long Beach, California 90840

Products Update Consultants

Robert Bachman
R.E. Bachman Consulting Structural Engineers
25152 La Estrada Dr.
Laguna Niguel, California 92677

Jack Baker
Haselton Baker Risk Group, LLC
728 Cherry Street, Suite C
Chico, California 95928

Dustin Cook
Haselton Baker Risk Group, LLC
728 Cherry Street, Suite C
Chico, California 95928

Scott Hagie
John A. Martin and Associates, Inc.
950 S. Grand Ave. 4th Floor
Los Angeles, California 90015

Angie Harris
19413 Broadacres Ave.
Carson, California 90746

Curt Haselton
Haselton Baker Risk Group, LLC
728 Cherry Street, Suite C
Chico, California 95928

Wyatt Henderson
Magnusson Klemencic Associates
1301 Fifth Avenue, Suite 3200
Seattle, Washington 98101

Monica Huang
Carbon Leadership Forum
Center for Integrated Design
1501 East Madison St. Suite 200
Seattle, Washington 98122

Gilberto Mosqueda
University of California, San Diego
Department of Structural Engineering
9500 Gilman Drive, Suite 8085
La Jolla, California 92093

Farzad Naeim
Farzad Naeim, Inc.
100 Spectrum Center Drive, Suite 900
Irvine, California 92618

Barbara Rodriguez
Carbon Leadership Forum
Center for Integrated Design
1501 East Madison St. Suite 200
Seattle, Washington 98122

Kathrina Simonen
Carbon Leadership Forum
Center for Integrated Design
1501 East Madison St. Suite 200
Seattle, Washington 98122

Siavash Soroushian
K.N. Toosi University of Technology
Department of Civil & Environmental Engineering
Tehran, Iran

Katherine Wade
Haselton Baker Risk Group, LLC
728 Cherry Street, Suite C
Chico, California 95928

Farzin Zareian
University of California, Irvine
Department of Civil and Environmental
   Engineering
Irvine, California 92697

FIRST EDITION PROJECT TEAM

Federal Emergency Management Agency

Mike Mahoney (Project Officer)
Federal Emergency Management Agency
400 C Street, SW
Washington, D.C. 20472

Robert D. Hanson (Technical Monitor)
Federal Emergency Management Agency
5885 Dunabbey Loop
Dublin, Ohio 43017

Applied Technology Council

Christopher Rojahn (Project Executive Director)
Applied Technology Council
201 Redwood Shores Parkway, Suite 240
Redwood City, California 94065

Ayse Hortacsu
Applied Technology Council
201 Redwood Shores Parkway, Suite 240
Redwood City, California 94065

Jon A. Heintz (Project Manager)
Applied Technology Council
201 Redwood Shores Parkway, Suite 240
Redwood City, California 94065

Project Management Committee

Ronald O. Hamburger (Project Technical Director)
Simpson Gumpertz & Heger
100 Pine Street, Suite 1600
San Francisco, California 94111

Peter J. May
University of Washington
3630 Evergreen Point Road
Medina, Washington 98039

John Gillengerten
1055 Rivermeade Dr.
Hebron, Kentucky 41048

Jack P. Moehle
University of California, Berkeley
3444 Echo Springs Road
Lafayette, California 94549

William T. Holmes (ex-officio)
Rutherford + Chekene
375 Beale Street, Suite 310
San Francisco, California 94105

Maryann T. Phipps (ATC Board Contact)
Estructure
1144 65th Street
Oakland, California 94608

Steering Committee

William T. Holmes (Chair)
Rutherford + Chekene
375 Beale Street, Suite 310
San Francisco, California 94105

Anne Bostrom
University of Washington
Parrington Hall, Room 327
Seattle, Washington 98195

Roger D. Borcherdt
U.S. Geological Survey
345 Middlefield Road, MS977
Menlo Park, California 94025

Bruce Burr
Burr & Cole Consulting Engineers
3485 Poplar Avenue, Suite 200
Memphis, Tennessee 38111

Kelly Cobeen
Wiss, Janney, Elstner Associates, Inc.
2200 Powell Street, Suite 925
Emeryville, California 94608

Anthony B. Court
A.B. Court & Associates
4340 Hawk Street
San Diego, California 92103

Terry Dooley
Morley Builders
2901 28th Street, Suite 100
Santa Monica, California 90405

Dan Gramer
Turner Construction Company
830 4th Avenue South, Suite 400
Seattle, Washington 98134

Michael Griffin
CCS Group, Inc.
1415 Elbridge Payne Road, Suite 265
Chesterfield, Missouri 63017

R. Jay Love
Degenkolb Engineers
1300 Clay Street
Oakland, California 94612

David Mar
Mar Structural Design
2629 Seventh Street, Suite C
Berkeley, California 94710

Steven McCabe
National Institute of Standards and Technology
100 Bureau Drive, MS 8630
Gaithersburg, Maryland 20899

Brian J. Meacham
Worcester Polytechnic Institute
Dept. of Fire Protection Engineering
100 Institute Road
Worcester, Massachusetts 01609

William J. Petak
University of Southern California
School of Policy Planning and Development
Los Angeles, California 90089

Risk Management Products Team

John D. Hooper (Co-Team Leader)
Magnusson Klemencic Associates
1301 Fifth Avenue, Suite 3200
Seattle, Washington 98101

Craig D. Comartin (Co-Team Leader)
Comartin Engineers
7683 Andrea Avenue
Stockton, California 95207

Mary Comerio
University of California, Berkeley
Dept. of Architecture
232 Wurster Hall
Berkeley, California 94720

Allin Cornell (deceased)
Stanford University
Dept. of Civil & Environmental Engineering
110 Coquito Way
Portola Valley, California 94028

Mahmoud Hachem
Degenkolb Engineers
1300 Clay Street
Oakland, California 94612

Gee Heckscher
Architectural Resources Group
1301 53rd Street
Port Townsend, Washington 98368

Judith Mitrani-Reiser
National Institute of Standards and Technology
100 Bureau Drive
Gaithersburg, Maryland 20899

Peter Morris
AECOM
2020 L Street
Sacramento, California 95811

Farzad Naeim
Farzad Naeim, Inc.
100 Spectrum Center Drive, Suite 900
Irvine, California 92618

Keith Porter
University of Colorado
Dept. of Civil, Environmental, and Architectural
  Engineering
1111 Engineering Drive
Boulder, Colorado 80309

Hope Seligson
MMI Engineering
2100 Main Street, Suite 150
Huntington Beach, California 92648

Risk Management Products Consultants

Travis Chrupalo
Degenkolb Engineers
375 Beale St., Suite 500
San Francisco, California 94105

D. Jared DeBock
California State University, Chico
400 West 1st Street
Chico, California 95929

Armen Der Kiureghian
ADK & Associates
1974 18th Avenue
San Francisco, California 94116

Scott Hagie
John A. Martin & Associates, Inc.
950 South Grand Avenue
Los Angeles, California 90015

Curt B. Haselton
Haselton Baker Risk Group, LLC
728 Cherry Street, Suite C
Chico, California 95928

Russell Larsen
Magnusson Klemencic Associates
1301 Fifth Avenue, Suite 3200
Seattle, Washington 98101

Juan Murcia-Delso
University of California, San Diego
9500 Gilman Drive, MC0085
La Jolla, California 92093

Scott Shell
Esherick Homsey Dodge & Davis Architects
500 Treat Avenue, Suite 201
San Francisco, California 94110

P. Benson Shing
University of California, San Diego
Dept. of Structural Engineering
409 University Center
9500 Gilman Drive, MC0085
La Jolla, California 92093

Mohamed M. Talaat
  Simpson Gumpertz & Heger
100 Pine Street, Suite 1600
San Francisco, California 94111

Farzin Zareian
University of California, Irvine
Department of Civil and Environmental Engineering
Irvine, California 92697

Structural Performance Products Team

Andrew S. Whittaker (Team Leader)
University at Buffalo
Dept. of Civil, Structural and Environmental
  Engineering
230 Ketter Hall
Buffalo, New York 14260

Gregory Deierlein
Stanford University
Dept. of Civil & Environmental Engineering
Blume Earthquake Engineering Center, MC 3037
Stanford, California 94305

John D. Hooper
Magnusson Klemencic Associates
1301 Fifth Avenue, Suite 3200
Seattle, Washington 98101

Yin-Nan Huang
University at Buffalo
127 Paramount Parkway
Buffalo, New York 14223

Laura Lowes
University of Washington
Dept. of Civil and Environmental Engineering
233C More Hall, Box 352700
Seattle, Washington 98195

Nicolas Luco
U.S. Geological Survey
Box 25046, DFC, MS 966
Denver, Colorado 80225

Andrew T. Merovich
A.T. Merovich & Associates, Inc.
1950 Addison Street, Suite 205
Berkeley, California 94704

Structural Performance Products Consultants

Jack Baker
Stanford University
Dept. of Civil & Environmental Engineering
240 Terman Engineering Center
Stanford, California 94305

Dhiman Basu
University at Buffalo
230 Ketter Hall
Buffalo, New York 14260

J. Daniel Dolan
Washington State University
Dept. of Civil and Environmental Engineering
405 Spokane Street, Sloan 101
Pullman, Washington 99164

Charles Ekiert
University at Buffalo
12 Hillcrest Drive
Hamlin, New York 14464

Andre Filiatrault
University at Buffalo
Dept. of Civil, Structural and Environmental
  Engineering
134 Ketter Hall
Buffalo, New York 14260

Aysegul Gogus
University of California, Los Angeles
5731 Boelter Hall
Los Angeles, California 90095

Kerem Gulec
University at Buffalo
230 Ketter Hall
Buffalo, New York 14260

Dawn Lehman
University of Washington
Dept. of Civil and Environmental Engineering
214B More Hall
Seattle, Washington 98195

Jingjuan Li
University of Washington
4747 30th Avenue NE B118
Seattle, Washington 98105

Eric Lumpkin
University of Washington
6353 NE Radford Drive, Apt. #3917
Seattle, Washington 98115

Juan Murcia-Delso
University of California, San Diego
9500 Gilman Drive, MC0085
La Jolla, California 92093

Hussein Okail
University of California, San Diego
9500 Gilman Drive, MC0085
La Jolla, California 92093

Charles Roeder
University of Washington
Dept. of Civil and Environmental Engineering
233B More Hall
Seattle, Washington 98195

P. Benson Shing
University of California, San Diego
Dept. of Structural Engineering
409 University Center
9500 Gilman Drive, MC0085
La Jolla, California 92093

Christopher Smith
Stanford University
MC:4020, Building 540
Stanford, California 94305

Victor Victorsson
Stanford University
1742 Sand Hill Road, Apt. 308
Palo Alto, California 94304

John Wallace
University of California, Los Angeles
Dept. of Civil Engineering
5731 Boelter Hall
Los Angeles, California 90095

Nonstructural Performance Products Team

Robert E. Bachman (Team Leader)
RE Bachman Consulting
25152 La Estrada Drive
Laguna Niguel, California 92677

Philip J. Caldwell
Schneider Electric
7 Sleepy Hollow Lane
Six Mile, South Carolina 29682

Andre Filiatrault
University at Buffalo
Dept. of Civil, Structural and Environmental
    Engineering
134 Ketter Hall
Buffalo, New York 14260

Robert P. Kennedy (deceased)
RPK Structural Mechanics Consulting, Inc.
28625 Mountain Meadow Road
Escondido, California 92026

Helmut Krawinkler (deceased)
Stanford University
Dept. of Civil & Environmental Engineering
240 Terman Engineering Center
Stanford, California 94305

Manos Maragakis
University of Nevada, Reno
Dept. of Civil Engineering,
Mail Stop 258
Reno, Nevada 89557

Eduardo Miranda
Stanford University
Dept. of Civil & Environmental Engineering
240 Terman Engineering Center
Stanford, California 94305

Gilberto Mosqueda
University at Buffalo
Dept. of Civil, Structural, and Environmental
    Engineering
Buffalo, New York 14260

Keith Porter
University of Colorado
Dept. of Civil, Environmental, and Architectural
    Engineering
1111 Engineering Drive
Boulder, Colorado 80309

Nonstructural Performance Products Consultants

Richard Behr
Pennsylvania State University
Dept. of Architectural Engineering
104 Engineering Unit A
University Park, Pennsylvania 16802

Gregory S. Hardy
Simpson Gumpertz & Heger
4000 MacArthur Boulevard, Suite 710
Newport Beach, California 92660

Christopher Higgins
Oregon State University
School of Civil and Construction Engineering
220 Owen Hall
Corvallis, Oregon 97333

Gayle S. Johnson
Halcrow
500 12th Street, Suite 310
Oakland, California 94607

Paul Kremer
Pennsylvania State University
430 Canterbury Drive
State College, Pennsylvania 16802

David L. McCormick
Simpson Gumpertz & Heger
100 Pine Street, Suite 1600
San Francisco, California 94111

Ali M. Memari
Pennsylvania State University
Dept. of Architectural Engineering
104 Engineering Unit A
University Park, Pennsylvania 16802

William O'Brien
Pennsylvania State University
The Pointe
501 Vairo Boulevard
State College, Pennsylvania 16803

John Osteraas
Exponent
149 Commonwealth Drive
Menlo Park, California 94025

Xin Xu
7 Xibei Xincun, Room 403
Wuxi, Jiangsu 214062, P.R. China

Fragility Review Panel

Bruce R. Ellingwood
Colorado State University
Dept. of Civil and Environmental Engineering
Fort Collins, Colorado 80523

Robert P. Kennedy (deceased)
RPK Structural Mechanics Consulting, Inc.
28625 Mountain Meadow Road
Escondido, California 92026

Stephen Mahin (deceased)
University of California, Berkeley
Dept. of Civil Engineering
777 Davis Hall
Berkeley, California 94720

Validation/Verification Team

Charles Scawthorn (Chair)
C. Scawthorn & Associates
744 Creston Road
Berkeley, California 94708

Jack Baker
Stanford University
Dept. of Civil & Environmental Engineering
240 Terman Engineering Center
Stanford, California 94305

David Bonneville
Degenkolb Engineers
375 Beale St., Suite 500
San Francisco, California 94105

Hope Seligson
MMI Engineering
2100 Main Street, Suite 150
Huntington Beach, California 92648

Special Reviewers

Thalia Anagnos
San Jose State University
General Engineering Office 169
San Jose, California 95192

Fouad M. Bendimerad
125B 24th Avenue
San Mateo, California 94403